The University of Nottingham

UNITED KINGDOM · CHINA · MALAYSIA

The role of miRNA regulation in response to hypoxia in gliomas

Louise Smith, BSc, MSc

A thesis submitted to the University of Nottingham for the degree of Doctor of Philosophy, November 2022

Supervisors: Mr Stuart Smith, Dr Alan McIntyre, Dr Anbarasu Lourdusamy

Abstract

Glioblastoma multiforme (GBM) is the most aggressive and frequent adult brain tumour. Current therapy consists of debulking surgery followed by radiotherapy and temozolomide chemotherapy. The median survival is only 14 months post-therapy due to the high rates of recurrence. GBMs are known to be very heterogenous both within the tumour and between patients, this is a key contributor to GBM recurrence. Solid tumours, including GBM, often harbour hypoxic regions which are areas of low oxygen, often around 1% or lower. Physiologically, the brain is usually at 7% oxygen and can vary often between 12.5% and 2.5%. Hypoxia is a tumour microenvironment which is known to exacerbate and accelerate tumorigenesis. As tumours proliferate and become denser, a hypoxic gradient occurs with less oxygenated cells at the core and more oxygenated cells towards the periphery. Although hypoxic pockets can be found throughout the tumour. Hypoxia causes hypoxia-induced transcription which consequently up or downregulates genes that are important within different hallmarks of cancer. These processes are regulated by many factors including miRNAs. miRNAs are small non-coding sequences which bind to complimentary sequences which cleaves target mRNA and subsequently causes mRNA degradation, translation inhibition or deadenylation. miRNAs regulate gene expression; however, their expression can be affected by many microenvironmental conditions such as hypoxia.

Different screening techniques were employed to determine significantly changed miRNA expression in response to hypoxia, in order to select hypoxia-sensitive miRNAs. This research aims to identify changed miRNAs in response to hypoxia, to then explore the depths of this response further including functional changes and gene target expression. Two miRNAs, miR-149-5p and miR-92a-3p were identified as significantly up and downregulated respectively, in response to hypoxia in glioblastoma cell lines. These findings were mostly also seen within glioblastoma tissue samples. Using miRNA mimics and inhibitors, the level of apoptosis is affected by hypoxia and changed expression of miRNAs. Further work analysed the gene targets of the selected miRNA and the effects of hypoxia on their expression using the mimics and inhibitors. The final aspect of this work identified that miR-149-5p is potentially a hypoxia-induced miRNA. This work highlights the importance of hypoxia in tumours at the molecular level and provides a basis of which individual miRNAs and their gene targets may be exploited to combat hypoxia in glioblastomas.

Research Outputs

Conference oral presentations

- **British Neuro-Oncology Association Annual Meeting (2022)** University of Liverpool, UK

Conference poster presentations

- **European Neuro-Oncology Association Annual Meeting (2022)** Vienna, Austria

Covid Impact Statement

Unfortunately, the work in this thesis was significantly impacted by the Covid-19 pandemic. The pandemic caused immediate closure of research labs in March 2022 and remained closed until the beginning of September 2022. On return to the laboratory, many aspects of research were still impacted by the pandemic such as intensive logistical issues including capacity restrictions and long supply and reagent delays. Whilst all efforts were made to mitigate the loss of research time, this was not always possible due to the practical nature of the project. This work has been completed with an extension of 8 weeks to enable some practical work to be conducted which otherwise would not have been completed due to the loss of laboratory access during Covid-19 pandemic. Further mental health issues (anxiety/depression) have been exacerbated due to the pandemic which caused difficulties when the laboratories reopened and a long adjustment period. Appropriate measures were put in place

including attending regular therapy and medications to ensure the best management of my mental health to help with the continuation of the PhD in the best possible way.

Acknowledgements

To my supervisors Mr Stuart Smith and Dr Alan McIntyre, thank you for your unwavering support and guidance not only through the PhD but also with the pandemic and personal issues. Without your encouragement I really would not have been able to complete it.

To my parents, my brothers, Athena and my grandad, thank you for always supporting me and listening to me when they had no idea what I was talking about. Especially for their support when I was truly struggling and for giving me motivation when I needed it most.

To my partner Thomas, thank you for being there every day whether it was good or bad and being my rock. I can never thank you enough for your love, support and encouragement and without you by my side, this thesis would not be complete.

To my best friend Liv, thank you for being there to listen to me stress, panic and moan over countless dinners and drinks – it's your turn next!

Thank you to Sajib for his expert help with my bioinformatics analysis, you are a star. To everyone at the CBTRC both past and present, specifically Michaela Griffin, Phoebe McCrorie and Jonathan Rowlinson, thank you for the daily encouragements and help. Without any of you, I would have really struggled (even more so) to complete my PhD, so thank you.

Table of Contents

Abstract 2
Research Outputs 4
Covid Impact Statement 4
Acknowledgements 6
Table of Contents 7
List of Figures 11
List of Tables 18
List of Common Abbreviations 20
1 Chapter 1: Introduction 23
1.1 Brief cancer overview 23
1.1.1 What is cancer? 23
1.1.2 Hallmarks of cancer 24
1.2 Gliomas and Glioblastomas 26
1.2.1 Glioma/Glioblastoma WHO classification 26
1.2.2 Molecular biology of gliomas/GBM 29
1.2.3 Adult GBM incidence and risk factors 33
1.2.4 Adult GBM treatment and prognosis 34
1.2.5 Low-grade glioma incidence, treatment and prognosis 35
1.2.6 Paediatric GBM incidence, treatment and prognosis 37
1.3 Hypoxia 37
1.3.1 HIF-2 induced hypoxia 39
1.3.2 Hypoxia detection 40
1.3.3 Hypoxia-activated endogenous markers 43
1.4 Micro-RNA (miRNA) 44
1.4.1 miRNA biogenesis 45
1.4.2 Functions of miRNA 47
1.4.3 miRNA in cancer 48
1.4.4 miRNAs in hypoxia 52
1.4.5 miRNAs as therapeutics 54
1.5 Hypotheses and aims 58
2 Chapter 2: Methods 60
2.1 Cell lines 60

2.2 Exposure to Normoxic and Hypoxic Conditions 62
2.3 Obtaining and Snap Freezing Cell Pellets 62
2.4 RNA Extraction of Cell Pellets 63
2.5 miRNA Microarray 64
2.6 Raw Data Analysis and Normalization by R-packages 65
2.6.1 NanoStringNorm 65
2.6.2 NanoStringDiff Package 65
2.6.3 Quality control 66
2.6.4 Principal component analysis 66
2.7 cDNA Synthesis and qPCR 66
2.7.1 LNA miRCURY Reverse Transcriptase (RT) 66
2.7.2 LNA miRCURY Custom qPCR Panel Protocol 67
2.7.3 cDNA synthesis 69
2.7.4 qPCR 70
2.7.5 GeneGlobe Analysis software 72
2.8 Downstream Bioinformatics analyses 72
2.8.1 Differential expression analysis and visualization 72
2.8.2 Hierarchical clustering 73
2.8.3 Pathway analysis and Visualization 73
2.9 Transfection of glioma with small RNAs 76
2.9.1 Transfection protocol 77
2.10 Caspase-glo assay 79
2.11 Senescence β-galactosidase cell staining assay (cell signalling) 80
2.11.1 Solution preparation 80
2.11.2 Senescence assay protocol 81
2.12 Western Blot 81
2.12.1 Protein Extraction 81
2.12.2 Bradford Assay 82
2.12.3 Preparing the gel 82
2.12.4 Conducting the Western Blot 83
2.13 Tissue Sections and Tissue Microarrays (TMAs) 84
2.14 Immunohistochemistry 85
2.14.1 Removal of paraffin and hydration 85
2.14.2 Antigen Retrieval 85

2.14.3 Antibody Probing 86
2.14.4 Antibody Detection and Counterstaining 86
2.14.5 Mounting the slides 87
2.15 Immunofluorescence (IF) 87
3 Chapter 3: Microarray analysis of glioma samples 89
3.1 Introduction 89
3.2 Microarray results 92
3.2.1 RNA yield and purity 92
3.2.2 Microarray analysis 93
3.3 Summary 117
4 Chapter 4: LNA miRCURY custom qPCR analysis of glioma samples 123
4.1 Introduction 123
4.2 RNA yield and reverse transcriptase 126
4.3 qPCR custom plate layout 126
4.4 GeneGlobe Analysis 155
4.4.1 Normalisation methods 155
4.5 miRNA screening results 170
4.5.1 Overall cell line analysis 172
4.5.2 GIN cell line analysis 181
4.6 Summary 188
4.6.1 miRNA screening of all glioma types 188
4.6.2 miRNA screening summary of low-grade gliomas 194
4.6.3 miRNA screening summary of glioblastomas 197
4.6.4 hsa-miR-149-5p 201
4.6.5 hsa-miR-92a-3p 202
5 Chapter 5: Hypoxia-specific miRNAs 205
5.1 Introduction of hypoxia and gliomas 205
5.2 Assessing hypoxia gradients in glioblastomas 205
5.3 Introduction of miRNA selected targets and hypoxia 212
5.4 The expression of miR-92a-3p and miR-149-5p in tumour samples and other functions 213
5.4.1 miRNA and tumour sample expression 214
5.4.2 Knock-ins and knock-out effectiveness 216
5.4.3 Caspase-glo assay with knock-ins and outs 222
5.4.4 Senescence assays 224

5.5 miRNA targets and enrichment 225
5.5.1 qPCR of associated genes and miR-149-5p expression 231
5.5.2 qPCR of associated genes and miR-92a-3p expression 246
5.5.3 qPCR of core vs rim of target genes 257
5.5.4 Immunofluorescence of RAN 262
5.5.5 Immunohistochemical staining of RAN 264
5.6 Summary 270
5.6.1 Hypoxia in tumours samples 270
5.6.2 miR-92a-3p expression differences between cells and tissues 273
5.6.3 miR-149-5p expression validated in tumour samples 274
5.6.4 Apoptotic and senescence assays 274
5.6.5 miR-92a-3p gene target expression 276
5.6.6 miR-149-5p gene target expression 280
5.6.7 miRNAs indirectly affecting non-target gene expression 284
5.6.8 RAN expression in glioblastoma tumour tissue samples 289
6 Chapter 6: Discussion, conclusions, and future work 293
6.1 Overview and conclusions 293
6.2 Future work 297
6.2.1 Luciferase assay 297
6.2.2 Other avenues of research 308
7 References 313

List of Figures

Figure 1. The gradient of hypoxia within a tumour. The cells nearest the blood supply are most oxygenated and a gradient is created until cells before necrotic, usually in the core of the tumour. 38

Figure 2. Hypoxia pathway. The schematic shows the molecular pathway of HIFs in normoxic and hypoxic conditions. 40

Figure 3. miRNA biogenesis. Schematic depicting miRNA biogenesis starting with its transcription in the nucleus, cleaving by DROSHA and DICER, entering the cytoplasm and being loaded onto the RISC complex. 46

Figure 4. LNA miRCURY custom panel plate layout 74

Figure 5. Microarray process of screening the expression of hundreds of different miRNAs. 91

Figure 6. A boxplot of the raw data from the microarray analysis with no normalisation or correction across the 12 samples..... 93

Figure 7. A boxplot of the microarray data after background correction, which subtracts the expression of the negative controls from the miRNA expression values. This is followed by normalisation with the ligation controls. 93

Figure 8. A boxplot of the data with only the ligation normalisation applied. Background correction has not been performed. 94

Figure 9. Histograms showing the distribution of miRNA expression in each of the samples following ligation normalisation without background correction. 95

Figure 10. A principal component analysis of the 12 different samples that were analysed by the NanoString microarray. Each two dots represent a hypoxic and normoxic sample for each category. For GIN and LGG categories, three cell lines were analysed..... 96

Figure 11. Volcano plot of all cell lines, annotating the miRNAs which are significant in hypoxia compared to normoxia. Downregulated miRNAs are blue, and the upregulated miRNAs are red. 100

Figure 12. A heatmap showing the statistically significant differentially expressed miRNAs over all cell lines..... 100

Figure 13. Volcano plot of the primary GIN cell lines, red dots are significantly upregulated in hypoxia compared to normoxia. 102

Figure 14. A heatmap showing the statistically significant differentially expressed miRNAs in the primary glioblastoma (GIN) cell lines..... 102

Figure 15. Volcano plot of the primary low-grade cell lines, annotating the miRNAs which are significantly downregulated in hypoxia compared to normoxia. 104

Figure 16. A heatmap showing the statistically significant differentially expressed miRNAs in the primary low grade gliomas cell lines. 104

Figure 17. A pathway schematic showing the relevant pathways of the mRNA targets of the significant miRNA across all cell lines in hypoxia compared to normoxia.. 106

Figure 18. Dot plot of disease ontology pathways for the significant miRNAs in hypoxia compared to normoxia in all cell lines. 107

Figure 19. Dot plot of KEGG pathways for the significant miRNAs in hypoxia compared to normoxia in all cell lines. 108

Figure 20. Dot plot of wikipathways for the significant miRNAs in hypoxia compared to normoxia in all cell lines. 109

Figure 21. Dot plot of reactome outputs for the significant miRNAs in hypoxia compared to normoxia in all cell lines. 110

Figure 22. A pathway schematic of the relevant pathways of the mRNA targets of the significant miRNA across GIN cell lines in hypoxia compared to normoxia. 111

Figure 23. Dot plot of disease ontology pathways for the significant miRNAs in hypoxia compared to normoxia in GIN cell lines. 112

Figure 24. Dot plot of KEGG pathways for the significant miRNAs in hypoxia compared to normoxia in GIN cell lines. 113

Figure 25. Dot plot of WikiPathways for the significant miRNAs in hypoxia compared to normoxia in GIN cell lines. 114

Figure 26. Dot plot of Reactome outputs for the significant miRNAs in hypoxia compared to normoxia in GIN cell lines. 115

Figure 27. A schematic of miRCURY LNA technology. Step 1 shows cDNA single stranded synthesis. Step 2 shows the PCR amplification using LNA-miRNA-specific primers followed by SYBR green detection. Image created using BioRender. 124

Figure 28. A PCA plot for the geNorm normalisation method. The blue dots are GBMs, green dots are low-grade gliomas and orange dots are paediatric samples. 158

Figure 29. Heatmap produced for the samples using the geNorm normalisation method. 159

Figure 30. A PCA plot for the NormFinder normalisation method. The blue dots are GBMs, green dots are low-grade gliomas and orange dots are paediatric samples. 163

Figure 31. Heatmap displaying the expression of the miRNAs using the NormFinder normalisation method. 164

Figure 32. A PCA plot showing the samples using the gobaI ct mean of expressed miRNAs normalisation method. 167

Figure 33. Heatmap from qPCR data following normalisation using the global Ct mean of expressed miRNAs method. 168

Figure 34. Principle component analysis of the glioma samples. 172

Figure 35. Site of expression of significant hypoxic-miRNAs. 173

Figure 36. A bubble plot of the hypoxic significant miRNAs within the three categories. 174

Figure 37. A miRNA network showing the significant miRNAs in hypoxia compared to normoxia in all cell lines. 175

Figure 38. Dot plot of the disease ontology of the significant miRNAs for all cell lines in hypoxia compared to normoxia. 176

Figure 39. Dot plot of the KEGG analysis of the significant miRNAs for all cell lines in hypoxia compared to normoxia. 177

Figure 40. Dot plot of the WikiPathways analysis of the significant miRNAs for all cell lines in hypoxia compared to normoxia. 178

Figure 41. Dot plot of the Reactome analysis of the significant miRNAs for all cell lines in hypoxia compared to normoxia. 179

Figure 42. A miRNA network showing the significant miRNAs in hypoxia compared to normoxia in GIN cell lines. 181

Figure 43. A schematic showing the site of expression of the significantly expressed miRNAs from the GIN category. 182

Figure 44. Dot plot of the disease ontology of the significant miRNAs for GIN cell lines in hypoxia compared to normoxia. 183

Figure 45. Dot plot of the KEGG analysis of the significant miRNAs for GIN cell lines in hypoxia compared to normoxia. 184

Figure 46. Dot plot of the WikiPathways analysis of the significant miRNAs for GIN cell lines in hypoxia compared to normoxia. 185

Figure 47. Dot plot of the Reactome analysis of the significant miRNAs for GIN cell lines in hypoxia compared to normoxia. 186

Figure 48. A graph showing the CA9 expression in the core and rim sections of glioblastoma tissues to assess the degree of hypoxia within the different regions. 205

Figure 49. CA9 immunohistochemical staining in different GBM regions. 206

Figure 50. Immunohistochemical staining of CA9 in GBM and temporal lobe. 207

Figure 51. CA9 staining in tumour samples in TMA2. 207

Figure 52. CA9 staining in tumour samples in TMA3. 208

Figure 53. CA9 staining in tumour samples in TMA4. 208

Figure 54. CA9 staining intensity correlation with age of GBM patients. 209

Figure 55. Schematic of low and high CA9 expression amongst GBM patients. 209

Figure 56. CA9 survival curve in GBM patients using TCGA dataset of 540 patients. 210

Figure 57. Western blot of HIF-1a protein expression in normoxic and hypoxic cultures of glioblastoma cell lines. 211

Figure 58. miR-92a-3p expression within glioblastoma tissue samples within the different regions, core and rim 214

Figure 59. miR-149-5p expression within glioblastoma tissue samples within the different regions, core and rim. 215

Figure 60. Transfection of GIN28 with SiGLO and non-targeting control. A) bright field image of GIN28 cells that are transfected with siGLO. B) Fluorescent image of GIN28 cells transfected with siGLO showing in the bright green spots. C) Bright field image of GIN28 cells that are transfected with a non-targeting control. D) Fluorescent image of GIN28 cells transfected with the non-targeting control with no fluorescence seen..... 216

Figure 61. Transfection of GIN31 with SiGLO and non-targeting control. A) bright field image of GIN31 cells that are transfected with siGLO. B) Fluoresent image of GIN31 cells transfected with siGLO showing in the bright green spots. C) Bright fied image of GIN31 cells that are transfected with a non-targeting control. D) Fluorescent image of GIN31 cells transfected with the non-targeting control with no fluorescence seen..... 217

Figure 62. Showing the expression of miR-92a-3p using miR-92a-3p mimics on GIN28 and GIN31, 48 and 72hrs after initial transfection. 219

Figure 63. Showing the expression of miR-149-5p using miR-149-5p mimics on GIN28 and GIN31, 48 and 72hrs after initial transfection. 219

Figure 64. Showing the expression of miR-92a-3p using miR-92a-3p inhibitors on GIN28 and GIN31, 48 and 72hrs after initial transfection. 220

Figure 65. Showing the expression of miR-149-5p using miR-149-5p inhibitors on GIN28 and GIN31, 48 and 72hrs after initial transfection. 220

Figure 66. Apoptotic assay using mimics and inhibitors of miR-92a-3p and miR-149-5p in GIN28 cells..... 221

Figure 67. Apoptotic assay using mimics and inhibitors of miR-92a-3p and miR-149-5p in GIN31 cells..... 222

Figure 68. Senescence assay of GIN28 using control, miR-92a-3p mimic and inhibitor in normoxic and hypoxic conditions. 224

Figure 69. Senescence assay of GIN28 using control, miR-92a-3p mimic and inhibitor in normoxic and hypoxic conditions. 224

Figure 70. Enrichment pathway analyses of the gene targets of miR-149-5p. 225

Figure 71. Kaplan Meier curve showing the disease-free survival data of the 8 hypoxic genes that are targets of miR-149-5p. The low expression signatures are patients with expression levels below the median and high signature group are those with expression above the median.. 227

Figure 72. Kaplan Meier curve showing the overall survival data of the 8 hypoxic genes that are targets of miR-149-5p. The low expression signatures are patients with expression levels below the median and high signature group are those with expression above the median.. 228

Figure 73. Enrichment analyses of the gene targets of miR-92a-3p.. 229

Figure 74. Effects of miR-149-5p mimics and inhibitors on SRSF1 expression in normoxic and hypoxic conditions in GIN28 cells. 231

Figure 75. Effects of miR-149-5p mimics and inhibitors on SRSF1 expression in normoxic and hypoxic conditions in GIN31 cells. 232

Figure 76. Effects of miR-149-5p mimics and inhibitors on RAN expression in normoxic and hypoxic conditions in GIN28 cells. 233

Figure 77. Effects of miR-149-5p mimics and inhibitors on RAN expression in normoxic and hypoxic conditions in GIN31 cells. 234

Figure 78. Effects of miR-149-5p mimics and inhibitors on HNRNPU expression in normoxic and hypoxic conditions in GIN28 cells. 236

Figure 79. Effects of miR-149-5p mimics and inhibitors on HNRNPU expression in normoxic and hypoxic conditions in GIN31 cells. 237

Figure 80. Effects of miR-149-5p mimics and inhibitors on ACAA1 expression in normoxic and hypoxic conditions in GIN28 cells. 239

Figure 81. Effects of miR-149-5p mimics and inhibitors on ACAA1 expression in normoxic and hypoxic conditions in GIN31 cells. 240

Figure 82. Effects of miR-149-5p mimics and inhibitors on ACADS expression in normoxic and hypoxic conditions in GIN28 cells. 241

Figure 83. Effects of miR-149-5p mimics and inhibitors on ACADS expression in normoxic and hypoxic conditions in GIN31 cells. 242

Figure 84. Effects of miR-149-5p mimics and inhibitors on SUCLG1 expression in normoxic and hypoxic conditions in GIN28 cells. 243

Figure 85. Effects of miR-149-5p mimics and inhibitors on SUCLG1 expression in normoxic and hypoxic conditions in GIN31 cells. 244

Figure 86. Effects of miR-92a-3p mimics and inhibitors on ACAA1 expression in normoxic and hypoxic conditions in GIN28 cells. 245

Figure 87. Effects of miR-92a-3p mimics and inhibitors on ACAA1 expression in normoxic and hypoxic conditions in GIN31 cells. 246

Figure 88. Effects of miR-92a-3p mimics and inhibitors on ACADS expression in normoxic and hypoxic conditions in GIN28 cells. 247

Figure 89. Effects of miR-92a-3p mimics and inhibitors on ACADS expression in normoxic and hypoxic conditions in GIN31 cells. 248

Figure 90. Effects of miR-92a-3p mimics and inhibitors on SUCLG1 expression in normoxic and hypoxic conditions in GIN28 cells. 249

Figure 91. Effects of miR-92a-3p mimics and inhibitors on SUCLG1 expression in normoxic and hypoxic conditions in GIN31 cells. 250

Figure 92. Effects of miR-92a-3p mimics and inhibitors on SRSF1 expression in normoxic and hypoxic conditions in GIN28 cells. 251

Figure 93. Effects of miR-92a-3p mimics and inhibitors on SRSF1 expression in normoxic and hypoxic conditions in GIN31 cells. 252

Figure 94. Effects of miR-92a-3p mimics and inhibitors on RAN expression in normoxic and hypoxic conditions in GIN28 cells. 253

Figure 95. Effects of miR-92a-3p mimics and inhibitors on RAN expression in normoxic and hypoxic conditions in GIN31 cells. 254

Figure 96. Effects of miR-92a-3p mimics and inhibitors on HRNRPU expression in normoxic and hypoxic conditions in GIN28 cells. 255

Figure 97. Effects of miR-92a-3p mimics and inhibitors on HRNRPU expression in normoxic and hypoxic conditions in GIN31 cells. 256

Figure 98. Graph showing SRSF1 expression in the core and rim of three glioblastoma patients..... 257

Figure 99. Graph showing RAN expression in the core and rim of three glioblastoma patients..... 258

Figure 100. Graph showing HNRNPU expression in the core and rim of three glioblastoma patients..... 259

Figure 101. Graph showing ACAA1 expression in the core and rim of three glioblastoma patients..... 259

Figure 102. Graph showing ACADS expression in the core and rim of three glioblastoma patients..... 260

Figure 103. Graph showing SUCLG1 expression in the core and rim of three glioblastoma patients..... 260

Figure 104. Immunofluorescence of RAN in GIN28 cells. 261

Figure 105. Immunofluorescence of RAN in GIN31 cells. 262

Figure 106. Immunofluorescence of RAN in GIN8 cells. 262

Figure 107. Immunohistochemical RAN expression in different GBM regions using patient tissues. 263

Figure 108. IHC staining of RAN in GBM core and temporal lobe. 264

Figure 109. RAN staining in tumour samples in TMA2. 265

Figure 110. RAN staining in tumour samples in TMA4. 265

Figure 111. RAN staining intensity correlation with age of GBM patients. 266

Figure 112 Schematic of low and high RAN expression amongst GBM patients. 267

Figure 113. Schematic of female and male prevalence within high RAN expression amongst GBM patients. 267

Figure 114. RAN survival curve in GBM patients using TCGA dataset of 540 patients 268

Figure 115. A schematic highlighting the possible avenues of future research to further investigate the hypoxic-inducible miR-149-5p in glioblastomas..... 309

List of Tables

Table 1. WHO 2021 classification of CNS tumours. 27

Table 2. Molecular characteristics of primary cell lines. 61

Table 3. Age and gender of patient primary cell lines. 61

Table 4. Glioma categories of the 12 different cell lines. 62

Table 5. Reverse transcription reactions 67

Table 6. Reaction setup for miRCURY LNA Custom PCR Panel 68

Table 7. LNA miRCURY Custom PCR Panel PCR Cycling Conditions 68

Table 8. A table showing the volumes required of the cDNA synthesis kit for one reaction 69

Table 9. A table showing the temperatures and time of the thermocycler programme for cDNA synthesis. 70

Table 10. qPCR master mix components and volumes. 71

Table 11. Primer sequences of miRNA downstream targets. 71

Table 12. qPCR Cycling Conditions 72

Table 13. miRIDIAN miRNA product information. 77

Table 14. Transfection mixture steps and volumes. 79

Table 15. Components and volumes for B-galactosidase staining solution. 80

Table 16. Table defining the number of cores and patients per each TMA. 85

Table 17. Fold change of miRNAs which had a p-value < 0.01 in hypoxia compared to normoxia. 99

Table 18. A table showing a list of the handpicked miRNAs from the miRCURY qPCR panel and the reasons from the literature searches. 127

Table 19. miRNAs selected as reference miRNAs in geNorm normalisation, based on their stability factor being less than 1.5. 156

Table 20. Average arithmetic Ct mean of the selected reference miRNAs for the geNorm method. 157

Table 21. Table of reference miRNA selected using the NormFinder normalisation method. 161

Table 22. Table of the average arithmetic Ct mean of the selected reference miRNAs for the NormFinder method. 162

Table 23. Table of the global Ct mean of expressed miRNAs for each triplicate of each sample. 166

Table 24. The tables hows the significant miRNAs and fold changes for each category; overall, GBM (GIN) and low-grade (LGG), from the LNA miRCURY qPCR analysis. 171

Table 25. Table showing overlapping significant miRNAs in microarray and qPCR analysis. 188

Table 26. Sequences of 3’UTRs cloned into the LightSwitch 3’UTR vector..... 299

Table 27. Co-transfection solutions per replicate. 305

Table 28. LightSwitch luciferase assay solution mixture..... 306

List of Common Abbreviations

α-KG	Alpha-ketoglutaric acid
AGO	Agonaute
AKT	RAC-alpha serine/threonine-protein kinase
AR	Androgen receptor
BOLD-MRI	Blood-oxygen-level-dependent MRI
CA9	Carbonic anhydrase 9
cDNA	Complimentary DNA
CFTR	cystic fibrosis transmembrane conductance regulator
DCE-MRI	Dynamic contrast-enhanced MRI
DMEM	Dulbecco's modified eagle medium
DMSO	Dimethyl sulfoxide
DNA	Deoxyribonucleic acid
EDTA	Ethylenediaminetetraacetic acid
EGFR	Epidermal growth factor receptor
EMT	Epithelial to mesenchymal transition
FBS	Foetal bovine serum
FDR	False discovery rate
F-MISO	Fluoromisonidazole
GBM	Glioblastoma multiforme
GCE	Primary cells derived from the GBM core
GIN	Primary cells derived from the GBM invasive edge
GLUT	Glucose transporter
GSEA	Gene set enrichment analysis
GSH	Glutathione

HBSS	Hanks’s balanced salt solution
HIF-1α	Hypoxia-inducible factor 1-alpha
HIF-1β	Hypoxia-inducible factor 1-beta
HRE	Hypoxia response element
IDH	Isocitrate dehydrogenase
IHC	Immunohistochemical
KEGG	Kyoto encyclopaedia of genes and genomes
LGG	Low-grade glioma
LNA	Locked nucleic acids
lncRNA	Long non-coding RNA
MAPK	Mitogen-activated protein kinases
MET	Tyrosine-protein kinase Met
MGMT	O-6-methylguanine-DNA methyltransferase
miRNA	microRNA
MMP	Matrix metalloproteinase
MRI	Magnetic resonance imaging
mTor	Mechanistic target of rapamycin kinase
NGS	Normal goat serum
PBS	Phosphate buffered saline
PCA	Principal component analysis
PCR	Polymerase chain reaction
PET	Positron emission tomography
PI3K	Phosphatidylinositol 3-kinase
PTEN	Phosphatase and tensin-homolog
QC	Quality control

RAS	Rat sarcoma virus GTPase
RIN	RNA integrity number
RNA	Ribonucleic acid
ROS	Reactive oxygen species
siRNA	Small interfering RNA
TIMP	Tissue inhibitor of metalloproteinase
TMA	Tissue microarray
TMZ	Temozolomide
UTR	Untranslated region
UV	Ultraviolet
VEGF	Vascular endothelial growth factor
VHL	von-Hippel-Lindau syndrome
WHO	World health organisation

1 Chapter 1: Introduction

1.1 Brief cancer overview

The history of cancer is thought to have been recorded by ancient Egyptians and Greeks (1) and throughout time since then. It is a disease that has been found in most organisms from humans to fish, including the possibility of dinosaurs (2). However, with the eradication and control of various diseases such as polio and smallpox which were endemic to the UK, cancer has come into the limelight throughout recent decades. Since then, cancer is a word that has become used ever more frequently within society's vocabulary, due to increased incidence via increased screening and detection. In the UK between 2016 and 2018, around 375,400 new cancer cases occurred and during 2017 - 2019 around 167,142 people died from cancer (3). These statistics show that cancer has become a prominent disease, and the vast amount of on-going international cancer research across all cancer types reflects this.

1.1.1 What is cancer?

Definitively, cancer is known to be the rapid proliferation of abnormal cells that can occur in nearly every organ of the body. Many tumours are solid masses of rapidly dividing cells. However, leukaemia and other blood malignancies are cancer in its liquid form with malignant cells residing within the bone marrow and blood (4). Underpinning all the molecular changes that occur with every type of cancer, stems from genetic mutations which favour oncogenic transformations resulting in oncogenic phenotypes. There are features that occur in cancer which have been

labelled the ‘hallmarks of cancer’ (5). However along with genetic alterations, post-transcriptional and post-translational changes have been shown to heavily contribute to oncogenic features.

1.1.2 Hallmarks of cancer

The hallmarks of cancer are acquired capabilities of cancer cells to ensure and enhance tumour growth. These were originally described by Hanahan and Weinberg in 2000 (6), then reviewed again in 2011 (5) adding an additional four traits. Nearly two decades on these features remain the focal points of most cancer research.

1.1.2.1 Genomic instability and mutations

Underpinning most features of malignancies are changes in the genetic code. Other hallmarks, which are described later, often arise due to mutations in particular genes. Carcinogenesis is a multistep progression which arises due to the acquisition of multiple mutations over time (7). Mutations in this process are described as either driver or passenger mutations (8). Driver mutations result in an advantage for the cancer i.e. a mutation that drives uncontrollable proliferation, whereas passenger mutations occur naturally but do not aid the progression of tumorigenesis (9).

1.1.2.2 Angiogenesis

As with normal cells and tissues, malignant cells require constant blood supply to deliver oxygen in order to proliferate profusely, alongside the delivery of other micronutrients and the removal of waste products (10).

The formation of new blood vessels from existing ones is defined as angiogenesis. Vascular endothelial growth factor-A (VEGF-A) is a gene which is heavily involved in the formation of blood vessels via signalling from VEGF-A ligand binding to one of three VEGF receptors which are tyrosine kinases (10). This signalling is upregulated in both tumorigenesis and hypoxia (11). Many other genes and receptors are involved in the formation of tumour vasculature. Aberrant angiogenesis in tumorigenesis often produces blood vessels which are porous and leaky with spontaneously sprouting micro-vessels (11). The vasculature of tumours often prevents efficient delivery of chemotherapeutic or targeted drugs to the tumour.

1.1.2.3 Maintaining proliferative signalling

As seen with VEGF in angiogenesis, in malignancies, many pro-proliferative signals enable and sustain rapid and constant cell division. Many different pathways have been identified in different tumours and are constitutively active such as MAPK pathway in melanomas and the PI3-kinase pathway which results from mutations in the PI3 kinase causing hyperactive signalling (12). In contrast, anti-proliferative signals that are used to regulate proliferation in normal cells are often switched-off preventing control of proliferation in cancer. PTEN phosphatase, a well-known tumour suppressor, also involved in the PI3-kinase pathway, is affected by mutations which causes loss of function and consequently contributes to sustained proliferation by PI3-kinase (13). The proliferative signalling is sustained in many different ways by many mutations in both

pro- and anti-proliferative genes, which contributes to one of the most well-known characteristics of cancer.

1.2 Gliomas and Glioblastomas

Gliomas are brain tumours which derive from glial cells that surround neurons. Multiple cell types are classified as glial cells such as astrocytes, oligodendrocytes, ependymal cells and microglia. These different types of glial cells can give rise to the different subtypes of gliomas defined by the World Health Organisation (WHO).

1.2.1 Glioma/Glioblastoma WHO classification

In 2016, the glioma classification was issued. Glioblastomas can be abbreviated to GB or GBM, however in this thesis GBM will denote glioblastomas. This thesis focuses on gliomas which are grouped into, glioblastomas, diffuse astrocytic and oligodendroglial tumours which is a branch of tumours that will be discussed in further detail. These tumours range from grade 2 to grade 4. This classification is based on both molecular and genetic characteristics of the tumours. Three main subgroups of molecular characterisations have arisen to diagnose gliomas. These are: isocitrate dehydrogenase (IDH) mutant and 1p/19q codeleted, IDH-mutant and 1p/19q non-codeleted and IDH wild-type. Histology and genetics are used to diagnose diffuse gliomas. However, when the histological diagnosis does not match the diagnosis made by genetic testing, the diagnosis is determined on the outcome of the genetic test (14). In cases where genetic testing in unable to be performed, the diagnosis is determined by the results of histology and often annotated

with ‘not otherwise specified’ (NOS). However, during this research, the WHO classification of gliomas and glioblastomas was updated in 2021. The change of classification altered so that glioblastomas are grade 4 IDH-wildtype tumours, and that astrocytomas are grade 2, 3 and 4 IDH-mutant tumours with oligodendrogliomas are grade 2 and 3, IDH-mutant with 1p/19q codeletion (15) as shown in table 1.

Table 1. WHO 2021 classification of CNS tumours.

WHO CNS Tumours	Tumour Grade
Glioblastoma, IDH-wildtype	4
Astrocytoma, IDH-mutant	2, 3, 4
Oligodendroglioma, IDH-mutant, 1p/19q codeletion	2, 3

1.2.1.1 Isocitrate dehydrogenase (IDH) mutant/wildtype

Mutations within isocitrate dehydrogenase were one of the first genetic changes discovered to aid diagnosis in gliomas. Gliomas that harbour IDH mutations are often of a lower grade (2 or 3) but can be grade 4 as of the new 2021 classification, grade 4 IDH-mutated gliomas are classified as grade 4 astrocytomas. IDH 1 and 2 proteins produce reduced nicotinamide adenine dinucleotide phosphate (NADPH) from NAPD+ by catalysing the oxidative decarboxylation of isocitrate to α-ketoglutarate (α-KG) outside of the Krebs cycle (16). It has also been noted that cells with low amounts IDH 1 and 2 proteins are more

susceptible to oxidative stress via free radicals and reactive oxygen species (ROS), indicating IDH plays a role in protecting against oxidative damage (17). Mutations identified in IDH1 in gliomas are a single amino acid missense mutation in residue arginine 132 and this residue is within the active site of the protein and required for binding to isocitrate (18). Mutation of arginine 132 inactivates its binding capabilities and also eradicates its normal catalytic activity (16). Mutations in IDH1 also result in a reduction of NADPH and α-KG which are required to maintain normal levels of reduced glutathione (GSH) to protect against ROS (19). Mutations in IDH2 are a single amino acid missense mutation of the analogous residue arginine 172 (19). Though the mechanism of how IDH and its mutations contribute to oncogenesis is widely disputed, IDH wild-type/mutated proteins are associated with the hypoxic pathway (20). Prolyl-hydroxylase enzymes are required for the hydroxylation and degradation of hypoxia inducible factor 1 (HIF-1) (21). These particular enzymes require α-KG and iron (Fe^{2+}), however, the IDH mutations cause a decrease in the amount of α-KG and Fe^{2+} (16)[c]. This results in an accumulation and stabilisation of HIF-1 which consequently promotes many HIF-induced cancer pathways such as angiogenesis (22). As HIF1 can be stabilised due to IDH mutations without the presence of hypoxia, it can be defined as ‘psuedohypoxia’ (16). GBMs that contain IDH mutations (now classified as grade 4 astrocytomas) have higher amounts of HIF-1α protein than GBMs which contain wildtype-IDH (16). A study has found that R-2-HG can substitute for α-KG to increase the hydroxylation activity of PHD (23) and therefore promote the degradation

of HIF-1α. However, a gene expression analysis study showed that IDH mutations reduced expression of HIF-target genes (16). Though it seems clear that IDH mutations play a role in HIF-1α stabilisation, more specific elucidation of its role is required for a solid understanding of its mechanism.

IDH mutations are more widely observed in the lower grade gliomas (2 and 3) (24). In astrocytic tumours, IDH mutations are accompanied by *TP53* mutation whereas in oligodendrogliomas with IDH mutations are accompanied by 1p/19q codeletion (25). These genetic alterations are mutually exclusive and determine the type of glioma. The presence of IDH mutations in lower grade gliomas suggests that these mutations are obtained early on in tumorigenesis and often precedes *TP53* mutation or 1p/19q codeletion. Patients whose tumours harbour IDH mutations are common in adolescents of 14 years old or more and are often younger than those without IDH mutations (26). Following multiple prospective analyses glioma patients that carry IDH mutations have a significantly longer overall survival than patients with wildtype-IDH (18).

1.2.2 Molecular biology of gliomas/GBM

Molecular information about glioblastomas along with WHO classification and histological classification allows for a comprehensive diagnosis and prediction of the response and prognosis of the tumour.

Clinical molecular subtyping has changed and advanced throughout the years of glioma research with the first subtype classification developed by Phillips *et al* identifying three groups; proliferative, mesenchymal and proneural (27). In 2010, this classification was expanded and altered by Verhaak *et al* changing the glioma subtypes to classical, mesenchymal, proneural and neural (28). High PDGFRA gene expression and high frequency of harbouring IDH-mutations is characteristic of proneural subtype found often in younger patients (28). Though proneural subtypes do not show a favoured response to chemo or radiotherapy, survival rates of proneural are the highest of the subtypes (29). Neural subtypes are more responsive to chemotherapy and radiotherapy and have similar gene expressions to normal brain and express markers such as Neurofilament Light Polypeptide (NEFL) and Synaptotagmin 1 (SYT1) (30). The classical subtype can harbour genetic aberrations such as chromosome 7 amplification, chromosome 10 loss, focal 9p21.3 homozygous deletion as well as high expression of Sonic hedgehog and Notch pathways (30). Aggressive chemo and radiotherapy can significantly improve the mortality of classical subtype patients. Mesenchymal subtypes have the worst prognosis of the four groups even though it is reported to be responsive to chemo and radiotherapy (29). Mesenchymal gliomas are characterised by deletion of tumour suppressor genes; P53, PTEN, NF1, increased expression of tumour necrosis factor family of genes, upregulation of angiogenesis gene and extensive inflammation and necrosis (30). Also a variety of angiogenic genes specifically were shown to be upregulated in mesenchymal

subtype including VEGFA, VEGFB and angiopoietin 1 (31). Further studies have shown that mitogen-activated protein kinase (MAPK) pathways, PI3K/AKT pathways and extracellular-signal related kinase (ERK) and Wnt pathways are associated with mesenchymal subtypes and those with PIK3R1 or protein piccolo (PCLO) have an increased poorer prognosis (32). In 2019, Teo *et al* , have combined the proneural and neural subtype as one entity (33).

Other classifications have also been developed such as prognostic subtyping of gliomas as invasive (poor prognosis), intermediate and mitotic (favourable prognosis) (34). A methylated MGMT promoter is associated with mitotic subtype which indicates the increased likelihood of a positive response to TMZ (34). Invasive subtypes require aggressive therapeutic intervention (30). Though this subtyping classification is generated by transcription profiles and survival times and some genetic features have been shown to identify with a certain subtype. Gliomas that harbour IDH-mutations, ATRX mutations and DNA methylation are only seen in mitotic subtypes, associated with a more favourable prognosis (34).

Particular gene mutations are important indicators and markers within GBM such as IDH-mutations, 1p/19q co-deletion (oligodendroglioma-specific), PTEN mutations, TP53 mutations, Telomerase Reverse Transcriptase (TERT) gene promoter mutations Alpha Thalassemia/Mental Retardation Syndrome X-linked (ATRX) mutations

and EGFR mutations (30). PTEN catalyses the dephosphorylation of the inositol ring in phosphatidylinositol-3,4,5-triphosphate (PIP3) to produce phosphatidylinositol-3,4,5-biphosphate (PIP2) which is vital to inhibit the AKT pathway (35). The lack or loss of PTEN activates the modulation of the cell cycle pushing towards an aggressive cell phenotype (30). TERT promoter mutations are associated with poor prognosis, linked with elderly patients and correlates overall with a shorter overall survival (30). EGFR amplification or high rate of EGFR mutations are characteristic of primary GBM and seen in around 50% of cases (36).

IDH-mutations, as discussed earlier, promote a favourable prognosis comparative to IDH-wildtype. IDH-wildtype glioblastomas are characterised by atypical nuclei, polymorphic cells, diffuse growth patterns, mitotic activity, microvascular proliferation and necrosis (30). There are also some IDH-wildtype glioblastomas variants including giant cell GBM, gliosarcoma and epithelial-like GBM (37). There are a few genetic differences noted between the GBM variants including a lack of EGFR amplification, PTEN, TP53 mutations and CDKN2A deletion for giant cell glioblastoma (38). In gliosarcoma, CDKN2A deletion, EGFR amplification is uncommon and unlikely to harbour TP53 mutations (39). Epithelial-GBM is more likely to occur in children, and often has a BRAF V600E mutation (40), lack of EGFR amplification, PTEN loss and hemizygous deletion of ODZ3 (41).

Epigenetic changes such as methylation are important markers in many cancers including GBM. Extensive DNA methylation of CpG islands in multiple promoter regions in gliomas is known as, glioma-CpG island methylator phenotype (G-CIMP), is linked to the proneural subtype (28) and thus associated with a more favourable prognosis. MGMT gene can confer resistance to alkylating chemotherapeutic agent, TMZ, by reversing mutagenic O6- alkyl-guanine back to guanine (42). G-CIMP clusters increase the likelihood of MGMT promoter methylation which causes silencing of the MGMT gene and correlates with improved response to TMZ (43).

1.2.3 Adult GBM incidence and risk factors

Glioblastomas are the most frequent and aggressive primary brain tumour in adults. Overall Caucasians have a higher incidence rate of GBM than all other ethnicities (44). Along with ethnicity, the incidence of primary GBM is higher in males than females (45), however GBM recurrence incidence is higher in females (46). As with most cancers increasing age is a risk factor for GBM. In particular the mean age of diagnosis of a primary GBM is around early sixties, with a median age of 64 (47), (44), (46). Annual age-adjusted incidence rate for GBM in the UK was 2.05 per 100,000 persons and 3.19 per 100,000 persons in the US, although these figures vary largely between countries (46). Several hereditary tumour syndromes are linked with an increased risk of GBM including Li-Fraumeni syndrome, often due to the TP53 germline mutation in the majority of cases, neurofibromatosis type 1 and 2 and

Turcot syndrome (45). Glioblastomas are predominately located in the supratentorial region with the highest incidence rates in the frontal lobe, followed by tumours overlapping multiple lobes, temporal and parietal lobes (44), (46).

1.2.4 Adult GBM treatment and prognosis

The current gold standard regime for the treatment of GBM consists of surgical resection of the tumour. Unfortunately, often tumour deposits are left behind. This is then followed by adjuvant radiotherapy (60 Gray) and temozolomide (TMZ) chemotherapy (48). TMZ has been used for decades and though it has a low IC_{50}, it effectively crosses the blood brain barrier which has secured its constant use in glioblastoma treatment. The mean survival with the most optimal treatment regime results in approximately 14 month survival (49) and only 8% of treated GBM patients reach long-term survival of 2.5 years (48). However, few patients can receive optimal regime due many variables including the success of the resection, the health of the patient as to whether optimal doses of radio and chemotherapy can be administered and acquired radio/chemoresistance. With years of persistent and excellent research focusing on GBM to find new therapies, the gold standard treatment regime has hardly changed in decades, due to tumour heterogeneity, crossing the blood brain barrier and therapeutic delivery issues.

1.2.5 Low-grade glioma incidence, treatment and prognosis

As of the 2021 WHO classification, low-grade gliomas are grade 2 and 3 astrocytoma that harbour IDH-mutations or oligodendrogliomas which also harbour IDH-mutations as well as 1p/19q co-deletion. Low-grade gliomas are characterised by IDH-mutations which is indicative of a more favourable prognosis compared to high-grade IDH-wildtype tumours (50). The distinction between the two low-grade tumour types, astrocytoma and oligodendroglioma is the 1p/19q deletion only seen in oligodendroglioma. Other markers can assist in distinguishing astrocytomas from oligodendrogliomas are; TP53 which are present in more than 60% of astrocytomas (51), ATRX inactivation associated with around 86% of IDH-mutant astrocytomas (25) and TERT promoter mutations which are present in more than 90% of oligodendrogliomas (52). In this research, all low-grade gliomas refer to low-grade astrocytomas with IDH-mutations. Low-grade gliomas, astrocytomas and oligodendrogliomas, represent 15% of all gliomas and have a highest incidence between the ages of 35-40 with increased prevalence in Caucasian males (53). The average overall survival of low-grade gliomas is between 5-6 years with a wider range of between 3 and 10 years (54). However, there are a selection of factors which are associated with a more negative outcome such as; over 40 years of age, tumours larger can 6cm in diameter, non-seizure symptoms and neurological defects at presentation, astrocytoma rather than oligodendroglioma, tumours crossing the midline and increasing at a rate of over 8mm a year (50)(53). Low-grade gliomas are generally slow growing and three stages of

disease progression highlighted for low-grade gliomas which are: 1) pre-symptomatic phase – not aware of the presence of the tumour unless discovered accidentally, 2) symptomatic period of around 7 years after initial presentation which is usually a seizure, 3) transformational stage lasting between 2 and 3 years which tumour accelerates and dedifferentiates into grade 3 or 4 astrocytoma/glioblastoma (53). Biopsies and pre-operative contrast enhancement are not reliable enough to establish a low-grade glioma diagnosis. T2/FLAIR-weighted MRI and baseline neuropsychological tests are preferred diagnostic techniques for low-grade gliomas (50). Surgical resection is the main treatment option of choice for low-grade gliomas and is favoured over biopsy and observation if possible (55). Complete surgical resection compared with subtotal resection is associated with improved seizure control (53). Adjuvant chemotherapy of procarbazine, lomustine, vincristine (PCV) or TMZ and radiotherapy doubles progression-free survival (PFS), overall survival and quality of life, often benefits oligodendroglioma patients slightly more (53). As younger patients often do not display any major neurological defects, the wait-and-see policy is often used as an overall survival is usually between 6 and 7 years or following initial aggressive resections, the average survival can be around 10 years from diagnosis and increased up to 15 years with personalised multi-staged therapies (50).

1.2.6 Paediatric GBM incidence, treatment and prognosis

In comparison to adult glioblastomas, GBM is less frequent in children making up around 3-7% of childhood primary brain tumours (56). The prognosis of GBM in children is similar to that of adults with a median survival of between 13 and 43 months (57). Generally, paediatric patients often survive longer than adult patients with GBM, suggesting that paediatric GBM has distinctive differences to its adult counterpart (56). As paediatric GBM is uncommon, reports and studies on the disease is limited, but in the literature the mean age of childhood GBM ranges between around 9 and 13 years (58). There is also a ratio of 3:2 male to female of childhood GBM, which is similar to the male predominance seen in adult GBM (57). Patients which have MGMT promoter methylation is favourable for long-term survival, contrasting other molecular changes such as PTEN and p53 mutations (58). Treatment for paediatric GBM is surgical resection of the tumour followed by radiotherapy and/or chemotherapy, however, the chemotherapeutic regimes differ and a standardised regime is still in investigation (59). Maximal resection of the tumour is associated with improved prognosis and overall survival and has been observed in many studies (56).

1.3 Hypoxia

The normal physiological percentage of oxygen (O_2) in the brain is around 7% (60), but varies between 12.5% and 2.5% (61). Hypoxia is often defined as the deficiency of oxygen to tissues, with a percentage of <1% oxygen, and in GBM, hypoxic oxygen levels have been suggested to be between 2.5% and 0.1% (61)(62). This state is often caused by a

rapidly proliferating mass of tumour cells which exceeds the rate of which vasculature inside the tumour is produced (63) causing a shortfall of oxygen delivery within the centre of the tumour. This phenomenon has been reported in many solid tumours, noting that the core is very hypoxic and sometimes necrotic compared to the rim and invasive edge of tumours which are relatively normoxic (64), depicted in figure 1. The lack of oxygen within the tumour often affects treatment as hypoxia contributes to chemoresistance (65) and radio-resistance (66). The depletion of oxygen initiates a change in gene expression due to the induction and stabilisation of Hypoxia-Inducible Factors (HIFs) and other transcription factors (67). HIF-1 is a heterodimer comprised of 2 subunits (HIF-1α and HIF-1β) which are each active in differing oxygen concentrations (68). In normoxia, HIFs bind to Von Hippel-Lindau (VHL) a tumour suppressor protein, which contains E3 ubiquitin ligase activity (69). Once ubiquitination has occurred, the 26S proteasome degrades HIFs, preventing transcription of hypoxia-inducible genes (60). However, in depleted oxygen levels, HIF-1α is not degraded and accumulation and stabilisation of this subunit and subsequently results in hypoxia-induced transcription after binding to the hypoxia response element (HRE) in the nucleus (70) depicted in figure 2. This particular HIF, HIF-1α, is thought to be more prominent in acute hypoxia (71).

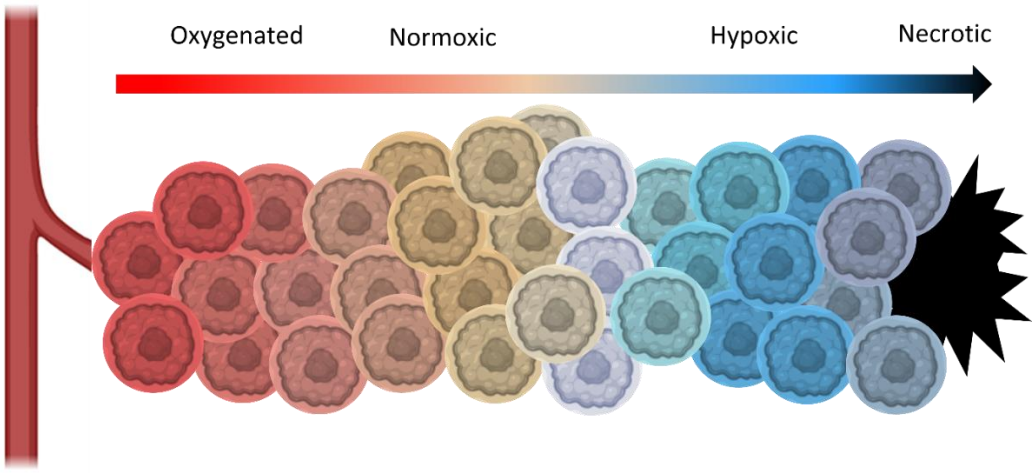

Figure 1. The gradient of hypoxia within a tumour. The cells nearest the blood supply are most oxygenated and a gradient is created until cells before necrotic, usually in the core of the tumour.

1.3.1 HIF-2 induced hypoxia

During chronic hypoxia another HIF is proposed to be more dominant, HIF-2, which is also split into two subunits (α and β) like HIF-1 (72). HIF-2α has been studied in hypoxia, though limited compared to HIF-1 studies, and its expression has been identified as unique to glioma stem cells (73). HIF2α regulates many downstream genes that are involved in tumorigenesis such as *myc* (73), *p-53, m-TOR* and *β-catenin* (74). As Zhao *et al* have studied, HIF-2 is involved and effects many important aspects of malignancy development and formation including altering proliferation and apoptosis, inhibiting DNA damage pathways, mediating the reprogramming of metabolism, regulating signal transduction pathways and mediating chemo- and radio-resistance (74). One of the most well-known genes that is induced by hypoxia is VEGF, which mediates angiogenesis, the formation and growth of blood vessels (75). As HIF-2 is preferentially expressed in chronic hypoxia, it signals for the downstream expression of VEGF (73). In comparison to low grade

tumours, higher levels of VEGF expression are seen in glioblastoma (76)(77) as well as high levels of hypoxia. Furthermore, as hypoxia aids angiogenesis, this microenvironmental factor also induces many other changes within tumours.

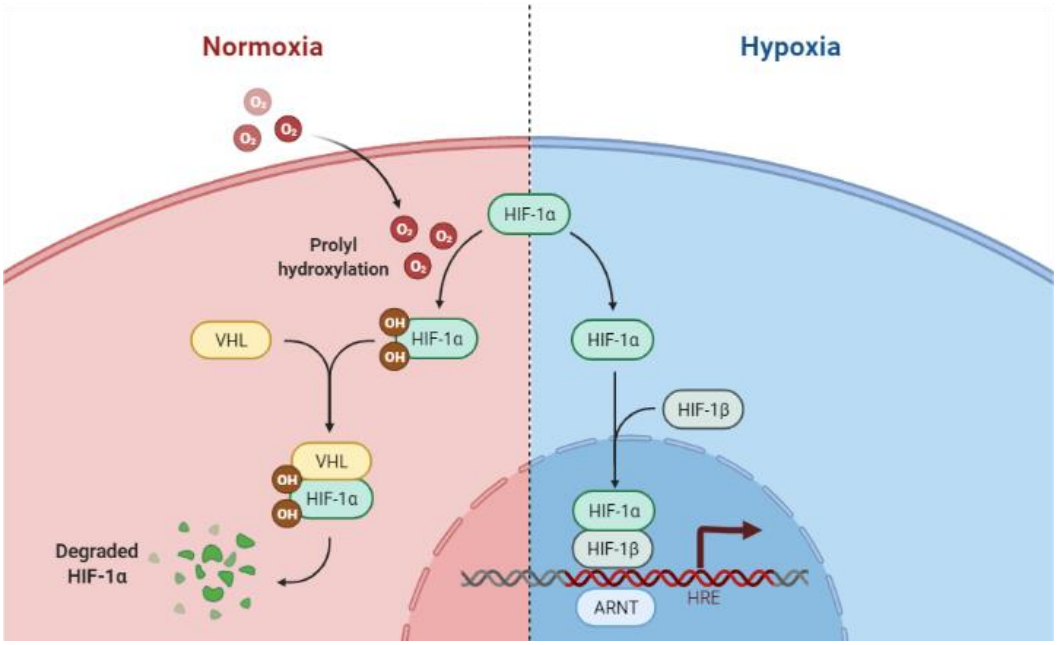

Figure 2. Hypoxia pathway. The schematic shows the molecular pathway of HIFs in normoxic and hypoxic conditions.

1.3.2 Hypoxia detection

Accurately detecting and monitoring oxygen concentrations within the brain and inside brain tumours is understandably difficult. Throughout the years, different technologies have been developed to detect hypoxia as well as to overcome issues such as the invasiveness of the procedure and representative sampling.

1.3.2.1 Fluorescent/phosphorescent and oxygen-sensitive probes

Many variations of probes have been developed including fluorescent/phosphorescent probes and oxygen-sensitive probes. Fluorescent or phosphorescent probes produce fluorescence or phosphorescence respectively, when in the presence of O_2 which occurs by complexes being excited in the ultraviolet (UV) or infrared wavelength ranges (78). Oxygen-sensitive probes were one of the first to be developed, most notably created by Leland Clark who produced an oxygen permeable coating on a platinum electrode which allowed the measurement of partial pressure of oxygen (PO_2) (79) (80). However, due to the large size and invasiveness of the probe, it can disrupt normal oxygen concentrations causing inaccurate the measurements (80). Also the sampling is restricted to a small region which is not representative of the whole tumour/area (80). This has predictably rendered oxygen-sensitive probes to become superseded by newer technologies.

1.3.2.2 Imaging

Imaging has recently become a technology that is widely used to detect hypoxia in tumours, using two different techniques, positron emission tomography (PET) and magnetic resonance imaging (MRI). Corroyer-Dulmont *et al* produced an in-depth review analysing a variety of MRI and PET techniques that measure the oxygen level in differing physiological compartments such as tissue, blood vessels and at a cellular level (81). ^{18}F-MISO is a 2-nitroimidazole compound that is widely used for assessing hypoxia using PET (82). ^{18}F-MISO is a regular procedure for

cancer patients, and is relatively low in radiation dose, approximately 250MBq (83). As well as the low radiation dose, ^{18}F-MISO diffuses easily across the blood-brain barrier, which is ideal for assessing hypoxia in brain tumours, though it is often limited by the low signal to noise ratio (83). There are other radionuclide agents that can be used for PET such as ^{64}Cu-diacetyl-bis(N4-methylthiosemicarbazone) (Cu-ATSM) (84) and 1-(2- [^{18}F] fluoro-1-[hydroxymethyl]ethoxy)methyl-2-nitroimidazole (85). There are also multiple MRI techniques that are used to indirectly give information on tumour hypoxia (83). T_1-weighted oxygen enhanced MRI uses the fact that molecular oxygen dissolves in the blood and tissue plasma distorts the MRI signal by increasing the relaxation rate of the protons (86). Dynamic contrast-enhanced MRI (DCE-MRI) measures blood flow, vascularity and parenchymal contrast (87) using low molecular weight contrast agents (83). Another MRI that is often used is the Blood oxygenation level dependent MRI (BOLD-MRI). BOLD-MRI indirectly measures tumour oxygenation (83) as the paramagnetic effects of deoxygenated haemoglobin is detected (88). Each of the various techniques of MRI imaging used to detect hypoxia has its advantages and limitations. They have each been used in the assessment of hypoxia in gliomas with varying success.

1.3.2.3 Immunohistochemistry

Immunohistochemical (IHC) methods are routinely used in laboratories and are often used to classify the tumour in relation to the staining of hypoxic markers, which can also go on to predict the likelihood of recurrence and prognosis (89). However, IHC methods are limited as the

technique is restricted to a biopsy, whereas ideally samples that are representative of the whole tumour are required (81). Nitroimidazoles and its derivatives can be administered externally, the low oxygen levels bio-reduce the nitroimidazoles bind to cellular macromolecules and are trapped intracellularly (90) (91) (83). Antibodies produced against these markers are then used in IHC techniques (92) (83).

1.3.3 Hypoxia-activated endogenous markers

Hypoxia induces a change in the environment of cells and tumours, which results in a change in both gene and protein expression. There are certain proteins that are indicative of hypoxia such as HIF-1α and HIF-2α and are present in most hypoxic solid tumours. Kolenda *et al* observed that hypoxia increases markers associated with a tumour stem cell-like phenotype such as CD133, podoplanin, BMI-1, nestin and Sox-2 alongside two markers which indicate chemoresistance, TIMP-1 and Lamp-1 in glioblastoma-derived spheroids (93). Other proteins are HIF-induced, and these proteins can be used as markers indicative of the presence of hypoxia.

1.3.3.1 Carbonic Anhydrase 9 (CA9)

CA9 is HIF-1α dependent and is consistently upregulated due to hypoxia (94). CA9 are catalysts involved in the reaction of reversible hydration of carbon dioxide to bicarbonate ($CO_2 + H_2O \leftrightarrow HCO_3^- + H^+$) (95). CA9 results from transcription initiated by HIF-1α binding to the hypoxic response element (HRE) in hypoxic conditions (96). CA9 is required for

pH regulation and cell adhesion (97). This marker has been shown to be upregulated in glioblastoma cells, D247-MG, at both the mRNA and protein level after a 24 hour exposure to 1.5% oxygen (98). CA9 upregulation under hypoxic conditions has been shown in multiple cancers including head and neck carcinoma (99), renal cell carcinoma (100) and cervical cancer (101). CA9 is often used in IHC to determine the hypoxic response within the tumour and, as with hypoxia and HIF-1α, overexpression often correlates with poorer outcomes (102).

1.3.3.2 Glucose Transporter 1 (GLUT-1)

GLUT-1 is also a hypoxia-responsive gene which is used to assess hypoxia and, as with CA9, GLUT-1 expression is associated with a negative impact (102). However, using GLUT-1 in IHC for the detection of hypoxia may not be a suitable marker as studies of GLUT-1 induction in normoxic conditions have been reported (94).

1.4 Micro-RNA (miRNA)

MicroRNAs (miRNAs) are small single-stranded, non-coding sequences that are transcribed from either intronic or exonic DNA sequences (103). Approximately between 18 and 22 nucleotides in length, these miRNAs play a very important role in the regulation of gene expression across numerous biological processes and pathways (104). By binding to the 3' untranslated region (UTR) of mRNA, miRNAs supress gene expression (105) by degradation of mRNA, translational repression or mRNA deadenylation.

1.4.1 miRNA biogenesis

The production of miRNAs has been separated into two pathways: canonical and non-canonical. The main difference between these pathways is the type of miRNA precursor with which the process begins. Non-canonical pathways begins with miRNA precursors such as short hairpin RNA (shRNA), mirtrons which are pre-miRNA from intronic sections of mRNA and 7-methylguanosine-capped pre-miRNA (106). During this study, we will only focus on the canonical pathway, depicted in figure 4, which uses pri-miRNA as its precursor (106), as we can assess all the components of the biogenesis process. This is also because the canonical pathway generates the majority of mammalian miRNAs (107)(108). Firstly, the miRNA is transcribed from DNA by RNA Pol II to produce pri-mRNA (around 1kb in length) (109). This pri-miRNA contains a stem-loop structure which contains the mature miRNA sequences (110). As with general transcription of all genetic material, it is open to regulation by many transcription factors, which may alter the expression of particular miRNAs (110). One enzymatic complex required for canonical biogenesis is the DGCR8/Drosha complex which acts within the nucleus of cells, is known as the microprocessor complex (111). This complex cleaves the pri-mRNA, leaving the loop-structure miRNA of around 65 nucleotides (112)(113). The product (pre-miRNA) is then translocated to the cytoplasm often by exportin protein 5 (EXP5) through the nuclear pore complex (114). The pre-miRNA is then cleaved by DICER, an endonuclease containing two RNA III domains (115). The cleaving by Dicer removes the terminal loop and produces a mature

miRNA duplex (116). The directionality of the mature miRNA depends upon whether it has originated from the 5’ or 3’ end of the pre-miRNA hairpin, which determines the name of miRNA, either 5p or 3p respectively (106). As miRNAs regulate numerous processes, it is unsurprising to note that DICER can also be regulated by miRNAs such as let-7 miRNA (117), which will be discussed in more detail later. This mature miRNA is then loaded onto the miRNA-induced silencing complex (miRISC) containing argonaute (AGO) proteins (118). Once loaded onto the complex, the miRNA is unwound, removing the passenger strand of the miRNA, resulting in the single strand miRNA (119). The active strand is known as the guide strand and many factors are involved in determining which strand becomes the guide strand, including the instability of the 5’ terminus and the first nucleotide, typically uracil (120). The passenger strand after being separated from the guide strand is then degraded (121).

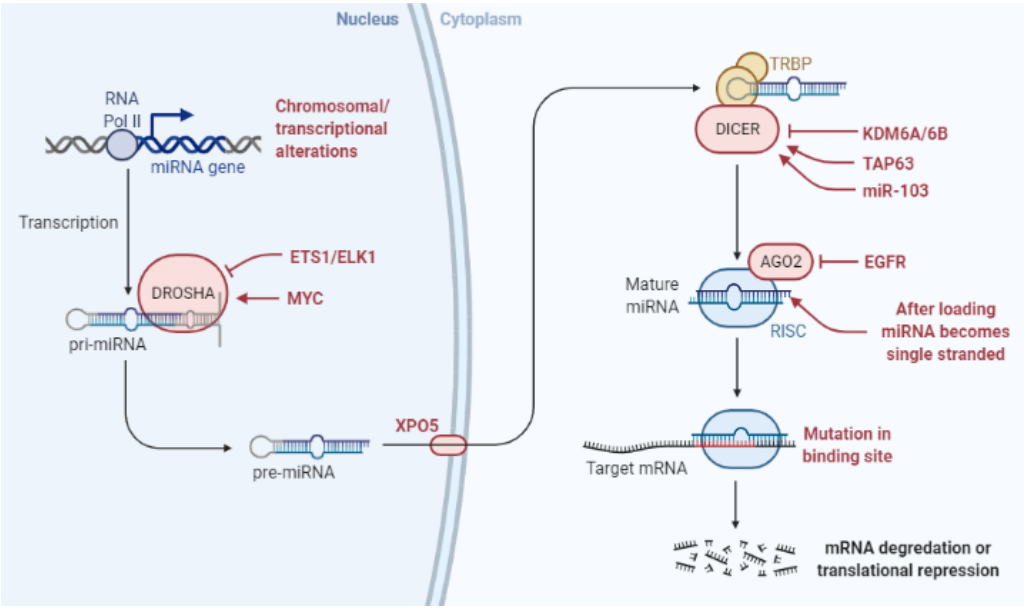

Figure 3. miRNA biogenesis. Schematic depicting miRNA biogenesis starting with its transcription in the nucleus, cleaving by DROSHA and DICER, entering the cytoplasm and being loaded onto the RISC complex.

1.4.2 Functions of miRNA

As mentioned, miRNAs can suppress gene expression by mRNA degradation or translation repression. The target specificity of the miRNA within the miRISC complex depends on the degree of complementarity to the miRNA response elements (MREs) sequences on the target mRNA (122). If the interaction between the miRNA and MREs are fully complementary, this induces AGO2 endonuclease activity and causes cleavage of the mRNA sequence (122). This interaction destabilises the association between AGO proteins and miRNA which initiates its degradation (123). However, many miRNA:MRE interactions are not fully complementary and contain mismatches between the guide miRNA strand which prevents the AGO2 endonuclease activity and instead has a mediator role of RNA interference (106), though the mechanism of translation repression is not fully understood. Proteins of the GW182 family make up the scaffold for the miRISC which then enables the recruitment of other effector proteins such as poly(A)-deadenlyase complexes including PAN2-PAN3 and CCR4-NOT which bind following the miRNA and target mRNA interaction (124). Poly(A)-deadenylation of the target mRNA is initiated by PAN2-PAN3 and completed by CCR4-NOT (106). Following successful deadenylation, decapping occurs by decapping enzyme DCP2, followed by degradation of the mRNA by the cytoplasmic 5’ to 3’ exonuclease XRN1 (125).

Whilst miRNA function largely focuses on gene silencing, there are reports of miRNAs being involved with the upregulation of genes. AGO2

and fragile-x-mental retardation protein 1 (FXR1) are associated with AU-rich elements at the 3' UTR to activate translation (126). Vasudevan and Steitz found multiple miRNAs interact with AGO and FXR1 to activate translation during the cell cycle arrest but inhibit translation within proliferating cells. miR-10a has been found to bind to the 5' UTR region of mRNA that encode for ribosomal proteins and enhance their translation during amino acid starvation (127). As miRNAs are usually associated with the silencing of genes, these reports have shown that under specific conditions, miRNAs can also contribute to the upregulation of genes.

1.4.3 miRNA in cancer

Within malignancies, miRNA are involved in the regulation of many hallmarks of cancer, including tumour progression, cell proliferation, migration and invasion (5)(128). An individual miRNA can interact with multiple mRNA transcripts (129) widening the downstream effects of these small nucleic sequences, thus adding another layer of complexity and interactions within the miRNA regulation. As previously noted, regulation of vital pathways in cancer are often modulated by microRNAs. Particular miRNAs that are involved in proliferative and anti-apoptotic signalling are elevated in cancer such as miR-17-92 cluster, which is located on chromosome 13q31 (130). He *et al* assessed the role of this cluster in Eμ-Myc transgenic mice, a model for B-lymphoma driven by oncogene *myc*. Interrogation of this cluster, noted that one of their functions is to supress cell death, driving an anti-apoptotic phenotype

(131). Other miRNAs are involved in pro-apoptotic signalling and anti-proliferative effects which are similar to tumour suppressor functions, and are often decreased in cancers such as let-7 miRNAs (130). Let-7 has been shown to be expressed in lower levels compared to normal cells in lung cancer, with lower let-7 levels being linked to shorter post-operative survival (132). These are just two of the hundreds of miRNAs that are involved in cancer initiation, development, progression, invasion and migration.

1.4.3.1 miRNAs in glioblastoma

As this research focuses on glioblastoma, it is important to know miRNAs that have already been studied within glioblastomas and their roles. miRNAs are usually denoted as oncogenic miRNAs (oncomiRs), which are upregulated and contribute to a malignant phenotype or tumour suppressor miRNAs that have anti-cancer roles but are often downregulated in cancer to allow for tumorigenesis and progression.

miR-21 is a well-researched oncogenic miRNA in glioblastoma. miR-21 is upregulated in glioblastomas compared to controls and associated with anti-apoptotic factors and increased tumour growth (133). Chan *et al* further showed that inhibition of miR-21 induces the activation of caspases and therefore increases apoptosis and cell death within glioblastomas (134). This miRNA was one of the first to have a role specifically identified within glioblastomas and highlights how important the roles of miRNAs are to tumorigenesis. Another oncogenic miRNA in

glioblastoma is miR-10b-5p whose expression is associated with higher grade gliomas (135). miR-10b is highly expressed in glioma cells but not detected in normal brain cells (136). Gabriely *et al* showed that the inhibition of miR-10b led to a decrease of glioma cell growth and an increase in cell cycle arrest and that autophagy and apoptosis are induced as a result of miR-10b inhibition. The upregulation of these miRNAs, silences genes which are involved in anti-cancer pathways such as apoptosis and shows the importance of their involvement in glioblastoma development.

In contrast there are also a multitude of different miRNAs which have been reported to be downregulated in glioblastoma which are described as tumour suppressor miRNAs. miR-181b-5p is downregulated in glioblastoma tissues compared with normal brain tissues and its overexpression has been shown to sensitise glioblastoma cells to temozolomide and subsequently induces apoptosis (137). EGFR was determined as a target of miR-181b-5p and inhibits EGFR expression, which itself is overexpressed in GBM and promotes glioma cell proliferation and invasion (137). Interestingly Chen *et al* found that overexpression of EGFR reversed the chemosensitivity to TMZ which miR-181b-5p induces. Similarly, another group looked at the chemosensitivity of miR-181b-5p but examined a different target gene, Bcl-2. Bcl-2 is an anti-apoptotic factor, whose expression decreases with increased expression of miR-181b-5p, and is further lowered with the combined therapy of miR-181b-5p overexpression and TMZ (138). These

studies show that increasing the level of miR-181b-5p in glioblastoma, increases glioma sensitivity to temozolomide and enhances TMZ-induced apoptosis. Another miRNA is miR-34a which is also downregulated in glioblastomas compared to normal brain and has tumour suppressive functions such as blocking cell proliferation, promoting cell cycle arrest and enhancing apoptosis (139). PD-L1, a ligand of PD-1, is a target of miR-34a and PD-L1 overexpression is associated with increased paclitaxel resistance in glioma cells (140). PD-L1 expression negatively correlates with miR-34a expression, and Wang and Wang showed that increased miR-34a expression, with miR-34a mimics, attenuates the chemoresistance effect of PD-L1 and exerts anti-tumour effects (140). This shows the anti-cancer effects some miRNAs have on glioblastomas and are lowly expressed in order to promote tumorigenesis. Increasing the levels of these tumour suppressive miRNAs can potentially enhance efforts to combat glioblastoma.

These examples are just four out of hundreds of miRNAs that are important for regulating pathways and gene expression vital for glioblastoma development. Understanding and highlighting these miRNAs allows for a deeper insight into the many molecular pathways of glioblastomas and the potential to exploit them to develop novel therapies or to enhance existing ones, such as increasing chemosensitivity.

1.4.4 miRNAs in hypoxia

Similarly to miRNAs in glioblastoma, miRNAs can also be associated with microenvironmental conditions such as hypoxia. miR-210 is a widely researched miRNA which is upregulated in hypoxia and known as a hypoxamiR. miR-210 expression is regulated by HIFs and HIF-1α directly binds to the HRE directly proximal to the miR-210 promoter (141). The HRE is located 40bp upstream of the transcriptional target site which suggests that this HRE element is responsible for the hypoxic induction of the miR-210 transcript known as, AK123483 located on chromosome 11p5.5, and coordinates expression of downstream target genes (142). This specific HRE has been shown to be conserved highlighting the importance of miR-210 regulation by hypoxia across species (142). The increased expression of miR-210 by hypoxia has been shown to also increase the stabilisation of HIF-1α itself, which creates a positive feedback loop (143). miR-210 has gene targets which have an impact on many molecular and biological processes, of which hypoxia induction influences their expression. Elevated miR-210 in hypoxic conditions downregulates downstream target, Max's Next Tango (MNT) a transcription factor, which in normoxic conditions competes with c-MYC for Max to regulate cell cycle entry and progression (144). The downregulation of MNT allows c-MYC to push cells through the cell cycle, showing that miR-210 indirectly affects c-MYC and promotes cell cycle progression (144). Increased miR-210 has also been associated with disruption of DNA repair and increased genomic instability. Members of the homology-dependent repair (HDR) DNA repair pathway such as

RAD51, RAD52, BRCA1 and BRCA2 are downregulated in hypoxia (145). RAD52 and BRCA2 have similar roles in HDR which involves recruiting RAD51 to the break sites in order to repair the DNA along with Replication Protein A (RPA); RAD52 is commonly involved in the process in BRCA2 deficient cells (146). miR-210 directly binds to the 3' UTR of RAD52 which degrades the protein and is therefore unable to participate in DNA repair (144). In hypoxia more DNA double strand breaks were reported along with lower levels of RAD52 and increased miR-210 compared to normoxic cells (147). miR-210 is also involved in the evasion of apoptosis by downregulating many components including apoptosis-inducing factor mitochondrion-associated 3 (AIFM3) which localises to the mitochondria and mediates the release of cytochrome-c to the cytosol within caspase-dependent apoptosis (148). Downregulation of AIFM3 prevents the release of cytochrome-c and results in inhibition of caspase-dependent apoptosis (147). Another pro-cancer pathway that elevated miR-210 promotes is angiogenesis. Increased miR-210 levels affect mitochondrial metabolism which switches oxidative phosphorylation to lactic acid fermentation that causes an increase in GLUT-1, a hypoxic biomarker (144). GLUT-1 upregulation causes the upregulation of Vascular Endothelial Growth Factor (VEGF) and Platelet-Derived Growth Factor (PDGF) which primes the extracellular environment for angiogenesis (149). miR-210 highlights the broad effects that just one individual miRNA can have on multiple gene targets as a result of the influence of hypoxia and its importance in promoting and sustaining tumorigenesis.

1.4.5 miRNAs as therapeutics

miRNAs have been identified as important components within many biological pathways and molecular networks which are able to regulate gene expression. One way these miRNAs can assist in the clinical environment is as non-invasive prognostic predictors and biomarkers. Multiple studies and research groups have identified many miRNAs which are indicative of prognosis or survival of cancers, including gliomas such as the upregulation miR-21 associated with poor prognosis and overall survival, along with the downregulation of miR-7 which corresponds to more invasive subtypes and poorer post-treatment outcomes (150). An advantage of using miRNAs as biomarkers is the lack of invasive procedures such as biopsies as miRNAs can be obtained through blood and cerebrospinal fluid, however reproducibility of results is a major issue in using miRNAs as biomarkers (150). Many components of processing such as using different bio-fluids, non-standardised internal controls and different detection methods such as qPCR, sequencing and microarrays causes differences in results between laboratories (150). miRNAs are unstable sequences, which poses a difficulty when considering their use as a biomarker. miRNA expression alters in different tissues, in order to obtain accurate expression readings miRNA will have to be extracted from the cell type required which may be inaccessible. Another challenge of using miRNAs as biomarkers is that the change in miRNAs expression levels may not be specific to a particular disease state such as glioblastoma (150). This particular issue

is combated by increasing research and solidifying the results of previous groups to link a particular miRNA with that disease state. Due to this, there is currently no miRNA that is used specifically in the clinic as gold standard prognostic markers for glioblastoma and gliomas. However, further research and testing will need to continue before the use of miRNAs as biomarkers for glioblastoma is possible.

miRNAs also have the potential to be modulators of efficacy of chemo and radiotherapy. As discussed, multiple miRNAs have been associated with sensitising or inferring resistance of glioma cells to chemotherapy such as miR-21 and TMZ (151). Silencing miR-21 can enhance the cytotoxic effect of a range of chemotherapeutic agents such as TMZ, paclitaxel, sunitinib and doxorubicin (151). Conversely, miRNAs such as miR-370-3p, can have the opposite effect as enhancing their expression can restore chemosensitivity towards TMZ by targeting MGMT expression (152). In GBM cell lines, miR-199a-5p was found to be downregulated, but when miR-199a-5p levels were up-regulated by the overexpression of bone morphogenetic protein 2 (BMP2), an inhibition of cell viability and enhanced cytotoxicity of TMZ was observed (153). Another miRNA whose expression is downregulated in GBM cells and upregulation enhances TMZ sensitivity is miR-128-3p. In both *in vitro* and *in vivo* experiments, overexpression of miR-218-3p was associated with the suppression of proliferation, invasion and migration of GBM cells which subsequently enhanced the chemosensitivity of GBM cells to TMZ (154). The mechanism by which it was discovered that miR-218 causes

these effects, was by inhibition of pro-EMT proteins including PDGFRα, Notch1 and Slug as well as directly targeting c-Met to inhibit cell viability (154). The method of using miRNAs as a therapy alongside chemotherapeutics of radiotherapy to enhance the effectiveness of treatment has not yet been brought into the clinic. Further studies need to be performed to analyse the safety of the combinatorial approach and which individual miRNAs enhance specific chemotherapeutic agents to achieve the most efficacious and safe result.

Nanoparticle delivery systems have the potential to be used as vehicles in order to enhance transfection efficiencies of miRNA and also control drug release in GBM (151). miRNAs can be delivered in nanoparticles into solid cancers to promote anti-cancer effects, of which there have been many pre-clinical and *in vivo* studies. In 2016, Shatsberg *et al* were successful in delivering tumour suppressor miRNA, miR-34a, in a polymeric nanogel to combat GBM in mouse models (155). Similarly, miR-34a loaded CXCR4 receptor-stimulated lipoprotein-like nanoparticle (SLNP), reduced the expression of Y-box 2 and Notch which inhibited stemness and chemoresistance and prolonged the survival glioma-initiating cell (GIC) bearing mice (156). A cationic carrier system, dendritic polyglycerol amine (dNG-NH_2) carrying miR-34a is stable in plasma and in a human GBM mouse model, able to cross the blood brain barrier whilst having anti-tumour effects such as inhibiting tumour growth. (157).

However, miRNAs are not clinically approved as current therapies to combat gliomas and glioblastomas. This is because using miRNA as a therapeutic poses many issues. Consequences of off-target effects must be evaluated before pursuing miRNA further. As miRNAs are able to target multiple genes, it is important to ensure that miRNA therapy is specifically targeting the desired genes and pathways and to ensure that no off-target cytotoxicity occurs from delivering miRNA as a therapeutic. Another difficulty of miRNAs is the low stability and short half-life, which has been reported *in vivo* due to the degradation by ribonucleases (158). However chemical modifications can increase miRNA stability and protect from RNases by modifying the 2' position of the ribose sugar backbone (43). Efficient delivery of the miRNA across the blood brain barrier (BBB) is another challenge faced by miRNA therapeutics. The BBB is made up of a vast number of cells such as astrocytes, endothelial cells , microglia, pericytes and a large amount of structural proteins of the basement membrane which include collagen, laminin, occludin, cytoplasmic proteins and junction adhesion molecule-1 to form tight barrier to protect the brain and to prevent entry from circulating molecules, specifically hydrophilic agents (159). Hydrophilic solutes require energy-dependent passage through glucose transporters, which has been exploited for passage into the brain. Glucose-RGD (Glu-RGD) a synthetic ligand has been favoured to selectively target and accumulate liposomes containing paclitaxel (PTX) in glioma cells which has been more effective than the pure drug alone (160). However, during tumorigenesis, overexpression of the multi-drug transporter P-

glycoprotein at the brain capillary is responsible for the expulsion of drugs and exogenous molecules which results in a reduced rate of bioavailability within the brain (159). Although many more miRNA therapies are being tested *in vivo*, it is important to note that these studies do not necessarily accurately reflect the response of GBM in a human patient. *In vivo* studies are established by using subcutaneous or intracranial injection of GBM cells, requiring miRNA-therapy to be pre-administered *ex vivo* or injected into the GBM xenografts which is not representative of how GBMs would be treated in human patients (161). Furthermore, many of the mouse models use immunodeficient mice that may limit the understanding of immunogenicity towards miRNA-therapies (43). Potential resistance to miRNA therapies may occur and become a possible drawback to this therapeutic approach. However, this is likely to be overcome by targeting whole miRNA families or using a combination of miRNAs to reduce the possibility of resistance (43).

All of these issues need to be overcome before an efficient, effective and safe miRNA therapy is developed to combat glioblastoma. However, pre-clinical studies show just how important miRNAs are within glioblastoma tumorigenesis and that refinement of using miRNA as a therapeutic, needs to continue.

1.5 Hypotheses and aims

This thesis focuses on the three main components discussed in this section: gliomas, miRNAs and hypoxia. This study hopes to use

screening techniques to identify individual and significant miRNAs which are up or down regulated in hypoxia compared to normoxia in gliomas. Furthermore, to follow on from selecting possible targets, in-depth studies will follow their expression and the effects on downstream gene targets as well as their function within hypoxia. This project aims to highlight the importance of particular miRNAs within hypoxia, an important microenvironmental factor in gliomas, especially GBM. This will facilitate the potential to highlight novel targets that can be exploited to help combat GBM as well as to further our understanding of the complex intricacies of gene regulation within these particular brain tumours.

For this study, it is hypothesised that:

1) miRNA expression levels will differ (up or downregulated) in hypoxia compared to normoxic samples.
2) miRNA expression levels will differ between glioma sub-types, including high grade (GBM), low-grade (LGG), paediatrics and commercially available cell lines.
3) Individual miRNAs changing expression in hypoxia compared with normoxia will affect downstream target gene mRNA expression.
4) Changing miRNA expression will affect biological pathways such as apoptosis and senescence in hypoxia compared to normoxia.

2 Chapter 2: Methods

2.1 Cell lines

12 different cell lines were used and divided into four categories: commercial/established, primary GBM, primary low-grade gliomas and paediatric. U87 and T98G of the commercial/established group were obtained from Dr Alan McIntyre at Cancer Biology at the University of Nottingham. GIN 8, GIN28 and GIN 31 were derived from the infiltrative region of the tumour. LGG-11, LGG-19 and LGG-24 were derived from the core of the tumour. The primary paediatric cell line GCE62 was derived from the core of the GBM tumour of a teenage patient. Molecular details of the primary cell lines and patient age and gender are available in tables 2 and 3 respectively. Cell lines U251, SF188, KNS42 are established and paediatric lines that are used within the Children's Brain Tumour Research Centre (CBTRC). Table 4 shows the division of cell lines into categories used throughout this research.

Table 2. Molecular characteristics of primary cell lines.

Cell line	IDH Status	1p19 co-deletion	ATRX Status	MGMT Status
GIN8	Wt	No	-	-
GIN28	Wt	No	Wt	No methylation
GIN31	Wt	No	Wt	No methylation
LGG11	R132H	No	Mutant	-
LGG19	R132H	No	Wt	No methylation
LGG24	R132H	No	Wt	Low methylation
GCE62	Wt	No	Wt	No methylation

Table 3. Age and gender of patient primary cell lines.

Cell line	Gender	Age
GIN8	Female	54
GIN28	Male	71
GIN31	Female	57
LGG11	Female	19
LGG19	Male	33
LGG24	Male	31
GCE62	Male	19

Table 4. Glioma categories of the 12 different cell lines.

Primary GBM		
GIN8	GIN28	GIN31
Low-Grade Gliomas		
LGG11	LGG19	LGG24
Paediatric GBM		
GCE62	SF188	KNS42
Established/Commercial GBM lines		
U87	U251	T98G

2.2 Exposure to Normoxic and Hypoxic Conditions

Each cell line was cultured to give two flasks of ~55% confluency. Once this confluency was reached, one flask was labelled normoxia and kept in the incubator at 37°C at room oxygen % (~21%). The other flask was labelled hypoxia and put into a hypoxic chamber at 37°C and at 1% oxygen. The flasks were put into their respective conditions at the same time and left to incubate for 24 hours.

2.3 Obtaining and Snap Freezing Cell Pellets

Once the cells had been exposed to the allocated condition, the media was removed. The cells were then washed with 5mls of HBSS. The cells were detached from the flask using 3mls of trypsin followed by a 5-minute incubation period at 37°C. The cells and trypsin solution were neutralised with 5mls of media. The whole solution was then transferred into a 50ml Falcon tube and centrifuged at 800rpm (104xg) for 5 minutes. The

supernatant was removed from the cell pellet. The cell pellet was re-suspended in 1ml of media and transferred into a 1.5ml Eppendorf tube. The cell suspension was then micro-centrifuged at 100xg for 5minutes. The supernatant was removed, leaving only the cell pellet. The Eppendorf containing the cell pellet was put into a canister containing liquid nitrogen (-210°C), snap freezing the cell pellet. The cell pellets were then stored at -80°C.

2.4 RNA Extraction of Cell Pellets

The RNA extraction was conducted using the *mir*Vana miRNA Isolation Kit (Ambion). The cell pellets were re-suspended using 300µl of Lysis/Binding Buffer and were mixed via pipetting until the pellet was fully broken up and all visible clumps were dispersed. The 30µl of miRNA Homogenate Additive was added and the lysate was vortexed (WhirliMixer; ThermoFisher Scientific). The vortexed lysate was then left on ice for 10 minutes. Afterwards, 300µl of Acid-Phenol:Chloroform (Ambion) was added to the lysate and vortexed for 1 minute before being centrifuged at 10,000xg for 5 minutes. The centrifuging of the lysate and Acid-Phenol:Chloroform (ThermoFisher Scientific) causes two distinct phases to form. The aqueous upper phase contains nucleic acids and was transferred to a new Eppendorf tube with 375µl of 70% ethanol. The lysate/ethanol mixture was vortexed before being pipetted onto a filter cartridge into a collection tube. The lysate/ethanol mixture was centrifuged at 10,000xg for 1 minute. The flow through was discarded. Then, 700µl of miRNA Wash Solution 1 was added onto the filter

cartridge and centrifuged at 10,000xg for 1 minute and the flow through was discarded. Afterwards, 500µl of miRNA Wash Solution 2/3 was added to the filter cartridge and centrifuged at 10,000xg for 1 minute, then flow through was discarded, this step was repeated. Once the flow through was discarded, the filter cartridge was centrifuged again at 10,000xg for 1 minute to remove any residual fluid. The filter cartridge was then transferred into a new Eppendorf tube. Nuclease-free water was pre-heated to 95°C and 50µl was pipetted onto the filter cartridge and left for 1 minute before centrifuging at 10,000xg for 1 minute. The RNA was stored at -80°C.

Following the results of the Nanodrop regarding the 260/230 ratio, the RNA extraction protocol was optimised for the commercial, primary GBM and paediatric cell lines. The volumes of Lysis/Binding Buffer and Acid-Phenol:Chloroform were increased to 400µl, 70% ethanol to 500µl and miRNA Homogenate Additive to 40µl to increase the size of the upper aqueous phase. The wash step using the Wash Solution 2/3 was repeated for a third time. The elution of the nuclease-free water was split into 2 separate elutions, the first one of 25µl and the second of 50µl.

2.5 miRNA Microarray

The quantification of the RNA was determined using Qubit 4 Fluorometer (ThermoFisher) using the broad range RNA kit. The RNA integrity number (RIN) was analysed using TapeStation and all of the RNA samples fell between the values of 8 and 10, indicating that the RNA was

intact. Once the RNA was quantified, it was diluted to a concentration of 33ng/µl before being sent to Nanostring, Seattle for nCounter miRNA expression panel microarray. To begin the process the miRNA underwent a miRNA-tag ligation. Once the ligation is complete, the ligation reaction is diluted 1:10 and 5µl of the miRNA-tag ligation is added to the hybridisations. The panels analysed around 800 miRNAs.

2.6 Raw Data Analysis and Normalization by R-packages

2.6.1 NanoStringNorm

NanoStringNorm is a package available in R which optimises the normalisation of Nanostring nCounter data (162). It allows the use of multiple normalisation methods. For this particular data, following graphical representation, quantile normalisation was the most suitable normalisation method for this data.

2.6.2 NanoStringDiff Package

The package NanoStringDiff is a specific R package which allows the identification of differentially expressed miRNAs/genes from nCounter microarray data using a generalised linear model of the negative binomial family which allows for a multi-factor design (163). This package incorporates functions to allow the pre-processing to be performed which includes the normalisation and log transformation. The likelihood ratio is a test to determine differentially expressed miRNAs within the comparisons between hypoxic status or GBM category selected.

2.6.3 Quality control

The impact of different normalization algorithms including ligation normalisation and background correction on reducing the variability across the samples were checked by plotting the Log2 expression and analysing the distribution of Log2 expression values across samples with ggplot2 R-package (Wickham H (2016). ggplot2: Elegant Graphics for Data Analysis. Springer-Verlag New York. ISBN 978-3-319-24277-4).

2.6.4 Principal component analysis

After determining the optimal normalisation method, a dimension reduction analysis in the form of principal component analysis (PCA) was performed to analyse the differences between the samples by using The R Stats Package (R Core Team (2012). R: A language and environment for statistical computing. R Foundation for Statistical Computing, Vienna, Austria. ISBN 3-900051-07-0, URL http://www.R-project.org/).

2.7 cDNA Synthesis and qPCR

2.7.1 LNA miRCURY Reverse Transcriptase (RT)

Using the extracted RNA, each sample was diluted to 5ng/µl. The reverse transcription reactions were prepared on ice following Table 5 using RT kit (Qiagen cat no. 339340).

Table 5. Reverse transcription reactions

Component	Volume for x1 reaction (µl)
5x miRCURY SYBR Green RT Reaction Buffer	2
RNase-free water	5
10x miRCURY RT Enzyme Mix	1
Template RNA (5ng/ul)	2
Total reaction volume	10

Once the reactions were prepared, they were incubated at 42°C for 60 minutes, followed by 95°C for 5 minutes and held for 4°C. The cDNA can be stored at 2-4°C for up to 4 days or at -30 to -15°C for up to 5 weeks.

2.7.2 LNA miRCURY Custom qPCR Panel Protocol

The cDNA was diluted 1:80. For a 384 well-plate and a custom PCR panel (Qiagen, cat no. 339330) configuration of 4 x 96 (4 samples per plate). The miRNA probe layout on the custom panels is shown in figure 4. The cDNA dilution + nuclease-free water is 5µl cDNA and 395µl of nuclease-free water for each sample. The reaction mixes were then are prepared as stated in table 6 using the miRCURY SYBR Green PCR kit (Qiagen, cat no. 339346).

Table 6. Reaction setup for miRCURY LNA Custom PCR Panel

Component	Volume per reaction (µl)
2x miRUCRY SYBR Green Master Mix	5
cDNA template (diluted 1:80)	4
RNAse-free water	1
Total reaction volume	10

The reaction mix was vortexed thoroughly and 10µl of the reaction mix were dispensed into each well per PCR panel plate. The plate was sealed and centrifuged at room temperature and left for 5 minutes to allow the primers to dissolve in the reaction mix. The plates were loaded onto the BioRad cfx384 qPCR machine and followed the program stated in table 7. The initial data analysis was performed using the software, Geneglobe Analysis.

Table 7. LNA miRCURY Custom PCR Panel PCR Cycling Conditions

Step	Time	Temperature
PCR initial heat activation	2 minutes	95°C
2-step cycling		
Denaturation	10 seconds	95°C
Combined annealing/extension	60 seconds	56°C
Number of cycles	40	
Melting curve analysis		60-95°C

2.7.3 cDNA synthesis

A different protocol was used for cDNA synthesis and qPCR when testing for target genes instead of miRNA. The cDNA synthesis kit used was the Applied Biosystems High-Capacity cDNA Reverse Transcription Kit 200 reaction (catalog no. 4368814). The RNA for this protocol came from RNA already extracted from tumour samples. The amount of RNA used was 20ng. A reverse transcription master mix was prepared on ice using the following components (table 8). The amount of master mix made was dependent on the number of samples. A final volume of 10µl of 20ng RNA was added to a fresh PCR tube along with 10µl of the master mix.

Table 8. A table showing the volumes required of the cDNA synthesis kit for one reaction

Component	Volume (µl)
10x RT buffer	2.0
25x dNTP mix (100mM)	0.8
10x Rt Random Primers	2.0
Ultra-Pure Water	4.2
MultiScribe Reverse Transcriptase	1.0
Total volume for 1 reaction	10

Once the RNA and master mix solutions were combined, the tubes were loaded onto the thermocycler and followed the following programme. Once the programme was completed (table 9) the samples were diluted 1 in 10 and stored at -20°C.

Table 9. A table showing the temperatures and time of the thermocycler programme for cDNA synthesis.

	Step 1	**Step 2**	**Step 3**	**Step 4**
Temperature °C	25	37	85	4
Time	10 min	120 min	5 min	∞

2.7.4 qPCR

This qPCR protocol is used to detect the expression of genes using the LightCycler 480 SYBR Green 1 Master from Roche. This 2x all in one master mix and contains FastStart Taq DNA polymerase, reaction buffer, dNTP mix, SYBR green 1 dye and $MgCl_2$. The primers displayed in table 11 are provided at a stock concentration of 100µM. The primers (Sigma-Aldrich, KiCqStart primers) are diluted 1 in 10 with ultra-pure water to result in a working concentration of 10µM. A master mix was made for each primer pair using the following volumes for one reaction shown in table 10. Once the master mixes are prepared, 2µl of the relevant cDNA was pipetted into each well and 18µl of the corresponding master mix was pipetted on top of the cDNA. The plates were sealed with a lid, and centrifuged. The plates were then run on the qPCR machine (BioRad cfx384) with the programmed shown in table 12.

Table 10. qPCR master mix components and volumes.

Component	Volume (µl)
Forward primer (10µM)	1
Reverse primer (10µM)	1
Ultra-pure water	6
2x Master Mix	10
Total reaction volume	18

Table 11. Primer sequences of miRNA downstream targets.

Gene	Forward Primer (5'-3')	Reverse Primer (3'-5')
ACAA	GGGGATAACCTCTGAGAATG	CAATCTCAGCTTGGAAACAG
ACADS	AGTTACACACCATCTACCAG	AGAGATGTTCCTTATCCACC
SUCLG1	ATTGGAATATGGCACCAAAC	GCCTCCTTCACAGTATTAAAG
SRSF1	GCAGGTGATGTATGTTATGC	TCTCCCTCATGAGATCTAAAC
RAN	CAGTACTACGACATTTCTGC	TCTAAGTCGTGCTCATACTG
HNRNPU	AAGTTGTGATGATGATTGGC	TATTTCCCTGGATTTTCTGC
CA9	CTTGGAAGAAATCGCTGAG	TGGAAGTAGCGGCTGAAGT
B-Actin	ATTGGCAATGAGCGGTTC	GGATGCCACAGGACTCCAT

Table 12. qPCR Cycling Conditions

Step	Time	Temperature
PCR initial heat activation	10 minutes	95°C
2-step cycling		
Denaturation	15 seconds	95°C
Combined annealing/extension	60 seconds	60°C
Number of cycles	40	
Melting curve analysis		60-95°C

2.7.5 GeneGlobe Analysis software

The data from the LNA miRCURY custom plates were analysed using the free-web Qiagen software GeneGlobe Analysis which is specifically designed for analysing miRNA miRCURY qPCR results.

2.8 Downstream Bioinformatics analyses

2.8.1 Differential expression analysis and visualization

Differential expression analysis (DEA) was carried by a two-sample student's t-test followed by false discovery rate (FDR) calculations in order to identify the significant difference of miRNA expression between hypoxic and normoxic conditions. The threshold for unadjusted p-value and FDR was set to FDR < 0.05. In case where no significant hits were found by applying FDR threshold, the unadjusted p-value cut-off was set to < 0.01 to increase the stringency of the statistical test. The procedure was performed by using Perseus software tool (REF:

https://www.nature.com/articles/nmeth.3901). The results of the DEA were visualized by using ggplot2 R-package.

2.8.2 Hierarchical clustering

The expression values of the significant miRNAs as identified by DEA were subjected to Hierarchical clustering where Euclidean distance algorithm was employed to cluster the columns (samples) and rows (miRNAs). To achieve this, first the Log2 expression values of the significant miRNAs were scaled by z-scoring method. The z-scored expression values were then clustered and visualised as heatmaps by using the MORPHEUS – an open access matrix visualization and analysis software (https://software.broadinstitute.org/morpheus) from Broad Institute, USA.

2.8.3 Pathway analysis and Visualization

For pathway analysis first, miRNA-gene network analysis was performed by using the web tool - MIENTURNET (Licursi V et al. MIENTURNET: an interactive web tool for microRNA-target enrichment and network-based analysis. BMC Bioinformatics 20, 545 (2019) doi:10.1186/s12859-019-3105-x) to identify the target genes of the differentially regulated miRNAs. After extracting the target genes of the miRNAs, Molecular Signatures Database v7.5.1 (MsigDB) (REF: PMID: 26771021) was used to perform the gene-set enrichment analysis (GSEA). The extracted the hallmark gene sets from MsigDB was then utilized for GSEA. For visualization purpose, the miRNA-gene network and GSEA results were combined

together and visualized using CytoScape tool (REF: PMID: 31477170) which is widely used for networking analysis.

Further pathway enrichment analysis based on the target genes of the differentially expression miRNAs were carried out by the enrichment algorithm as implemented in MIENTURNET. For enrichment analysis, gene-sets for Disease ontology, KEGG, WikiPathways, and RNAs were used.

	1	2	3	4	5	6	7	8	9	10	11	12	13	14	15	16	17	18	19	20	21	22	23	24	
A	miR-21-5p	miR-21-5p	miR-606	miR-606	miR-30e-5p	miR-30e-5p	miR-34a-5p	miR-34a-5p	miR-362-5p	miR-362-5p	miR-7-5p	miR-7-5p	miR-92a-3p	miR-92a-3p	miR-132-3p	miR-132-3p	miR-331-3p	miR-331-3p	miR-152-3p	miR-152-3p	miR-335-5p	miR-335-5p	miR-106b-5p	miR-106b-5p	A
B	miR-21-5p	miR-21-5p	miR-606	miR-606	miR-30e-5p	miR-30e-5p	miR-34a-5p	miR-34a-5p	miR-362-5p	miR-362-5p	miR-7-5p	miR-7-5p	miR-92a-3p	miR-92a-3p	miR-132-3p	miR-132-3p	miR-331-3p	miR-331-3p	miR-152-3p	miR-152-3p	miR-335-5p	miR-335-5p	miR-106b-5p	miR-106b-5p	B
C	miR-125b-5p	miR-125b-5p	miR-17-5p	miR-17-5p	miR-495-3p	miR-495-3p	miR-210-3p	miR-210-3p	miR-96-5p	miR-96-5p	miR-92a-3p	miR-92a-3p	miR-451a	miR-451a	miR-222-3p	miR-222-3p	miR-128-3p	miR-128-3p	miR-26b-5p	miR-26b-5p	miR-425-5p	miR-425-5p	miR-216a-5p	miR-216a-5p	C
D	miR-125b-5p	miR-125b-5p	miR-17-5p	miR-17-5p	miR-495-3p	miR-495-3p	miR-210-3p	miR-210-3p	miR-96-5p	miR-96-5p	miR-92a-3p	miR-92a-3p	miR-451a	miR-451a	miR-222-3p	miR-222-3p	miR-128-3p	miR-128-3p	miR-26b-5p	miR-26b-5p	miR-425-5p	miR-425-5p	miR-216a-5p	miR-216a-5p	D
E	miR-29b-3p	miR-29b-3p	miR-146a-5p	miR-146a-5p	miR-149-5p	miR-149-5p	miR-199a-3p	miR-199a-3p	miR-487b-3p	miR-487b-3p	miR-130a=3p	miR-130a=3p	miR-210-3p	miR-210-3p	miR-155-5p	miR-155-5p	miR-185-5p	miR-185-5p	miR-296-5p	miR-296-5p	miR-100-5p	miR-100-5p	miR-16-5p	miR-16-5p	E
F	miR-29b-3p	miR-29b-3p	miR-146a-5p	miR-146a-5p	miR-149-5p	miR-149-5p	miR-199a-3p	miR-199a-3p	miR-487b-3p	miR-487b-3p	miR-130a=3p	miR-130a=3p	miR-210-3p	miR-210-3p	miR-155-5p	miR-155-5p	miR-185-5p	miR-185-5p	miR-296-5p	miR-296-5p	miR-100-5p	miR-100-5p	miR-16-5p	miR-16-5p	F
G	miR-31-5p	miR-31-5p	miR-142-5p	miR-142-5p	miR-27a-3p	miR-27a-3p	miR-31-5p	miR-31-5p	miR-148b-3p	miR-148b-3p	miR-107	miR-107	miR-199a-5p	miR-199a-5p	miR-26a-5p	miR-26a-5p	miR-382-5p	miR-382-5p	miR-181a-5p	miR-181a-5p	miR-205-5p	miR-205-5p	miR-9-5p	miR-9-5p	G
H	miR-31-5p	miR-31-5p	miR-142-5p	miR-142-5p	miR-27a-3p	miR-27a-3p	miR-31-5p	miR-31-5p	miR-148b-3p	miR-148b-3p	miR-107	miR-107	miR-199a-5p	miR-199a-5p	miR-26a-5p	miR-26a-5p	miR-382-5p	miR-382-5p	miR-181a-5p	miR-181a-5p	miR-205-5p	miR-205-5p	miR-9-5p	miR-9-5p	H
I	miR-374b-5p	miR-374b-5p	miR-376c-5p	miR-376c-5p	miR-19a-3p	miR-19a-3p	miR-148a-3p	miR-148a-3p	miR-93-5p	miR-93-5p	miR-191-5p	miR-191-5p	miR-151a-5p	miR-151a-5p	miR-106a-5p	miR-106a-5p	miR-24-3p	miR-24-3p	miR-27b-3p	miR-27b-3p	miR-10a-5p	miR-10a-5p	miR-186-5p	miR-186-5p	I
J	miR-374b-5p	miR-374b-5p	miR-376c-5p	miR-376c-5p	miR-19a-3p	miR-19a-3p	miR-148a-3p	miR-148a-3p	miR-93-5p	miR-93-5p	miR-191-5p	miR-191-5p	miR-151a-5p	miR-151a-5p	miR-106a-5p	miR-106a-5p	miR-24-3p	miR-24-3p	miR-27b-3p	miR-27b-3p	miR-10a-5p	miR-10a-5p	miR-186-5p	miR-186-5p	J
K	miR-181b-5p	miR-181b-5p	miR-23b-5p	miR-23b-5p	miR-29a-3p	miR-29a-3p	miR-628-5p	miR-628-5p	miR-23a-5p	miR-23a-5p	miR-20a-5p	miR-20a-5p	miR-488-3p	miR-488-3p	miR-99b-5p	miR-99b-5p	miR-137	miR-137	miR-30d-5p	miR-30d-5p	miR-141-3p	miR-141-3p	miR-324-5p	miR-324-5p	K
L	miR-181b-5p	miR-181b-5p	miR-23b-5p	miR-23b-5p	miR-29a-3p	miR-29a-3p	miR-628-5p	miR-628-5p	miR-23a-5p	miR-23a-5p	miR-20a-5p	miR-20a-5p	miR-488-3p	miR-488-3p	miR-99b-5p	miR-99b-5p	miR-137	miR-137	miR-30d-5p	miR-30d-5p	miR-141-3p	miR-141-3p	miR-324-5p	miR-324-5p	L
M	miR-4454	miR-4454	miR-365a-3p	miR-365a-3p	miR-379-5p	miR-379-5p	miR-181c-5p	miR-181c-5p	miR-221-3p	miR-221-3p	miR-335-5p	miR-335-5p	miR-99a-5p	miR-99a-5p	miR-29c-3p	miR-29c-3p	miR-140-5p	miR-140-5p	miR-184	miR-184	miR-145-5p	miR-145-5p	miR-15b-5p	miR-15b-5p	M
N	miR-4454	miR-4454	miR-365a-3p	miR-365a-3p	miR-379-5p	miR-379-5p	miR-181c-5p	miR-181c-5p	miR-221-3p	miR-221-3p	miR-335-5p	miR-335-5p	miR-99a-5p	miR-99a-5p	miR-29c-3p	miR-29c-3p	miR-140-5p	miR-140-5p	miR-184	miR-184	miR-145-5p	miR-145-5p	miR-15b-5p	miR-15b-5p	N
O	Let=7b-5p	Let=7b-5p	miR-218-5p	miR-218-5p	miR-98-5p	miR-98-5p	miR-421	miR-421	miR-154-5p	miR-154-5p	miR-25-5p	miR-25-5p	UniSp3	UniSp3	UniSp6	UniSp6	Cel-39-3p	Cel-39-3p							O
P	Let=7b-5p	Let=7b-5p	miR-218-5p	miR-218-5p	miR-98-5p	miR-98-5p	miR-421	miR-421	miR-154-5p	miR-154-5p	miR-25-5p	miR-25-5p	UniSp3	UniSp3	UniSp6	UniSp6	Cel-39-3p	Cel-39-3p							P
	1	2	3	4	5	6	7	8	9	10	11	12	13	14	15	16	17	18	19	20	21	22	23	24	

Figure 4. LNA miRCURY custom panel plate layout

2.9 Transfection of glioma with small RNAs

Reverse transfection was decided as the transfection method of choice due to its shorter timeframe and its flexibility to test different concentrations of the small RNA. In this project three different types of small RNA were used: siGlo Green Transfection Indicator Control, miRNA mimcs, miRNA hairpin inhibitors, products described in table 11. siGlo Green is a fluorescent oligonucleotide complex that localises to the nucleus and acts as a transfection indicator. The translocation of siGlo Green to the nucleus, was detected using a fluorescent microscope at a wavelength between 488 and 507, is indicative of efficient uptake of small RNA into the nucleus of the cells of interest. DharmaFECT 1 transfection reagent (Horizon Discovery, T-2001-02), is a lipid-based transfection reagent that is designed for effective transfection of small RNAs with low cytotoxicity. The optimisation of the volumes of DharmaFECT and number of cells to use in this transfection protocol was determined by Huda Alfardus (43). miRNA mimics are used to overexpress miRNAs, as they are double-stranded RNAs chemically enhanced to preferentially load RISC (RNA-induced silencing complex). miRNA hairpin inhibitors knock down levels of miRNAs. These are single-strand RNAs which are designed to bind and to sequester the complimentary the mature miRNA strand. Universal non-targeting mimic/inhibitor negative controls are modified mature sequences based on Cel-miR-67, which has minimal sequence similarity with miRNAs targets in human. The non-targeting mimic/inhibitor controls were used to distinguish mimicry/inhibitory effect from background effect.

Table 13. miRIDIAN miRNA product information.

miRNA	Product type	Product code (Horizon Discovery)	miRNA sequence
Cel-miR-67	miRNA mimic negative control	CN-001000-01-05	UCACAACCUCCUAGAAAGAGUAGA
	miRNA inhibitor negative control	IN-001005-01-05	UCACAACCUCCUAGAAAGAGUAGA
Hsa-miR-92a-3p	miRNA mimic	C-300511-07-0010	UAUUGCACUUGUCCCGGCCUGU
	miRNA inhibitor	IH-300510-06-0050	UAUUGCACUUGUCCCGGCCUGU
Hsa-miR-149-5p	miRNA mimic	C-300631-07-0050	UCUGGCUCCGUGUCUUCACUCCC
	miRNA inhibitor	IH-300631-08-0050	UCUGGCUCCGUGUCUUCACUCCC

2.9.1 Transfection protocol

The transfection protocol was performed in a 6-well plate. The 5x siRNA buffer (Horizon Discovery, B-002000-UB-100) is diluted to 1x siRNA buffer. This 1x siRNA buffer is used to dilute each miRNA products to 5µM. The miRNA mimics/inhibitors and controls were diluted in serum-

free media for a final concentration of 25nM (tube 1). In parallel, serum-free media was added to the transfection reagent, Dharmafect and incubated for 5 minutes at room temperature (tube 2). Once tube 1 and tube 2 were made, they were combined at a ratio of 1:1 (tube 3) and incubated at room temperature for 20 minutes, which allows the encapsulation of the small RNAs by the transfection reagent. 400µl of tube 3 were dispensed into each well of a 6-well plate. Pre-warmed (37°C) culture medium containing 3.125×10^4 cells/ml were added on top of the transfection solution in each well, as displayed in table 12. The cells were then incubated at 37°C in 5% CO_2 humidified atmosphere for 24 hours. The transfection media was replaced with fresh cell culture media after 24 hours and continued to incubate for a further 72 hours.

Table 14. Transfection mixture steps and volumes.

	Contents of tubes	**1 Well of a 6-well plate (µl)**
Tube 1	miRNA mimic/ inhibitor/ negative control	10
	Serum-free media	190
Tube 2	DharamFECT	2
	Serum-free media	198
Tube 3	Tube 1	200
	Tube 2	200
Tube 4	Cells in serum-supplemented culture media	1,600
	Total volume of transfection media	2,000

2.10 Caspase-glo assay

Once the transfections were set up as described in the previous section but scaled down using a 96-well black-walled optical bottom plates (ThermoFisher) which one of the plates exposed to hypoxia in the hypoxic chamber. The cells were ready for the apoptotic caspase-glo 3/7 assay (Promega). The caspase-glo 3/7 buffer and lyophilised caspase-glo 3/7 substrate thawed and reach room temperature before mixing

together in a 1:1 ratio into the substrate amber glass bottle. The plates of cells are removed from the incubator to reach room temperature. 100µl of the caspase glo solution was added to each well, including media only serving as a blank. The plate was incubated for 30 minutes at room temperature and shook at 500rpm for 30 seconds before the luminescence being read on the plate reader.

2.11 Senescence β-galactosidase cell staining assay (cell signalling)

2.11.1 Solution preparation

The 10x fixative solution was diluted to 1x with distilled water. The 10x staining solution was agitated and heated to 37°C to redissolve and then diluted to 1x with distilled water. 20mg of X-Gal was dissolved into 1ml of DMSO to prepare a solution of 20mg/ml. The components in the table 13 make up the β-galactosidase staining solution. Once the solution was made, the pH was measured and adjusted accordingly to be within the range of 5.9 – 6.1.

Table 15. Components and volumes for B-galactosidase staining solution.

Component	Volume for a single well of a 6-well plate (µl)
1x Staining solution	930
100x solution A	10
100x solution B	10
20mg/ml X-Gal	50

2.11.2 Senescence assay protocol

The media was removed from cultured cells in 6-well plates and rinsed with PBS. 1ml of 1x fixative solution was added to each well and allowed to fix for 10 minutes at room temperature. The wells were rinsed again twice with PBS. 1ml of the β-galactosidase staining solution was added to each well and the plates were sealed with parafilm to prevent evaporation, as this can cause crystallisation of the stain. The plates were incubated overnight at 37°C in a dry incubator (without CO_2), as carbon dioxide can alter the pH which can affect the staining results. For long term storage of the plates, remove the β-galactosidase staining solution and overlay with 70% glycerol and store at 4°C.

2.12 Western Blot

2.12.1 Protein Extraction

Corning 10mm^3 plates were seeded with 0.5 million cells. These plates were left in the incubator for 6 hours before moving the hypoxia condition plates into the hypoxic chamber at 1% oxygen for 24 hours. 5µl of 10% sodium dodecyl sulfate (SDS) and 10µl of 10mM of dithiothreitol (DTT) were added to 1ml of urea lysis buffer. The plates were removed from the incubator/hypoxic chamber and placed on ice. The media was removed from the plates and the cells washed with PBS. The PBS was removed from the plates and 200µl of lysis buffer was added to each plate and left for 5 minutes on ice. A cell scraper was used in a circular motion for 5 minutes to ensure maximum extraction of the cells. The cell lysate was

pipetted into labelled Eppendorf tubes kept on ice. The lysates were sonicated for 10 cycles of 30 seconds on and 30 seconds off. Once complete, the lysates were kept on ice for 15 minutes. The lysates were centrifuged at 4°C, at max speed 13.2 for 10 minutes. The lysates were stored at -80°C in the freezer.

2.12.2 Bradford Assay

A stock solution of 50mg/ml bovine serum albumin (BSA) was created by dissolving 0.5g BSA powder in 10ml distilled H_2O. Serial dilutions were performed to create standards of the following concentrations (µg/ml); 4000, 2000, 1000, 500, 250, 125, 62.5, 31.25, 15.625, 7.8125, 3.90625 and 0. The lysates were thawed on ice and diluted 1 in 15 with ultra-pure water. 10µl of standards and sample were added to separate wells. The BioRad dye was diluted 1 in 5 with distilled H_2O and 200µl of dye was added to each well. The plate is read using a spectrophotometer at 620nm wavelength. The results are used to calculate the amount of sample required to load the gel.

2.12.3 Preparing the gel

The website www.cytographica.com/lab/acryl2.html was used to calculate the volumes of each component for the gel. When analysing HIF proteins, the resolving gel was 8% and the stacking gel was 4% with a thickness of 1ml, using 40% acrylamide. The components for the resolving gel are as follows; ddH_2O, 40% acrylamide, 1.5M Tris pH 8.8, 10% SDS, 10% ammonium persulfate (APS),

tetramethylethylenediamine (TEMED). The components for the stacking gel are as follows; ddH_2O, 40% acrylamide, 0.5M Tris pH 6.8, 10% SDS, 10% APS and TEMED. Once setting up the glass plates and clamp, the resolving gel is poured in. On top 1ml of isopropanol is pipetted on top of the gel to remove any bubbles and to even the surface. Once set, the isopropanol is removed and rinsed twice with distilled water. The stacking gel is then poured on top, the appropriate comb inserted and left to set. The gels are stored at 4°C in running buffer if not used immediately.

2.12.4 Conducting the Western Blot

The Laemmli working solution was made up of 900ul of Laemmli solution and 100ul of 2-mercaptoethanol. The sample solution was made up of 3-parts sample and 1-part Laemmli working solution. The sample solutions were boiled at 95°C for 5 minutes. 3ul of Precision Plus Protein Dual Color Standards (BioRad) ladder (10-250kDa) was loaded on the gel. The samples were then loaded onto the gel (60ug when looking for HIF protein). The gel ran at 80 volts through the stacking gel and then at 120 volts through the resolving gel. A dry transfer is carried out using the TransBlot turbo system (BioRad), turbo transfer buffer, tissue stacks, nitrocellulose membrane, the gel and another tissue stack. The excess liquid is removed and the BioRad high molecular weight programme was selected. The membrane was then moved into a small container or falcon tube and blocked for an hour at room temperature with the appropriate blocking buffer (3% milk in tris buffered saline with 0.1% tween20 (TBS-T) for HIF1a and 5% BSA in TBS-T for HIF2a). The membrane was

incubated at 4C overnight with the appropriate primary antibody in the appropriate buffer (HIF1a 1 in 500, HIF2a 1 in 500, b-actin 1 in 1000). The membrane was washed in TBS-T for 5 minutes, 3 times. The membrane was then incubated for one hour at room temperature with the appropriate secondary antibody (green anti-mouse, 1 in 10,000 for HIF1a and red anti-rabbit, 1 in 10,000 for HIF2a). The membrane can be stored in 1x tris buffered saline (TBS) at 4C. The blots are imaged at 700 and 800nm wavelengths depending on the antibodies used.

2.13 Tissue Sections and Tissue Microarrays (TMAs)

Control sections of duodenum were collected by the histopathology unit in the Queen's Medical Centre, Nottingham UK. Whole sections of GBM tumours were collected from patients by Dr Stuart Smith, Queen's Medical Centre, Nottingham UK. Sections from the three regions: core, rim and invasive edge were obtained from each GBM patient. Adult GBM TMAs were created from cores of the sections of the three regions of each patient. The paediatric TMAs were collected from the Children's Brain Tumour Research Centre, Nottingham UK. Collection of all tissues from patients was obtained prior to surgery in accordance with the Human Tissue Authority (HTA) codes of practice for research.

Table 16. Table defining the number of cores and patients per each TMA.

TMA Name	No. of Cores	No. of Patients
Adult GBM TMA 2	81	9
Adult GBM TMA 3	81	9
Adult GBM TMA 4	81	9

2.14 Immunohistochemistry

2.14.1 Removal of paraffin and hydration

Formalin, the fixative used for fixing tissues, can prevent the binding to antibodies by forming crosslinks with antigens. To deparaffinise the tissue slides, they were kept at 60°C overnight before being placed in xylene (Fisher Chemicals) for 15 minutes. The slides were rehydrated in a series of ethanol concentrations, beginning with 10 minutes in absolute ethanol, followed by 5 minutes in 90% ethanol, 5 minutes in 80% ethanol, 5 minutes in 70% ethanol. The slides were then washed in running tap water.

2.14.2 Antigen Retrieval

The slides were placed at 98°C preheated ethylenediaminetetraacetic acid (EDTA) pH 8.0 for 20 minutes in a steamer for CA9 antibody. For heat-induced epitope retrieval, the slides were immersed in the steamer in the preheated EDTA at 98°C for 40 minutes. The slides using RAN antibody were placed using the sixth sense mode on the microwave which boiled for 10 minutes using sodium citrate at pH 6.0. The slides were put into a glass container with PBS and was agitated for 2 minutes.

The tissues were encircled using a hydrophobic pen (Vector Laboratories) and blocked with 20% normal goat serum (NGS) inside a humidifier chamber (a plastic lidded container, filled with wet blue roll) for 20 minutes at room temperature. The slides were then washed in PBS for 5 minutes before peroxidase blocking solution (Dako) was applied which was then left to incubate for 5 minutes at room temperature inside the humidifier chamber.

2.14.3 Antibody Probing

The tissues were then washed in PBS for 5 minutes and then incubated in the primary antibodies. CA9 mouse monoclonal antibody (Anti-human carbonic anhydrase IX [M75], Absolute Antibody) was diluted 1 in 1000 and left for 2 hours at room temperature inside the humidifier chamber. RAN mouse monoclonal antibody (MA5-38621, Invitrogen) was diluted 1 in 200 and left for 2 hours at room temperature inside the humidifier chamber. After the primary antibody incubation, the tissues were then washed in PBS for 5 minutes followed by 3 drops of secondary antibody (Dako Reagent A) which is left to incubate for 30 minutes at room temperature in the humidifier chamber. The slides are then washed in PBS for 5 minutes.

2.14.4 Antibody Detection and Counterstaining

The antibodies were detected using 3,3′-Diaminobenzidine (DAB) which was diluted 1:50 in DAB buffer solution (Dako). The DAB solution was applied to the slides and left to incubate for 5 minutes before being rinsed

with distilled water. To counter stain, the slides were agitated in Harris Haematoxylin (TCS Bioscientific) for 10 seconds, then washed in running water. The slides were then washed in Lithium Carbonate for 5 seconds until the nuclei were stained then washed in running water. The slides were then dehydrated spending 5 minutes in each concentration of ethanol (70%, 80%, 90% and 100%) and then washed in xylene.

2.14.5 Mounting the slides

The slides were mounted with a coverslip using DPX (Sigma-Aldrich) and placed on a hotplate to dry before viewing under the microscope.

2.15 Immunofluorescence (IF)

Cells were seeded at a density of 10,000 cells per well of the chamber slides (Millicell EZ slides, Merck). The cells were left to adhere overnight, before being exposed to either 1% oxygen in the hypoxic chamber or 21% oxygen in the incubator for 24 hours. For each well, the media was aspirated off, washed with PBS and then removed. 100µl of 4% paraformaldehyde (PFA) was added to each well and left for 15 minutes at room temperature. PBX (PBS with 0.1% triton-X) was made up, and 100µl pipetted into each well and left to permeabilise the cells for 30 minutes at room temperature. The wells were washed with PBS. 100µl of NGS was added per well for blocking and was incubated for an hour inside a humidity box. The blocking solution was removed, and a 1:200 dilution of RAN antibody (MA5-38621, Invitrogen) was diluted in NGS, 100µl applied to each well of the chamber slide and incubated for another

hour inside the humidity box. The wells were washed with PBT (PBS with 0.1% Tween20) three times for 5 minutes. The secondary antibody, Alexa Fluor 488 goat anti-mouse IgG (H + L) (2379467, Invitrogen) was diluted 1 in 100 with NGS and 100µl applied to each well and incubated for 1 hour in the humidity box and protected from the light. The wells were washed again with PBT, three times for 5 minutes. 300nM of DAPI was made up with PBS and 100µl added to each well and incubated for 5 minutes at room temperature protected from the light. The wells were washed twice with PBS, and coverslips mounted and sealed with nail polish. The slides were stored at 4°C in the dark. The slides were viewed using a fluorescence microscope (Nikon).

3 Chapter 3: Microarray analysis of glioma samples

3.1 Introduction

As discussed previously, different stages and types of tumours, including those of the same type and stage, vary greatly from patient to patient, including their expression of genes and expression of miRNA. However, fundamental differences of miRNA expression between low and high grades are not known. In addition, the altered miRNA expression associated pathways in response to hypoxic strain has not been fully investigated in a range of gliomas.

The nature of low-grade gliomas, including a generally slower growth rate and typically different molecular features such as IDH mutations, indicates a difference in biological processes which are potentially regulated by miRNA. Furthering investigation of miRNA expression within low-grade gliomas may provide an insight into the role miRNAs play in low-grade glioma development and their differing responses to microenvironmental changes such as lower oxygen levels.

Alongside investigating the roles of miRNA in low-grade gliomas, it is also beneficial to assess the altered miRNA expression in glioblastomas. Though more is known about miRNAs in glioblastomas, the direct impact of hypoxia on individual miRNAs is yet to be determined. Hypoxia is largely cited as a tumour progressive microenvironment for glioblastomas, which is a concentrated region of hypoxia with lower O_2

availability in the core of the tumour that follows a gradient through to the invasive rim and peripheral cells. Screening large numbers of miRNA will identify those with a significant link to hypoxia which may lead to its exploitation for a novel therapeutic target.

Understanding the miRNA landscape of gliomas will involve and generate a large amount of information on the expression of hundreds of miRNAs. This information is also the precursor to understanding the intricate regulatory mechanisms and identifying the genes controlled by miRNAs. As part of their regulatory roles, miRNAs alter the degree of their gene suppression depending on environmental changes and their own regulatory mechanisms.

To analyse such a broad number of miRNAs at once, in normoxic and hypoxic samples, a few techniques can be employed. This can include sequencing, microarrays and qPCR panels. The technique of choice for this investigation was using NanoString nCounter miRNA expression microarray panel (figure 5) which counted the expression of 827 individual human miRNAs. This particular technique was chosen for its breadth of miRNAs, making it an ideal screening method to analyse the expression of hundreds of miRNAs. Microarray technology uses optical molecular barcodes to label individual miRNA transcripts. Two different types of probes are used for each miRNA; a capture probe and a reporter probe, both of which have 50 nucleotides to bind to the miRNA. The capture probe contains a biotin molecule at the end which is used to bind

to the sample and then immobilise it. The reporter probes are a fluorescent barcode which is made up of 6 spots and each spot can be one of four different colours. Each gene/miRNA is assigned a specific and unique colour combination and it is this barcode that is counted at the end of the process. These two probes along with the RNA sample and hybridisation buffer are pipetted together in a tube and placed on a thermocycler overnight at 65°C. This method is completely enzyme free, not requiring any reverse transcriptase or amplification. Once the hybridisation complexes have formed, the RNA will be bound to both the capture and reporter probe by binding to the 50 nucleotides of each probe. The two probes fit adjacently and complementary to the RNA with no gaps between the two probes. The hybridisation reactions are loaded onto compatible instruments such as nCounter sprint profiler. Once loaded onto the machine, a purification step occurs. Two rounds of magnetic bead purification occur which is used to remove the excess reporter and capture probes. Next the probe is bound to the slide. The biotin on the end of the capture probe is utilised in this step to immobilise the purified sample onto the slide surface by a biotin-streptavidin interaction. For the final stage of the process, an electric current is passed through the sample which makes the complexes lie-down flat against the slide surface and allows the molecules to be orientated in the same direction. A fixative is applied to keep the molecules in place so the slide can be imaged for single molecule counting and data collection. The raw counts of the slide account for the actual number of molecules present in the sample. This data is entered into the nSolver Analysis

Software which conducts QC checks and normalises the data against a set of internal controls and reference genes.

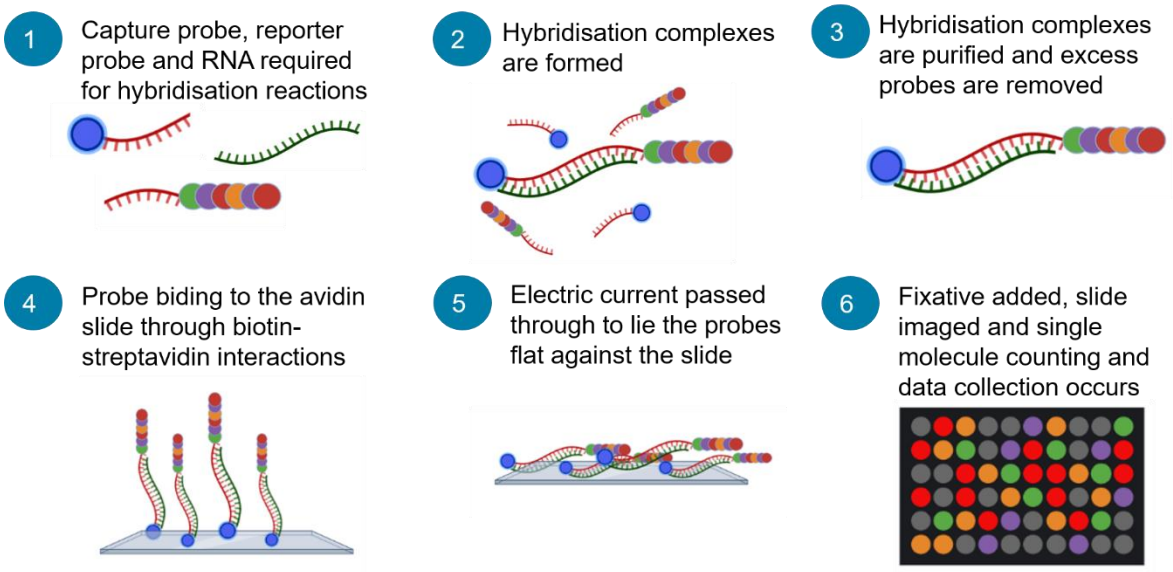

Figure 5. Microarray process of screening the expression of hundreds of different miRNAs.

Hypothesis 1: Individual miRNA levels are differentially expressed in hypoxic gliomas compared to normoxic gliomas.

Hypothesis 2: Differentially expressed miRNAs in hypoxia compared to normoxia differs in high-grade gliomas compared to low-grade gliomas.

3.2 Microarray results

3.2.1 RNA yield and purity

RNA was extracted from 12 different cell lines which are outlined in (table 4). The purity of the total RNA was measured using the A260/A280 and A260/A230 ratios in which the ratios nearest to 1.8 indicated the absence of contaminants that absorb at A280 and A230 respectively. The quality

of the RNA was also assessed using the RNA integrity number (RIN). The values of RIN range from 1 to 10 with values close to 1 indicating that the RNA has degraded and a value of 10 indicates that the RNA is completely intact. All the RNA samples had a minimum RIN of 9.2 which assumes that the RNA is almost intact after the RNA extraction process.

3.2.2 Microarray analysis

3.2.2.1 Normalisation

After analysing the quality and purity of the RNA samples, all of the samples were fit (RIN > 5 and absorbance ratio of between 1.6 and 2.0) to proceed with the microarray analysis.

After initial quality control (QC) analysis followed by normalisation, it was found that many of the miRNA expression counts were similar to the background level. The QC analysis were satisfactory; however, it is noted that if the capture probe is not added last to the hybridisation reactions before loading onto the thermocycler, it can cause a greatly increased background due to non-specific binding. Due to the uncertainty of the normalisation, the samples were graphically represented as not normalised (figure 6), with background correction (figure 7) and without background correction (figure 8). The background correction subtracted the expression of negative controls from the miRNA expression values. This is then followed by normalisation with the ligation controls. When performing the background correction before the ligation normalisation due to the expression of most of the miRNAs being at background level,

564 miRNAs out of 800 would be discarded. To be able to analyse as many miRNAs as possible, background correction was excluded but ligation normalisation was performed.

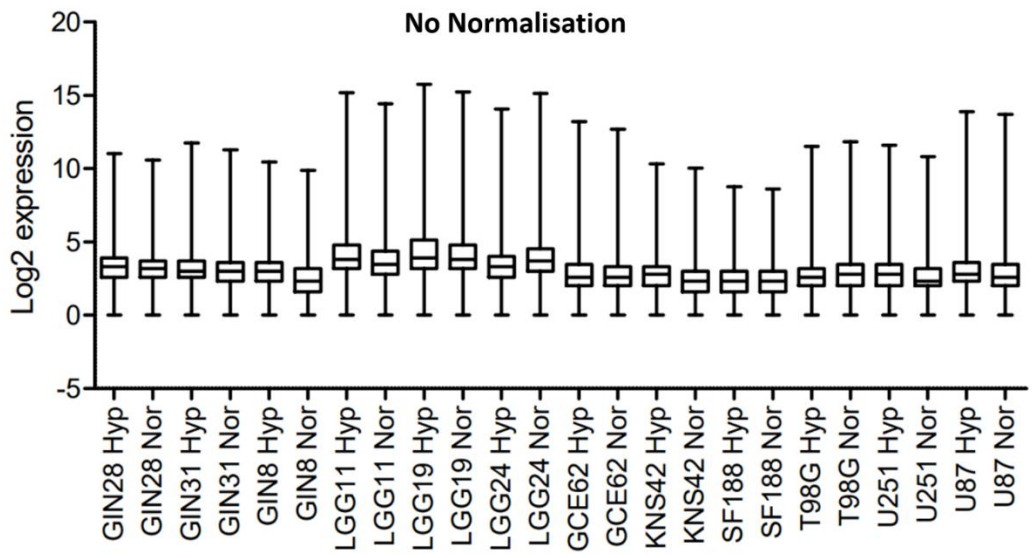

Figure 6. A boxplot of the raw data from the microarray analysis with no normalisation or correction across the 12 samples.

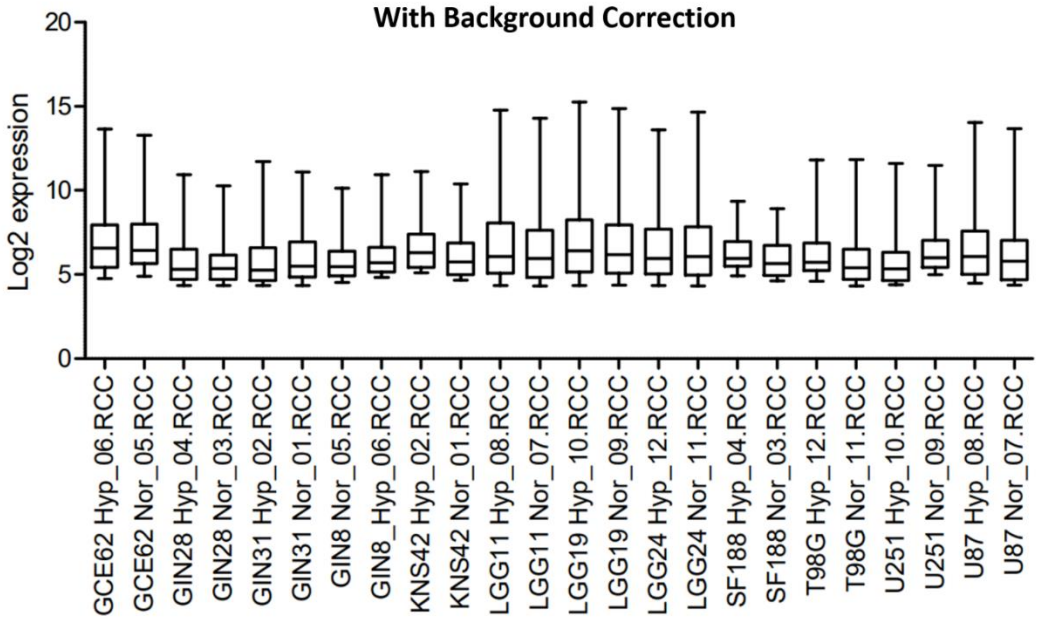

Figure 7. A boxplot of the microarray data after background correction, which subtracts the expression of the negative controls from the miRNA expression values. This is followed by normalisation with the ligation controls.

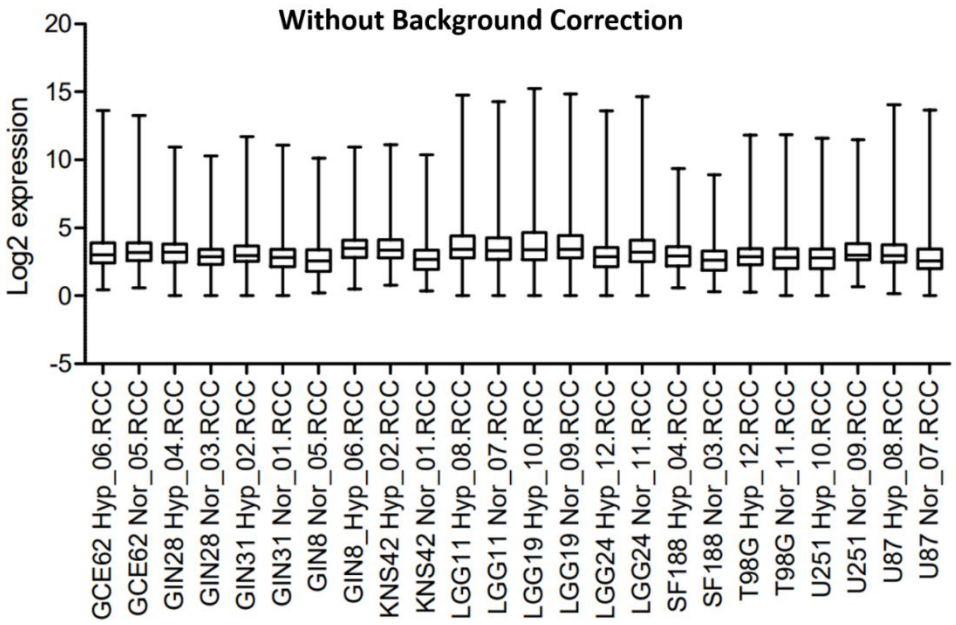

Figure 8. A boxplot of the data with only the ligation normalisation applied. Background correction has not been performed.

The ligation normalisation without background correction reduced the variability across the samples and created a normal distribution of miRNA expression in each of the samples. This is indicative that the normalisation has had the desired effect for each sample and can be seen in figure 9.

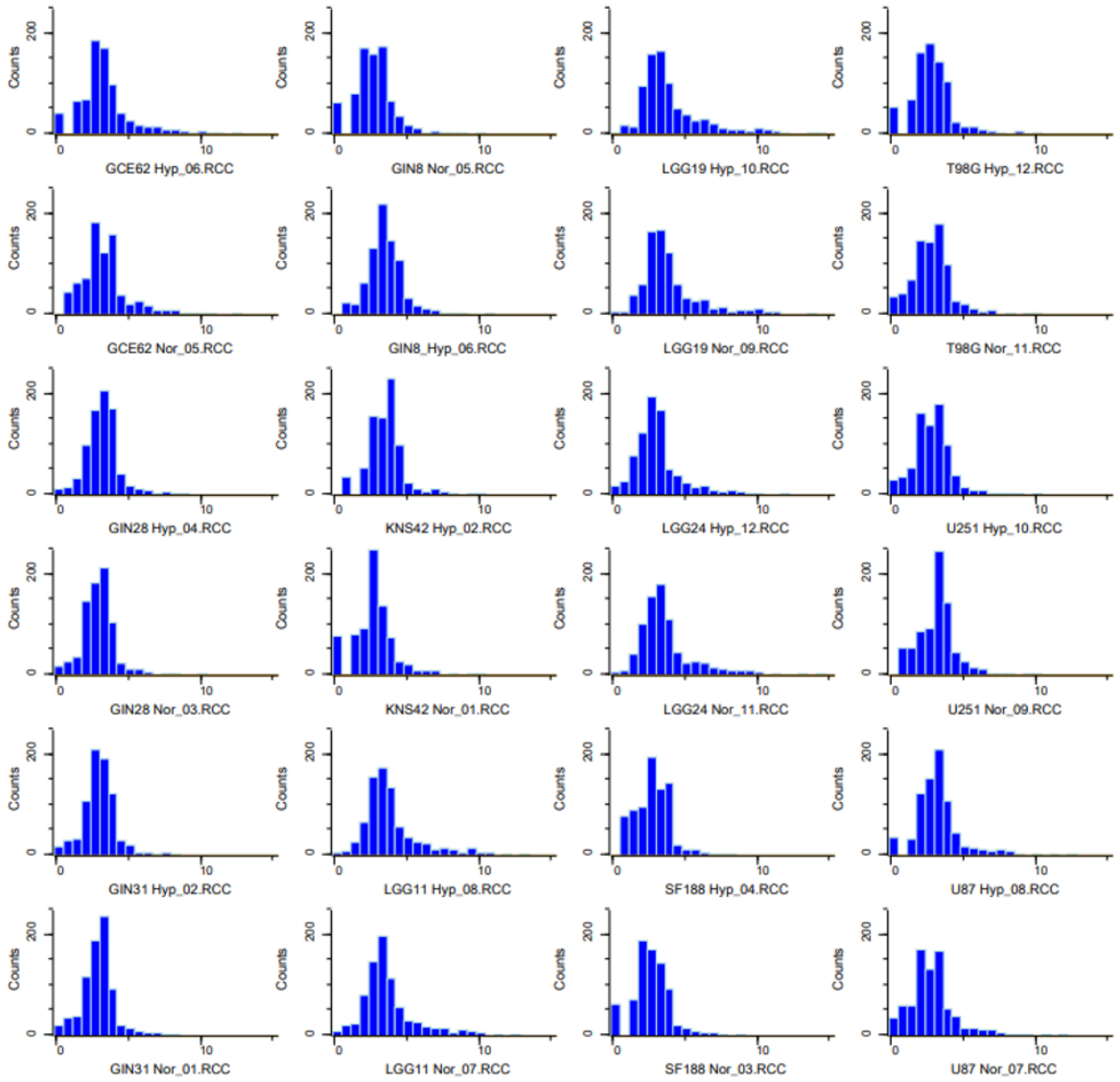

Figure 9. Histograms showing the distribution of miRNA expression in each of the samples following ligation normalisation without background correction.

3.2.2.2 Clustering

After the normalisation method was determined, a principal component analysis (PCA) (figure 10) was performed to analyse the differences between the samples. The analysis shows the separation of the samples largely based on their primary categories including low grade, high grade, paediatric and commercially available cell lines. The low-grade samples

have all grouped together as have the primary high-grade cell lines (GIN). The commercially available cell lines and the paediatric samples are more diverse with the U87 and GCE62 being more distinct from the other samples in their respective groups. Each category contains 3 cells lines and each cell line has a normoxic and hypoxic sample. The PCA plot shows that the different categories separate the cell lines more than the hypoxic status.

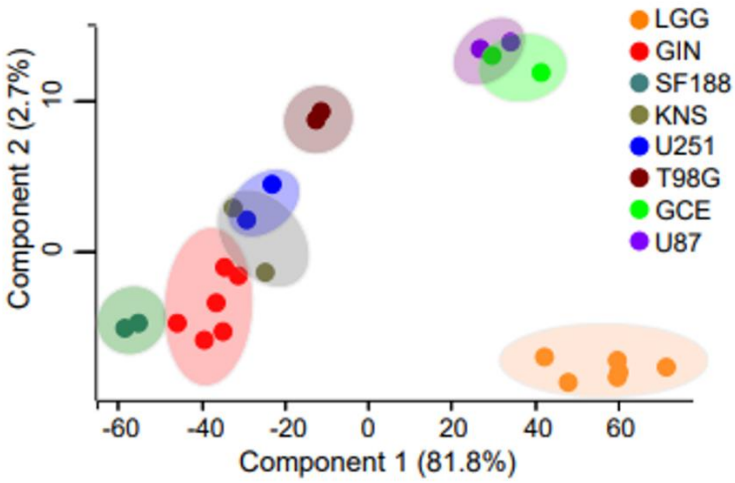

Figure 10. A principal component analysis of the 12 different samples that were analysed by the NanoString microarray. Each two dots represent a hypoxic and normoxic sample for each category. For GIN and LGG categories, three cell lines were analysed.

3.2.2.3 Statistical analysis

Statistical analysis was carried out in the form of a two-sample student's t-test to identify the significant miRNA expression in hypoxia compared to normoxia. The categories that were analysed were overall hypoxia *vs* normoxia, GIN hypoxia *vs* normoxia and LGG hypoxia *vs* normoxia. GIN and LGG samples were looked at particularly due to the availability of

primary samples and any research conducted on these primary samples provides a stronger clinical association. Once false discovery rate (FDR) was applied, no miRNAs were significant, p-value < 0.05. To allow analysis to be conducted on the data, the unadjusted p-value cut-off was p-value < 0.01 to increase the stringency since no FDR was applied. The p-values and fold changes are displayed in table 17. A selection of miRNAs was deemed significant in hypoxia compared to normoxia using the new parameters for each group (overall, GIN and LGG) and are visualised using volcano plots (figures 11, 12 and 13). The miRNA points in red are overexpressed in hypoxia compared to normoxia and the miRNA blue points are under-expressed in hypoxia compared to normoxia. Analysing the significant miRNAs overall the samples (figure 11) show a small number of significant miRNAs which are upregulated and miR-494-5p which is downregulated across all twelve cell lines.

Table 17. Fold change of miRNAs which had a p-value < 0.01 in hypoxia compared to normoxia.

Overall Hypoxia vs Normoxia	Student's t-Test log2 Fold change	GIN Hypoxia vs Normoxia	Student's t-Test log2 Fold change	LGG Hypoxia vs Normoxia	Student's t-Test log2 Fold change
hsa-miR-2110	0.928445748	hsa-miR-1193	1.080245018	hsa-miR-2053	-0.862955014
hsa-miR-320a	0.739031076	hsa-miR-128-1-5p	0.916840633	hsa-miR-217	-0.659039497
hsa-miR-328-3p	0.880330165	hsa-miR-138-5p	0.535958449	hsa-miR-3615	-0.491241693
hsa-miR-412-3p	0.890960885	hsa-miR-210-5p	1.088476102	hsa-miR-494-5p	-0.855932156
hsa-miR-450b-3p	0.641052842	hsa-miR-218-5p	0.909828981	hsa-miR-506-6p	-0.634440581
hsa-miR-491-5p	0.765570501	hsa-miR-301b-5p	0.806286891	hsa-miR-606	-2.238622109
hsa-miR-494-5p	-0.665201724	hsa-miR-302a-5p	0.8567969		
hsa-miR-508-3p	0.884228831	hsa-miR-412-3p	1.336175799		
		hsa-miR-4425	1.284610192		

		hsa-miR-4461	0.746825933		
		hsa-miR-4741	0.601069371		
		hsa-miR-490-5p	1.757540941		
		hsa-miR-549a	1.169620355		
		hsa-miR-575	0.940525293		
		hsa-miR-576-3p	0.739831209		
		hsa-miR-608	0.794635137		
		hsa-miR-616-3p	0.665755113		
		hsa-miR-766-5p	2.536768243		

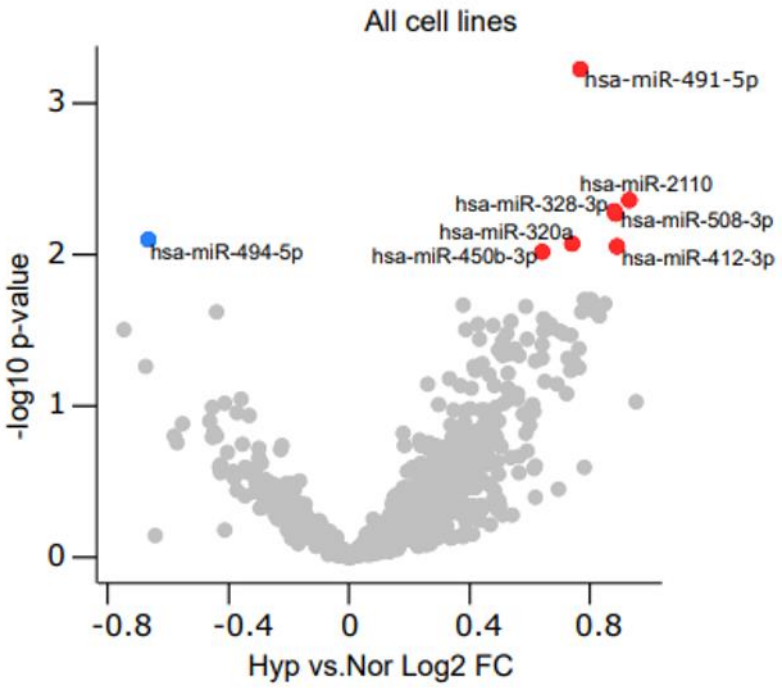

Figure 11. Volcano plot of all cell lines, annotating the miRNAs which are significant in hypoxia compared to normoxia. Downregulated miRNAs are blue, and the upregulated miRNAs are red.

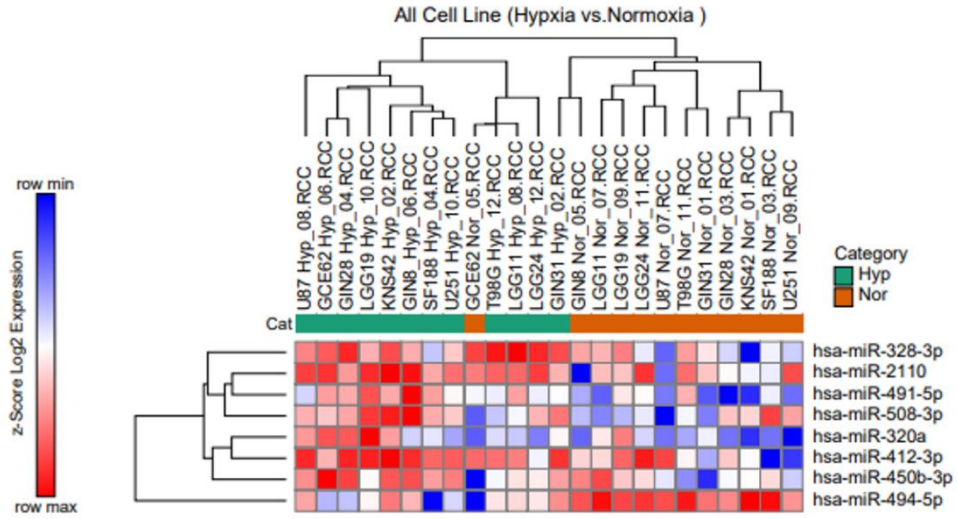

Figure 12. A heatmap showing the statistically significant differentially expressed miRNAs over all cell lines.

Over all of the cell lines, 8 miRNAs out of the 827 screened were statistically significant, as shown in figure 11. miR-494-5p is the only miRNA to be downregulated in hypoxia compared to normoxia across the

12 cell lines. miR-491-5p, miR-2110, miR-328-3p, miR-320a, miR-450b-3p, miR-508-3p and mir-412-3p are upregulated in hypoxia compared to normoxia across all 12 cell lines. The significant miRNAs across all samples were displayed in a heatmap in figure 12. The hierarchical clustering of the heatmaps shows that the cell lines are separated based on the hypoxic status rather than differing cell origins. The GCE62 normoxic sample is an outlier as it clusters within the hypoxic samples. Overall, this result uncovers the miRNAs that exhibit elevated expression levels in hypoxic strain. Thus, the differentially regulated miRNAs have the potential to be utilized as biomarkers for exploring the hypoxic pressure in GBM.

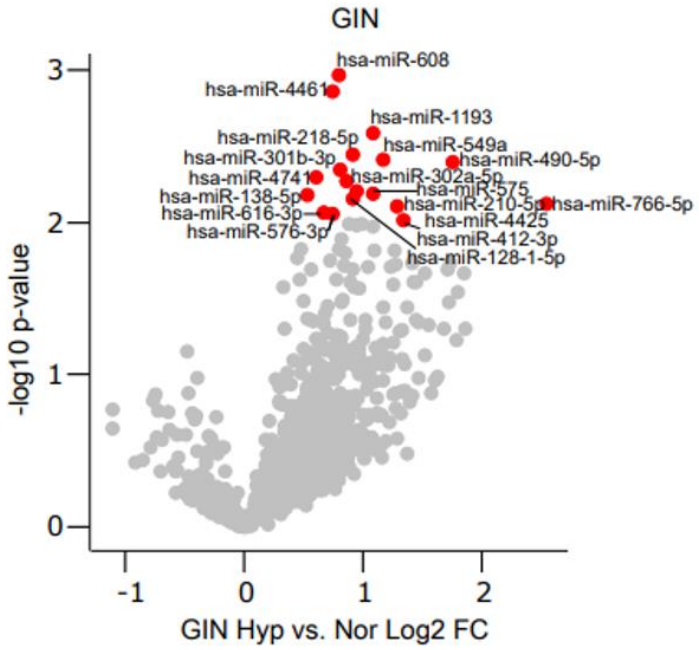

Figure 13. Volcano plot of the primary GIN cell lines, red dots are significantly upregulated in hypoxia compared to normoxia.

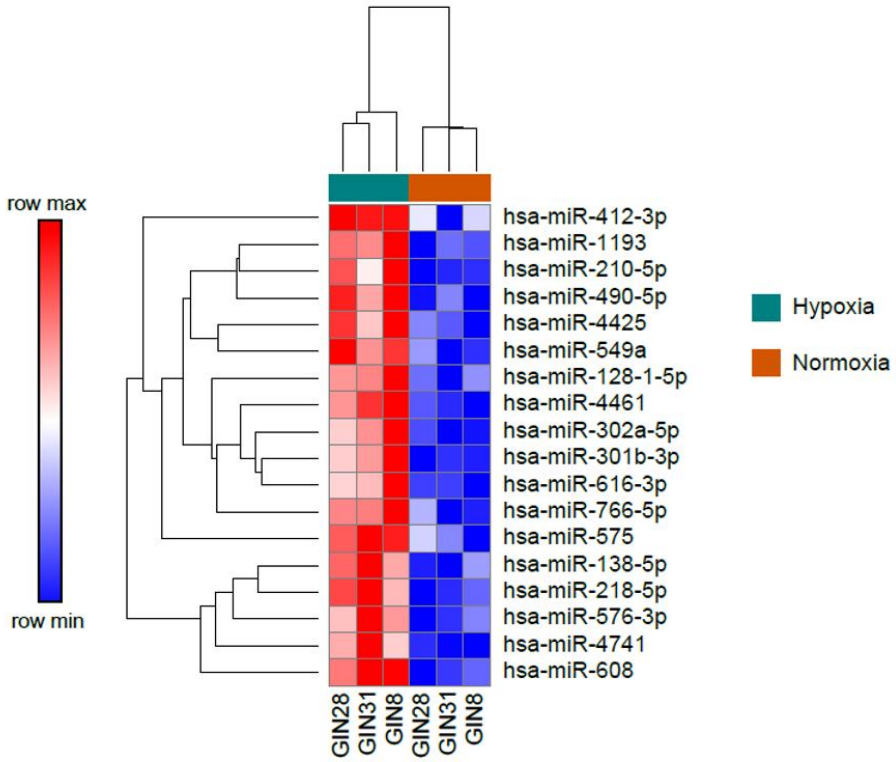

Figure 14. A heatmap showing the statistically significant differentially expressed miRNAs in the primary glioblastoma (GIN) cell lines.

In the GIN samples, 18 miRNAs were significantly upregulated in hypoxia compared to normoxia and no miRNAs were significantly downregulated, seen in figure 13. The upregulated miRNAs include miR-608, miR-4461, miR-218-5p, mir-301b-3p, miR-4741, miR-138-5p, miR-616-3p, miR-576-3p, miR-1193, miR-549a, miR-490-5p, miR-320a, miR-575, miR-210-5p, miR-766-5p, miR-142-3p, miR-218-1-5p. It should be noted that not all GIN hypoxia upregulated miRNAs are upregulated in the overall glioma cell lines (figure 11). This is because the overall cell line category combines commercial, GIN, low-grade and paediatric miRNA hypoxia vs normoxia expression as a whole average and these miRNAs are only upregulated in hypoxia compared to normoxia in the GIN cell lines only. This also accounts for the differences seen between the low-grades and overall categories. Figure 14 shows the separation of the hypoxic and normoxic samples of primary glioblastoma cells with the 18 significant miRNAs. The differentially regulated miRNAs exhibit the power to distinguish between hypoxic and normoxic conditions.

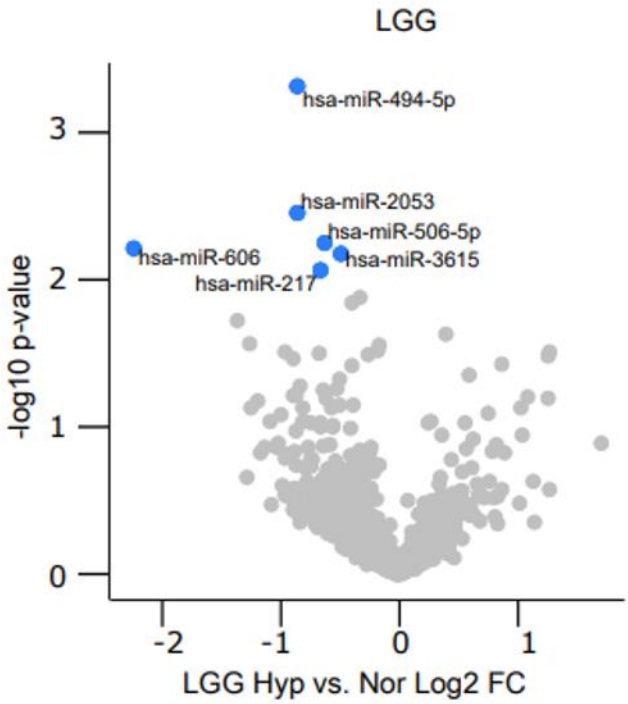

Figure 15. Volcano plot of the primary low-grade cell lines, annotating the miRNAs which are significantly downregulated in hypoxia compared to normoxia.

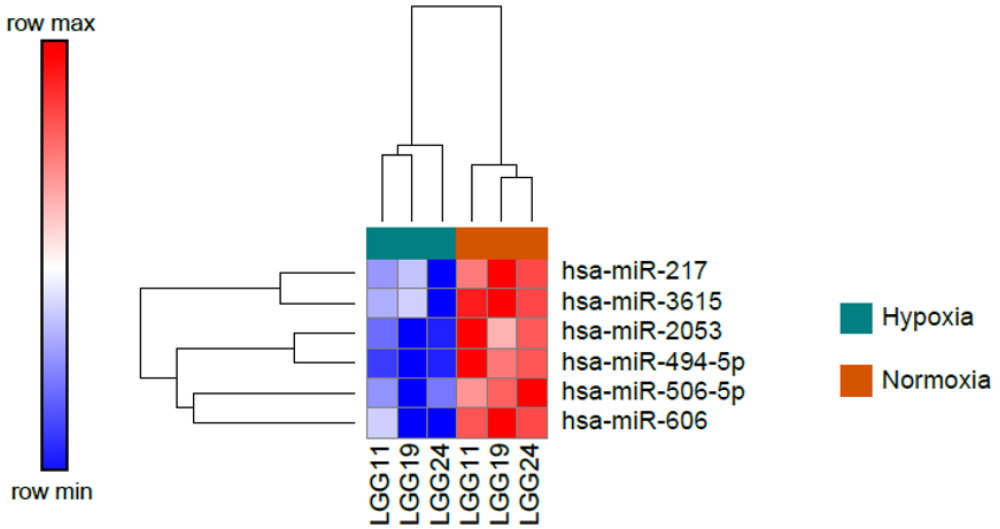

Figure 16. A heatmap showing the statistically significant differentially expressed miRNAs in the primary low grade gliomas cell lines.

The 6 miRNAs were downregulated significantly in hypoxia compared to normoxia and no miRNAs were significantly upregulated in hypoxia. The

downregulated miRNAs in hypoxia in low-grade gliomas are miR-606, miR-127, miR-494-5p, miR-2053, miR-506-5p and miR-3615 as seen in figure 15. Similarly for the low-grade cell lines, figure 16 shows the heatmap which indicates the separation of hypoxic and normoxic samples based on the expression of the 6 miRNAs.

3.2.2.4 Pathway analysis

Pathway analysis was conducted on the three categories; overall, GIN and low-grade gliomas using the web tool Mienturnet http://userver.bio.uniroma1.it/apps/mienturnet/ for miRNA-gene network analysis and pathway enrichment Molecular Signatures Database v7.5.1 (MsigDB) was used to extract the hallmark gene sets for Gene Set Enrichment Analysis (GSEA). These results were combined together using CytoScape which is widely used for networking analysis. This analysis identified the target genes controlled by the significantly regulated miRNAs and revealed the biological processes that are significantly altered under hypoxic strain.

3.2.2.4.1 Pathway analysis of all cell lines

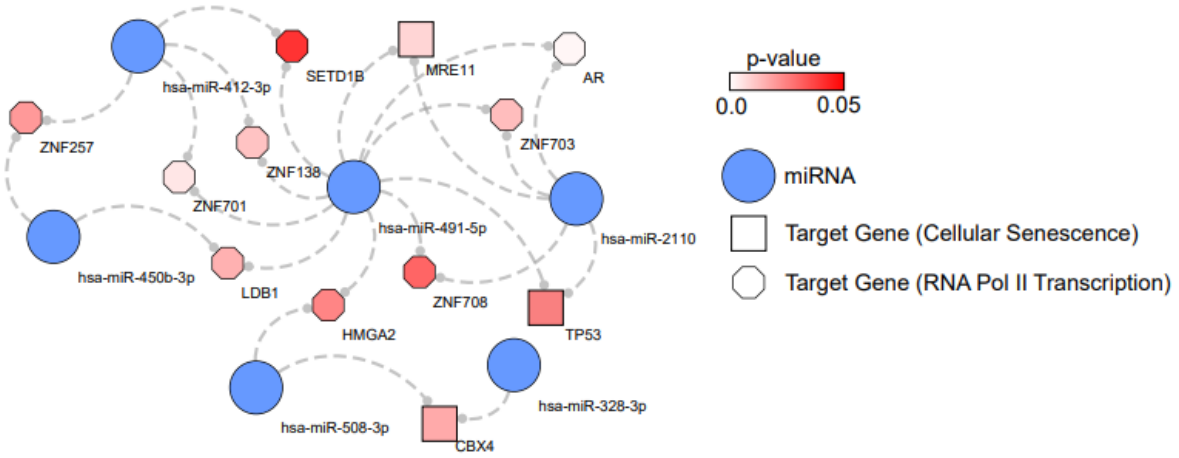

Figure 17. A pathway schematic showing the relevant pathways of the mRNA targets of the significant miRNA across all cell lines in hypoxia compared to normoxia..

For the category spanning all the cell lines, two major pathways were significantly associated with hypoxic strain; cellular senescence and RNA Pol II transcription which is shown in figure 17. Five different zinc-finger protein encoding genes associated with RNA Pol II transcription along with androgen receptor (*AR*), high-mobility group-AT-hook 2 (*HMGA2*) LIM-binding domain 1 (*LDB1*) and histone *SETD1B* are upregulated in response to hypoxic conditions. These genes are shown to interact with miR-412-3p, miR-450b-3p, miR-491-5p, miR-2110 and miR-508-3p. In addition, genes were associated with cellular senescence pathway including tumour protein 53 (*TP53*), chromobox 4(*CBX4*) and double-strand break repair protein *MRE11* were also significantly upregulated in hypoxia. These genes are shown to interact with miR-2110, miR-328-3p, miR-508-3p and miR-491-5p.

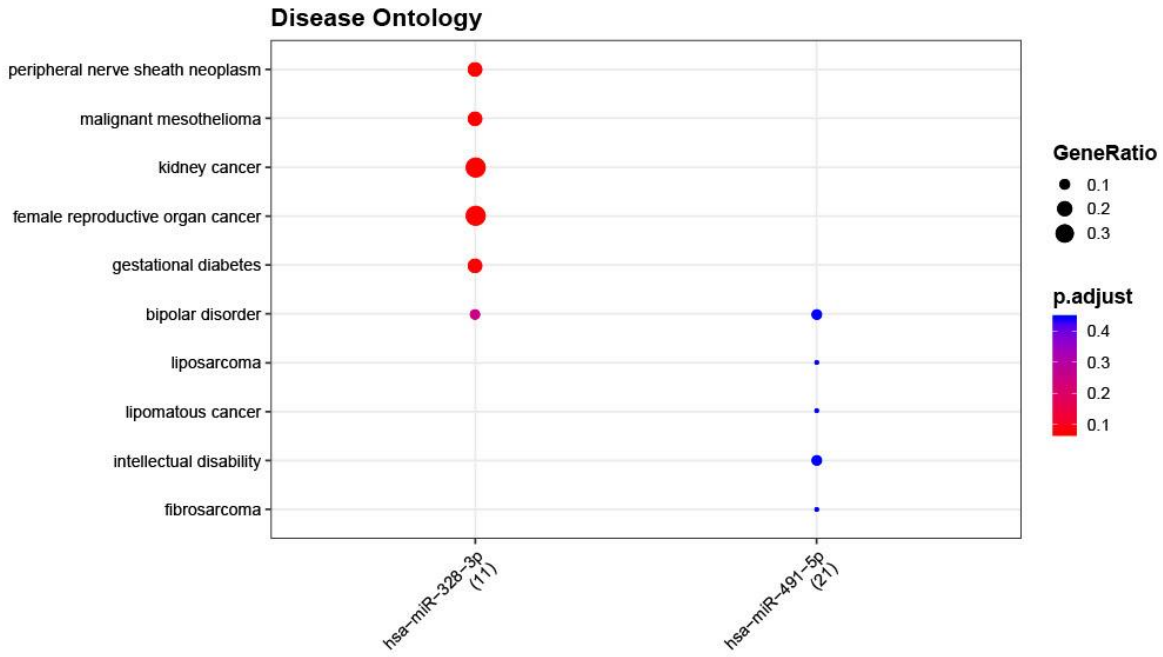

Figure 18. Dot plot of disease ontology pathways for the significant miRNAs in hypoxia compared to normoxia in all cell lines.

Further pathway enrichment analysis was conducted on target genes of the significant miRNAs for all the cell lines. Due to low enrichment values, p-values were used instead of the adjusted p-values from multiple correction tests. Using disease ontology, figure 18, the two miRNAs (miR-328-3p and miR-491-5p) which were significantly associated with hypoxia (figure 14). miR-328-3p is linked to peripheral nerve sheath neoplasm, malignant mesothelioma, kidney cancer, female reproductive organ cancer, gestational diabetes and bipolar disorder. Whereas miR-491-5p is linked to bipolar disorder, liposarcoma, lipomatous cancer, intellectual disability and fibrosarcoma.

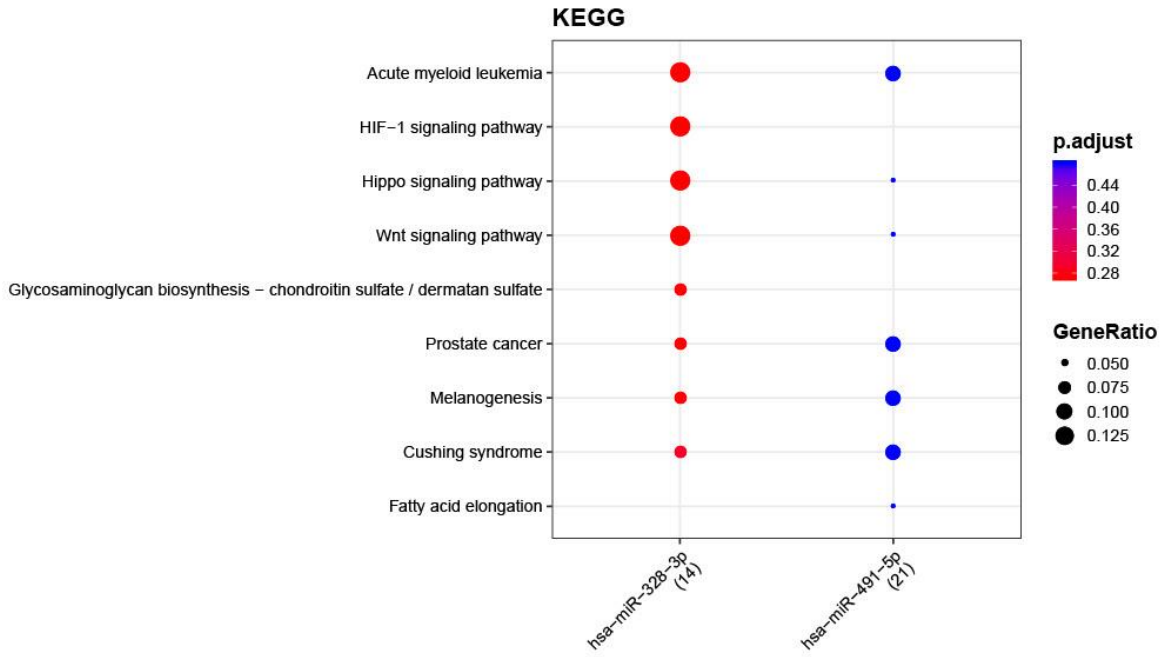

Figure 19. Dot plot of KEGG pathways for the significant miRNAs in hypoxia compared to normoxia in all cell lines.

In the KEGG pathway analysis, the same two miRNAs (miR-328-3p and miR-491-5p) that were associated with hypoxia were identified (figure 19). miR-328-3p is linked to acute myeloid leukaemia, HIF-1 signalling, Hippo signalling, Wnt signalling, glycosaminoglycan biosynthesis, prostate cancer, melanogenesis and Cushing's syndrome. miR-491-5p is linked to the same pathways as miR-328-3p except HIF-1 signalling and glycosaminoglycan biosynthesis and is also linked to fatty acid elongation.

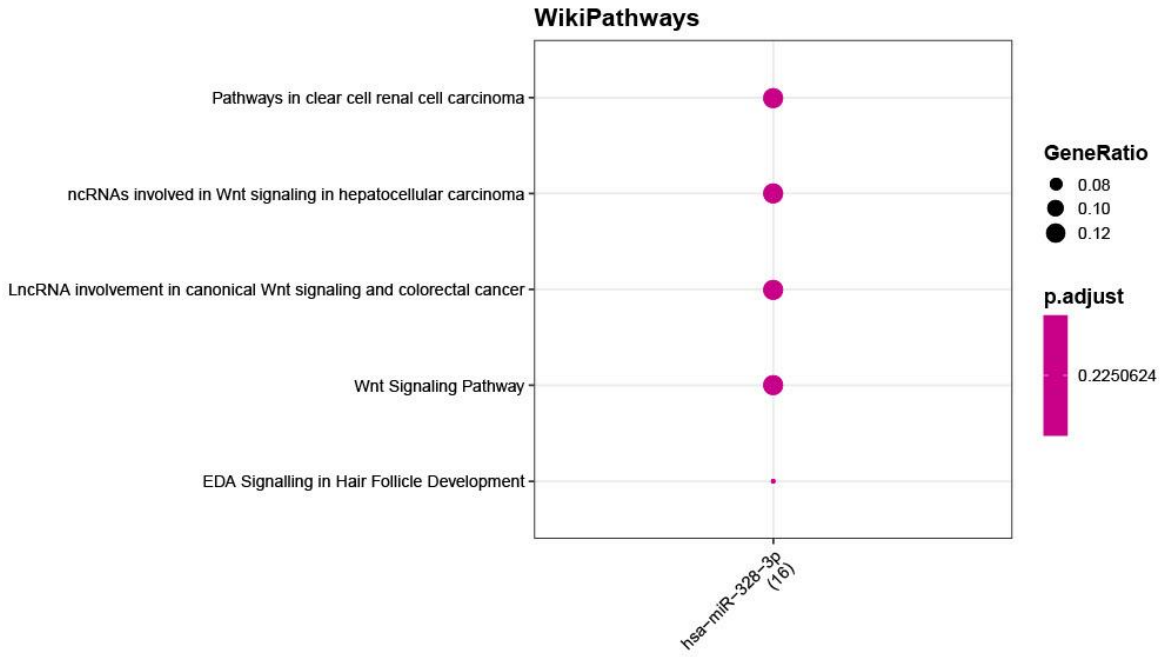

Figure 20. Dot plot of wikipathways for the significant miRNAs in hypoxia compared to normoxia in all cell lines.

Another regular pathway analysis involves wikipathways. miR-328-3p was the only significant miRNA for this analysis (figure 20) and is linked to pathways in clear cell renal cell carcinoma, ncRNAs involved in canonical Wnt signalling and colorectal cancer, Wnt signalling and EDA signalling in hair follicle development.

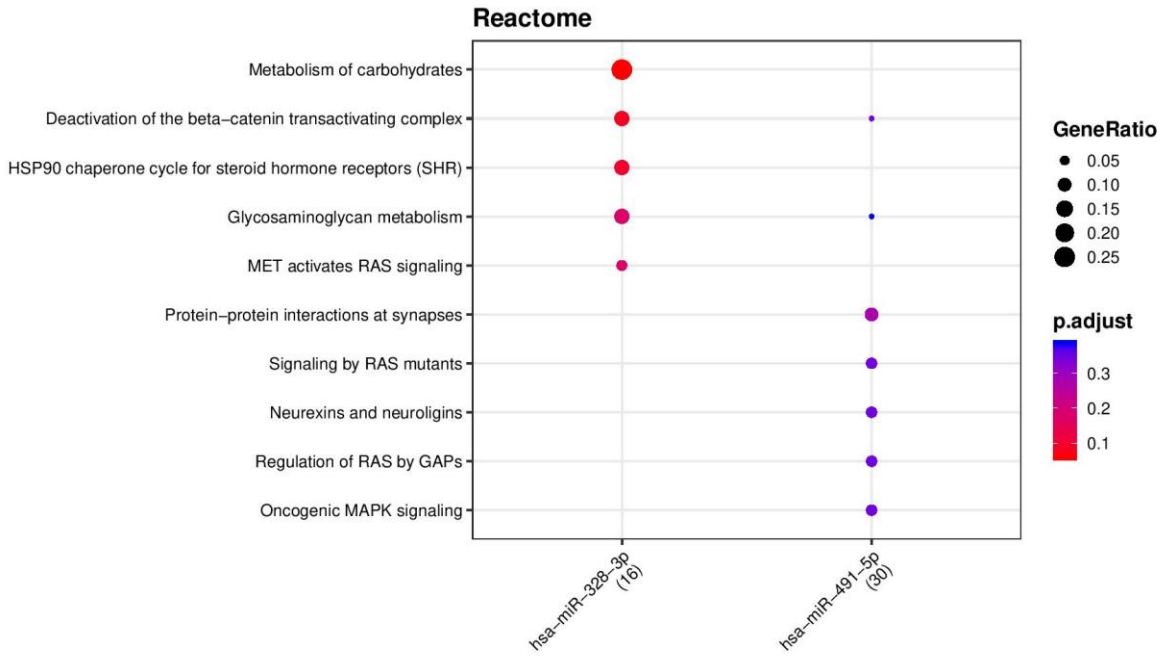

Figure 21. Dot plot of reactome outputs for the significant miRNAs in hypoxia compared to normoxia in all cell lines.

Reactome is a free online database which is readily used to find biological pathways of genes. miR-328-3p and miR-491-5p were also significant in reactome analysis (figure 21). miR-328-3p is linked to the metabolism of carbohydrates, deactivation of the beta-catenin transactivating complex, HSP90 chaperone cycler for steroid hormone receptors (SHR), glycosaminoglycan metabolism and MET activates RAS signalling. Using wikipathways, miR-491-5p is linked to deactivation of the beta-catenin transactivating complex, glycosaminoglycan metabolism, protein-protein interactions at synapses, signalling by RAS mutants, neurexins and neuroligins, regulation of RAS by GAPs and oncogenic MAPK signalling.

3.2.2.4.2 Pathway analysis of GIN cell lines

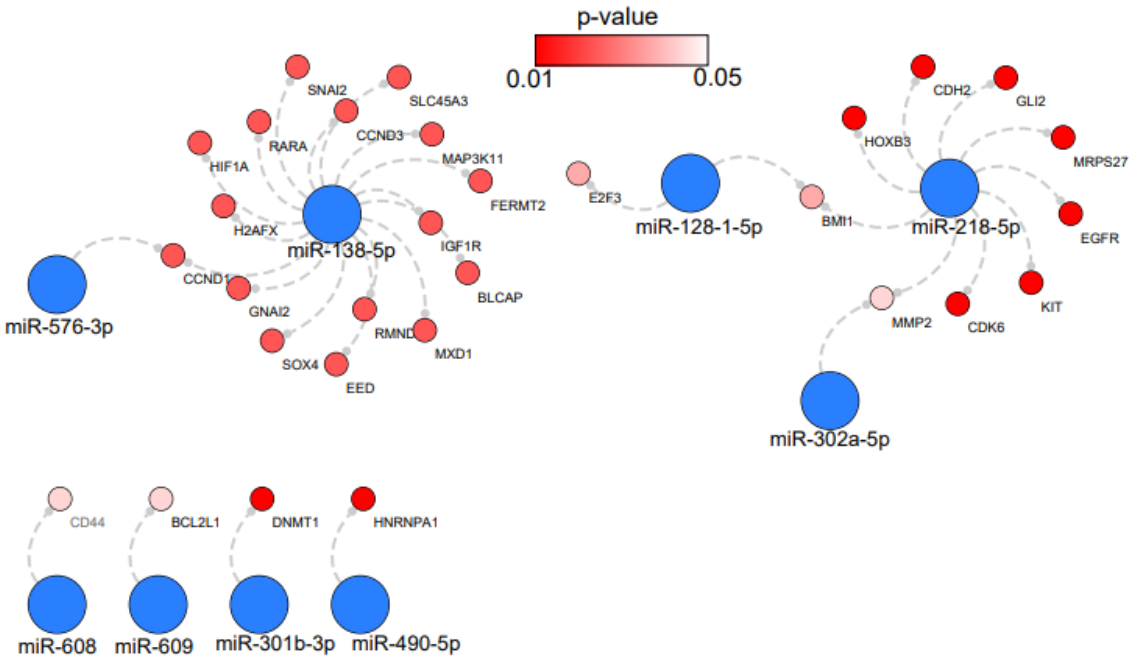

Figure 22. A pathway schematic of the relevant pathways of the mRNA targets of the significant miRNA across GIN cell lines in hypoxia compared to normoxia.

Pathway analysis in the GIN cell lines showed that miR-138-5p, miR-576-3p, miR-128-1-5p, miR218-5p, miR-320a-5p, miR-608, miR-609, miR-301b-3p and miR-490-5p have possible interactions with a number of genes that were significantly enriched seen in figure 22.

From the miRNAs which were significant in hypoxia compared to normoxia in GIN cell lines the following miRNAs; miR-128-1-5p, miR-138-5p, miR-218-5p, miR-301b-3p, miR-302a-5p, miR-490-5p, miR-576-3p and miR-608 were enriched in disease ontology, KEGG, wikipathways

and reactome analysis (figures 23, 24, 25 and 26 respectively). The dotplots have adjusted p-values and GeneRatios for each graph.

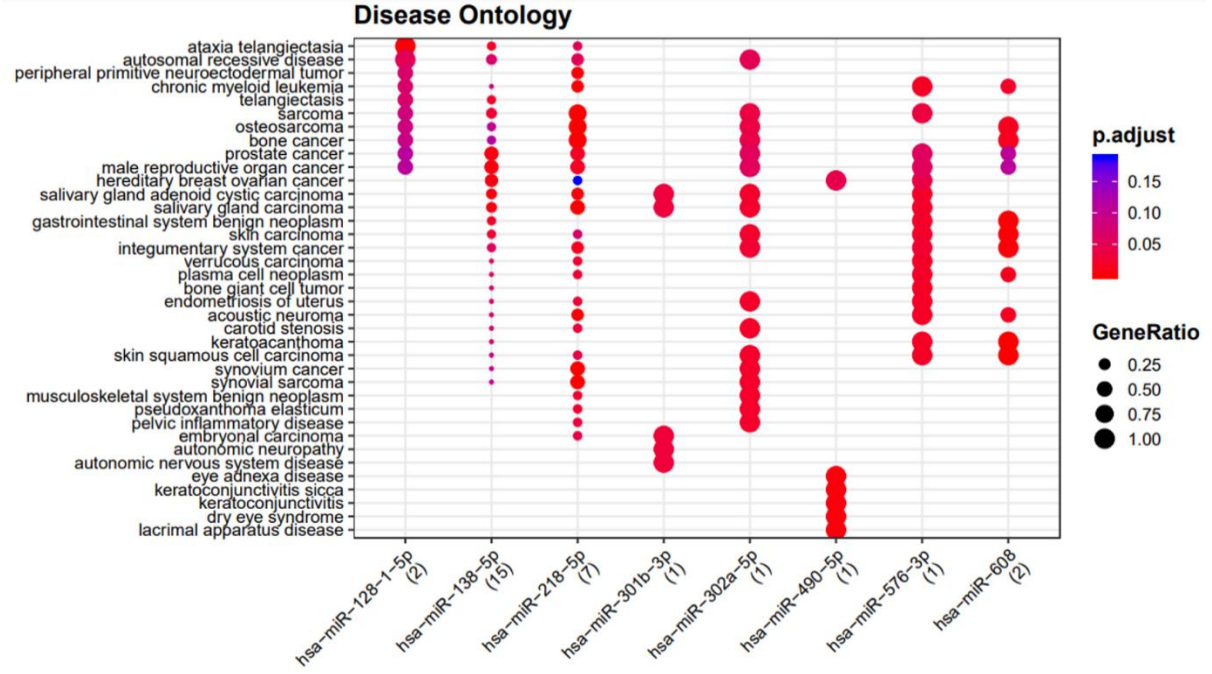

Figure 23. Dot plot of disease ontology pathways for the significant miRNAs in hypoxia compared to normoxia in GIN cell lines.

Using disease ontology, a large range of diseases was enriched with the significant miRNAs including bone cancer, osteosarcoma, salivary gland carcinoma, skin carcinoma (figure 23). As well as a number of cancers, other diseases which are linked to the significant miRNAs include ataxia telangiectasia, autosomal recessive diseases and endometriosis of uterus.

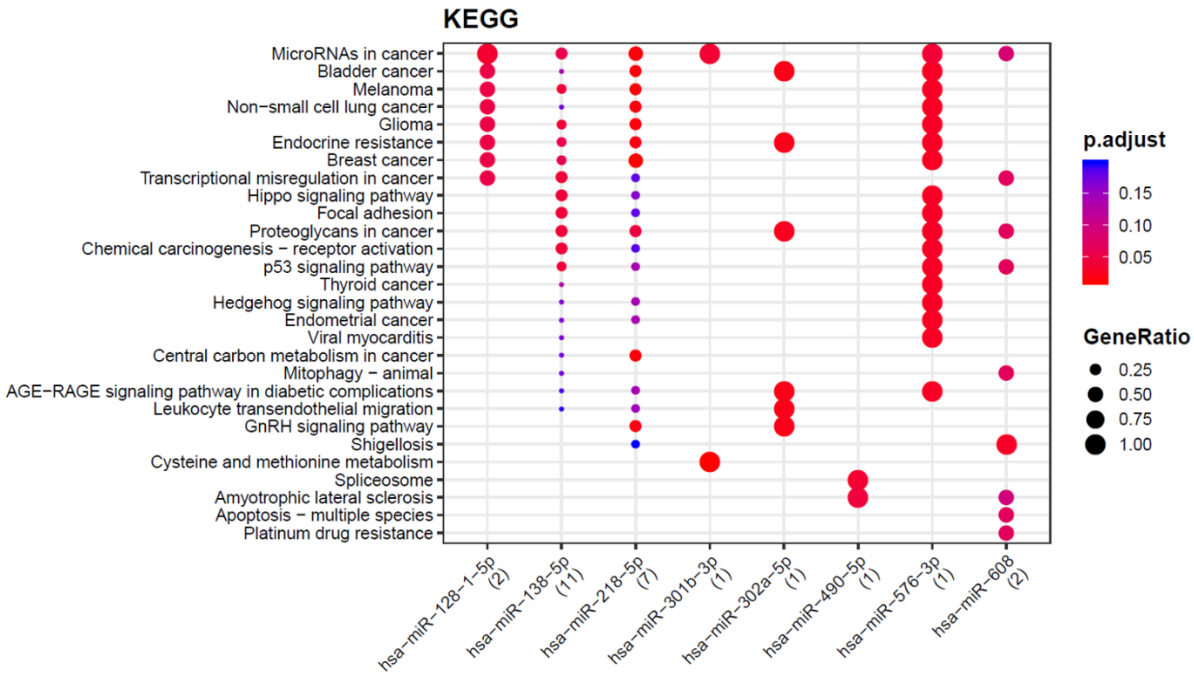

Figure 24. Dot plot of KEGG pathways for the significant miRNAs in hypoxia compared to normoxia in GIN cell lines.

The same miRNAs were enriched with KEGG pathway analysis (figure 24). One pathway, microRNAs in cancer, contained all the significant miRNAs except miR-302a-5p and miR-490-5p. Another important KEGG pathway showed that miR-128-1-5p, miR-138-5p, miR-218-5p and miR-576-5p were enriched in gliomas.

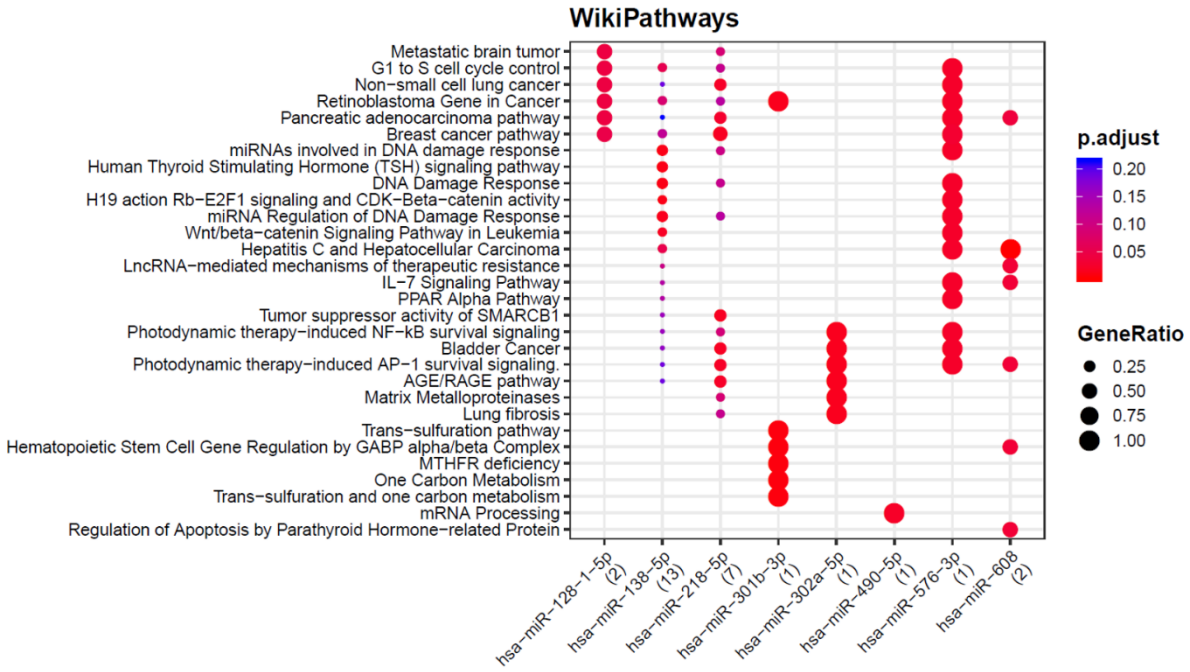

Figure 25. Dot plot of WikiPathways for the significant miRNAs in hypoxia compared to normoxia in GIN cell lines.

The WikiPathways analysis also revealed relevant pathways for the significant hypoxic miRNAs (figure 25). Metastatic brain tumour pathways were enriched for miR-128-1-5p and miR-218-5p. The analysis showed that the miRNAs were enriched for other cancers including non-small cell lung cancer, bladder cancer and Wnt/beta-catenin signalling pathway in leukaemia.

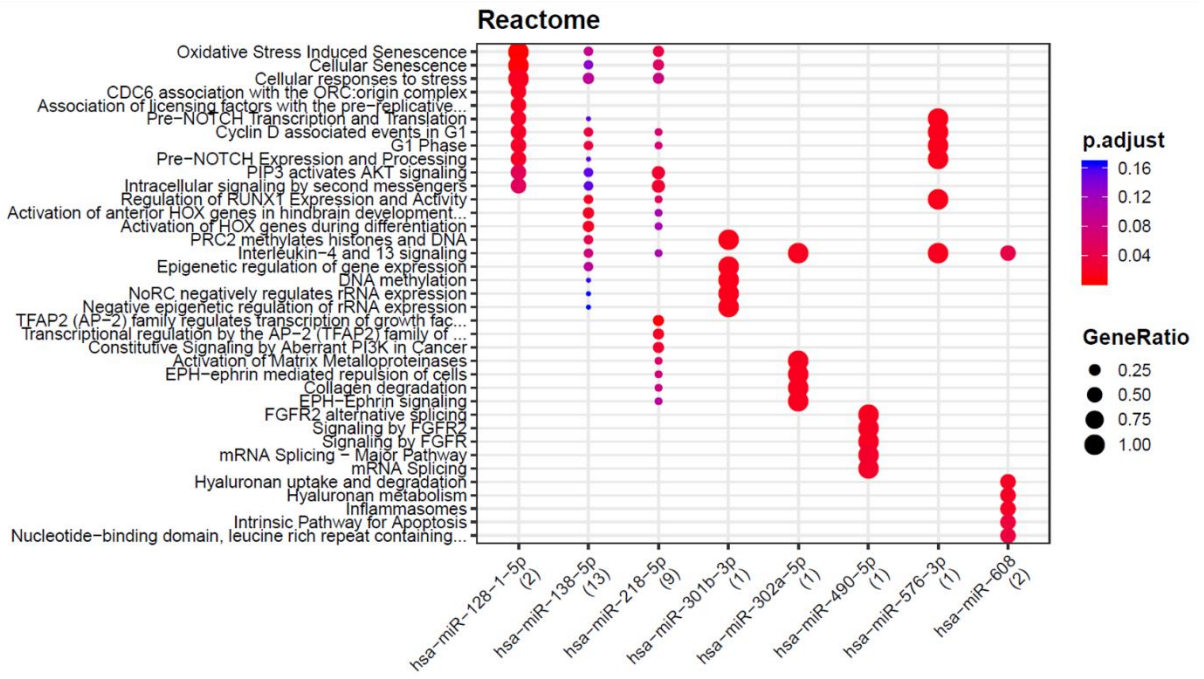

Figure 26. Dot plot of Reactome outputs for the significant miRNAs in hypoxia compared to normoxia in GIN cell lines.

A number of biological pathways were enriched with the significantly upregulated miRNAs for hypoxia using Reactome (figure 26). Oxidative stress induced senescence is enriched with miR-128-1-5p, miR-138-5p and miR-218-5p. The same three miRNAs were also enriched in cellular senescence and cellular responses to stress. A large range of pathways from splicing to interleukin signalling were enriched for these miRNAs, showing the diversity of their functions.

3.2.2.4.3 Pathway analysis of LGG cell lines

There was no pathway analysis for the low-grade cell lines, as none of the hypoxic significantly expressed miRNAs were significantly enriched in any pathways.

3.3 Summary

This first study used the microarray to screen 827 human miRNAs across 12 different glioma samples. The different samples included 3 paediatric and 3 commercially available cell lines. These samples were not taken forward for further analyses as it was determined to focus largely on high-grade gliomas (GIN cell lines) and low-grade gliomas. This was because these two categories are all primary cell lines derived from patients and less is known about the miRNA landscape of patient-derived tumours. Statistical analyses compared the miRNA expression with or without hypoxic strain in three categories; overall which encompasses all 12 cell lines (includes paediatrics and commercially), only GIN cell lines (GIN28, GIN31 and GIN8) and only the LGG cell lines (LGG19, LGG24 and LGG11).

Firstly, analysing the effect of hypoxia on all of the 12 cell lines, 8 miRNAs were statistically significant. One interesting miRNA, miR-491-5p, was identified as significant across all cell lines and was found to be 1.7 times upregulated in hypoxia compared to normoxia. miR-491-5p is noted to be tumour suppressor and involved in apoptotic pathways and cellular senescence (164), which was also indicated in the pathway analysis. Cellular senescence pathway included the gene *MRE11,* which is a direct target of miR-491-5p. The repression of *MRE11* can potentially decrease double-strand break repair by homologous recombination and cause cellular senescence (165). The effect of hypoxia on cellular senescence is not very clear with some reviews indicating it reduces cellular

senescence (166) and that the lack of oxygen can also increase senescence through different molecular pathways (167). The second pathway linked to miR-491-5p is RNA polymerase II transcription composed of many zinc-finger proteins including those shown in figure 13. RNA transcription is extremely important in hypoxia-induced cells, to enable hypoxia-induced transcription requiring polymerase II. Another miRNA, miR-328-3p is also significantly upregulated in hypoxia across all the cells around 1.8 times more than in normoxia. The pathway analysis of this miRNA shows that *CBX4* is a direct target. *CBX4* is linked to preventing cellular senescence (168), as miR-328-3p is increased and directly suppresses *CBX4*, this suggests a possible increase of cellular senescence. This is a similar effect to miR-491-5p repressing *MRE11.* Across all cell lines, in hypoxia there seems to be an increase in cellular senescence, based on miRNA expression and their targets.

The next grouped analysis focussed on the effects of hypoxia purely the GIN cell lines. 18 miRNAs were found to be significantly upregulated. miR-218-5p is 1.87 times upregulated in hypoxia and has multiple targeted genes and enriched in the pathway analysis. One pathway it is enriched in is oxidative stress induced senescence, and RNA polymerase II transcription similarly to the overall analysis. This particular miRNA is also indicated in the Wikipathways of signalling pathways in glioblastoma. Other pathways that are linked to miR-218-5p are apoptosis, angiogenesis, regulation of gene expression and metabolic processes. These are further confirmed when looking at the direct targets

of miR-218-5p in the pathway analysis. *EGFR* is linked to hypoxia, promotes angiogenesis, proliferation and effects cellular signalling. *MMP2* another target of miR-218-5p is linked to invasion of tumour cells.

Previously it has been shown that, higher expression of miR-21-5p in colon cancer cells induces β-catenin signalling by directly supressing KRIT1, thus contributing to angiogenesis and vascular permeability in colon cancer (PMID: 34088891). Further study is required to investigate whether a similar mechanism orchestrated by miR-21-5p in play to promote angiogenesis to counteract hypoxic strain in GBM.

Another miRNA that is upregulated 2-fold in hypoxia in GBM cell lines, though is not enriched in the pathway analysis is miR-210-5p. This miR-210-5p is a hypoxic marker, so it is encouraging to note that this miRNA is upregulated in hypoxia. miR-210-5p is also known as a hypoxamiR, which is notably upregulated in most cases of hypoxia. miR-210-5p increases cell cycle progression, genomic instability and angiogenesis (144).

In contrast to the other groups, the miRNAs that were statistically significant within the low-grade category were all downregulated. miR-606 was downregulated 4.7 times more in hypoxia compared to normoxia in low-grade glioma cell lines. This particular miRNA has not been studied largely in general, except for being related to cellular proliferation of sponging to miR-606 in pancreatic cancer (169), and there is no literature

regarding miR-606 in relation to gliomas and hypoxia. However, there are RNA polymerase II transcription, gene expression, and multiple metabolic processes are identified as pathways linked to miR-606 based on its predicted targets. It may identify this miRNA as important in either hypoxia and/or low-grade gliomas. It is still important to note, that although these miRNAs are significant ($p < 0.01$), none were significant when post-hoc correction was applied. Another miRNA that was downregulated in low-grade gliomas and overall, when analysing all 12 cell lines was miR-494-5p. This miRNA is linked to neurogenesis, nervous system development, DNA-binding transcription factor activity, developmental cell growth and neuron differentiation. The only potential pathway that has a more direct link to hypoxia and gliomas is cell migration. With little literature about this miRNA, it is hard to assume the impact of hypoxia on its function within low-grade gliomas. It is also noted that miR-210-3p, a hypoxic marker, is not upregulated in hypoxia in the low-grade gliomas compared to normoxia. As mentioned previously low-grade gliomas harbour IDH mutations which may cause HIF-1 stabilisation, therefore additional hypoxic pressure may not cause a significant difference in hypoxic-induced miRNAs or genes. However, the hypoxic exposure of low-grade gliomas may not have had a significant effect on the expression of hypoxic miRNA markers, further distinguishing their differences from glioblastomas. For the low-grade gliomas, during the pathway analysis of significant miRNAs, no pathways were enriched.

This chapter has shown the use of screening miRNAs using a microarray. As mentioned, a large benefit to using techniques such as the NanoString nCounter miRNA microarray is the ability to screen such a large a volume of miRNAs, in this instance 827 miRNAs. This allows for a thorough investigation of the miRNA landscape across a number of different samples. During the normalisation process, it was evident that a large proportion of the miRNAs had similar expression values to the background, which caused them to be excluded from the analysis. The most appropriate normalisation method was used to ensure the greatest number of miRNAs were involved in further analysis. However, as this experiment was outsourced, it is unknown what may have caused the undetectable expression counts. The quality checks of the experiment were as expected, so the cause remains unknown. It is routinely mentioned that miRNA expression is often lower than that of genes and there can be more difficult to measure. As the classification of significance of the miRNAs was altered to a p-value of 0.01 as adjusted p-values were not significant, other techniques are required to produce more statistically significant and robust results. Quantitative polymerase chain reaction (qPCR) is routinely used for validation of gene expression. Instead of individual PCRs for a specific gene (or miRNA), custom panels can be created to PCR a number of miRNAs at the same time. The number of miRNAs analysed at one time is a lot smaller than the microarray – around 92 target miRNAs on a 384-well plate. However, the method is widely used, it is not outsourced and relatively inexpensive and

quicker to run. This technique was chosen as the next smaller screening method, after using the miRNA microarray.

The hypotheses of this chapter are accepted. It has been shown that miRNAs are differentially expressed in hypoxia compared to normoxic conditions among the different glioma categories (overall, GIN and low-grade). The expression of the miRNAs differs between the categories, as the significant miRNAs are upregulated in glioblastomas but downregulated in low-grade gliomas. This chapter has revealed a set of hypoxic-specific set of miRNAs in glioma samples that are likely to play important role in counteracting the stress posed by hypoxic condition. It also confirms that different individual miRNAs are changed in the categories, there was no one miRNA that was significantly expressed across the three groups. The next step of this project is to use qPCR as a smaller screening method to produce more robust and statistically significant results of differentially expressed miRNAs.

4 Chapter 4: LNA miRCURY custom qPCR analysis of glioma samples

4.1 Introduction

After the difficulties faced from the NanoString microarray analysis, a second similar experiment was conducted to obtain miRNA expressions that are significantly changed in hypoxia compared to normoxia in glioma samples. A different methodology using qPCR was selected to assess microRNA expression levels. Custom panel qPCR 384-plates were created using Qiagen (locked-nucleic acids) LNA miRCURY technology with 90 manually picked miRNA probes, seen in figure 4.

LNA miRCURY technology was selected as it has been identified to improve generate accurate and reproducible miRNA analysis. Quantification of miRNA presents multiple challenges such as the close sequence identity (170). The Qiagen system was chosen because it is miRNA specific and uses locked-nucleic acids (LNA). LNAs are analogues that have a high affinity for RNA and the ribose ring is 'locked' in place. These locked nucleotides enable thermal stability during the hybridisation to complementary RNA or DNA strands. The melting temperature (T_m) of the duplex increases between 2 – 8 °C. This allows for more accurate discrimination between very similar and small targets. As the targets are often very small, the GC content of primers can vary massively. This can cause low robustness and introduce high uncertainty as the T_m of the miRNA duplex will vary based on the different GC content. However, as mentioned previously, the LNAs increase thermal

stability regardless of GC content of the miRNA. Another issue when amplifying miRNA, is the discrimination between very similar sequences. As they are small sequences, some miRNAs can differ by only a single nucleotide. This means that distinguishing between different miRNAs is important to ensure the miRNA of choice is being amplified. Another advantage of using LNAs is that they can enhance the discriminatory capabilities of the primers and increase affinity for its miRNA complementary strand which improves the specificity and sensitivity for all miRNA targets. As well as the benefits listed above, the data provided by PCR is expression data, which allows to see the expression level of each miRNA in the sample. With LNA technology, it is more certain that the results are specific and accurate for each individual miRNA chosen.

Using PCR to quantify miRNAs has always been difficult as the length of usual primers are often the same length as the miRNA itself. Often PCR primers designed for miRNAs result in primer-dimer generation. LNA technology can be used in the PCR setting to increase both specificity and sensitivity. LNAs are introduced into short primers which anneal directly to the miRNA sequence. The LNA miRCURY PCR system can be described in two steps, which can also be depicted in figure 27:

1) Convert the miRNA into cDNA using a miRNA-specific primer using reverse transcriptase.
2) Amplify the cDNA by using the miRNA-LNA containing short primer.

As the NanoString microarray technology struggled to produce statistically significant results with usual parameters ($p<0.05$ with adjusted p-values). Other methods of screening miRNAs were discussed before deciding upon the LNA miRCURY qPCR custom plate system such as RNA sequencing, however, qPCR of miRNAs was more appropriate for this investigation.

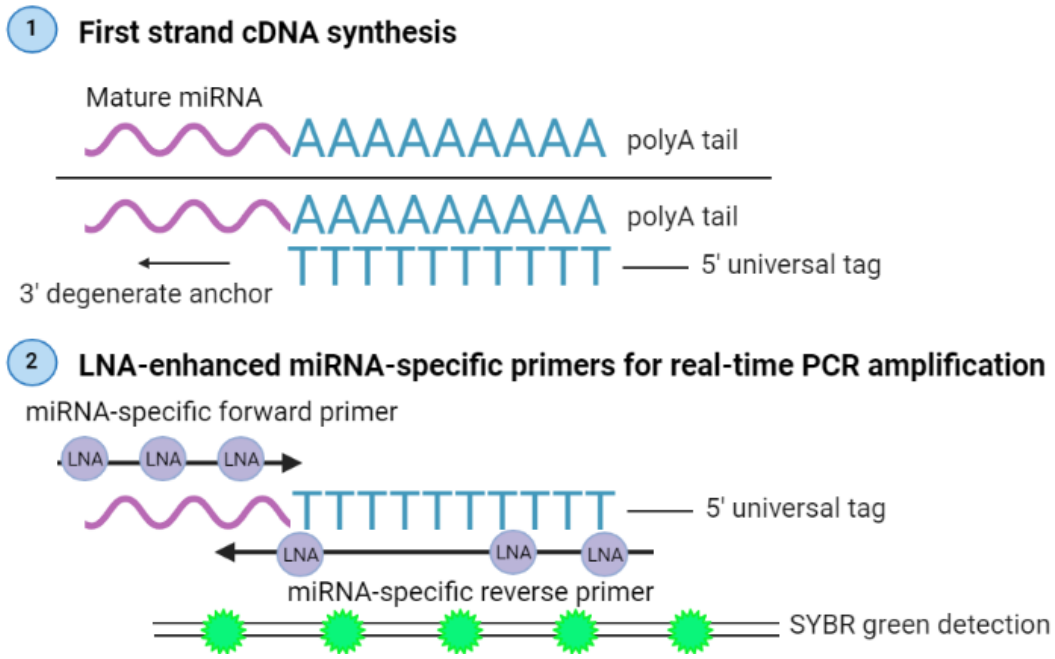

Figure 27. A schematic of miRCURY LNA technology. Step 1 shows cDNA single stranded synthesis. Step 2 shows the PCR amplification using LNA-miRNA-specific primers followed by SYBR green detection. Image created using BioRender.

Hypothesis 1: Individual miRNA levels are differentially expressed in hypoxic gliomas compared to normoxic gliomas.

Hypothesis 2: Differentially expressed miRNAs in hypoxia compared to normoxia differs in high-grade gliomas compared to low-grade gliomas.

4.2 RNA yield and reverse transcriptase

RNA was extracted from 4 primary cell lines (GIN28, GIN31, LGG19 and LGG24) and 2 commercially available cell lines (SF188 and U87). The RNA used was the same RNA used for the NanoString microarray. The RNA was re-quantified before use and analysed and fell into the parameters of a RIN number higher than 8 and A260/A280 and A260/A230 ratios in which the ratios nearest to 1.8.

4.3 qPCR custom plate layout

The format of the qPCR was available in many formats, including custom panels. The custom panels allow for ready-designed miRNA primer mixes to already be inserted into the wells before use. This enables a choice of multiple miRNA targets to be analysed at one time. The plate used was a 384-well plate, allowing four 96-sets of each layout on the plate to allow for 4 samples to be run at the same time.

The handpicked choice of the miRNAs was selected from thorough literature-based searches, and some were determined from the first preliminary analysis of the NanoString data. However, further in-depth NanoString analysis was completed after the qPCR panels were performed, which accounts for some miRNAs that are not featured in the qPCR panels. miR-218-5p, miR-210-3p and miR-606 are the only three miRNAs from the NanoString microarray which were included in the qPCR custom plate layout. The literature-based searches, focused on

individual miRNAs and whether they were researched in either gliomas and/or hypoxia. 90 miRNAs were chosen and are seen in table 18.

Table 18. A table showing a list of the handpicked miRNAs from the miRCURY qPCR panel and the reasons from the literature searches.

miRNA	Reason from literature
hsa-miR-21-5p	It is known to be overexpressed in glioblastomas. It is particularly associated with cell proliferation of glioblastomas (150).
hsa-miR-606	This miRNA was highlighted in the preliminary NanoString array, as potentially significant in low-grade gliomas.
hsa-miR-30e-5p	mir-30e-5p has been linked to hypoxia in a number of cell types including stem cell-derived cardio-myocytes (171) and lung adenocarcinomas (172). One paper links the expression of miR-30e-5p in gliomas with the use of demethylzeylasteral to inhibit glioma growth (173).
hsa-miR-34a-5p	miR-34a-5p is a known tumour suppressor in glioblastomas with low expression levels of miR-34a-5p related to poor survival prognosis (174).
hsa-miR-362-3p	Little is known about the role of miR-362-5p in gliomas however, miR-362-5p has been shown to regulation proliferation and invasion of trophoblastic

	cells in hypoxia (175). There are other studies of miR-362-3p involvement in hypoxia.
hsa-miR-7-5p	miR-7-5p is downregulated in glioblastoma cell lines and is a tumour suppressor in glioblastomas which inhibit cell migration and invasion (176).
hsa-miR-92a-3p	miR-92a-3p is linked into glioblastomas and has been shown to be regulated in glioblastomas and linked to signalling pathways such as Notch-1/Akt (177). miR-92a is part of the miR-17-92 cluster, of which many members are linked to hypoxia, though the knowledge of mir-92a-3p effect in hypoxia is limited.
hsa-miR-132-3p	The expression of mir-132-3p in glioblastomas has conflicting results in multiple papers (178). This miRNA has been shown to be induced in response to hypoxia in mouse and human brain microvascular endothelial cells (179).
hsa-miR-331-3p	mir-331-3p is a tumour suppressor whose expression in lowered in glioblastomas (180). It is also linked to long non-coding RNA GAPLINC which sponges miR-331-3p to promote growth of glioblastoma (181).
hsa-miR-152-3p	miR-152-3p is a tumour suppressor whose expression is decreased in glioblastoma cells and its function is linked to the proliferation, migration and invasion of tumour cells, with an increase in miR-152-

	3p resulting in the sensitising of glioblastoma cells to cisplatin. (182).
hsa-miR-335-5p	Few studies have looked at this particular miRNA in depth, there are very few papers looking at its relevance in glioblastomas and one paper characterising its association with the cystic fibrosis transmembrane conductance regulator (CFTR) gene in which validates that miR-335-5p regulates a number of genes including HIF1α (183).
hsa-miR-106b-5p	miR-106b-5p has been characterised in glioblastoma as an oncomiR which elevates tumorigenesis by targeting tumour suppressor genes such as RBL1, RBL2 and CASP8 (184). There are further studies assessing the functions of miR-106b-5p in glioblastomas linking it to macrophage polarisation (185) and long non-coding RNA GAS5-AS1 (186).
hsa-miR-125b-5p	miR-125b-5p is an oncomiR and has been shown to be upregulated in glioblastomas, its upregulation is a biomarker of poor prognosis and contributes to promoting cell proliferation, protection from apoptosis and increased chemoresistance (187). miR-125b has also shown to be downregulated in low-grade gliomas and low-grade paediatric tumours and its overexpression halts cell growth (188). There are a

	few studies linking miR-125b to hypoxic effect, but not in gliomas.
hsa-miR-17-5p	miR-17-5p is known to be upregulated in glioblastoma cell lines and shown to be upregulated between 3 and 6 fold with the induction of hypoxia (189). miR-17-5p could potentially be another marker of hypoxia in glioblastomas though it's direct affect and function in hypoxic glioblastoma is yet to be elucidated.
hsa-miR-495-3p	miR-495-5p has been studied in glioblastomas and is linked to tumour progression by acting as a sponge for circular RNA (190) and pseudogenes (191). miR-495-5p seems to be relevant to hypoxia but with little in-depth studies and no direct link between glioblastomas and hypoxia.
hsa-miR-210-3p (2 probes)	Mir-210-3p is a known hypoxic marker and has been shown to be increased in hypoxia in glioblastoma cell lines (192). This allows for this miRNA to be a positive control for hypoxic conditions. This miRNA was also identified in the NanoString microarray.
hsa-miR-96-5p	This miRNA was highlighted in the preliminary NanoString array, as potentially significant in low-grade gliomas.
hsa-miR-451a	This miRNA has been shown to be significantly different between glioblastoma patients and healthy

	controls, high levels of miR-451a correlated with positive MGMT expression (193).
hsa-miR-222-3p	miR-222-3p has been investigated in various studies in glioblastoma, with some studies suggesting elevated levels of mir-222-3p is indicative of poor prognosis and linked to increased DNA damage and tumour growth (194). There are various studies linking miR-222-3p with hypoxia, but non detailing the association within glioblastomas.
hsa-miR-128-3p	miR-128-3p has been studied in glioblastoma and has tumour suppressor functions in glioblastomas. miR-128-3p is downregulated in GBM tissues and cell lines and it was found that increased expression of mir-128-3p increases the chemosensitivity of glioblastoma to temozolomide, inhibits expression of proteins in EMT pathway and inhibits cell viability by targeting c-Met (154).
hsa-miR-26b-5p	There are limited studies of miR-26b-5p in glioblastoma and hypoxia, but none have investigated miR-26b-5p directly to characterise its function in either condition or jointly.
hsa-miR-425-5p	miR-425-5p has been shown to be increased in glioblastoma compared to normal brain and has been shown to be involved in the regulation of cell

	proliferation and apoptosis in glioma stem-like cells (195).
hsa-miR-216a-5p	miR-216a-3p has limited reports of its expression and function in glioblastoma but it has been loosely linked to hypoxia with its expression being linked to a marker of hypoxia, HIF1α (196).
hsa-miR-29b-3p	miR-29b-3p is a tumour suppressor miRNA whose expression is downregulated in glioblastoma and that its restoration exerts anti-cancer effects (197). There are a number of papers linking miR-29b-3p to hypoxia in cardiomyocytes but none linking miR-29b-3p to hypoxia in glioblastomas.
hsa-miR-146a-5p	miR-146a-5p has been identified within glioblastomas and linked with neural stem cell proliferation, differentiation and migration by regulating Notch1 (198).
hsa-miR-149-5p	miR-149-5p is upregulated in glioblastomas, which effects the target gene caspase 2, however it has also been reported that it can be downregulated in glioblastomas, effecting AKT1 which also enhances chemosensitivity to TMZ (199).
hsa-miR-199a-3p	miR-199a-3p has been studied in glioblastomas, including that it is under-expressed in glioma samples and that overexpression of miR-199a-3p suppresses cell proliferation by regulation of the Akt/mTOR

	pathway (200). There has recently been study looking at hypoxia-induced glioma-derived exosomal miR-199a-3p and its role promoting ischemic injury by inhibiting the mTOR pathway (201). However, there are few studies assessing the role of miR-199a-3p in hypoxia with GBM tumours.
hsa-miR-487b-3p	miR-487b-3p has been identified as a miRNA that co-regulates TP53 and Akt for glioma development and contributes to the mediation of glial cell line-derived neurotrophic factor induced proliferation and migration of glioma cells (202).
hsa-miR-130a-3p	miR-130a-3p is downregulated in GBM compared to human astrocyte cells and cells transfected with a miR-130a-3p mimic exhibited lower growth rate than the control, it also inhibits migration and TMZ resistance by targeting Sp1 (203). These miRNA is also involved with long non-coding RNAs and a feedback loop involving mTOR to inhibit tumorigenesis (204). miR-130a-3p has been shown to be involved in inhibiting glycolysis with long non coding RNAs under hypoxia and HIF1α is a target of miR-130a-3p in hepatocellular carcinoma cells (205), though no link has yet been reported in GBM.
hsa-miR-155-5p	miR-155-5p is a known oncomiR in glioblastoma and has been shown that when targeted with peptides

	that reduction of miR-155-5p induces capase-3 activation and apoptosis in TMZ-resistant glioma cell lines (206). miR-155-5p has also been identified in paediatric GBM and is significantly correlated with the expression of PD-L1 (207). miR-155-5p has been linked to the transcription factor ELK3 and the hypoxic response in endothelial cells (208). No similar studies have been conducted in GBM.
hsa-miR-185-5p	miR-185-5p has been shown to be involved in the PI3K/AKT pathway due to involvement with FoxD2-AS1 to promote glioma expression (209). There are many studies reporting its interaction with different long non-coding RNAs which affect glioma growth. Studies shows its interaction with long non-coding RNAs to attenuate hypoxia induced pyroptosis in cardiomyocytes (210). Though none have been reported in hypoxia in GBM.
hsa-miR-296-5p	miR-296-5p has been reported to enhances glioma invasiveness by downregulating caspase-8 and nerve growth receptor (211).
hsa-miR-100-5p	miR-100-5p is found to be decreased in glioblastoma cell lines, however, once restored a reduction in cell viability and proliferation is seen, this has been linked to the targeting of SMARCA5 and ErbB3 in tumour initiating cells (212). This miRNA has also been

	studied in hypoxia in endothelial cells, in which overexpression of miR-100-5p inhibits dysfunction of human placental microvascular endothelial cells (HPMECs) under hypoxia by downregulating HIPK2 to activate the PI3K/Akt pathway (213).
hsa-miR-16-5p	miR-16-5p is downregulated in glioma cell lines and its overexpression decreases cell viability, proliferation, induces caspase 3/7 activity and apoptosis (214). miR-16-5p has been linked to hypoxia in cardiomyocytes but no studies assessing miR-16-5p function in hypoxia in cancers.
hsa-miR-31-5p (2 probes)	Co-expression of miR-31-5p and miR-145-5p were shown to inhibit glioblastoma invasion in mesenchymal stem cells (215). In hypoxia, HIF1α-SP1 interaction disrupts a regulatory loop involving miR-31-5p to promote non-small cell lung cancer progression (216). This has not yet been investigated in glioblastomas.
hsa-miR-142-5p	BRD4 promotes glioma stemness by enhancing miR-142-5p mediation of the Wnt/β-catenin signalling pathway (217). In hypoxia, in cardiomyocytes, it has been reported that the suppression of miR-142-5p reduces hypoxia-induced apoptosis by targeting SIRT7 (218).

hsa-miR-27a-3p	miR-27a-3p has been reported in many studies, reporting its various roles in glioblastoma. One of these shows that miR-27a-3p is significantly lower expressed in GBM samples compared to normal brain tissue and has a negatively correlation of expression with *EGFR* (219). Studies has been conducted to look at the roles of miR-27a-3p in hypoxia-induced cells or cardiomyocytes but none looking specifically at the effect of hypoxia on miR-27a-3p in cancer or GBM.
hsa-miR-148b-3p	miR-148b-3p expression level was significantly higher in GBM cell lines than in control with overexpression of miR-148b-3p inhibiting MMP-2 and MMP-9 and downregulating Wnt1 protein, showing that miR-148b-3p has the ability to inhibit invasion and migration in GBM cell lines (220).
hsa-miR-107	miR-107 is downregulated in glioma cell lines (U87) and overexpression of miR-107 suppressed glioma proliferation, invasion and reduced MMP-12 expression (221). In colon cancers it has been shown the p53 regulates miR-107 which in turn can decrease hypoxia signalling by suppressing the expression of HIF1β (222). However, this pathway involving miR-107 has not been studied in glioblastoma.

hsa-miR-199a-5p	A few studies have looked at miR-199a-5p in glioblastoma, including that the expression of miR-199a-5p is reduced in glioma cell lines and its overexpression inhibits glioma proliferation, invasion and migration and miR-107 has a direct negative correlation of expression with magnesium transport 1 (MAGT1) with its increased expression leading to significantly increased glioma proliferation, invasion and migration (223). In multiple myeloma miR-199a-5p has been identified in a hypoxia/AKT/miR-199a-5p loop in which miR-199a-5p is downregulated in hypoxic multiple myeloma cells (224). Though miR-199a-5p has been directly linked to hypoxia, there are no studies specifically identifying miR-199a-5p in hypoxia in glioblastoma cells.
hsa-miR-26a-5p	There are few studies targeting miR-26a-5p in glioblastoma, however, one paper has shown that when glioma cell lines are treated with rapamycin, glioma growth is inhibited and autophagy promoted via a miR-26a-5p/DAPK1 axis (225), showing that mir-26a-5p has involvement within glioblastomas. Mir-26a-5p has been shown to protect cardiomyocytes from hypoxia/reoxygenation injury by targeting WNT5A and inhibiting the Wnt/β-catenin signalling pathway (226). miR-26a-5p protective

	function against hypoxia has not been reported in cancer or glioblastoma.
hsa-miR-382-5p	miR-382-5p expression is lower in glioma tissues compared to non-tumour brain tissues but found that miR-382-5p levels were high in U87 and U251 cell lines, though upregulation of miR-382-5p significantly decreased glioma cell proliferation (227). In gastric cancer, miR-382-5p has been shown to be induced by HIF-1α as a pro-angiogenic miRNA which targets a tumour suppressor phosphatase and tensin homolog (228). However, miR-382-5p link with hypoxia in glioblastoma as not yet been characterised.
hsa-miR-181a-5p	Multiple studies have been conducted investigating the various roles and functions of miR-181a-5p in glioblastoma. miR-181a-5p has been studied as a tumour suppressor in gliomas and is shown to inhibit proliferation and invasion of drug-resistant glioma cells by targeting the F-box protein 11 (229). miR-181a-5p also modulates osteopontin expression in glioblastoma cells (230). miR-181a-5p was also found to have a further 2-3 fold downregulation following hypoxia induction in glioma cells and Bcl-2 is a target of miR-181a-5p which allows for apoptotic escape (189).

hsa-miR-205-5p	miR-205-5p is decreased in glioblastoma cells which results in an increased expression of the long non coding RNA SNHG5 and consequently promotes glioma proliferation (231). Conversely to glioblastoma, miR-205-5p is significantly induced under hypoxia in cervical and lung cancer cells which promotes epithelial-mesenchymal transition by targeting ASPP2 (232).
hsa-miR-9-5p	miR-9-5p is found to be decreased in glioblastoma cells, and it has been found to mediate ABCC1 to increase the sensitivity of glioma cells to temozolomide (233). miR-9-5p has been found to mediate BNIP3 which is affected by circJARID2 to regulate hypoxia-induced injury in rat-derived cardiac cells (234).
hsa-miR-374b-5p	miR-374b-5p is downregulated in glioma cells and is a tumour suppressor and overexpression of miR-374b-5p reduced proliferation, migration, invasion and vasculogenic mimicry and that MMP14 is a direct target of miR-374b-5p (235). However, there is limited information and studies on miR-374b-5p in hypoxia in cancer.
hsa-miR-376c-5p	Little is known about this particular miRNA overall, so it was included in this screen to determine if it was affected by hypoxia in GBM. It Is known to be

	downregulated in breast cancer compared to normal breast tissue (236).
hsa-miR-19a-3p	miR-19a-3p has been shown to be upregulated in glioma tissues and cell lines with PTEN being a direct target of miR-19a-3p which in gliomas, causes PTEN downregulation in gliomas and consequently promotes cell proliferation, migration and invasion of glioma cells (237). miR-19a-3p is shown to mitigate hypoxia-induced apoptosis in cardiomyocytes by downregulating CCL20 and inactivating MAPK (238). However, these roles of miR-19a-3p in hypoxia have not been reported within cancer or glioblastoma.
hsa-miR-148a-3p	miR-148a-3p is overexpressed in GBM tissues compared with normal brain tissues and has been shown to target the factor inhibiting hypoxia (FIH1) to promote HIF1α and Notch signalling, this shows that miR-148a-3p and miR-31 can regulate glioma growth to activate angiogenesis even in normoxic conditions (239).
hsa-miR-93-5p	miR-93-5p has been shown to lesser expression in U87 glioma cell lines compared with normal human brain glial cell line, and MMP2 has been shown to be a direct target of miR-93-5p and increasing miR-93-5p expression, decreases MMP2 expression resulting in inhibition of proliferation in glioma cells

	(240). An *in vivo* study in mice shows that under hypoxia miR-93-5p is downregulated compared to the control and that the miRNA is sponged by circHIPK3 to activate the Rac1/PI3K/AKT pathway (241). There are no direct studies linking hypoxia to miR-93-5p expression and investigating its roles in cancer or glioblastoma.
hsa-miR-191-5p	miR-191-5p has been identified as an oncomiR in glioblastoma, which high expression levels compared to controls and its overexpression promoted increased growth of glioblastoma cells and considered a poor prognostic marker for GBM (242). Though no links to miR-191-5p to hypoxia in GBM have been reported, miR-191-5p has been shown to be hypoxia and estrogen responsive in breast cancer and promotes breast cancer cell proliferation and migration (243).
hsa-miR-151a-5p	miR-151a-5p has increased expression in lung cancer compared to peri-carcinomatous tissue (244) and miR-151a-5p has been shown to be associated with hypoxia in mesothelioma (245). No direct links to GBM with miR-151a-5p have been reported.
hsa-miR-106a-5p	Increased levels of miR-106a-5p are found in glioblastoma and is significantly associated with a lower probability of 2-year overall survival (194). miR-

	106-5p has been shown to target STAT3 and consequently downregulate the STAT3/HIF1α pathway in breast cancer and lower miR-106a-5p levels are associated with poor survival in breast cancer patients (246). However, the expression of miR-106a-5p in hypoxia was not quantified in this study compared to normoxia and has not been investigated in glioblastomas.
hsa-miR-24-3p	miR-24-3p is increased in glioma cells and has been shown to promote cell proliferation in glioma cells which has been found to occur by regulating MXI1 synergistically with miR-27a-3p (247). However in breast cancer miR-24-3p has been shown in induce chemoresistance and is shown to directly target FIH1, as miR-24-3p expression increases in hypoxic conditions, FIH1 decreases which consequently causes the upregulation of HIF1α (248).
hsa-miR-27b-3p	miR-27b-3p is a tumour suppressive miRNA which is downregulated in glioblastoma cells and overexpression of miR-27b-3p inhibits glioma proliferation migration and induces apoptosis, the inhibition of glioma tumours via overexpression of miR-27b-3p was also reported using xenografted glioma tumours *in vivo* (249). Though miR-27b-3p has not been assessed in glioblastoma in relation to

	hypoxia, miR-27b-3p levels in hypoxia in colorectal cancers have and showed that miR-27b-3p levels were higher in moderate hypoxia (2% O_2) than marked hypoxia (0.5% O_2) and hypoxia levels of mir-27b-3p were all higher than normoxic expression (250).
hsa-miR-10a-5p	Mir-10a-5p has been shown to be sponged by long non-coding RNA PTENP1 which prevents its targeting to PTEN and lower miR-10a-5p expression predicted better overall survival from gliomas and lower miR-10a-5p expression results in increased apoptosis with increased cleaved caspase-3 and Bax (251). No direct association between hypoxia and miR-10a-5p has yet been identified in cancer.
hsa-miR-186-5p	Mir-186-5p is a tumour suppressive miRNA which has been shown to be downregulated in glioma cell lines compared to normal brain cell lines, miR-186-5p expression represses invasiveness of glioma cell lines and migration and downregulates components of the NF-kB signalling pathway which is involved in proliferation and cell survival such as Erk1/2 and mir-186-5p was also shown to directly target FGF2 and RelA (252). In oesophageal squamous cell carcinoma, HIF1α was found to be a direct target of miR-186-5p, however the long non-coding RNA

	SNHG6 sponges miR-186-5p, lowering its expression which consequently promotes HIF1α expression (253). However, the effect of hypoxia itself was not identified and this relationship has not yet been confirmed within glioma cells.
hsa-miR-181b-5p	miR-181b-5p is reported as a tumour suppressor miRNA and that overexpression of miR-181b-5p sensitises glioblastoma cells to TMZ, this is as Bcl-2 is a target gene of miR-181b-5p whose expression decreases with the miRNA increase and also inhibited by TMZ to increase glioblastoma apoptosis (138). Interestingly miR-186-5p is upregulated in gall bladder cancer tumour tissue and a mir-181b-5p antagomir was used to show that it exacerbated the decrease of cell viability under hypoxia and glucose consumption was significantly upregulated in hypoxia and these changes were reverted by the miR-181b-5p antagomir of miR-181b-5p (254).
hsa-miR-23b-5p	miR-23b-5p is downregulated in glioma tissues and cell lines compared with normal human astrocyte cells and a miR-23b-5p mimic was used to show that miR-23b-5p overexpression inhibits proliferation, promotes apoptosis and increase chemosensitivity to TMZ (255). However, miR-23b-5p has not yet been studied under hypoxia in cancer or glioblastomas.

has-miR-29a-3p	miR-29a-3p is downregulated in glioma tissues compared to normal brain tissues and that its direct target Gab1 is upregulated, in miR-29a-3p downregulation, which promotes glioma cell proliferation (256). In paediatric tumours, mir-29a-3p levels are lower than non-neoplastic brain tissues and that Notch2 is a putative target of miR-29a-3p and low levels of miR-29a-3p and miR-107 and miR-181c-5p allow for the activation of Notch2 signalling (257). However, the influence of hypoxia on miR-29a-3p in cancers has not fully investigated.
hsa-miR-628-5p	miR-628-5p is suggested to be a tumour suppressive miRNA whose expression levels are downregulated in comparison to normal brain tissues and miR-628-5p overexpression results in reduced glioma proliferation and induced cell cycle arrest in G1, mir-628-5p also binds to DDX59 which is linked to p-AKT (258). Little is known about this miRNA in hypoxia in cancers.
hsa-miR-23a-5p	miR-23a-5p is thought to be an oncomiR in glioblastoma and its overexpression promotes cell migration and invasion and indirectly targets the repressor of MMP14 to promote glioma cell migration (259). Few studies have focussed on the direct effect of hypoxia on mir-23a-5p in cancers or glioblastoma.

hsa-miR-20a-5p	Increased mir-20a-5p levels are significantly associated with an increased hazard of death, lower probability of 2-year disease-free survival and miR-20a-5p upregulation is associated with advanced astrocytomas, glioma-genesis and promote invasiveness by targeting the tissue inhibitor of metalloproteinases-2 (TIMP2) (194). miR-20a-5p is found to be downregulated in hypoxia (0.2% O_2) compared to normoxia in GBM cell lines by more than 2-fold (260). However, no further studies has investigated the effects of hypoxia on miR-20a-5p in hypoxia.
hsa-miR-488-3p	This miRNA was highlighted in the preliminary NanoString array, as potentially significant in low-grade gliomas. Though mir-488-3p has been shown to be at a lower expression in glioma cell lines and tissues than normal brain tissues and astrocytes and the knockdown of miR-488-3p along with miR-190a-5p knockdown promotes malignant behaviours of gliomas due to their interactions with PVT1 (261).
hsa-miR-99b-5p	miR-99b-5p expression levels are reported to be lower in GBM compared with non-neoplastic brain tissues and decreased expression of miR-99b-5p is associated with aggressive tumour progression and overexpression of mir-99b-5p resulted in inhibition of

	glioma cell migration and invasion (262). No studies have yet reported the effect of hypoxia on miR-99b-5p in cancer or glioblastomas.
hsa-miR-137	miR-137 is under-expressed in GBM and is tumour suppressive miRNA, the enforcement of its expression has been shown to have many anti-tumour effects such as inhibition of glioma proliferation and stem cell differentiation, the induction of apoptosis, the inhibition of invasion and angiogenesis and the suppression of glioma stem cell development and stemness maintenance (263). One study has shown that miR-137 is downregulated in hypoxic conditions and consequently hypoxia-induced DNA methylation results in the downregulation of miR-137 in GBM cells (264). Though this study shows a link between miR-137 and hypoxia in glioma cells, further functional and mechanistic assays are required to show the effects of hypoxia on mir-137 more than the expression.
hsa-miR-30d-5p	miR-30d-5p levels are downregulated after surgical resection compared to pre-operation levels also miR-30d-5p levels are increased in GBM patients compared to control levels, also increased levels of miR-30d-5p is associated with increased risk of death (265).

hsa-miR-141-3p	miR-141-3p is significantly downregulated in glioma tissues and cell lines compared with normal brain tissues, the expression also decreased in GBM compared to low-grade glioma and decreased in low-grade glioma compared to normal brain tissues, a target of miR-141-3p ATF5, is repressed by miR-141-3p which inhibits glioma growth (266). miR-141-3p has been found to be downregulated in breast cancer cell lines in hypoxia and that miR-141-4p overexpression attenuates hypoxia-induced cell migration and inhibits the hypoxia-activated HMGB1/HIF1α signalling pathway in breast cancer (267).
hsa-miR-324-5p	miR-324-5p is downregulated in glioblastoma tissues compared to normal brain tissues as potentially significant in low-grade gliomas, circSERPINE2 has been shown to sponge miR-324-5p in glioblastomas to accelerate its degradation, BCL2 is a target of miR-324-5p and by decreases its expression allows for the upregulation of the anti-apoptotic gene BCL2 (268). An indirect link between hypoxia and miR-324-5p in glioblastomas has been suggested, HIF1α, a transcription factor, activates the hedgehog signalling pathway, which is regulated by SMO, a target of miR-

	324-5p (269). However, further investigations are required to confirm this assumption.
hsa-miR-4454	miR-4454 is downregulated in chemo-resistant cell lines compared to normal colorectal cancer cell lines and directly targets GNL3L which is associated with drug-resistance (270). miR-4454 is downregulated in hypoxia compared to normoxia in melanoma exosomes (271).
hsa-miR-365a-3p	miR-365a-3p has been shown have low expression in gastric cancer compared with normal tissues and that low expression of miR-365a-3p is a marker of poor prognosis (272). miR-365a-3p is linked to cerebral infarction and hypoxia-ischemic brain damage (273).
hsa-miR-379-5p	miR-379-5p is downregulated in glioma tissues and cell lines compared with normal human astrocytes, upregulation of mir-379-5p results in the inhibition of viability, migration and invasion of glioma cells and EMT by regulating microsomal glutathione transferase 1 (MGST1) (274). Though its response to hypoxia in GBM and cancer is unknown.
hsa-miR-181c-5p	This miRNA was highlighted in the preliminary NanoString array. miR-181c-5p has been linked to GBM as was differentially expressed in regards to MGMT expression (275). miR-181c-5p has also been

	loosely linked to hypoxia within glioblastoma with its regulation being increased under hypoxic conditions (189).
hsa-miR-221-3p	miR-221-3p is upregulated in glioblastomas, and upregulation of miR-221-3p in GBMs without MGMT promoter methylation has a significant negative prognostic association (187). A further 3-6 fold upregulation of miR-221-3p was seen under hypoxic conditions in GBM cell lines (189). However, further characterisation of the effect of hypoxia on miR-221-3p needs to be elucidated.
hsa-miR-335-5p	CCNB2 is a direct target of miR-335-5p, though the levels of miR-335-5p have not been identified in gliomas, the levels of CCBN2 are upregulated in gliomas as they are in lung adenocarcinoma and where miR-335-5p is downregulated (276). miR-335-5p is linked to hypoxia by HIF-1α and CFTR gene in bronchial epithelial cells (183).
hsa-miR-99a-5p	The deregulation of miR-99a-5p in controls compared to breast cancer tissues and plasma levels have suggested the use of miR-99a-5p as a potential non-invasive biomarker for breast cancer (277). Hypoxia has been shown to downregulate the expression of miR-99a-5p in H9c2 cells and that inhibition of long non-coding RNA THRIL has a protective effect

	against hypoxia-induced injuries by upregulation miR-99a-5p expression in H9c2 cells (278). This effect has not yet been studied or reported in GBM.
hsa-miR-29c-3p	miR-29c-3p has been shown to be involved in a regulatory loop in glioblastomas consisting of CD276, miR-29c-3p and Myc to combat natural killer cell cytotoxicity (279). In medulloblastoma, miR-29c-3p expression is suppressed by long non-coding RNA CRNDE which decreases chemosensitivity (280). In human bronchial epithelial cells, miR-29c-3p has been shown to target HIF3A (281) suggesting a hypoxic response.
hsa-miR-140-5p	miR-140-5p is decreased in glioblastomas compared to normal brain tissues and increased miR-140-5p suppresses cell proliferation and cell cycle and VEGFA and MMP2 are targets of miR-140-5p which are conversely correlated with miR-140-5p levels in glioblastomas (282). No reports link miR-140-5p to hypoxia in glioblastoma but there are reports of miR-140-5p being involved in protection from hypoxic injury (283).
hsa-miR-184	miR-184 is downregulated in GBM tissues and cells compared with normal brain, increased expression of mir-184 inhibits invasiveness and migration of U87 cells and directly targets STC2, whose

	overexpression is correlated with poor prognosis and is conversely associated with mir-184 (284). Conversely, a different study shows that mir-184 is upregulated in GBM glioma cells and that factor inhibiting HIF-1 (FIH-1) is a direct target of miR-184 which positively regulates HIF-1α (285).
hsa-miR-145-5p	miR-145-5p levels are lower in glioblastoma tissues compared with low-grade gliomas and with normal brain tissues and that low miR-145-5p is significantly associated with poor prognosis (286). miR-145-5p has been shown to be HIF-1 dependent and is significantly upregulated in hypoxia in glioblastoma (260). The differences between miR-145-5p expression in hypoxia and normoxia in glioblastomas need to be investigated and to show the functional and mechanical differences exerted by hypoxia.
hsa-miR-15b-5p	miR-15b-5p has been shown to be downregulated in glioma cell lines and tissues compared with normal brain, increased expression of miR-15b-5p prevents cell proliferation by inducing apoptosis and supresses cell migration and invasion and SALL4 is a direct target of miR-15b-5p which is a zinc-finger transcription factor (287). No information is yet available of the effect of hypoxia on miR-15b-5p in GBM or cancer.

hsa-let-7-5p	Let-7-5p is downregulated in gliomas which is also related to the resistance of glioblastomas to radiation (288). LIN28A a known regulator of let-7-5p has been shown to be induced by hypoxia in colon cancer and therefore consequently effects the expression of let-7-5p (289)
hsa-miR-218-5p	miR-218-5p is downregulated in glioma cell lines and tissues compared with normal brain and increased expression of miR-218-5p results in inhibition of glioma cell proliferation and induced cell cycle arrest and apoptosis and LHFPL3 is a direct target of miR-218-5p to regulate EMT (290). Little is known of miR-281-5p in response to hypoxia in cancer. This miRNA was also identified in the NanoString microarray.
hsa-miR-98-5p	miR-98-5p is downregulated in glioblastoma tissues compared with peritumour tissues and lncRNA NEAT1 promotes glioblastoma progression by regulating miR-98-5p/BZW1, an oncogene (291). A feedback loop consisting of DSCR8/miR-98-5p/STAT3/HIF-1α are important in the progression of ovarian cancer (292) as STAT3 is a direct target of mIR-98-5p, this miRNA is likely to be effected by hypoxia but no reports have shown this yet in glioblastomas.

hsa-miR-421	miR-421 is downregulated in glioblastoma compared to normal controls and is sponged by circular RNA circSCAF11 and positively regulates transcription factor SP1 which is shown to target VEGFA (293). Hypoxia has been shown to increase the levels of miR-421 in gastric cancer to promote metastasis and inhibit apoptosis by targeting e-cadherin and caspase-3 (294). The link between hypoxia and miR-421 has not yet been studied in glioblastomas.
hsa-miR-154-5p	miR-154-5p is downregulated in glioblastoma tissues and cell lines compared to normal controls and the overexpression of miR-154-5p inhibits the malignant behaviour of glioblastoma cells (295). miR-154-5p has been found to be involved in the lncRNA MAPKAPK5-AS1/PLAGL2/HIF-1α loop which promotes hepatocellular carcinoma progression and is important in hypoxic conditions (296). However, no studies have yet investigated this regulatory loop in glioblastomas.
hsa-miR-25-5p	miR-25-5p is characterised as an oncomiR is gliomas and shown to be overexpressed which increased glioma cell proliferation by targeting CDK inhibitor and increasing S/M phases in the cell cycle (297). In H9c2 cells, miR-25-5p is overexpressed and downregulates HMBG1 which inhibits apoptosis after

	hypoxia/reoxygenation (297). The effect of hypoxia on miR-25-5p has not been yet reported in glioblastomas.
UniSp3	A positive PCR control for the miRNA custom qPCR plate provided by Qiagen.
UniSp6	A reverse transcriptase control for the miRNA custom qPCR plate provided by Qiagen.
Cel-miR-39-6p	A non-human miRNA control that should not be present in human tissues/cells.

4.4 GeneGlobe Analysis

To analyse the output of miRNA expression was conducted using GeneGlobe analysis software by Qiagen which is compatible with the Qiagen LNA miRCURY qPCR technology. The cycle threshold (Ct) data was imported into the software and parameters were selected such as 40 Ct cut-off and unpaired t-test and 2-tail p-value.

4.4.1 Normalisation methods

GeneGlobe analysis software had three different normalisation methods available: geNorm, NormFinder and Global Ct mean of expressed miRNAs. Each of the methods were applied to the data, to determine the most appropriate normalisation method for further analysis to continue. The set-up of the custom panels only allowed for U87 samples to be run in duplicate rather than triplicate which skewed the data. From this point

forward U87 was removed from the GeneGlobe analysis. The following sections will describe each of the normalisation methods.

4.4.1.1 geNorm

The geNorm normalisation method produces a normalisation factor based on either predefined reference miRNA or up to 10 miRNAs from the panel which have the best geNorm-calculated stability measures if their values are less than 1.5. The stability measures are the average pairwise variation between a reference miRNA and all other reference miRNAs using stepwise exclusion of the worst scoring miRNAs. This method uses the principle that the expression ratio between any two reference miRNAs, in all samples, should be identical (298). Table 19 shows the miRNAs selected as the reference miRNAs based upon their stability factor.

Table 19. miRNAs selected as reference miRNAs in geNorm normalisation, based on their stability factor being less than 1.5.

miRNA	Stability Factor
hsa-miR-149-5p	0.0891
hsa-miR-27a-3p	0.0950
hsa-miR-181a-5p	0.0949
hsa-miR-19a-3p	0.0945
hsa-miR-24-3p	0.0913
hsa-miR-27b-3p	0.0943
hsa-miR-99b-5p	0.0951
hsa-miR-365a-3p	0.0919

hsa-miR-99a-5p	0.0930
hsa-miR-145-5p	0.0852

The Ct values of all the selected miRNAs were averaged for each triplicate of each sample to give an arithmetic mean and the arithmetic means were averaged to give an average arithmetic for each sample as shown in table 20.

Table 20. Average arithmetic Ct mean of the selected reference miRNAs for the geNorm method.

Sample	**Arithmetic Mean**	**Average Arithmetic Mean**
GIN28 Normoxic	32.36	32.28
	32.26	
	32.22	
GIN28 Hypoxic	34.04	33.83
	33.52	
	33.94	
SF188 Normoxic	32.44	32.32
	32.20	
	32.32	
SF188 Hypoxic	32.12	32.02
	31.84	
	32.11	
LGG19 Normoxic	27.65	28.12

	28.03	
	28.69	
LGG19 Hypoxic	27.85	28.45
	28.79	
	28.70	
LGG24 Normoxic	30.62	30.61
	30.77	
	30.45	
LGG24 Hypoxic	29.61	29.60
	29.68	
	29.53	
GIN31 Normoxic	32.41	33.35
	32.60	
	35.04	
GIN31 Hypoxic	33.85	33.92
	33.85	
	34.05	

This method considers the whole miRNA panel and avoids bias/affects by grouping. geNorm helps to robustly detect subtle changes within miRNA expression by normalising against specifically chosen reference miRNAs as opposed to the whole miRNA expression landscape.

To visualise the effect of the different normalisation methods, a principal component analysis (PCA) plot and a heatmap were created. Figures 29

and 30 show the PCA plot and heatmap respectively for the geNorm normalised data.

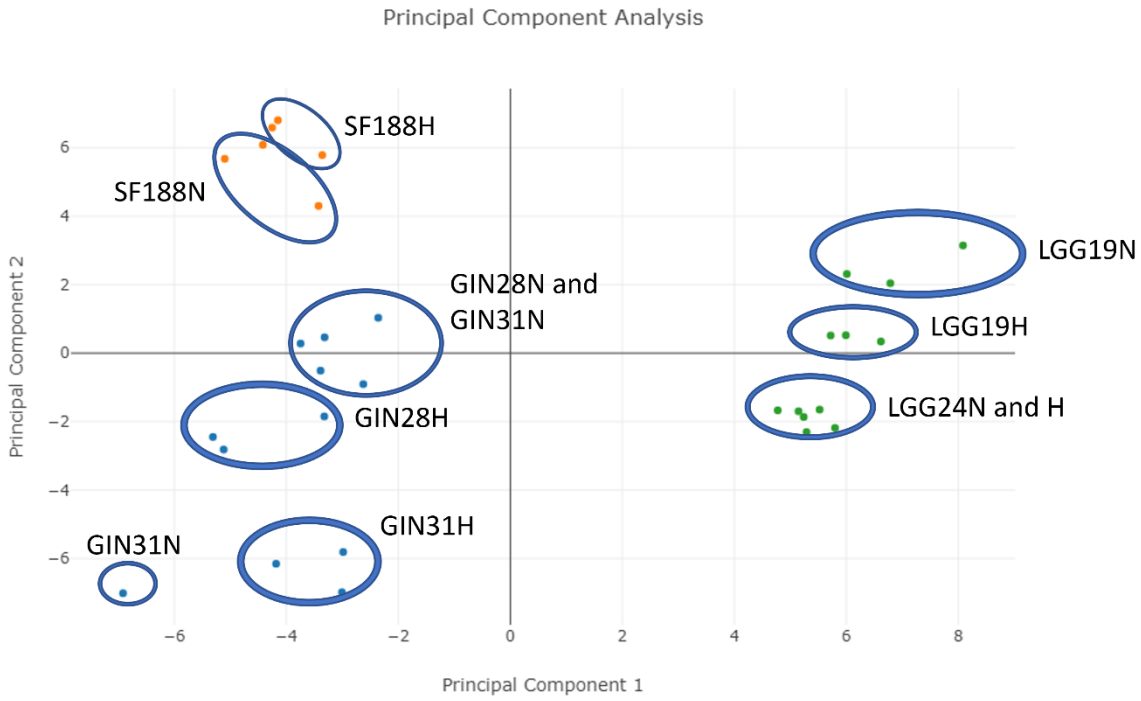

Figure 28. A PCA plot for the geNorm normalisation method. The blue dots are GBMs, green dots are low-grade gliomas and orange dots are paediatric samples.

The PCA plot in figure 28 shows the clustering of the samples. Using the geNorm method, the samples have clustered according to their category (low-grade, paediatric and GBM) which emphasises that the categories are distinctly different from each other even though they are all classed as gliomas. Within the categories, some samples have separated into distinct hypoxic and normoxic groups which is the case for LGG19 and GIN28. Figure 29 shows the heatmap using the geNorm method.

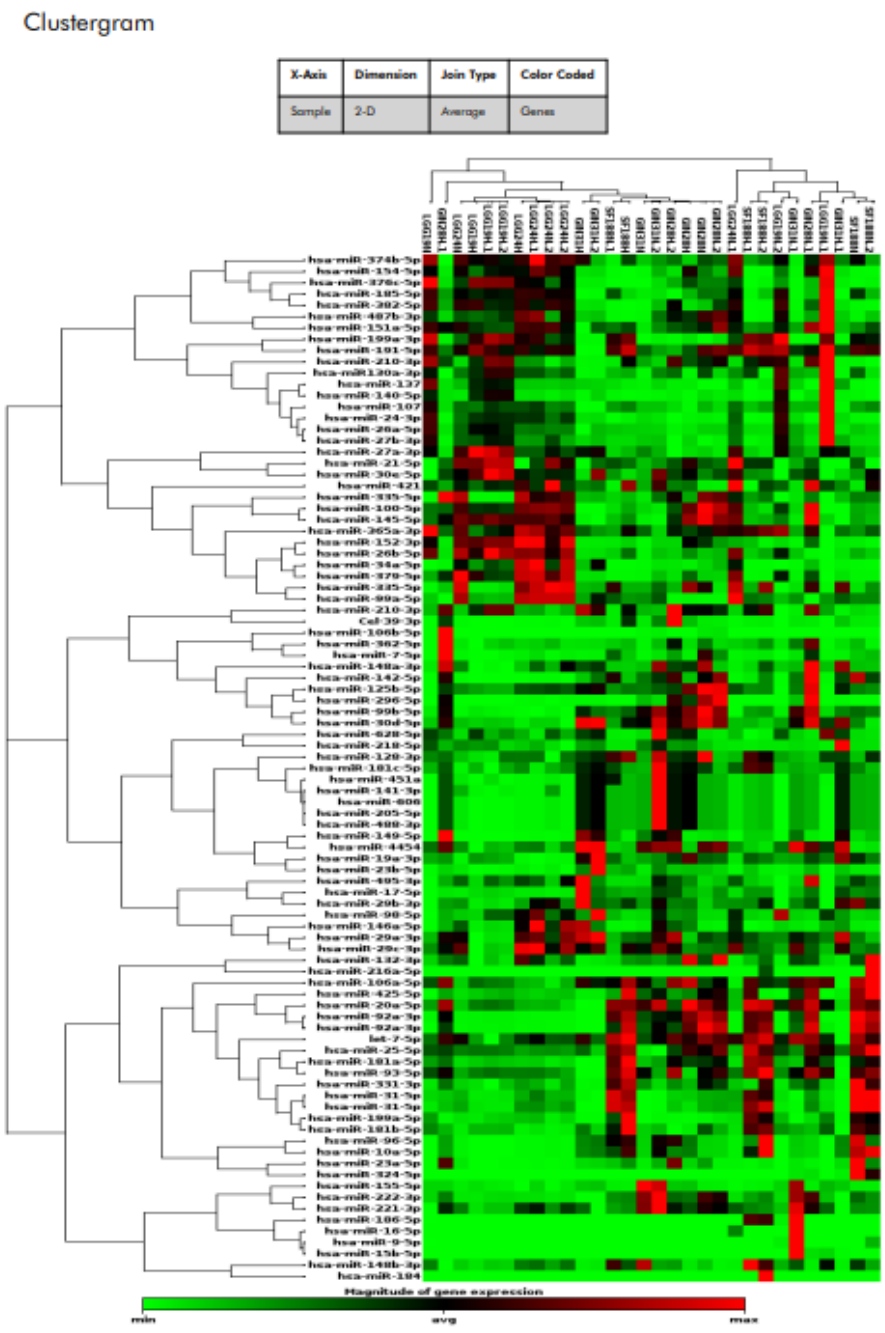

Figure 29. Heatmap produced for the samples using the geNorm normalisation method.

4.4.1.2 NormFinder

The second normalisation method, NormFinder, finds optimal reference miRNAs out of a group of candidate miRNAs using an algorithm. This method can also take into account the treatment groups of miRNAs, in

this case, hypoxic status or glioma type, which could result in compensating expression. Using NormFinder the following miRNAs displayed in table 21 are the reference miRNA set for this normalisation method.

Table 21. Table of reference miRNA selected using the NormFinder normalisation method.

miRNA	Standard Deviation
hsa-miR-181a-5p	0.19
hsa-miR-19a-3p	0.09
hsa-miR-27b-3p	0.3
hsa-miR-29a-3p	0.1
hsa-miR-99b-5p	0.19
hsa-miR-30d-5p	0.14
hsa-miR-4454	0.04
hsa-miR-365a-3p	0.18
hsa-miR-29c-3p	0.07
hsa-miR-145-5p	0.21

The ct values of all the selected reference miRNAs were averaged for each triplicate of each sample to give an arithmetic mean and the arithmetic means were averaged to give an average arithmetic for each sample as shown in table 22.

Table 22. Table of the average arithmetic Ct mean of the selected reference miRNAs for the NormFinder method.

Sample	Arithmetic Mean	Average Arithmetic Mean
GIN28 Normoxic	31.68	31.55
	31.41	
	31.56	
GIN28 Hypoxic	33.70	33.35
	33.08	
	33.27	
SF188 Normoxic	32.64	32.62
	32.55	
	32.66	
SF188 Hypoxic	31.92	32.02
	31.90	
	32.24	
LGG19 Normoxic	27.72	28.23
	28.07	
	28.89	
LGG19 Hypoxic	28.65	28.95
	29.09	
	29.11	
LGG24 Normoxic	30.73	30.80

	30.90	
	30.79	
LGG24 Hypoxic	29.67	29.70
	29.74	
	29.70	
GIN31 Normoxic	32.45	33.29
	32.48	
	34.94	
GIN31 Hypoxic	33.82	33.93
	33.89	
	34.09	

Similarly to the geNorm data, a PCA plot and heatmap were generated to assess the differences in the normalisation methods, figures 30 and 31 respectively. A similar grouping to the geNorm method was found when comparing PCA plots.

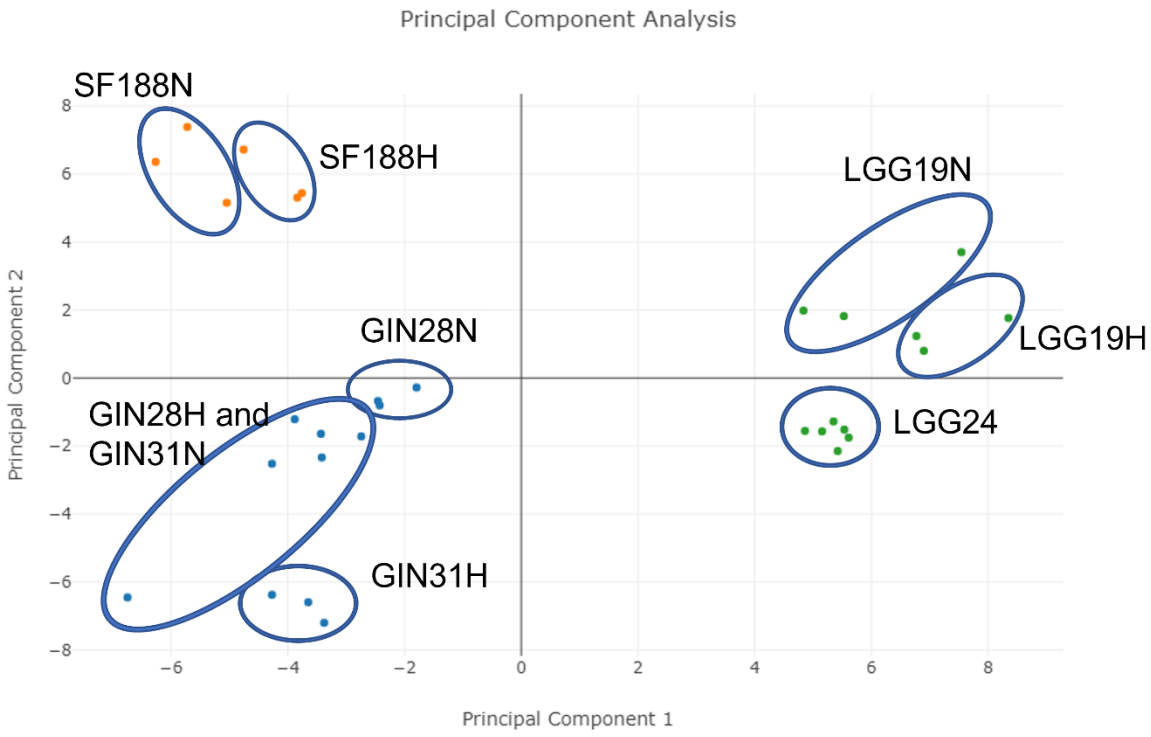

Figure 30. A PCA plot for the NormFinder normalisation method. The blue dots are GBMs, green dots are low-grade gliomas and orange dots are paediatric samples.

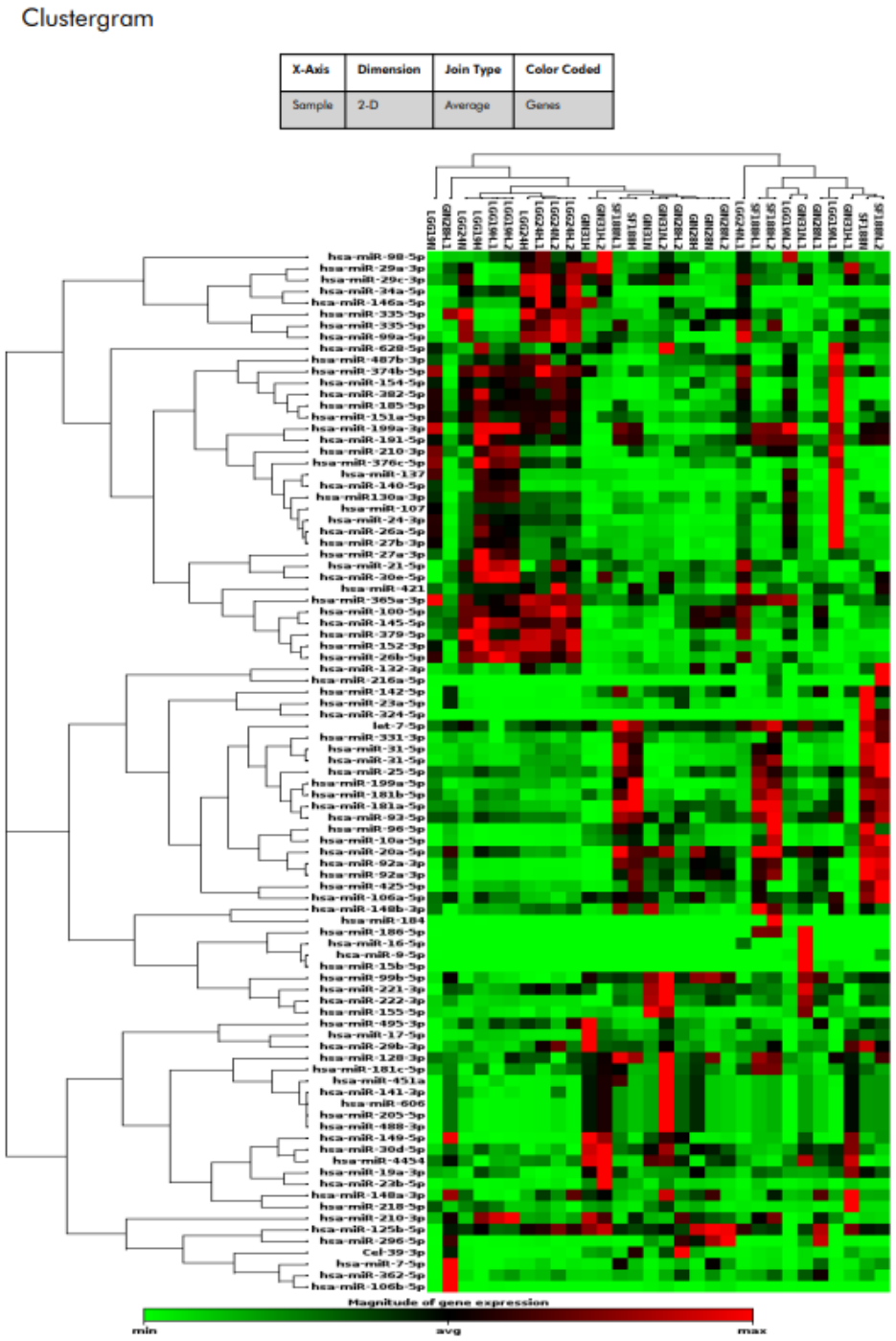

Figure 31. Heatmap displaying the expression of the miRNAs using the NormFinder normalisation method.

4.4.1.3 Global Ct mean of expressed miRNAs

Global Ct mean of expressed miRNAs is the most different normalisation method compared to geNorm and NormFinder. Instead of selecting a

group of miRNAs to be a reference group, this method calculates a global Ct mean for all the miRNA targets of each sample and uses that as a normalisation factor. A lower limit of detection was set at 40 and this determined whether an individual miRNA is expressed. Table 23 shows the global Ct mean for each triplicate of each group.

Table 23. Table of the global Ct mean of expressed miRNAs for each triplicate of each sample.

Sample	**Global Ct mean of expressed miRNAs**
GIN28 Normoxic	33.76
	32.27
	33.62
GIN28 Hypoxic	35.04
	34.72
	35.28
SF188 Normoxic	32.57
	34.08
	31.81
SF188 Hypoxic	33.64
	32.34
	31.67
LGG19 Normoxic	28.50
	30.75
	30.10

LGG19 Hypoxic	30.85
	31.56
	31.53
LGG24 Normoxic	33.17
	32.21
	33.02
LGG24 Hypoxic	31.98
	32.06
	31.89
GIN31 Normoxic	34.14
	29.05
	35.62
GIN31 Hypoxic	34.98
	33.13
	35.07

As with the other normalisation methods, a PCA plot and heatmap were generated using the global Ct mean of expressed miRNAs normalisation method. This method had the most differences, compared to the other normalisations which are particularly noticeable in the PCA plot, figure 32. The paediatric and GBM samples cluster together, whereas using the other normalisation methods, these samples are distinctly separate. However, the paediatric samples are glioblastomas and overall the GBMs/paediatrics are still clearly separated from the low-grade gliomas. The heatmap in figure 33 shows that a lot of miRNAs are over-expressed

in the low-grade gliomas compared to the other samples, which is also more prominent with this normalisation method compared to the others.

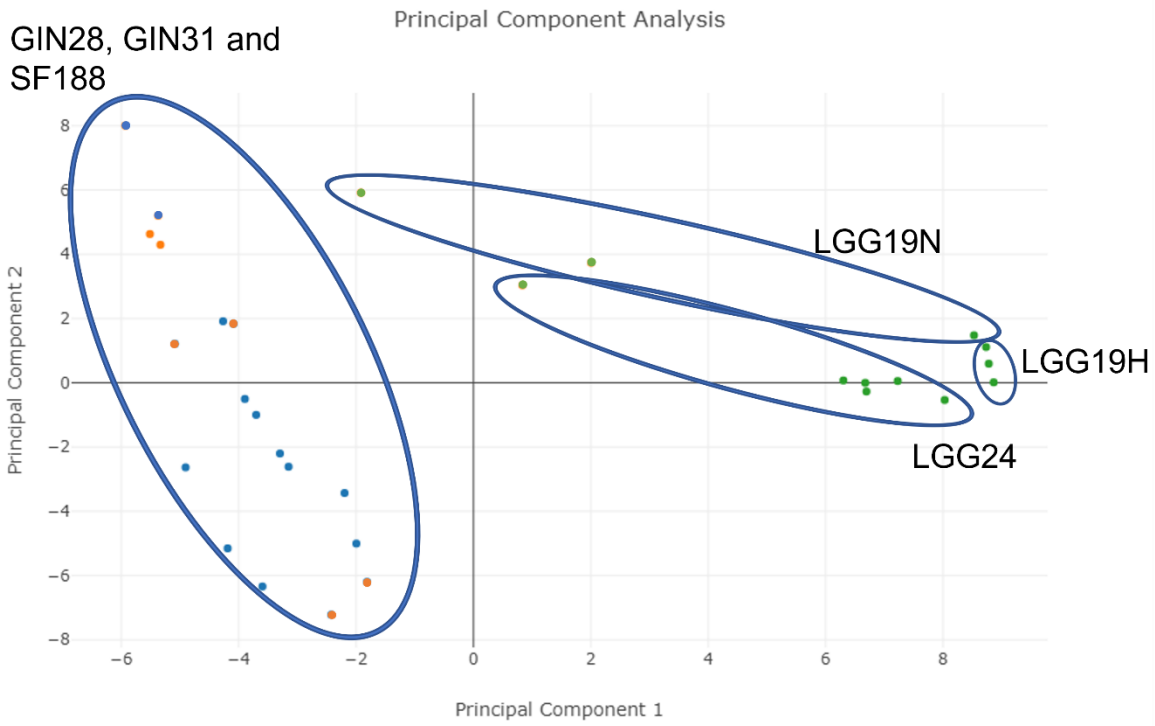

Figure 32. A PCA plot showing the samples using the gobal ct mean of expressed miRNAs normalisation method.

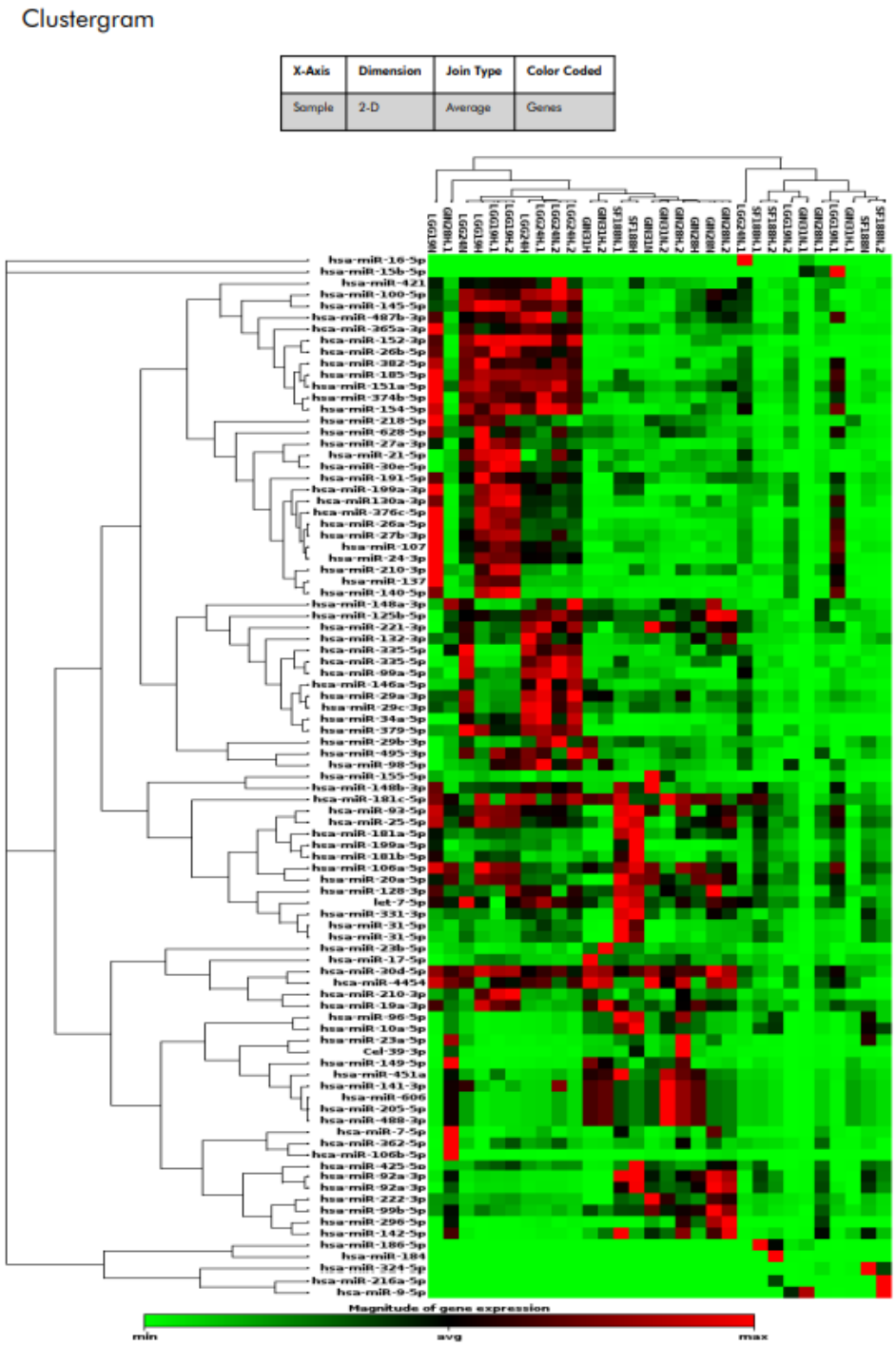

Figure 33. Heatmap from qPCR data following normalisation using the global Ct mean of expressed miRNAs method.

4.4.1.4 Normalisation conclusion

After applying the different normalisation methods to the data and analysing the outputs from each one, the geNorm method was the

normalisation method chosen to progress with. This method does not take into account the treatment of the samples which may result in compensating expression as such NormFinder. Also, using the global Ct mean of expressed miRNAs rather than using a small group of reference miRNA may hide the subtle differences that are associated with miRNA expression which could still have an important physiological/molecular impact. For these reasons geNorm is the normalisation method of choice.

4.5 miRNA screening results

Once a normalisation method was determined, statistical student t-tests were performed to identify significant miRNAs between hypoxic and normoxic between the three categories, the overall, GBM and low-grades. The significant miRNAs and the respective fold changes are displayed in table 24.

Table 24. The tables hows the significant miRNAs and fold changes for each category; overall, GBM (GIN) and low-grade (LGG), from the LNA miRCURY qPCR analysis.

Overall Hypoxia vs Normoxia	**Fold change**	**GIN Hypoxia vs Normoxia**	**Fold change**	**LGG Hypoxia vs Normoxia**	**Fold change**
hsa-miR-34a-5p	6.84	hsa-miR-149-5p	3.38	hsa-miR-34a-5p	40.43
hsa-miR-152-3p	2.34	hsa-miR-137	2.86	has-miR-152-3p	8.61
hsa-miR-210-3p	3.75	hsa-miR-92a-3p	0.03	hsa-miR-125b-5p	263.01
hsa-miR-92a-3p	0.26	hsa-miR-331-3p	0.29	hsa-miR-92a-3p	2.31
hsa-miR-92a-3p	0.22	hsa-miR-92a-3p	0.02	hsa-miR-296-5p	3.84
hsa-miR-222-3p	0.14	hsa-miR-222-3p	0.02		
hsa-miR-107	0.32	hsa-miR-425-5p	0.15		
hsa-miR-93-5p	0.4	hsa-miR-296-5p	0.23		
hsa-miR-191-5p	0.39	hsa-miR-100-5p	0.11		

hsa-let-7b-5p	0.23	hsa-miR-107	0.14		
		hsa-miR-181a-5p	0.39		
		hsa-miR-191-5p	0.19		

4.5.1 Overall cell line analysis

Similarly, to the NanoString analysis, a PCA plot (figure 34) using the GeneGlobe analysis was conducted to show that the types of gliomas is the main factor to separate the gliomas. The low-grade gliomas, both hypoxic and normoxic are all clustered together in the left bottom corner, the two paediatric samples are clustered together. Most of the GBM primary cell lines are together, except GIN31 hypoxic sample. However, the GIN normoxic samples are more distinct from the hypoxic GIN samples, compared to the other glioma categories, potentially showing that hypoxic affects GBM more so than the other categories. This PCA plot is similar to the clustering of the NanoString microarray.

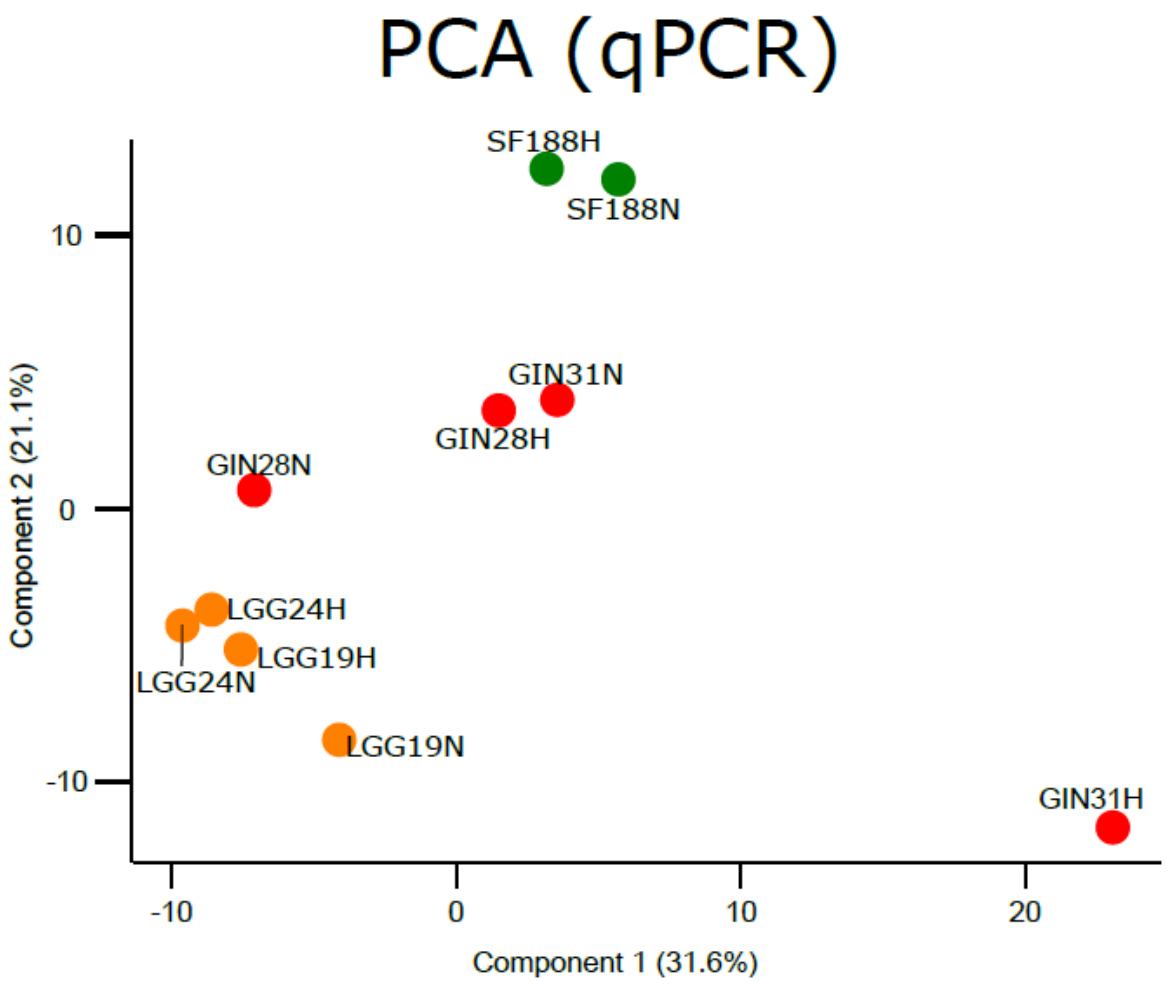

Figure 34. Principle component analysis of the glioma samples.

Using the FunRich a standalone software tool, for functional enrichment and interaction network analysis of genes, proteins and miRNAs, all the significant miRNAs were shown that their site of expression was significantly shown to be in malignant gliomas as depicted in figure 35, as well as the brain.

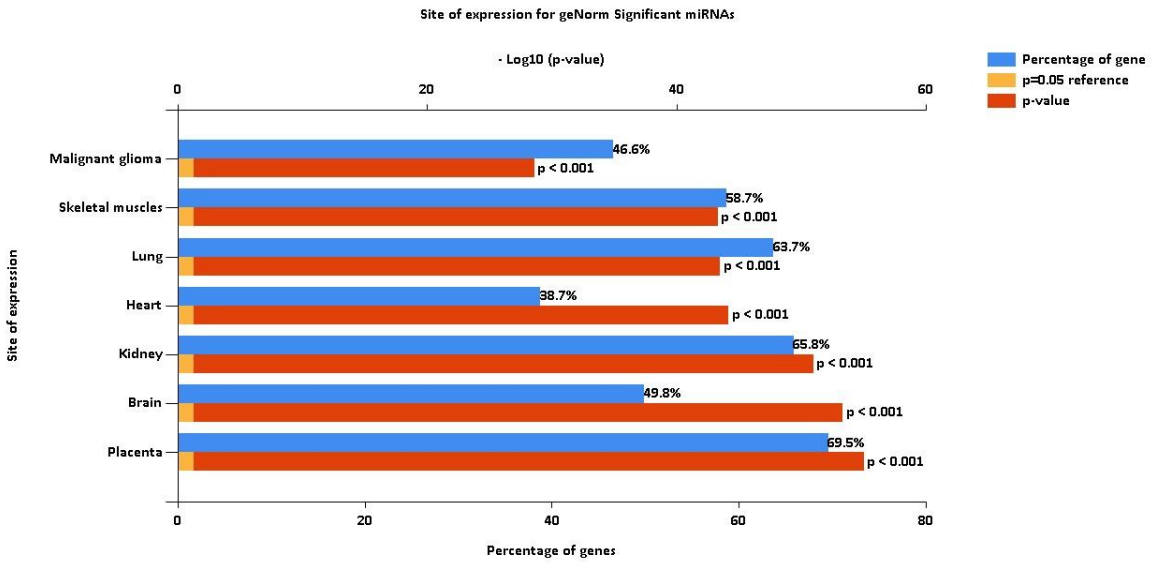

Figure 35. Site of expression of significant hypoxic-miRNAs.

The significant miRNAs are displayed in a bubble plot, figure 36, to show the significance of each miRNA in hypoxia compared to normoxia within the three categories, with an indication of the degree of fold change for each miRNA in the category.

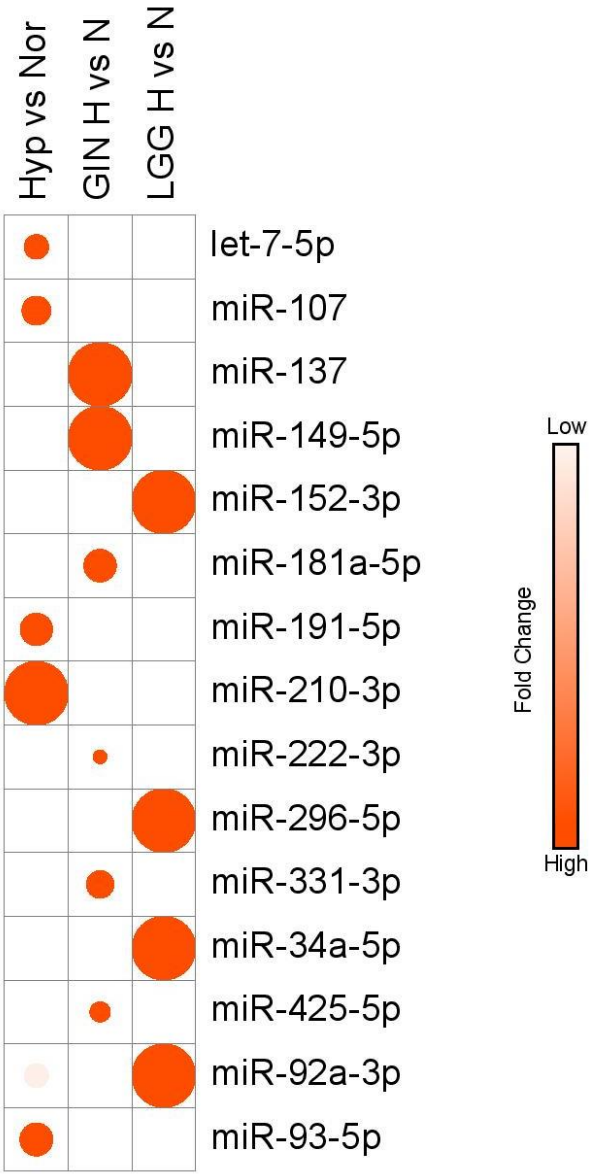

Figure 36. A bubble plot of the hypoxic significant miRNAs within the three categories.

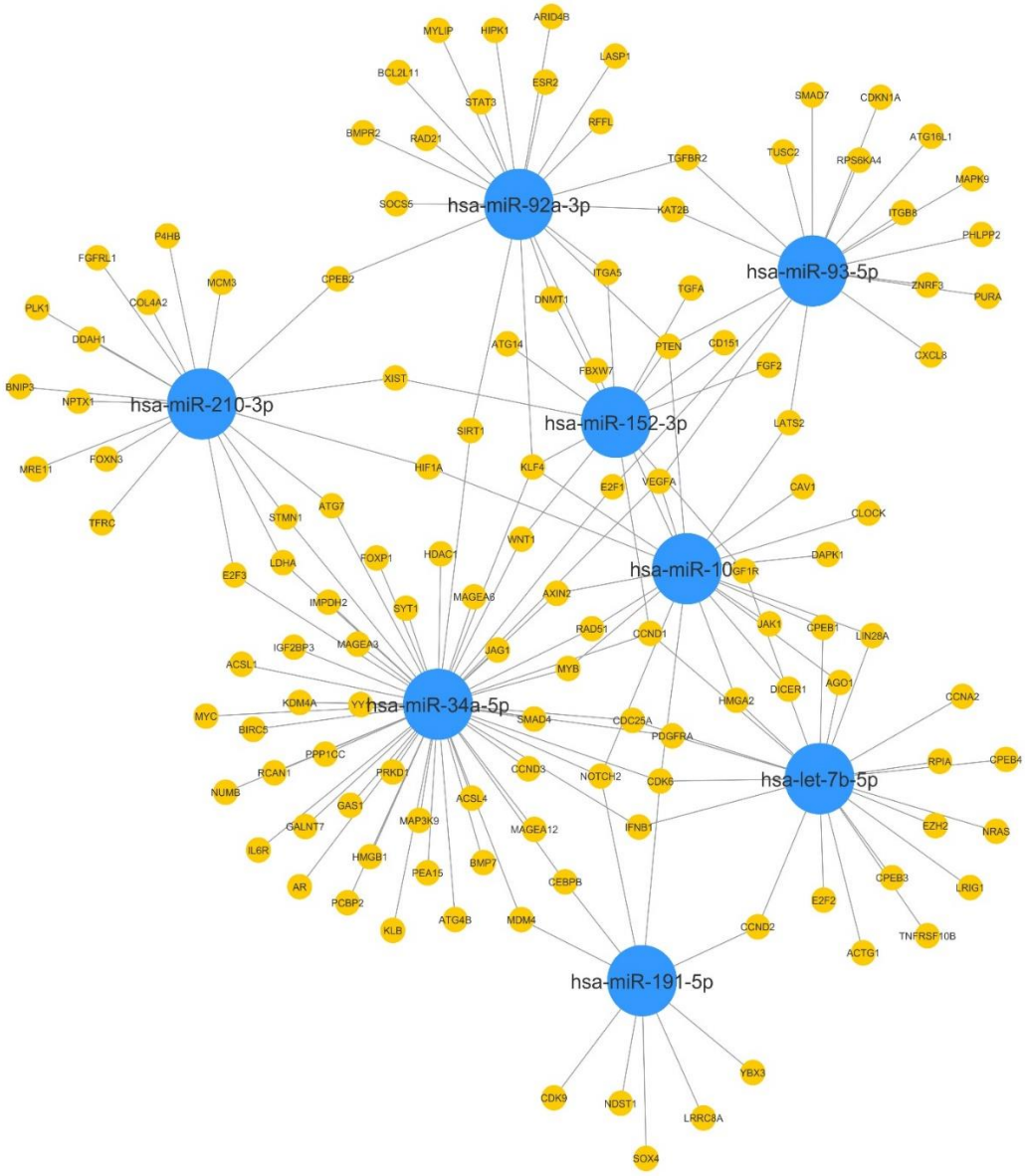

Figure 37. A miRNA network showing the significant miRNAs in hypoxia compared to normoxia in all cell lines.

The significant miRNAs are shown in figure 37 in the blue circles with the direct target genes shown in the yellow circles. It shows the interaction between the different significant miRNAs and their targets. Using the list of the significant miRNAs and using their targets a variety of pathway analysis was performed including disease ontology, Kyoto

Encyclopaedia of Genes and Genomes (KEGG), WikiPathways and Reactome. A selection of these miRNAs was identified in the pathway analysis which were the following: let-7b-5p, miR-107, miR-152-3p, miR-191-5p, miR-210-3p, miR-34a-5p, miR-92a-3p, miR-93-5p.

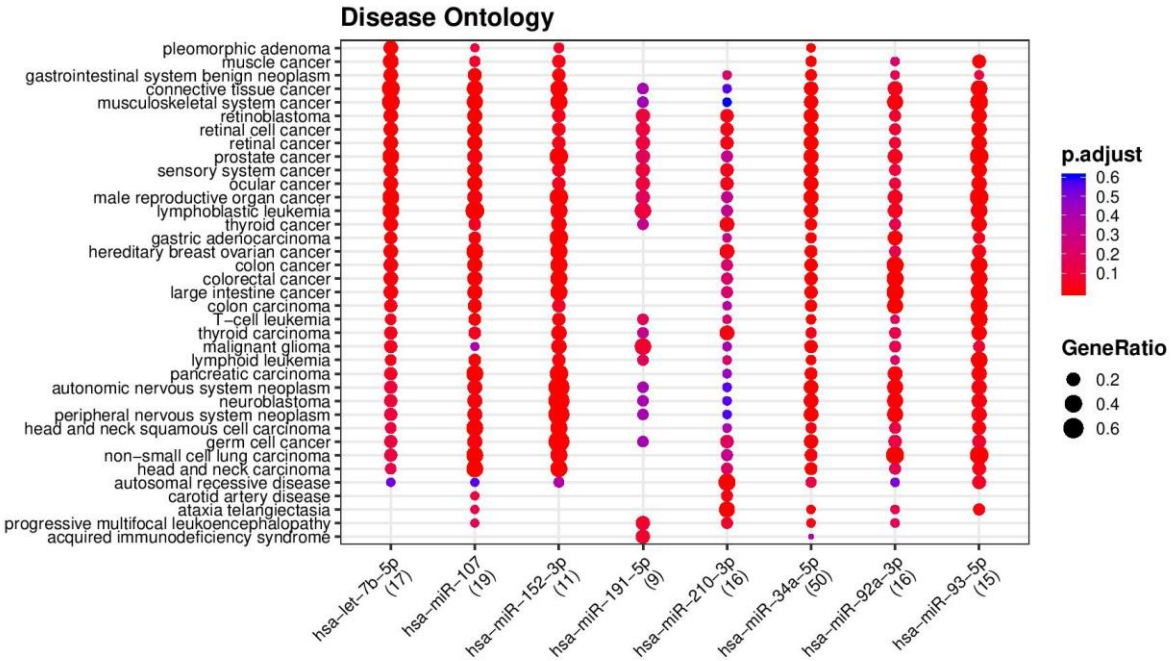

Figure 38. Dot plot of the disease ontology of the significant miRNAs for all cell lines in hypoxia compared to normoxia.

In disease ontology, figure 38, most diseases that were significantly related to the miRNAs were a variety of cancers, including malignant gliomas, neuroblastomas and colon cancer. This finding supports the expression of these miRNAs in malignant gliomas, which was the cell type these miRNAs were tested in.

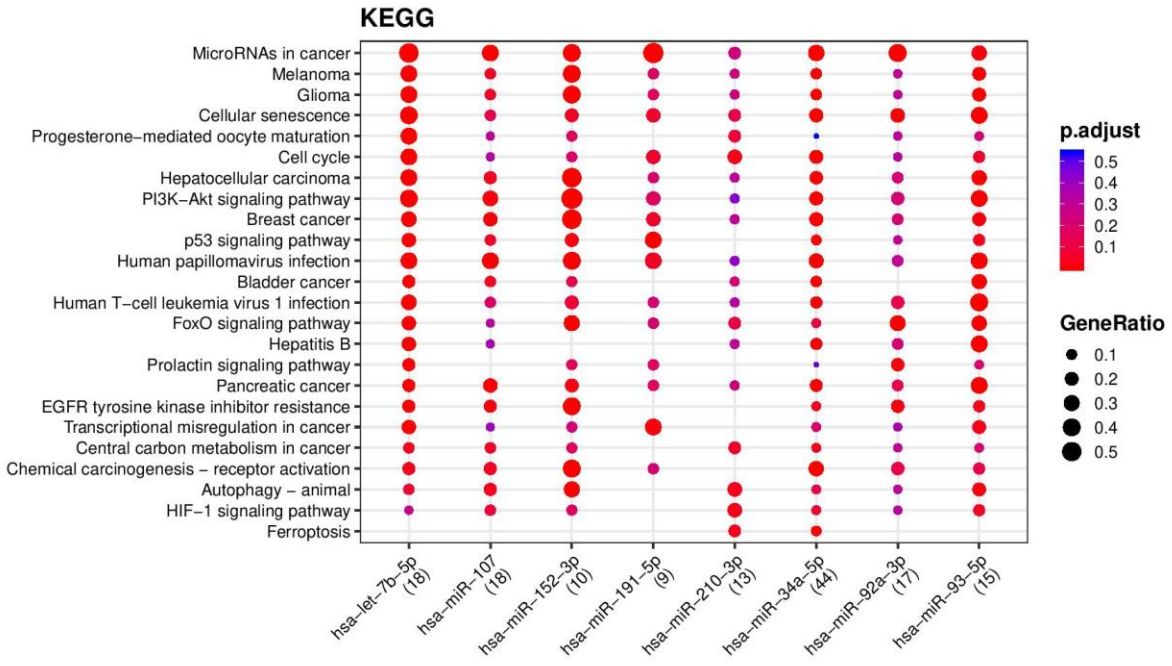

Figure 39. Dot plot of the KEGG analysis of the significant miRNAs for all cell lines in hypoxia compared to normoxia.

The KEGG analysis, figure 39, also supports the findings in the disease ontology analysis. One disease identified via KEGG, was gliomas. Other important pathways which were identified were miRNAs in cancer and cellular senescence, which was highlighted from the NanoString microarray data. HIF-1 signalling pathway was also identified in these hypoxia-regulated miRNAs, indicating that all of the miRNAs, excluding miR-191-5p, are involved within HIF-1 signalling. This is another piece of evidence, that these miRNAs have a role to play in response to hypoxia. Other pathways that were identified were a number of signalling pathways including FoxO, p53 and PI3K-Akt.

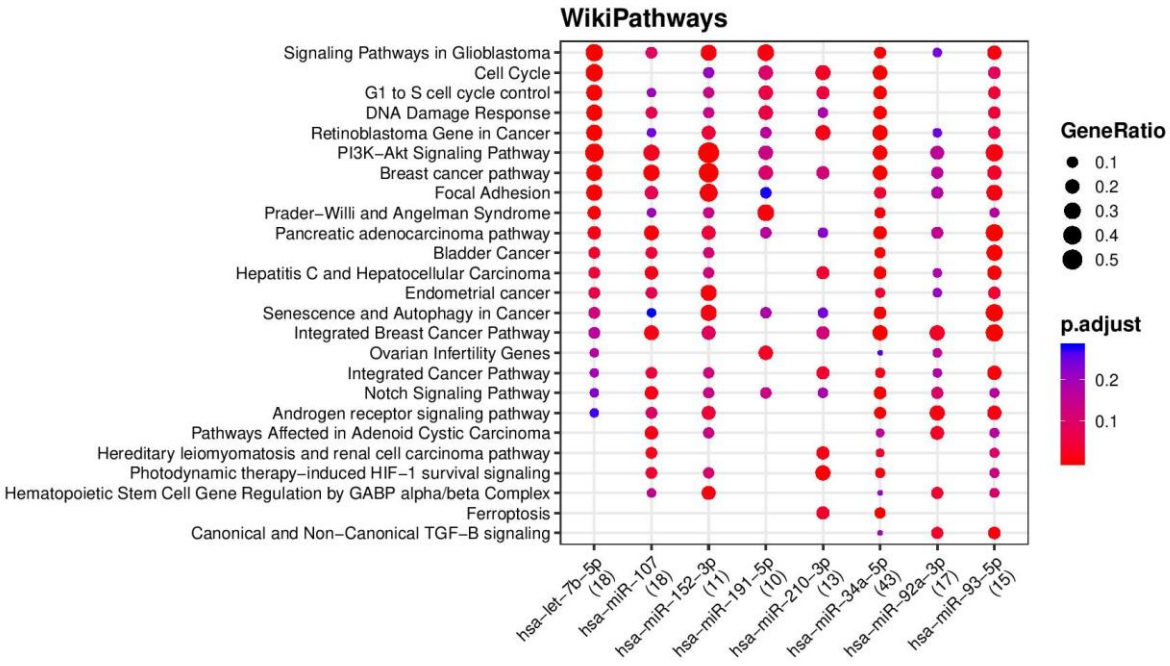

Figure 40. Dot plot of the WikiPathways analysis of the significant miRNAs for all cell lines in hypoxia compared to normoxia.

In figure 40, data from WikiPathways analysis also confirms the significance of these miRNAs in signalling pathways in glioblastoma. Another hypoxic related pathway was also identified; photodynamic therapy-induced HIF-1 survival signalling was significant amongst these miRNAs. Senescence and autophagy in cancer was also highlighted as a significant pathway, which has similarly showed up in other analyses. Alongside these pathways, a large range of signalling pathways were also identified as significant amongst these miRNAs over all the cell lines in hypoxia.

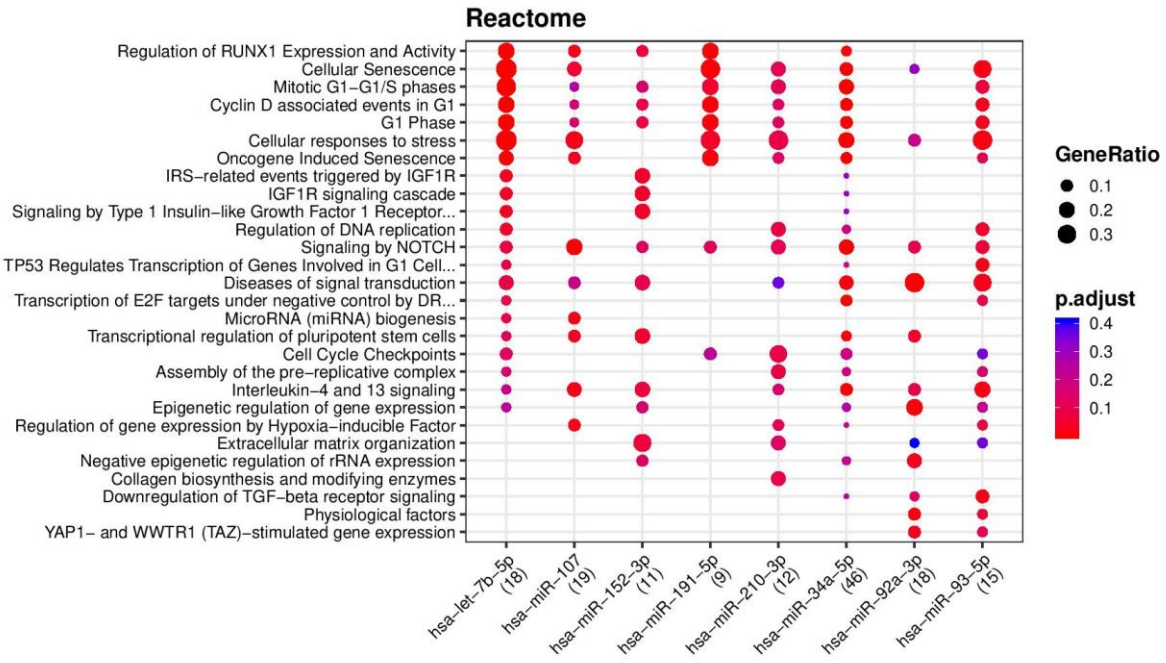

Figure 41. Dot plot of the Reactome analysis of the significant miRNAs for all cell lines in hypoxia compared to normoxia.

Figure 41 shows the dot plot of the reactome analysis for all cell lines, hypoxic-significant miRNAs. Regulation of gene expression by hypoxia-inducible factor is a pathway that is significant amongst the miRNAs. Similarly, to other analyses, cellular senescence and oncogene-induced senescence was also identified as significant. miRNA biogenesis was identified as a pathway along with cell cycle related pathways. Multiple signalling pathways were identified as well as multiple transcriptional regulation of different downstream targets.

Overall, the analyses of all the cell lines have identified that gliomas, hypoxia and miRNA regulation are associated with these miRNAs via their targets. Also, cellular senescence and signalling pathways were

identified as significant and important pathways associated with these miRNAs.

4.5.2 GIN cell line analysis

Analyses were also conducted looking at only the primary GBM cell lines. Figure 42 shows the network of interaction of the significantly expressed miRNAs and their gene targets. The significantly expressed miRNAs are highlighted in this network and it shows the intricacies and intertwining of the miRNAs and their targets.

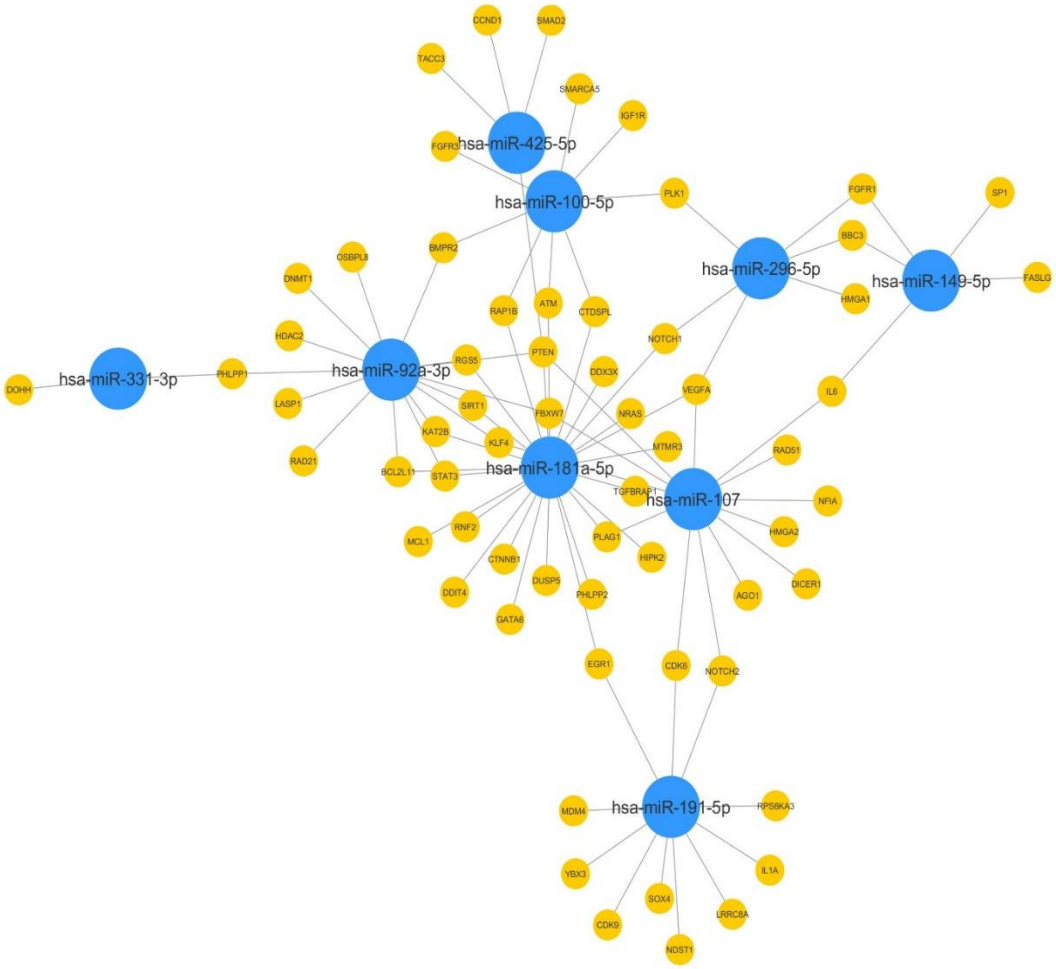

Figure 42. A miRNA network showing the significant miRNAs in hypoxia compared to normoxia in GIN cell lines.

Similarly, to the overall analysis, FunRich was used to show the site of expression of the significantly changed miRNAs in hypoxia compared to normoxia in glioblastoma cell lines and both the brain and malignant gliomas showed that they significantly expressed these miRNAs, seen in figure 43.

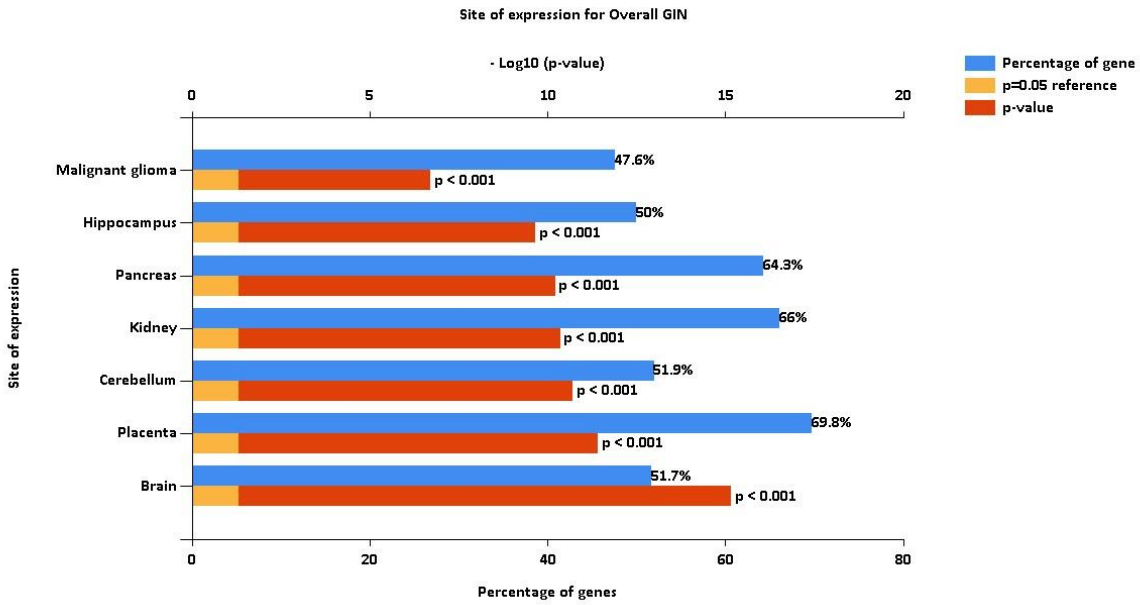

Figure 43. A schematic showing the site of expression of the significantly expressed miRNAs from the GIN category.

This emphasises the fact that miRNA expression not only affects the expression of genes, but also effect the expression to other miRNAs. Analyses of the hypoxic-GIN significant miRNAs looked at disease ontology, KEGG, WikiPathways, Reactome, the miRNAs identified in this analysis are miR-100-5p, miR-107, miR-149-5p, miR-181a-5p, miR-191-5p, miR-296-5p, miR-331-3p, miR-425-5p and miR-92a-3p.

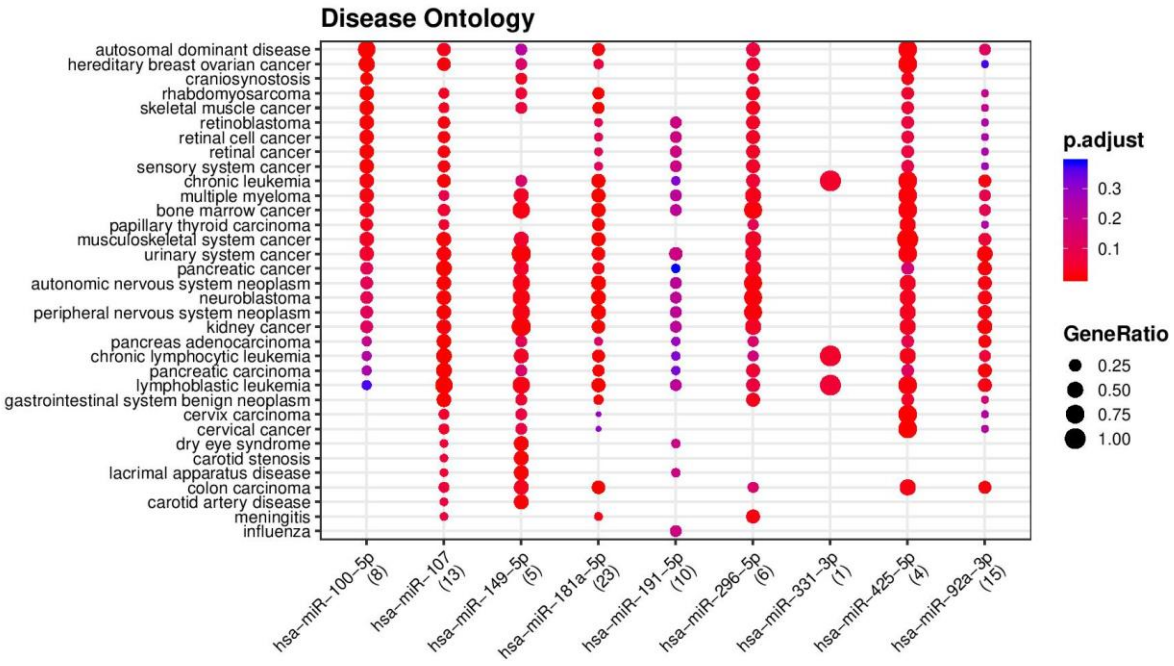

Figure 44. Dot plot of the disease ontology of the significant miRNAs for GIN cell lines in hypoxia compared to normoxia.

Figure 44 shows the results of the disease ontology analyses of the hypoxic-GIN cell line significant miRNAs. These miRNAs are linked to multiple cancers including ovarian cancer, kidney cancer, pancreatic cancer, thyroid cancer and leukaemia. Though gliomas were not significantly identified, diseases of the nervous system were found to be significant amongst the miRNAs.

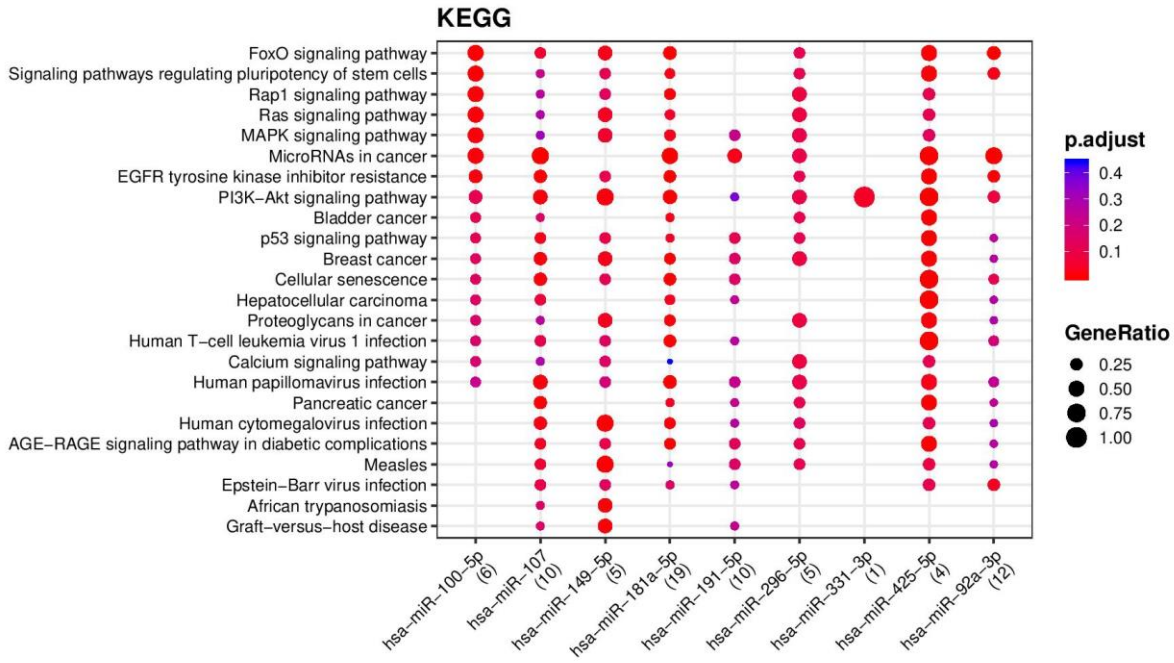

Figure 45. Dot plot of the KEGG analysis of the significant miRNAs for GIN cell lines in hypoxia compared to normoxia.

KEGG pathway analysis results are shown in figure 45 of the hypoxic-GIN significant miRNAs. To be expected, miRNAs in cancer was a pathway that was significantly associated with these miRNAs. As well, multiple signalling pathways including Rap1, RAS, MAPK, p53, and PI3K-Akt, many of which are known to be involved in malignancies, including gliomas. Another pathway which was noted, was cellular senescence. This pathway was highlighted as a pathway of interest using the NanoString data and in the qPCR analyses of all cell lines.

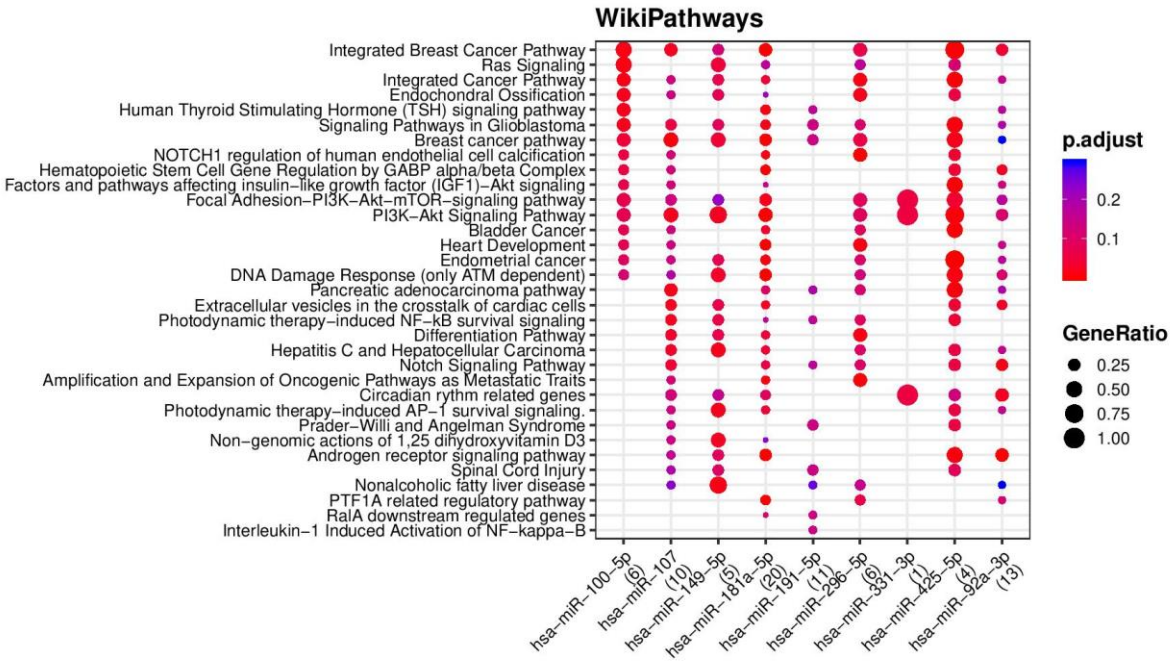

Figure 46. Dot plot of the WikiPathways analysis of the significant miRNAs for GIN cell lines in hypoxia compared to normoxia.

Interestingly, after reviewing the WikiPathways results of the GIN-hypoxic significant miRNAs, one pathway of interest was identified: signalling pathways in glioblastoma seen in figure 46. This enforces the presence of these miRNAs in glioblastomas, of which these miRNAs were tested in. Also is similar as the KEGG analysis brought to light many signalling pathways that the miRNAs were involved in and are identified in glioblastomas, as well as individually highlighting signalling pathways such as PI3K-Akt and Ras, which are well reported in glioblastomas.

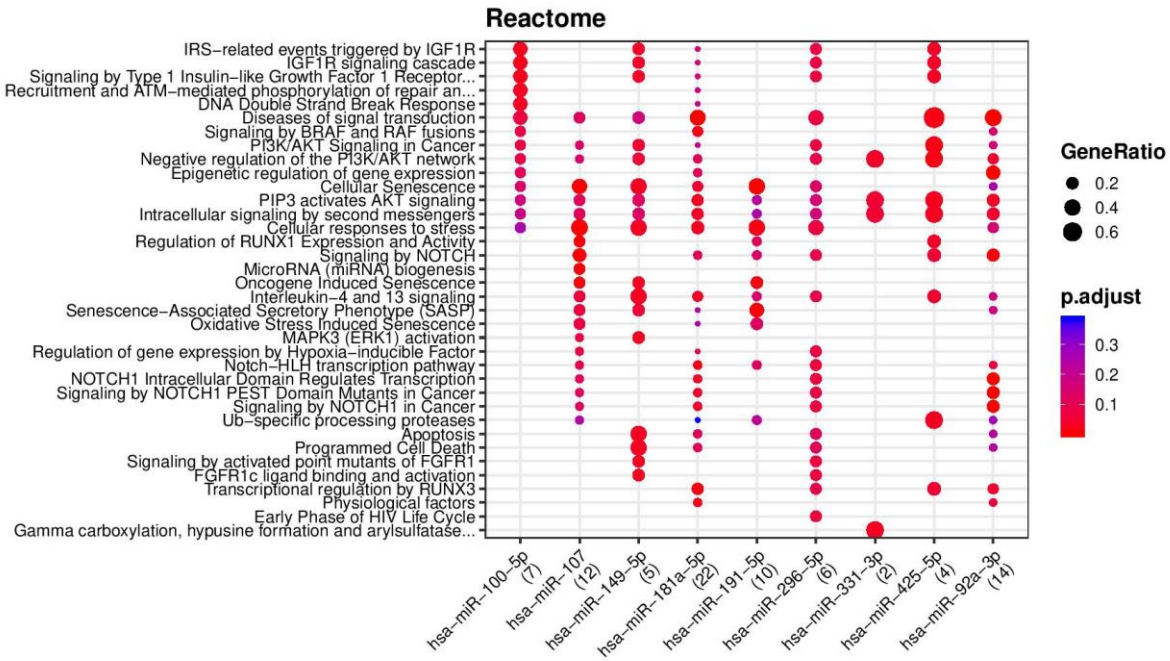

Figure 47. Dot plot of the Reactome analysis of the significant miRNAs for GIN cell lines in hypoxia compared to normoxia.

The Reactome analysis of GIN-hypoxic significant miRNAs also highlights cellular senescence, oncogene-induced senescence, apoptosis and programmed cell death in figure 47. This shows that these pathways may be of importance, miR-149-5p is involved in all of these. Again, multiple signalling pathways have been highlighted that are known to be involved in cancer such as NOTCH1 and PI3K/Akt. A pathway, regulation of gene expression by hypoxia-inducible factor was also identified, which further reenforces the idea that hypoxia has an effect on these miRNAs in gliomas.

4.6 Summary

Using the GeneGlobe analysis software, multiple analyses were made comparing hypoxia and normoxia miRNA expression in each group as well as observing the miRNA changes in normoxia between the different glioma samples. These analyses allow an insight into the alterations of the miRNA landscape depending on hypoxic status and glioma type. The results of this screening method, allowed for the identification of miRNAs to investigate further within hypoxia in glioblastomas. As mentioned, the samples were separated into categories; overall, LGG and GIN. As further in-depth analyses on microarray data proceeded the qPCR investigation, not all significant miRNAs found in the microarray were assessed using qPCR and the qPCR does not serve as an orthogonal validation for the microarray findings. However, the following significant miRNAs that were identified in NanoString microarray and were also significant in the qPCR analyses are displayed in table 25.

Table 25. Table showing overlapping significant miRNAs in microarray and qPCR analysis.

All Glioma cell lines	GIN lines only	LGG only
N/A	miR-218-5p	miR-606
	miR-210-3p	

4.6.1 miRNA screening of all glioma types

In the overall analyses, comparing miRNA expression in hypoxia compared to normoxia over three different glioma types, paediatric, low-

grade gliomas and glioblastomas there are 9 differentially expressed miRNA, 3 of which are upregulated in response to hypoxia and 5 that are down regulated in response to hypoxia. One of the most notable miRNAs is miR-210-3p which is upregulated 3.75-fold in hypoxia and is often reported as a hypoxic marker (192). miR-210-3p is often upregulated in hypoxia, described as a hypoxamiR, increases transcriptional activity of HIF and its target genes such as VEGF and CA9, it also promotes hypoxic survival and chemoresistance (260). miR-210-3p is the only significant miRNA that was identified from both the NanoString microarray and the qPCR analyses. Two other miRNAs which were upregulated in hypoxia were miR-34a-5p (6.48-fold) and miR-152-3p (2.34-fold). miR-34a-5p has been widely investigated within gliomas, and found that it's expression is downregulated when compared to normal brain (299). miR-34a-5p is reported as a tumour suppressor within gliomas and has many targets such as bcl-2, notch-1/notch-2, Fra-1 and MAP3K9 which are involved with anti-apoptotic function, cell cycle transition, invasion/metastasis and mitogen-activated protein kinase pathways (174). However, miR-34a-5p expression was upregulated overall in gliomas in response to hypoxia, though a link between miR-34a-5p and hypoxia within gliomas has not been largely investigated. The other upregulated miRNA, miR-152-3p, is also generally downregulated in gliomas compared to normal controls in normoxic conditions, and is also reported as a tumour suppressor and its downregulated results in decreased sensitivity to cisplatin (182). Similarly, to miR-34a-5p, though compared to normal brain, the expression levels are decreased, in

hypoxia, miR-152-3p are significantly increased. Potential compensatory mechanisms/feedback loops to counterbalance the hypoxic effect may cause these tumour suppressive miRNAs to be upregulated in hypoxia. The other miRNAs are significantly downregulated significantly in hypoxia compared to normoxia in the combined analyses; miR-92a-3p (3.8-4.54-fold), miR-222-3p (7.14-fold), miR-107 (3.13-fold), miR-93-5p (2.5-fold), miR-191-5p (2.56-fold) and let-7-5p (4.34-fold). All of these identified significantly down-regulated miRNAs are known to be important in glioma tumorigenesis. Low expression levels of miR-107 have been shown to promote angiogenesis within gliomas (300), and low expression of miR-107 is significant in hypoxic glioma cultures compared to normoxic and angiogenesis is a pro-tumour microenvironment which is facilitated within hypoxic conditions. miR-93-5p is also reported to have decreased levels of expression in glioma cell lines and tissues compared to normal brain, and a known gene target of miR-93-5p is MMP-2 (240). Lower expression levels of miR-93-5p, allow for an increase of MMP-2, an enzyme, in glioma cells which is associated with tumour growth, invasion and a prognostic marker for glioma recurrence (301). MMP-2 is increased in hypoxic conditions in gliomas, due to the increase of the transcriptional factor HIF-1α in hypoxia (302). As the expression levels of miR-93-5p are significantly lower than in gliomas, which are reported to already be decreased compared to normal controls, it can be predicted that this may be a factor that attributes to the increase of MMP-2 in gliomas in hypoxia. Let-7-5p has been shown to be significantly downregulated within glioma cell lines compared with normal astrocytes, which increases the

migration and invasion of glioma cells which is also linked to let-7-5p target E2F5 (303). In colon cancer, it has been assessed that hypoxia increased the expression of LIN28A, a RNA-binding protein, which subsequently supresses the expression of let-7-5p, which is exacerbated in hypoxia (289). Though this mechanism has not been shown in gliomas, further downregulation of let-7-5p in hypoxia compared to normoxia, could potentially occur via the increased production of LIN28A.

However, miR-92a-3p, miR-222-3p and miR-191-5p are all significantly downregulated in hypoxia compared to normoxia in gliomas, however, they are all reported to be significantly upregulated in gliomas compared to controls. In different situations miR-92a-3p has conflicting expressions under the influence of hypoxia. In mouse embryonic stem cells, an investigation studying the miR-92a/Sp1/MyoD axis, showed that under hypoxia miR-92a-3p expression is suppressed (304). However, within human endothelial progenitor cells, miR-92a-3p is elevated under hypoxic and high glucose injury which decreases the expression of GDF11 and consequently the downstream SMAD2/3/FAK/Akt/eNOS signalling pathway (305). No studies have directly assessed the miR-92a-3p expression within hypoxia in gliomas, which indicates further work is required to understand the mechanism involved under hypoxia influence in gliomas. One study has shown that hypoxia has no effect of miR-222-3p expression within MCF-7 breast adenocarcinoma cells (306), however no other studies within other cancers have explored miR-222-3p expression in hypoxia. As these miRNAs has reduced expression

levels in hypoxia compared to normoxia it is possible that under the influence of hypoxia, other regulatory or compensatory mechanisms/pathways cause the downregulation of these specific miRNAs in hypoxia.

This particular analysis shows that there is a difference of individual miRNA expression between hypoxic and normoxic cultures, indicating that hypoxia does affect miRNA expression which is likely affecting the expression of downstream target genes and proteins and pathways in glioma progression and growth.

Further analysis was conducted on these miRNAs, including identifying that these miRNAs are known to be involved in malignant gliomas using FunRich software shown in figure 44. The pathway enrichment analyses explored all the significant miRNAs within the overall category, excluding miR-222-3p, which did not have any significant results in the following analysis. Disease ontology identified many cancers of which some of these miRNAs have been reported to be involved in, including prostate cancer (307), lymphoblastic leukaemia (308) and colon cancer (309). Malignant glioma was also identified as cancer in which these significant miRNAs are associated with, which further solidifies our findings. This pathway analysis shows the importance of understanding these miRNAs, as they are widely associated with a wide variety of cancers indicating that, if exploited, these could be important markers or targets for cancer.

Another analysis that was performed was KEGG identifies associated diseases and biological pathways that a set of miRNAs are involved in. Agreeing with the disease ontology analysis, a main pathway that was elucidated was miRNAs in cancer. Further carcinomas were identified of the selected miRNAs being associated with including melanoma (310), bladder cancer (311) and again, malignant glioma. Interestingly many of these miRNAs from this analysis were highlighted to be involved in many signalling pathways which are dysregulated in cancers, including gliomas, such as PI3K-Akt, FoxO and p53 pathways as well metabolism and transcriptional in cancer was also identified. Also, an important pathway that the selected miRNAs are involved in, was the HIF-1 signalling pathway which is linked to hypoxia. This particular finding further emphasises the link of hypoxia with the identified miRNAs.

Similarly to KEGG, WikiPathways is another database allowing the input of data and to find its associated pathways. Similar malignancies and signalling pathways to those identified in KEGG were also found via WikiPathways. Other signalling pathways that were highlighted including androgen receptor signalling pathway, Notch pathway and photodynamic therapy-induced HIF-1 survival pathway, potentially suggesting a link between HIF and the associated miRNAs. Another important finding was the signalling pathways in glioblastoma was found using the selected miRNAs. Other biological pathways such as senescence, autophagy, DNA damage and cell cycle were associated with the miRNAs, and all of these are known to be potentially disrupted within cancer.

The final analysis used Reactome, which primarily specialises in human biological pathways. A large array of pathways was highlighted and some of these were related to pathways that were identified in WikiPathways analysis, including a variety of pathways involved in the cell cycle, senescence and oncogene induced senescence and Notch signalling. Regulation of gene expression by HIFs was also highlighted as an associated pathway to the miRNAs which are significantly expressed in hypoxia.

These analyses confirm that the miRNAs that were identified in the overall category, which are differentially expressed in hypoxia compared to normoxia, links to gliomas, cancer and hypoxia which increases the confidence within the results.

4.6.2 miRNA screening summary of low-grade gliomas

Five miRNAs were all significantly upregulated in hypoxia compared to normoxia in low-grade gliomas; miR-34a-5p was upregulated 40.34-fold, miR-152-3p is upregulated 8.61-fold, miR-125b-5p is upregulated 263-fold, miR-92a-3p is upregulated 2.31-fold and miR-296-3p is upregulated 3.84-fold. The significant miRNAs identified in the NanoString microarray were all downregulated in hypoxia, however all the significant miRNAs identified in qPCR are upregulated in hypoxia compared to normoxia. Though it is noted, that the significant miRNAs identified from each screening process are different. The expression values of miR-34a-5p

and miR-152-3p, in the qPCR analysis, are more increased in hypoxia compared to the overall, all-glioma analyses. Whilst there is no comparative data of miR-34a-5p levels in low-grade gliomas, miR-34a-5p is known to be downregulated in glioblastomas, compared to normal controls (299) but has been shown have significantly increased levels in hypoxia within cardiomyocytes and that that hypoxic-injury is exacerbated by miR-34a-5p overexpression and results in the downregulation of gene target zinc-finger E-box binding homoeobox1 (ZEB1) (312). Similarly to miR-34a-5p, miR-152-3p is downregulated in gliomas, both astrocytomas and glioblastomas compared to controls (313) but upregulated in our study in response to hypoxia, which has not yet been identified in other cancers. miR-125b-5p has been shown to have increased expression in low-grade gliomas compared to glioblastomas, though it's been reported to have contradicting roles as it has been described as an oncogene though is also noted to be downregulated in glioma-like stem cells and having anti-angiogenic functions (314). Unlike the increase in miR-125b-5p due to hypoxic exposure, it has been reported that miR-125b-5p was downregulated in response to hyperglycaemia and hypoxia in diabetic retinopathy (315). In contrast to overall and purely GIN cell lines, mir-92a-3p is significantly upregulated in glioblastomas in hypoxia compared to normoxia, whereas in the other categories it is significantly downregulated. This particular probe was inserted twice and thus solidifies the results even further. There are few studies that assess the role of miRNA within low-grade gliomas, however one bioinformatic study completed by Jeremais *et al*

highlights the significance and negative correlation between miR-92a-3p and heat-shock protein B8 (HspB8), and indicates that miR-92a-3p has importance within low-grade gliomas, though within the study was not able to identify the mechanism of the correlation, only that the two are negatively correlated (316). This study required further attention to determine the nature of the correlation and to determine whether the miRNA is up or downregulated within low-grade gliomas. The individual role of miR-92a-3p within hypoxia remains to be elucidated within low-grade gliomas to determine the differing roles within hypoxia between the different stages of glioma and to fully understand the breadth of regulation and functions of miR-92a-3p. Though miR-296-3p has not been exclusively examined within low-grade gliomas, it has been shown to have increased expression in glioblastomas which is associated with enhanced invasiveness and targets caspase-8 and nerve growth factor receptor to potentiate the invasiveness of glioblastoma cells (317). Though no further studies have explored miR-296-5p in response to hypoxia in cancers, its known role of increasing invasiveness may be further required when exposed to hypoxic conditions, which will need more investigation.

There are very few studies which report on the miRNA landscape particularly within low-grade gliomas and specifically in relation to their response within hypoxic conditions. Interestingly, four significant miRNAs were significant in other glioma groups, however, in low-grade gliomas these miRNAs are significantly more expressed in hypoxia. miR-34a-5p

and miR-152-3p are tumour suppressive miRNAs and their increase in hypoxia could potentially be a feedback/regulatory loop to counterbalance the pro-cancer effects of hypoxia. miR-296-5p has varied functions in different cancers, indicating that this particular miRNA requires further elucidation to confirm its role during hypoxia within gliomas. miR-92a-3p is reported as oncogenic, and the expression of this miRNA may be pushing the pro-hypoxia phenotype. No further analysis could be conducted on the significant miRNAs alone within the low-grade group as no enrichment pathways were identified as significant. Due to this, this prevented any of the low-grade miRNAs being assessed further. However, miRNA still remains a very interesting branch of low-grade glioma research that requires further experimental investigation to fully understand the impact of miRNA in low-grade gliomas and in response to these particular findings, why many of the miRNA are so vastly increased in hypoxia compared to normoxia and also compared to the glioblastoma group.

4.6.3 miRNA screening summary of glioblastomas

Glioblastomas are the most aggressive type of glioma and are known to harbour hypoxic regions. These areas of hypoxia add to the continuous heterogeneity of GBMs which alter the genome and post-transcriptional/translational mechanisms resulting in increased or reduced expression of particular molecular pathways that result in specific physiological effects. Hypoxia is known to increase growth and invasion of GBM cells, aid glioma-stem-like cells and increase

angiogenesis by directly or indirectly targeting a number of genes such as Notch1, VEGF, mTOR, PI3K and many others (318) (69).

The amount miRNAs that were significantly changed in response to hypoxia compared to normoxia in glioblastomas, was larger than in the other categories. Two miRNAs are significantly upregulated: miR-149-5p (3.38-fold) and miR-137 (2.86-fold). The other nine significant miRNAs are downregulated in hypoxia in glioblastomas which are: miR-92a-3p (33-50-fold), miR-222-3p (33-fold), miR-100-5p (9.1-fold), miR-107 (7.1-fold), miR-425-5p (6.7-fold), miR-191-5p (5.3-fold), miR-296-5p (4.4-fold), miR-331-3p (3.5-fold), miR-181a-5p (2.6-fold).

One of the upregulated miRNAs in hypoxia, miR-137, is generally described as a tumour suppressor within glioblastomas and is usually downregulated compared to normal brain and is associated with inhibiting cell proliferation and invasion, inducing apoptosis and suppressing glioma stem-cell development (263). Though in other cancers, including prostate cancer, miR-137 has been reported to be downregulated in response to hypoxia (319). Further pathways need to be investigated to determine the possibility for miR-137 upregulation in glioblastoma, as it could potentially trying to compensate against the hypoxic environment. One of the downregulated miRNAs, miR-100-5p is notably downregulated in glioblastomas compared to controls and is associated with initiating tumour growth (212). Though its expression in response to hypoxia has not been thoroughly investigated in

glioblastomas, it has been noticed that miR-100-5p is downregulated in hypoxia (320) and has been shown to be downregulated in hypoxia in hepatocellular carcinoma by being sponged by lncRNA RAET1K (321). miR-425-5p has been shown to have increased expression in glioblastomas compared with normal brain controls, and with positive correlation of SOX2 which consequently regulates RAB31 and FOXJ3 to promote the survival of glioma stem-like cells (195). The expression of miR-425-5p has been identified as downregulated in response to hypoxia in this study, though no papers have yet linked miR-425-5p with hypoxia in cancers. This is an avenue that has not yet been investigated. miR-331-3p has been shown to be downregulated in glioblastomas compared with normal brain in multiple studies (180) (181), our investigated shows downregulation of miR-331-3p in hypoxia comparative to normoxia, however, no studies have directly shown the response of miR-331-3p to hypoxia within cancer directly. miR-181a-5p is shown to be a tumour suppressor and downregulated in cancers such as breast and colon cancers (322) as well as glioblastomas (323). Macharia *et al* studied the expression level of miR-181a-5p in glioblastoma, which was significantly lower than controls, and within hypoxia which was reduced between an extra 4-10-fold change (189). This study shows a similar effect to our investigation which highlights the downregulation of miR-181a-5p in response to hypoxia within glioblastomas.

Disease ontology, KEGG, WikiPathways and Reactome analyses were conducted on the GIN significantly expressed miRNAs, similarly to those

in the overall category. Multiple cancers were identified to be associated with these miRNAs were similar to those in the overall category including lymphoblastic leukaemia, colon cancer, bladder cancer and hepatocellular carcinoma. Malignant glioma was also identified as an associated disease in WikiPathways analysis. Multiple important signalling pathways were highlighted in the KEGG analysis including, PI3k-Akt, FoxO, Rap1, Ras, MAPK and p53 pathways, many of which are known to be important in cancer and in glioblastomas. Similar to the overall analysis, senescence including oxidative-stress induced senescence was identified to be associated with the miRNAs from the GIN cell lines, other biological pathways were also significant including apoptosis and miRNA biogenesis. Reactome also highlighted regulation of gene expression by HIFs as a significant pathway from the miRNAs. These analyses also confer that the GIN-specific miRNAs do have an association with glioblastoma and hypoxia.

From the hypoxic-significant miRNAs, individual miRNAs need to be identified to pursue forward and to assess further changes within hypoxia of downstream targets and functional changes. The selected targets for further investigation were chosen from the GIN category, due to the long growth time of the low-grade gliomas and the large amount of different cell lines required for the overall category. The GIN cell lines are patient derived, which enhances the clinical relevance of the results from these glioblastoma cells. The data in table 24 shows the significant miRNAs and the fold changes of each. The two miRNAs selected for further

investigation are hsa-miR-149-5p and hsa-miR-92a-3p. miR-149-5p had the highest upregulated fold change, 3.38-fold, of all the significant miRNAs from the GIN group. The second miRNA chosen was miR-92a-3p which was one of the highest down-regulated fold changes, 33-50-fold, and one of the lowest fold changes in the overall group and interestingly, significantly upregulated in the low-grade gliomas group.

4.6.4 hsa-miR-149-5p

miR-149-5p has been studied in various cancers with various roles, including both tumour suppressor and oncogenic roles, sometimes in the same cancer including glioblastoma, which has been reported to have both increased, targeting caspase-2, and repressed expression, targeting Rap1Bq and Akt, compared to normal brain controls (199). He *et al* also noted that miR-149-5p can be upregulated in gliomas with a notable downstream target of JunB. miR-149-5p upregulation in glioblastoma has been linked to the downregulation of both caspase-2 and p53 which both influence cell cycle transitions. It was found that Wee1-like protein kinase (Wee1), important for the regulation of the transition between G2 and M phase, was significantly downregulated with miR-149-5p upregulation in glioblastoma cell lines and results in the promotion of glioma proliferation (324). In contrast, She *et al* showed that miR-149-5p was decreased in gliomas compared with normal controls and the expression of miR-149-5p is shown to suppress glioma proliferation, invasion and cytoskeletal remodelling by affecting Rap1B-associated GTPase (325). These studies show the different pathways

and regulation loops that involve miR-149-5p and is just a small insight into the breadth of its roles within glioblastomas. No studies have been identified that examine the effect of hypoxia on miR-149-5p within cancer. This study hopes to close the gap of the lack of understanding of miR-149-5p and its response to hypoxia within glioblastomas, as this study shows that miR-149-5p is significantly upregulated in GBM in response to hypoxia. The selection of this miRNA to investigate further hope to identify important downstream targets that are affected by the upregulation of miR-149-5p in hypoxia and to investigate their roles within glioblastomas.

4.6.5 hsa-miR-92a-3p

miR-92a-3p is widely associated with glioblastomas and is involved in a vast majority of pathways and genes and is defined as an oncogene and is upregulated in glioblastoma and gliomas compared to normal controls both in cell lines and tissues (177). By interactions with various genes and non-coding RNAs, there is a great understanding of the involvement of miR-92a-3p in proliferation and apoptosis in glioblastomas. Long non-coding RNA SNHG14 is downregulated within gliomas, its expression is negatively correlated with miR-92a-3p which highlights that the overexpression of miR-92a-3p promotes glioma progression whilst suppressing SNHG14 (326). Another studied showed the upregulation of miR-92a-3p in gliomas, and it's potential as a poor prognostic marker as well as the increase in glioma proliferation and invasion through the mTor-Akt signalling pathway due to miR-92a-3p overexpression (327).

This study found that Kruppel-like factor 4 (KLF4), which is thought to mediate p53 expression, is a target of miR-92a-3p and consequently downregulated in gliomas (327). As well as largely being associated with proliferation and invasion, miR-92a-3p is also associated with apoptosis. Niu *et al* found that Bim, a pro-apoptotic factor, is a target of miR-92a-3p and the Bim is significantly lower in glioma cells, indicating that miR-92a-3p contributes to an anti-apoptotic state which helps increase proliferation (328). Though miR-92a-3p is well documented in glioblastoma about its roles within proliferation and apoptosis, there are fewer studies assessing the effect of hypoxia on miR-92a-3p in any cancer. Ghosh *et al* shows that miR-92a-3p directly targets VHL, important factor in the hypoxic pathway, which increases the stabilisation of HIF-1α to allow it to combine with cofactors and phosphorylated STAT3 to produce a complex which directly promotes the transcription of VEGF within B-cell chronic lymphocytic leukaemia (329) (330), though this link with hypoxia is related to increase levels of miR-92a-3p which is the opposite seen in glioblastoma. In this study, miR-92a-3p has been found to be downregulated in hypoxia in GBM, which is opposite to many of the literature reports. Further experiments, including validating these findings in tumour tissue samples need be performed in order to confirm the expression of miR-92a-3p in hypoxia in GBM.

Together with the qPCR data and previous research, it is clear that both miR-149-5p and miR-92a-3p have important roles within glioblastoma and are significantly expressed in response to hypoxia compared to

normoxia. Further experiments are required to investigate the importance of the response of these selected miRNAs to hypoxia in GBM.

5 Chapter 5: Hypoxia-specific miRNAs

5.1 Introduction of hypoxia and gliomas

The micro-environmental condition of hypoxia has long been associated with cancers, especially solid tumours. As solid tumours are a mass of proliferative cells, the cells in the centre have access to less oxygen than those on the periphery of the tumour. This is because rate of angiogenesis is not sufficient to supply oxygen to the centre of the tumour and as the tumour increases in size, the diffusion of oxygen becomes inadequate (22). Even though angiogenesis is active within tumours, the vasculature is leaky, irregular and poorly functioning which often leads to hypoxic domains (331). Conceptually the tumour can be modelled as a ball of cells with a hypoxic gradient, with of hypoxia in the core/centre of the tumour which then slowly decreases through the tumour with cells adjacent to normal tissue having more access to oxygen. As hypoxia is known as a pro-cancer microenvironment the effect it has on miRNAs is of importance in glioblastomas. The selected miR-149-5p and miR-92a-3p are further investigated to determine if their change in expression affects downstream targets and pathways the targets are involved in.

5.2 Assessing hypoxia gradients in glioblastomas

Carbonic anhydrase 9 (CA9) is induced under hypoxic conditions and is known as a hypoxic marker. To indirectly assess the effect of hypoxia within the core and rim regions of glioblastomas, CA9 expression was analysed using qPCR in each of these sections, figure 48. Three different

individual glioblastoma pairs of tumour tissues were analysed, with one from the core region and the rim. The core identifies as cells from the centre of the tumour. The rim consists of cells on the outline of the tumour, and the invasive edge consists of cancer cells penetrating normal health brain. Increased hypoxia is associated with higher expression of CA9. In all three tumour tissue pairs assessed, CA9 expression was significantly higher in the core than in the rim, which suggests that hypoxia is more prevalent in the core of the tumour than the rim, indicating the gradient of hypoxia within glioblastomas.

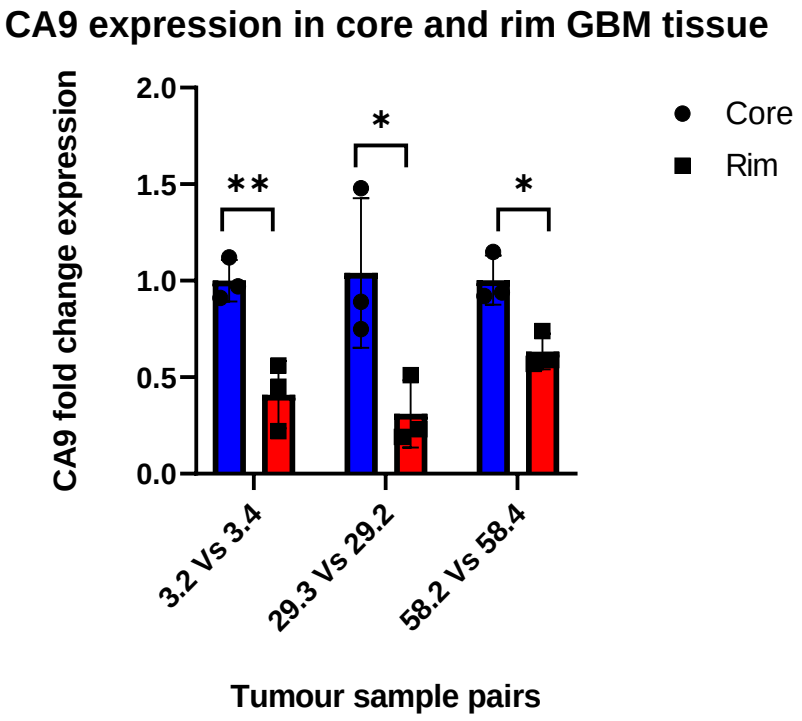

Figure 48. A graph showing the CA9 expression in the core and rim sections of glioblastoma tissues to assess the degree of hypoxia within the different regions.

To further validate the expression of CA9 in the tumour tissues, CA9 was stained for using immunohistochemistry on TMAs. In figure 49, CA9

staining is more significant in the core compared to the invasive edge, and though not significant against the rim regions, the data shows a clear increase in CA9 expression within the core. Figure 50 shows the staining of CA9 in a GBM core section, and the temporal lobe, where deeper staining is seen in the core. 27 different patient tissues are on the 3 tissue microarrays and figures 51, 52 and 53 show the CA9 cytoplasmic and nuclear staining for each tissue microarray. CA9 is mainly cytoplasmic stained, as seen in these figures, with very little nuclear staining.

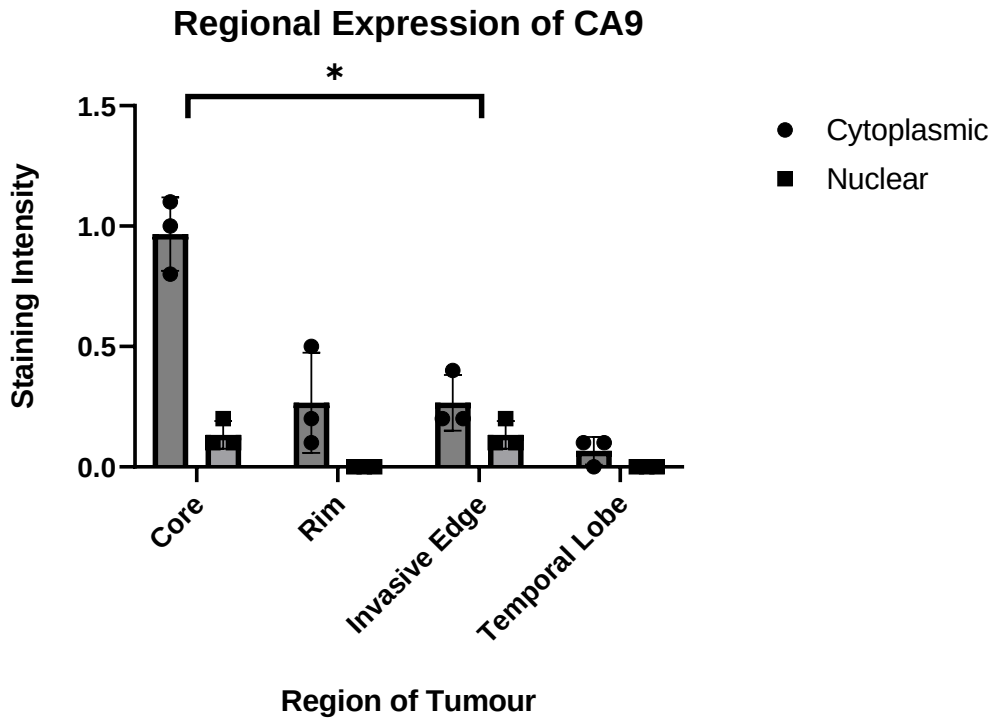

Figure 49. CA9 immunohistochemical staining in different GBM regions.

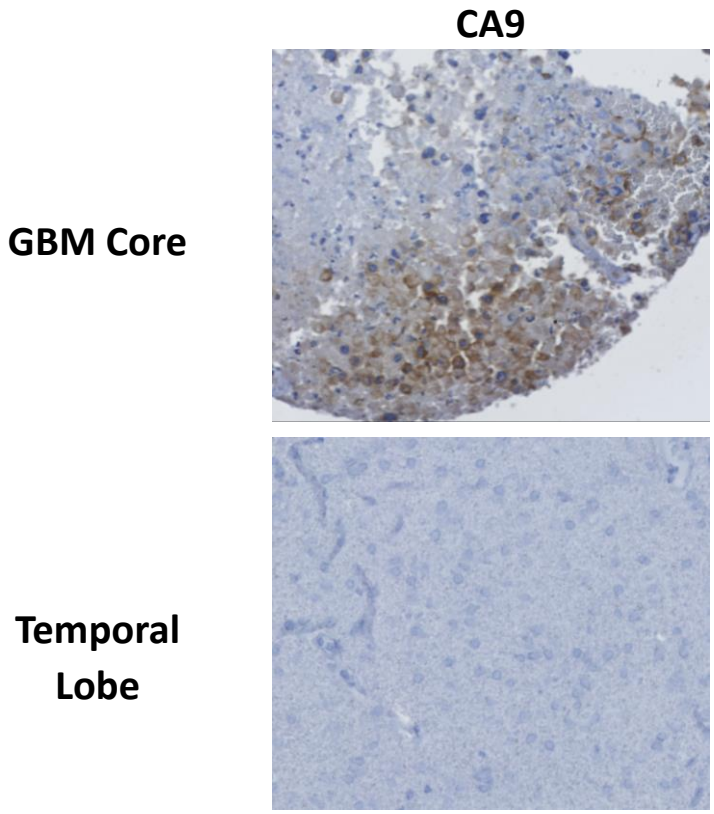

Figure 50. Immunohistochemical staining of CA9 in GBM and temporal lobe.

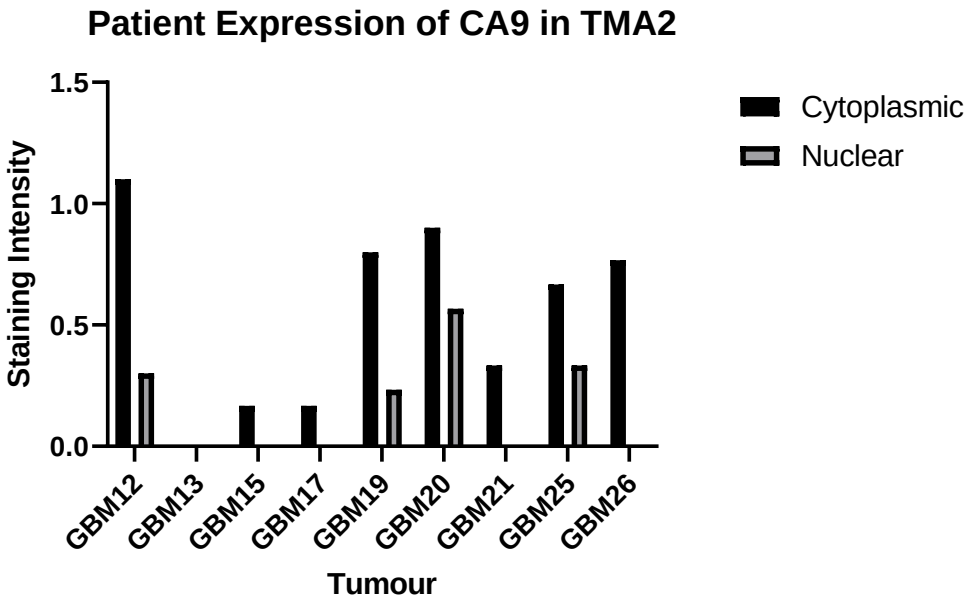

Figure 51. CA9 staining in tumour samples in TMA2.

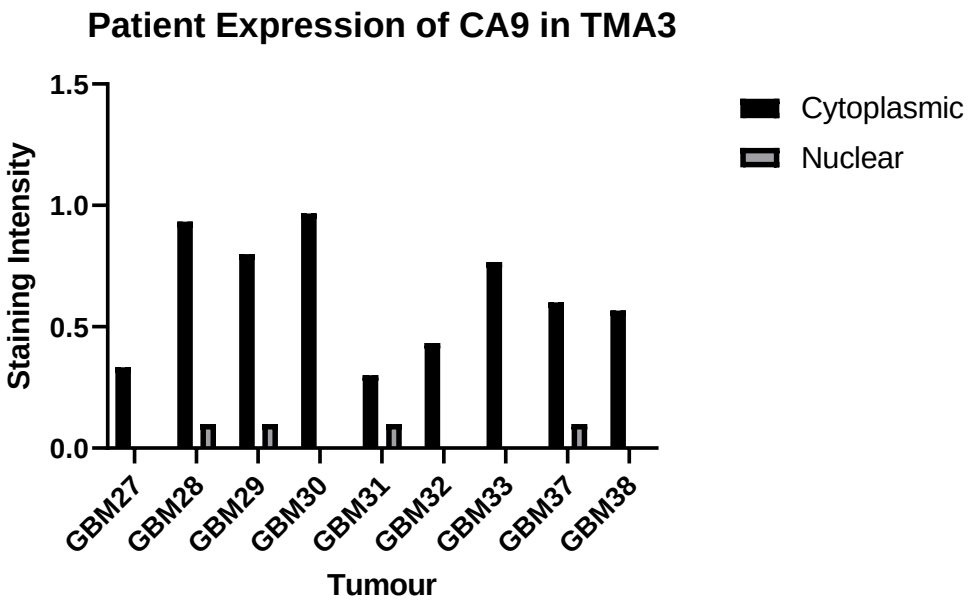

Figure 52. CA9 staining in tumour samples in TMA3.

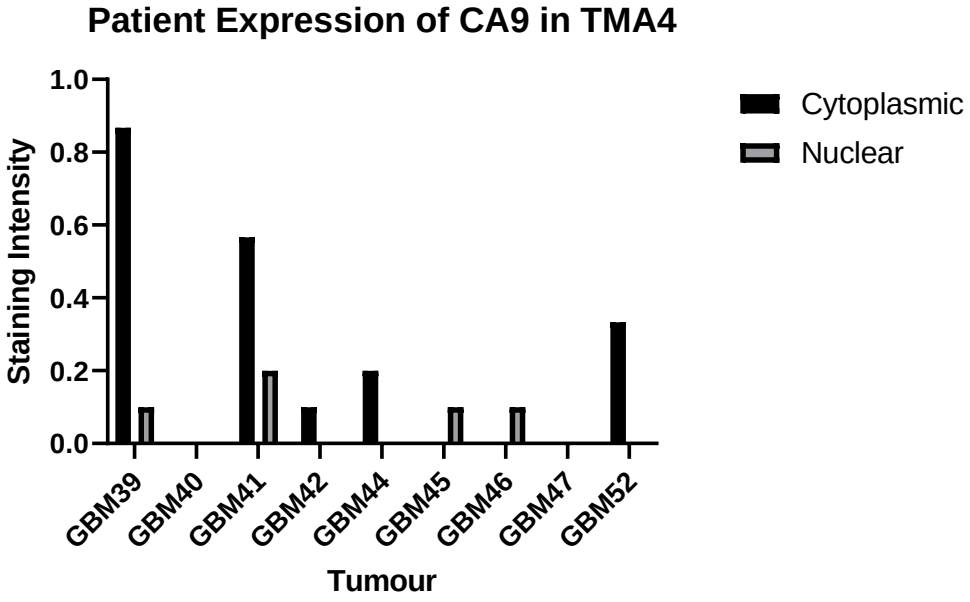

Figure 53. CA9 staining in tumour samples in TMA4.

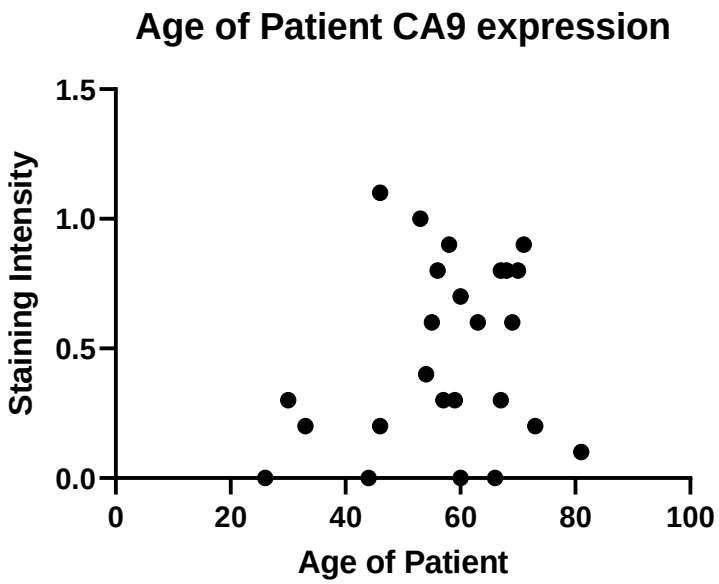

Figure 54. CA9 staining intensity correlation with age of GBM patients.

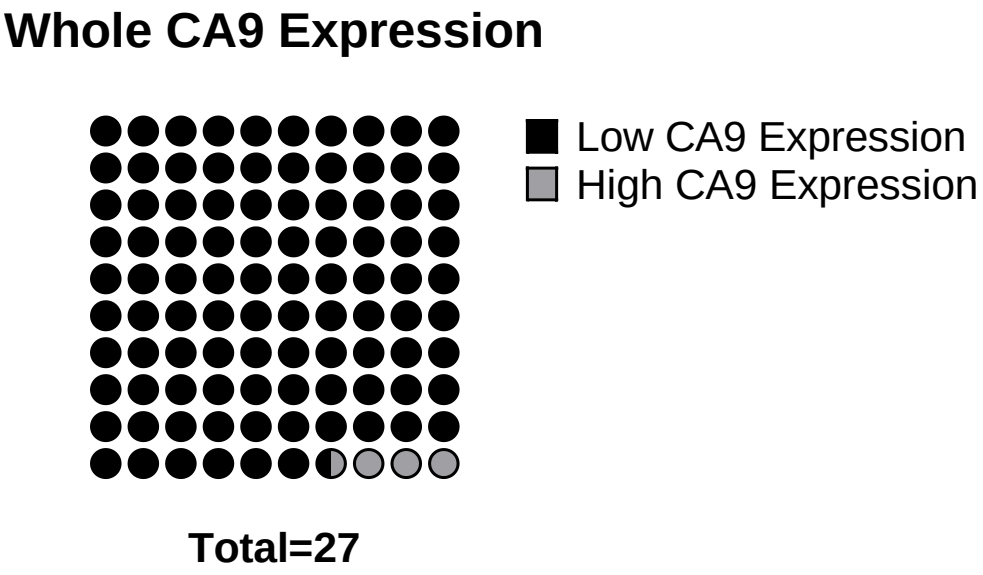

Figure 55. Schematic of low and high CA9 expression amongst GBM patients.

Using patient data from the TMAs, the ages of the patients were obtained to assess if there was a correlation of CA9 expression and age. In figure 54, no direct correlation between CA9 expression and age was determined. In these particular TMAs, all but 1 patient had relatively low

expression of CA9, as shown in figure 55. It was expected that there would be a higher or more intense staining of CA9, however the core regions accumulate most of the staining for CA9.

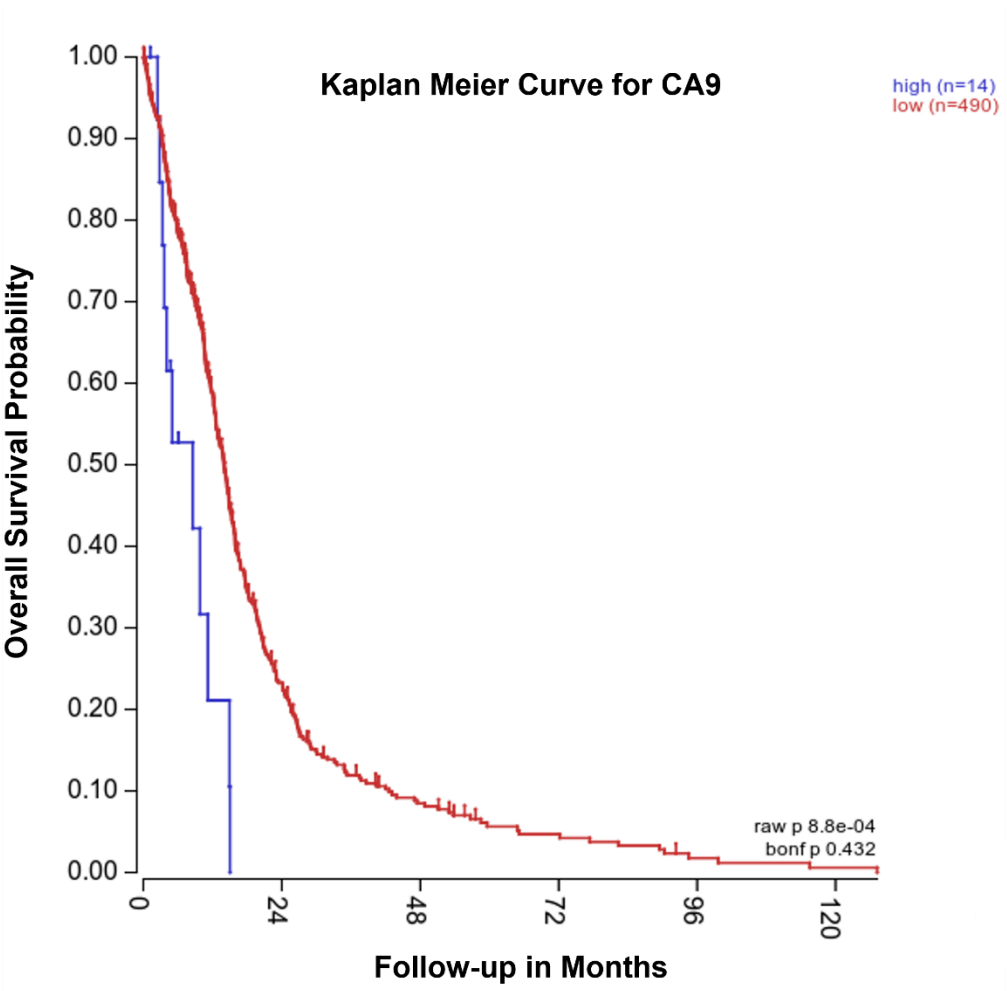

Figure 56. CA9 survival curve in GBM patients using TCGA dataset of 540 patients.

A Kaplan-Meier curve was produced using a TCGA dataset of glioblastomas with 540 patients as seen in figure 56 to determine the effect of CA9 expression of survival. The graph assesses high CA9 expression (n=14) and low CA9 expression (n=490). A larger portion of patients exhibiting low CA9 expression is similar to the trend seen in the TMA. Patients with higher CA9 expression have a much worse overall survival probability compared to patients with low CA9 expression.

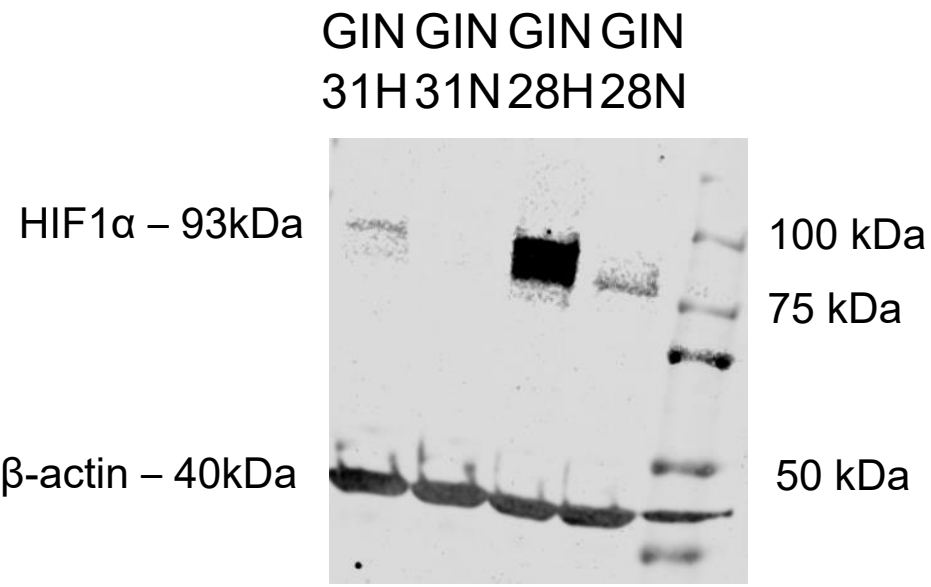

Figure 57. Western blot of HIF-1a protein expression in normoxic and hypoxic cultures of glioblastoma cell lines.

As well as qPCR analysis and IHC of CA9 to assess the presence of hypoxia, a western blot looking at the protein HIF-1α expression between the hypoxic and normoxic cultures was conducted to determine the presence of hypoxia, figure 57. The hypoxic cultures of the two glioblastoma cell lines, GIN28 and GIN31, has bands showing at 93kDa indicating the presence of HIF-1α protein. The normoxic cultures have no or lesser bands than the hypoxic cultures, showing the effect of hypoxia is stronger in the hypoxic conditions and that HIF-1α is expressed.

5.3 Introduction of miRNA selected targets and hypoxia

As miR-92a-3p and miR-149-5p are selected as important miRNAs in response to hypoxia in glioblastomas, further investigation is required to determine the impact of their changed expression levels due to the

change of oxygen levels. Our next hypotheses look into the effects of gene expression in response to hypoxia under the influence of miRNAs and ultimately how this could affect glioblastomas.

Hypothesis 1: miR-92a-3p is downregulated in response to hypoxia and this will cause the expression of target genes to be increased more in hypoxia.

Hypothesis 2: miR-149-5p is upregulated in response to hypoxia and this will cause the expression of target genes to be decreased more in hypoxia.

Hypothesis 3: Hypoxia effects biological processes such as apoptosis and senescence.

Hypothesis 4: Changed target gene expression in hypoxia is also seen in tumour tissue samples.

5.4 The expression of miR-92a-3p and miR-149-5p in tumour samples and other functions

The selected miRNAs, miR-149-5p and miR-92a-3p, are up and downregulated respectively in hypoxia in glioblastoma cell lines. To validate the changes seen in the cell lines, qPCR was performed to assess the expression levels of the miRNAs in tumour tissue samples.

5.4.1 miRNA and tumour sample expression

mir-92a-3p was a target selected from the qPCR data and it was significantly downregulated in the cell lines in hypoxia compared to normoxic conditions. Using the same three tumour tissue samples of core and rim regions, the expression of miR-92a-3p was analysed in these regions. Interestingly, the results are the opposite to those seen in the cell lines, with miR-92a-3p expression upregulated in the core compared with the rim in hypoxia as seen in figure 58. A potential reason for this change seen in the tumour tissue is that the cell load of the peripheral areas could be drastically lower than in the core which may artificially reduce the observed expression levels.

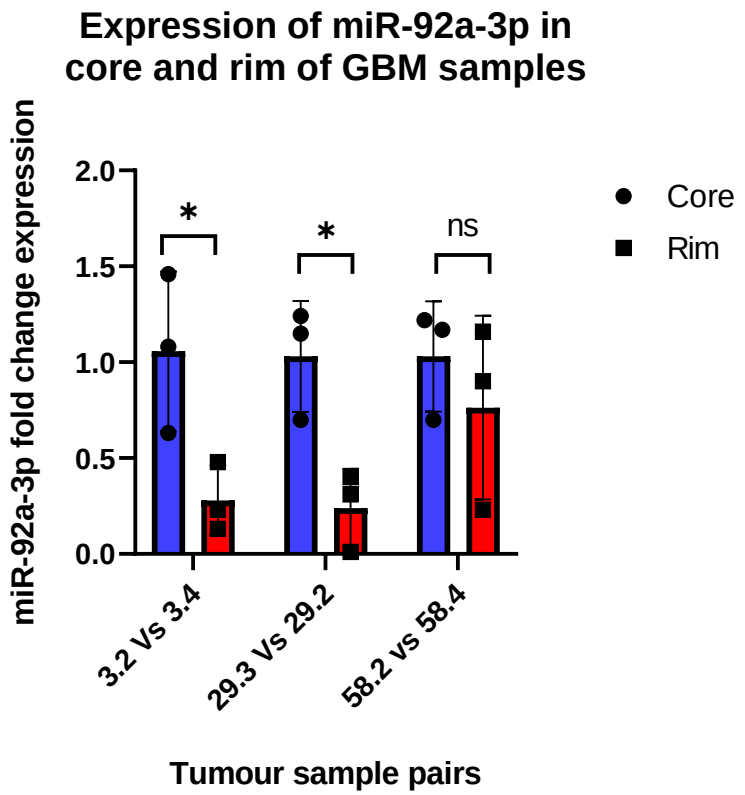

Figure 58. miR-92a-3p expression within glioblastoma tissue samples within the different regions, core and rim

The other selected target from the qPCR analysis is miR-149-5p. The expression of miR-149-5p within the tumour sample pairs was conducted and it was found that within two of the three pairs, miR-149-5p expression was significantly upregulated in the core compared with the rim as seen in figure 59. This coincides with the cell line expression of miR-149-5p, as upregulated in the core, suggests upregulation in hypoxia which was seen in the cell lines.

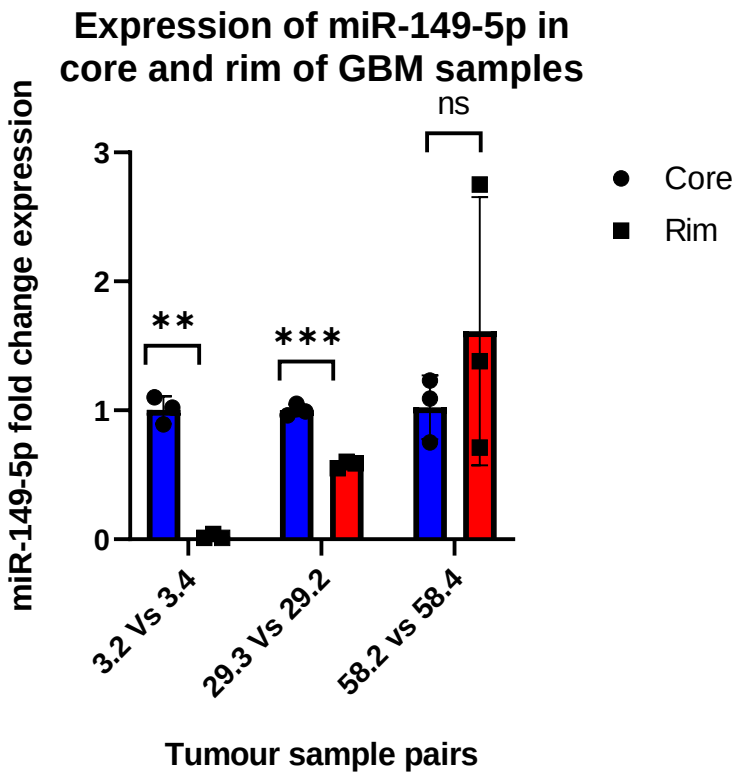

Figure 59. miR-149-5p expression within glioblastoma tissue samples within the different regions, core and rim.

5.4.2 Knock-ins and knock-out effectiveness

During the process of transfection, siGLO green transfection indicator, which is a fluorescent oligonucleotide that localises within the nucleus and fluoresces green, was transfected to visually confirm the efficiency of transfection. Figures 60 and 61 confirm the fluorescence of transfected siGLO compared to the non-transfected control in both GIN28 and GIN31 cell lines.

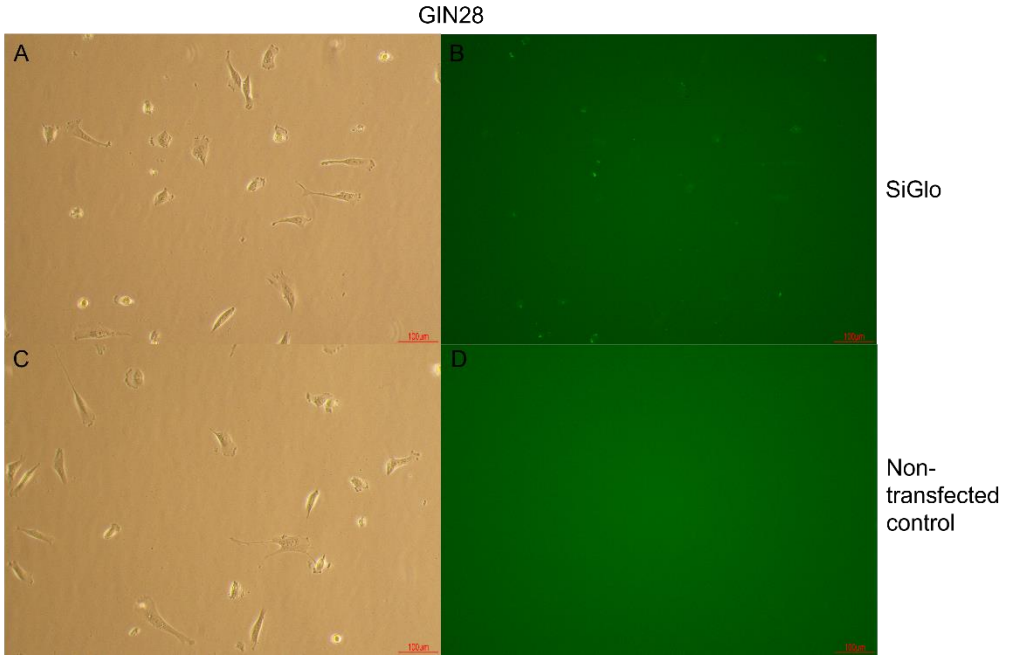

Figure 60. Transfection of GIN28 with SiGLO and non-targeting control. A) bright field image of GIN28 cells that are transfected with siGLO. B) Fluorescent image of GIN28 cells transfected with siGLO showing in the bright green spots. C) Bright field image of GIN28 cells that are transfected with a non-targeting control. D) Fluorescent image of GIN28 cells transfected with the non-targeting control with no fluorescence seen.

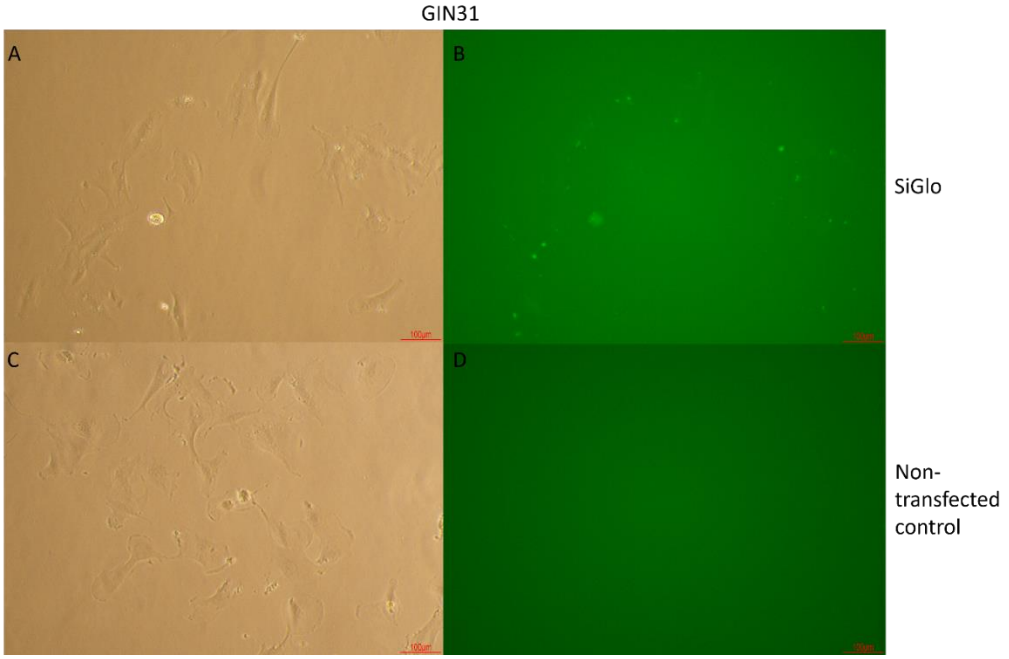

Figure 61. Transfection of GIN31 with SiGLO and non-targeting control. A) bright field image of GIN31 cells that are transfected with siGLO. B) Fluoresent image of GIN31 cells transfected with siGLO showing in the bright green spots. C) Bright fied image of GIN31 cells that are transfected with a non-targeting control. D) Fluorescent image of GIN31 cells transfected with the non-targeting control with no fluorescence seen.

To determine how long the transfection of the mimics and inhibitors would last, the expression of each miRNA was analysed using PCR after 48hrs and 72hrs of transfection, these preliminary investigations were all conducted within normoxic conditions. This was to confirm that after 24 hours of transfection incubation and 24 hours of hypoxic exposure, the effect of the mimic and inhibitors was still present for following experiments. The time points assessed were 48hrs, as this is the minimum amount of time required and then a 72hr time-point if longer experiments were required to see if the transfections were still at an acceptable level. In figures 62 and 63 the mimic expression of miR-92a-

3p and miR-149-5p respectively, is at its highest point at 48hrs compared to the non-targeting control and deteriorates by 72hrs in both cell lines.

The inhibitor effect was much more stable after 48hrs, showing a similar level of reduction of miRNA expression at the 72hr time-point for miR-92a-3p in both cell lines in figure 64. For the miR-149-5p inhibitor, peak repression of miR-149-5p was seen at 48hrs and at 72hrs the expression of miR-149-5p started to increase in figure 65.

Following on the results of the miRNA transfection efficiency, all follow-on experiments were conducted at 48hrs after transfection to allow for transfection uptake, and hypoxic/normoxic exposure. This time point was the most successful for both cell lines and both the mimics and inhibitors of both miRNAs, miR-92a-3p and miR-149-5p.

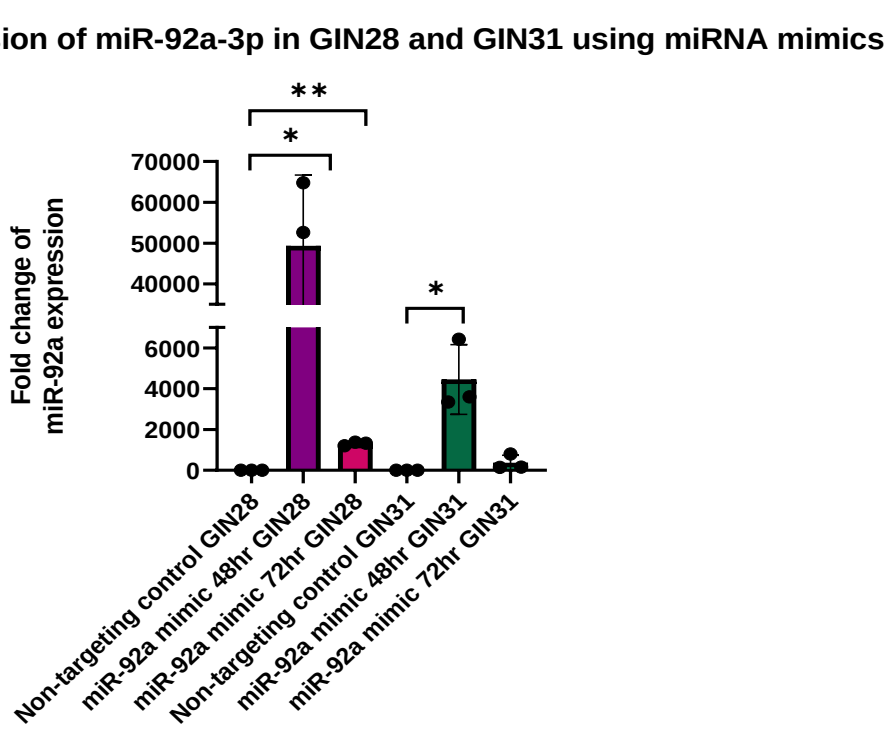

Figure 62. Showing the expression of miR-92a-3p using miR-92a-3p mimics on GIN28 and GIN31, 48 and 72hrs after initial transfection.

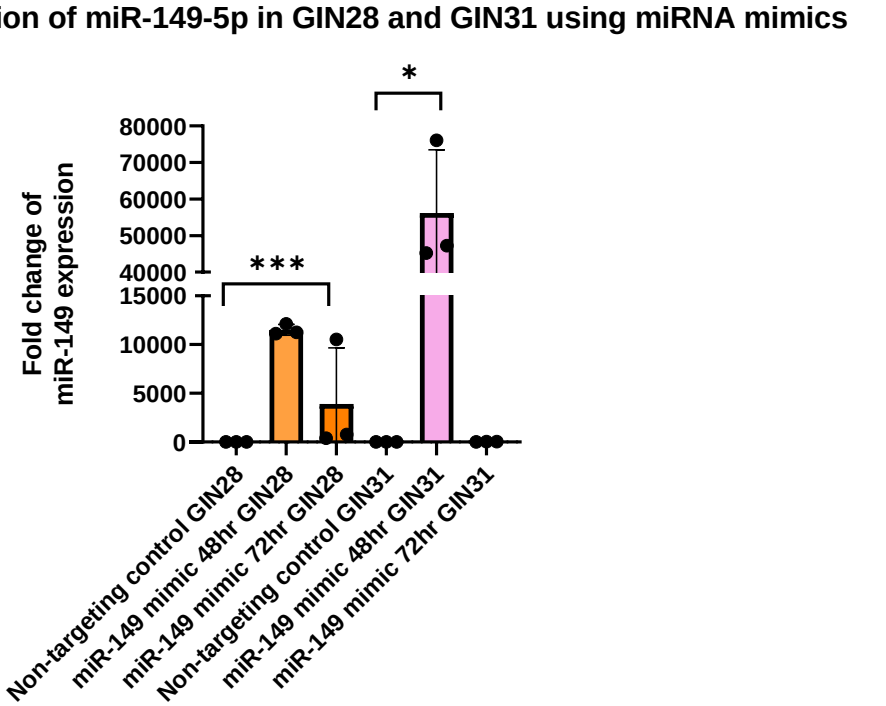

Figure 63. Showing the expression of miR-149-5p using miR-149-5p mimics on GIN28 and GIN31, 48 and 72hrs after initial transfection.

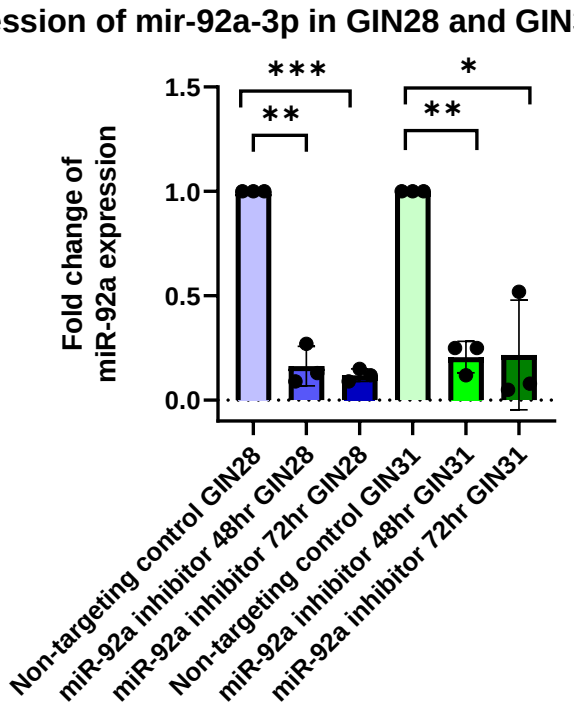

Figure 64. Showing the expression of miR-92a-3p using miR-92a-3p inhibitors on GIN28 and GIN31, 48 and 72hrs after initial transfection.

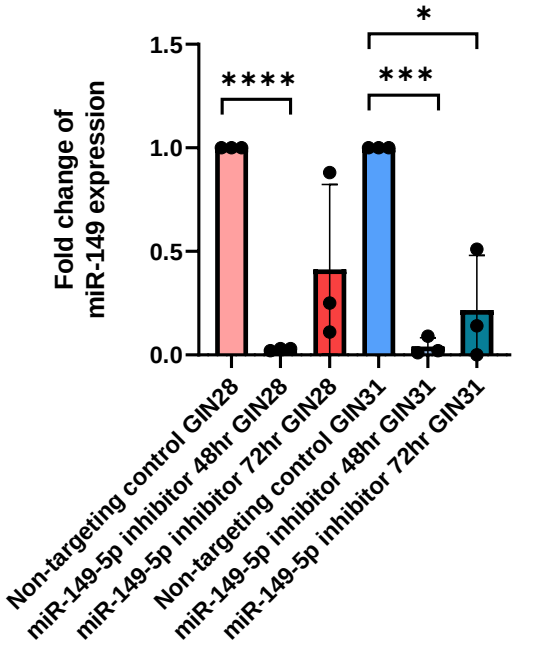

Figure 65. Showing the expression of miR-149-5p using miR-149-5p inhibitors on GIN28 and GIN31, 48 and 72hrs after initial transfection.

5.4.3 Caspase-glo assay with knock-ins and outs

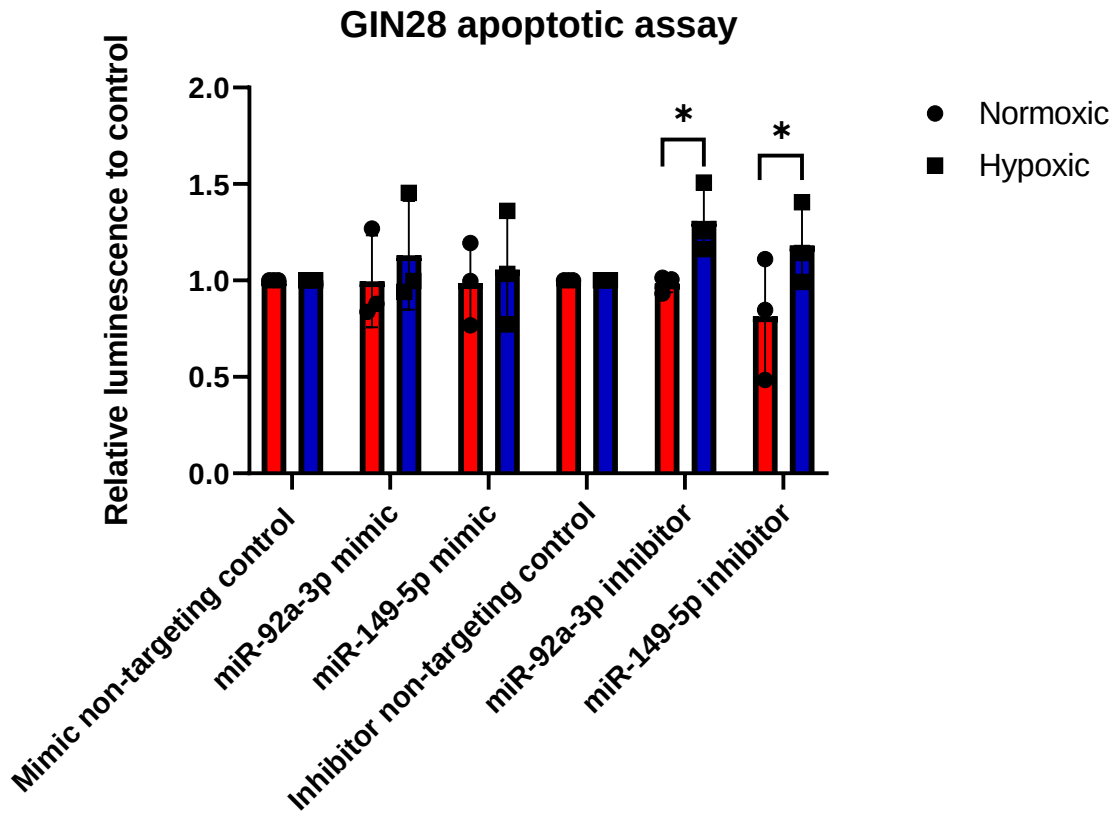

Figure 66. Apoptotic assay using mimics and inhibitors of miR-92a-3p and miR-149-5p in GIN28 cells.

To assess the effect of hypoxia on apoptotic activity and miRNA expression levels, the Caspase-glo assay (Promega) was performed using miR-92a-3p and miR-149-5p mimic and inhibitor transfected cells that were cultured in normoxic and hypoxic conditions.

The apoptosis assay, Caspase-Glo (Promega) contains a pro-luminescent caspase-3/7 DEVD-aminoluciferin substrate and a thermostable luciferase in a mixture which are both optimised for cell lysis. The addition of the mixture to cells results in cell lysis which results

in caspase cleavage of the substrate. This cleavage frees aminoluciferin which is catalysed by luciferase and generates a luminescent signal that is proportional to caspase-3/7 activity. The buffer system increases assay performance and prevents compound interference which is more likely in fluorescent or colorimetric assays.

In GIN28, apoptosis in significantly increased in normoxia compared to hypoxia with miR-149-5p inhibitor transfected cells as seen in figure 66.

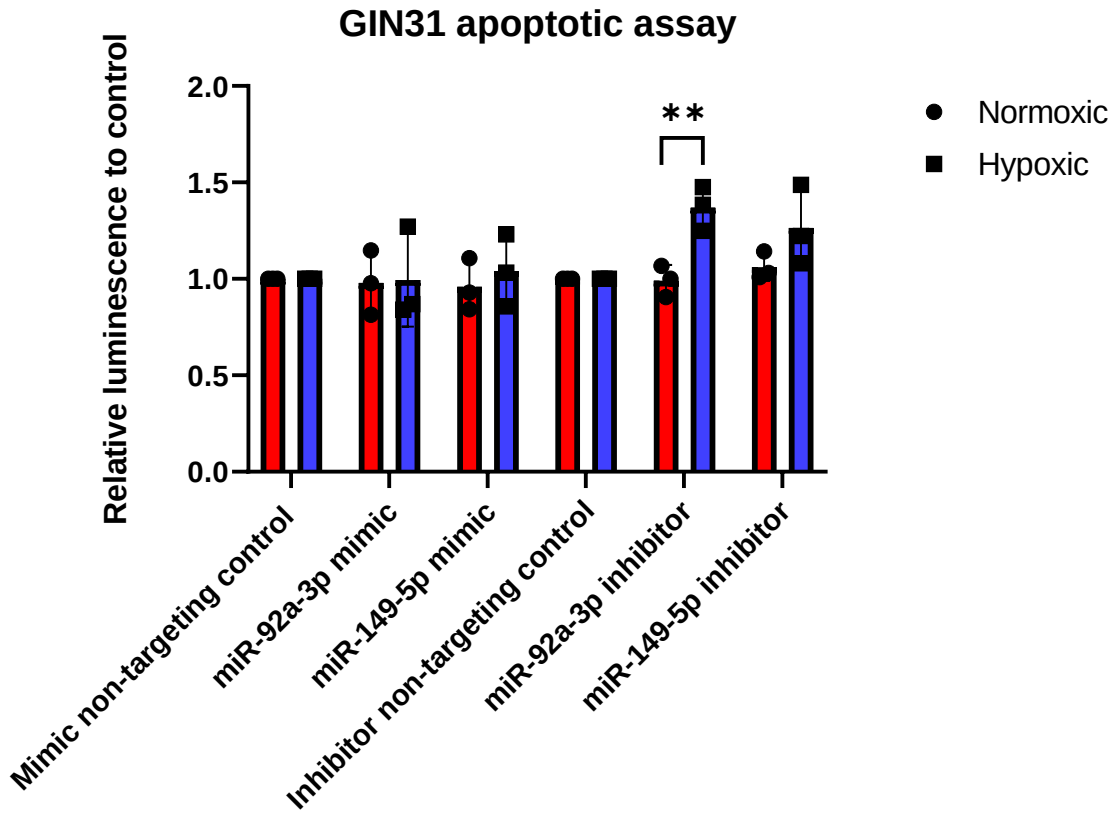

Figure 67. Apoptotic assay using mimics and inhibitors of miR-92a-3p and miR-149-5p in GIN31 cells.

In both GIN28 and GIN31 (figure 67) the amount of apoptosis was significantly increased in hypoxia compared to normoxia with transfected miR-92a-3p inhibitor. The transfected mimics of both miRNAs had no significant differences of apoptosis between hypoxic and normoxic conditions.

5.4.4 Senescence assays

Similar to apoptosis, senescence is a biological pathway that miR-92a-3p and miR-149-5p are significantly involved in, and was identified in the disease ontology, KEGG, wikipathways and Reactome analyses. Senescence assays were performed on miR-92a-3p and miR-149-5p mimic and inhibitor transfected GIN28 and GIN31 cell lines along with a control and used the β-galactosidase senescence staining kit (Cell Signalling). However, as seen in figure 68 and 69 for GIN28, the β-galactosidase staining solution crystalised which prevented accurate staining of cells in senescence. Crystallisation occurs when too much condensation forms within the plates. Further optimisation could also include ensuring the dissolving of staining solution by heating and agitating solutions simultaneously. Due to time limitations, optimisation of the protocol was not conducted, but for the future to analyse the effects of hypoxia and miRNA expression on senescence, this particular method requires further optimisation.

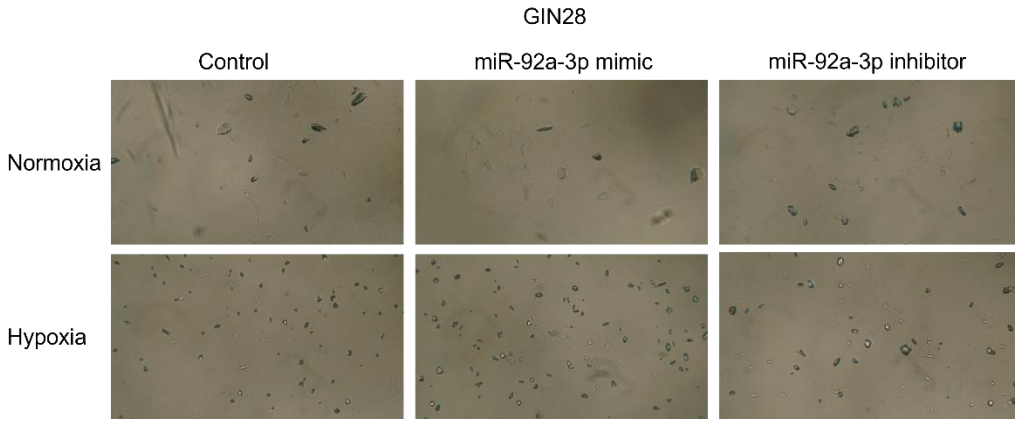

Figure 68. Senescence assay of GIN28 using control, miR-92a-3p mimic and inhibitor in normoxic and hypoxic conditions.

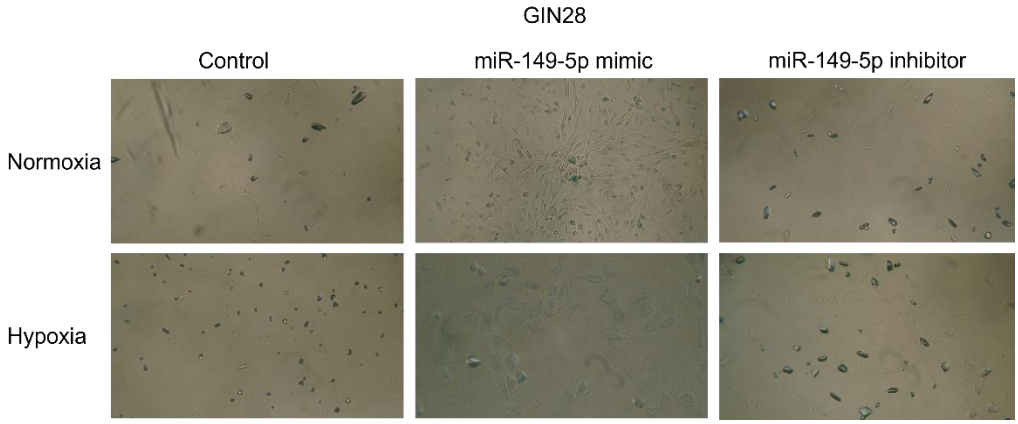

Figure 69. Senescence assay of GIN28 using control, miR-92a-3p mimic and inhibitor in normoxic and hypoxic conditions.

5.5 miRNA targets and enrichment

miR-149-5p and miR-92a-3p are selected as hypoxia-influenced miRNAs and to further understand their response to hypoxia, pathway enrichment analysis was conducted to identify the most significant pathways the miRNA targets are involved in and the most significant gene targets in significant pathways of the miRNAs.

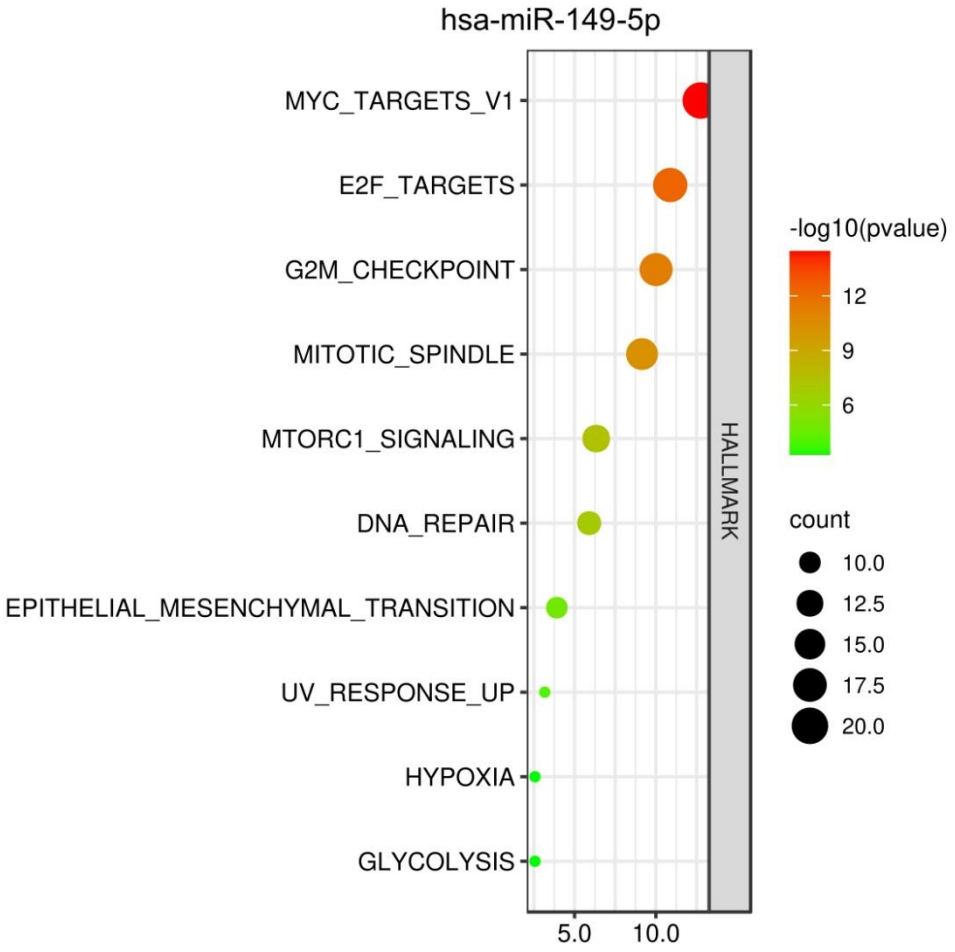

Figure 70. Enrichment pathway analyses of the gene targets of miR-149-5p.

The enrichment pathway analysis of miR-149-5p, figure 70, shows that both MYC and E2F targets are the most significant pathways that involve miR-149-5p target genes. G2M checkpoint and mitotic spindle pathways are significant which are both part of the cell cycle. Other pathways which are significant include mTOR pathway (involving mTORC), DNA repair pathway, EMT pathway, UV response and glycolysis. An important pathway that significantly involves miR-149-5p gene targets is hypoxia pathway. The top three gene targets of each miRNA will be investigated further, for miR-149-5p the top three genes in the most significant pathways are SRSF1, RAN and HNRNPU. SRSF1 is involved in MYC

targets, E2F targets, mitotic spindle, mTOR signalling, DNA repair, EMT, UV response, glycolysis and hypoxia. RAN is involved in MYC targets and G2M checkpoints and HNRNPU is involved in E2F targets.

Hypoxia was identified as a significant pathway from the gene targets of miR-149-5p. The 8 genes that were associated with hypoxia and miR-149-5p targets are MYH9, SLC2A1, PFKL, GPI, GAPDH, IL6, GPCI and JUN. Figure 71 and 72 shows the disease-free survival and overall survival of GBM patients with high and low expression of the hypoxia genes combined. High expression of these genes significantly reduce disease-free survival compared to low expression but though possibly showing a similar trend has no significant difference on overall survival.

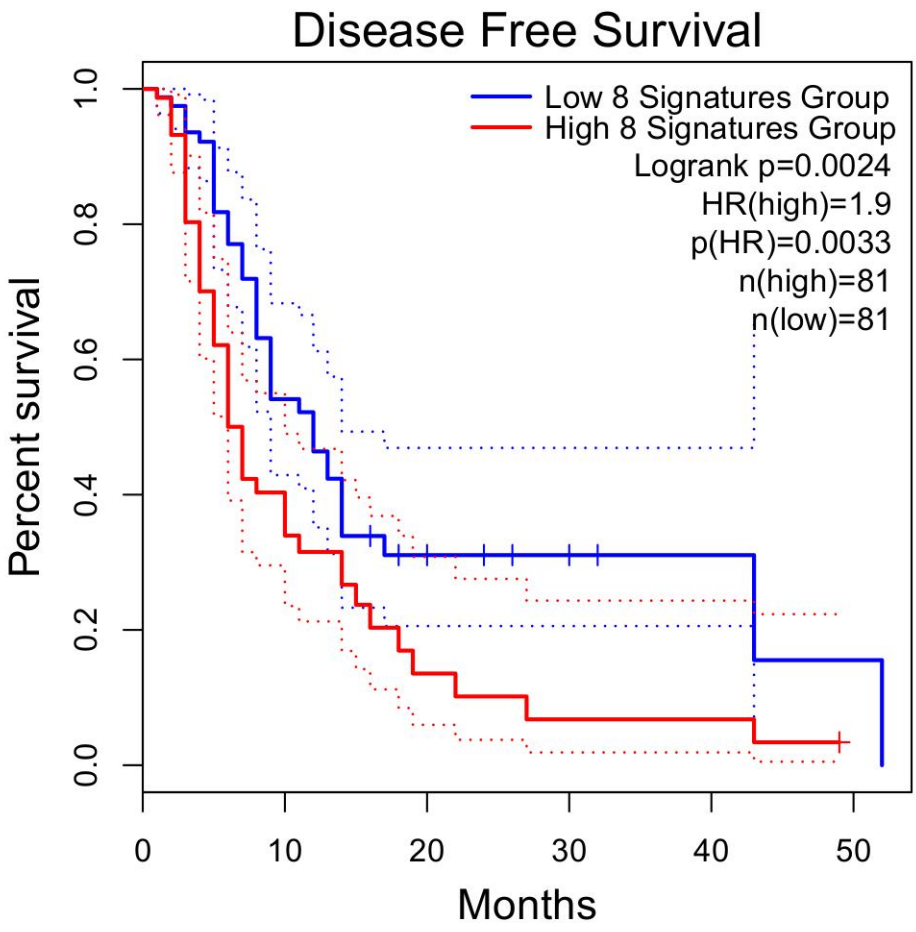

Figure 71. Kaplan Meier curve showing the disease-free survival data of the 8 hypoxic genes that are targets of miR-149-5p. The low expression signatures are patients with expression levels below the median and high signature group are those with expression above the median.

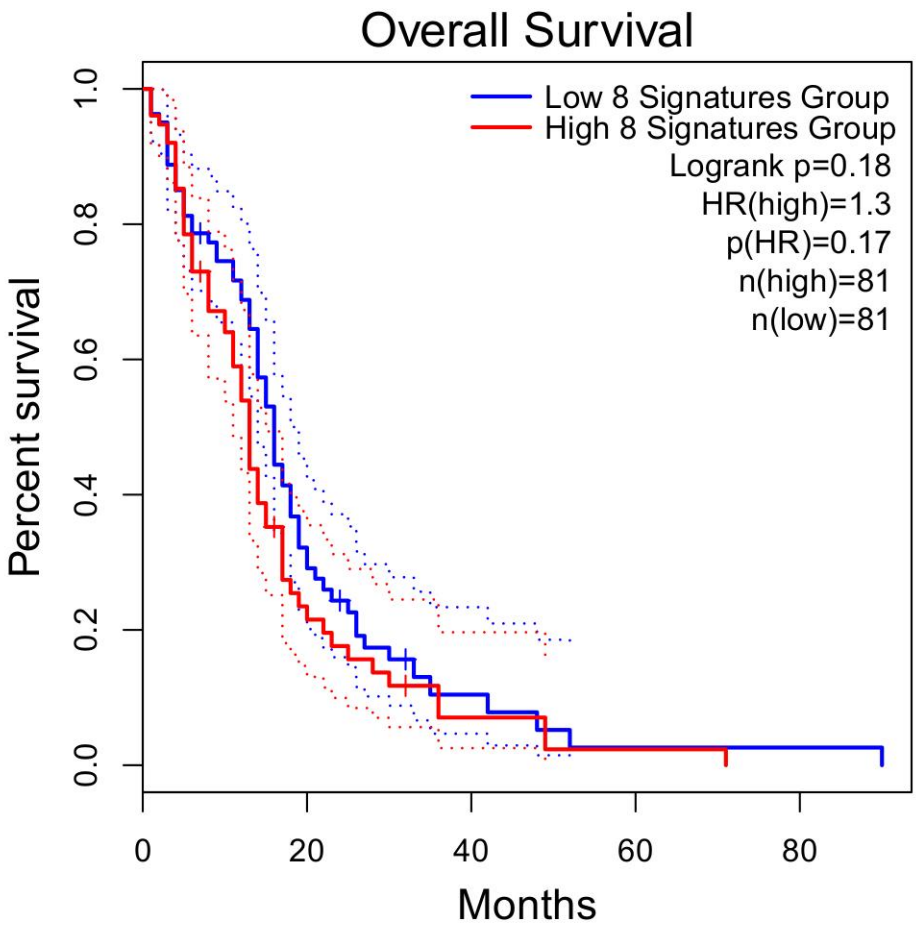

Figure 72. Kaplan Meier curve showing the overall survival data of the 8 hypoxic genes that are targets of miR-149-5p. The low expression signatures are patients with expression levels below the median and high signature group are those with expression above the median.

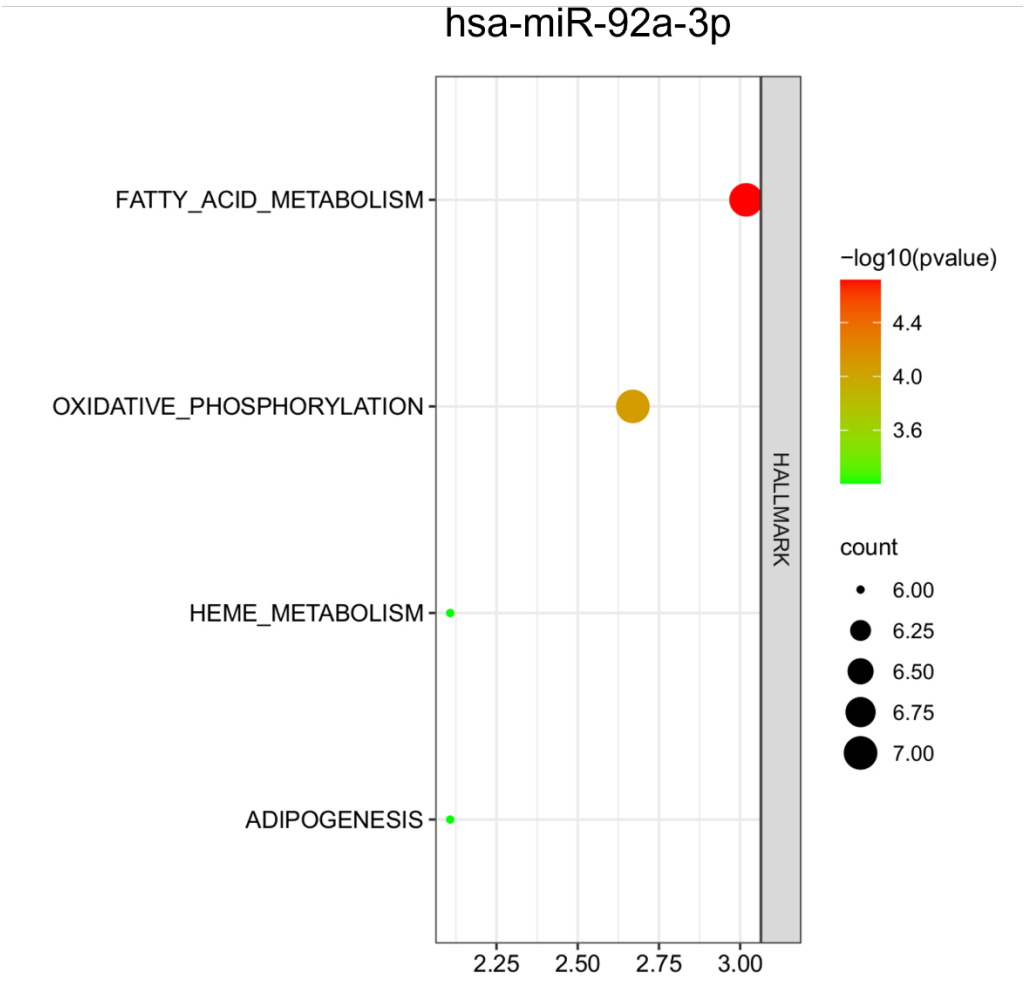

Figure 73. Enrichment analyses of the gene targets of miR-92a-3p.

The enrichment pathway analysis of miR-92a-3p, figure 73, shows that both fatty acid metabolism and oxidative phosphorylation are the most significant pathways that involve miR-92a-3p target genes. Other miR-92a-3p target significant pathways are haem metabolism and adipogenesis. The top three significant genes that are involved in both fatty acid metabolism and oxidative phosphorylation are SUCLG1, ACCA1 and ACADS. SUCLG1 is also involved in haem metabolism and adipogenesis and ACAA1 is also involved in adipogenesis.

In hypoxia, a downregulation of oxidative phosphorylation and fatty acid metabolism is expected as the fatty acid conversion to L-cartenine is suppressed in hypoxia.

5.5.1 qPCR of associated genes and miR-149-5p expression

Following from the enrichment of the target genes of miR-149-5p, the significant top three gene targets were selected; SRSF1, RAN and HNRNPU. All three genes were involved in the most enriched pathways as MYC targets, E2F targets and involved in the G2M checkpoint. The expression of these genes was assessed using non-targeting controls, miR-149-5p mimic and miR-149-5p inhibitor in both normoxic and hypoxic conditions. This was to enable to observe the effect of the miRNA expression on the gene expression in the different oxygen conditions.

SRSF1 is a serine/arginine-rich splicing factor 1 involved in pre-mRNA splicing and has been reported to be a proto-oncogene. In GIN28, the miR-149-5p mimics and inhibitors have the opposite effect in normoxia compared to SRSF1 expression seen in hypoxia. The mimic reduces the amount of SRSF1 expression significantly and the inhibitor significantly increases SRSF1 expression in hypoxia as seen in figure 74. In GIN31, figure 75, there are no significant changes to SRSF1 expression in response to the mimics and inhibitors in normoxia and hypoxia. This emphasises the differences and heterogeneity of glioblastoma tumours.

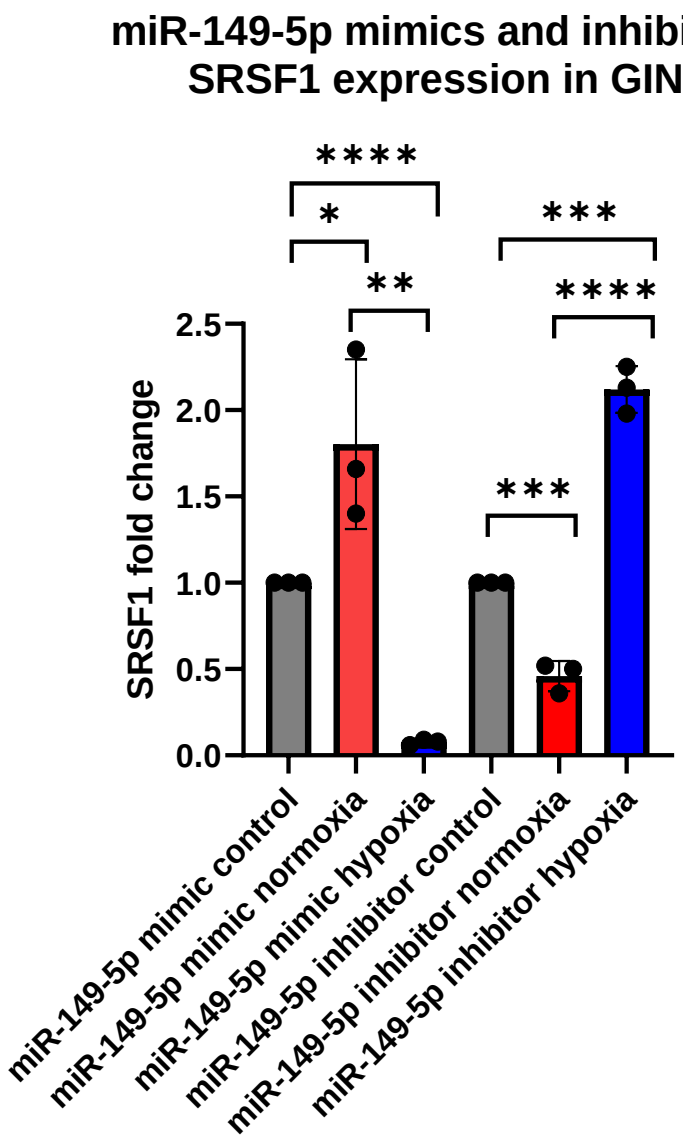

Figure 74. Effects of miR-149-5p mimics and inhibitors on SRSF1 expression in normoxic and hypoxic conditions in GIN28 cells.

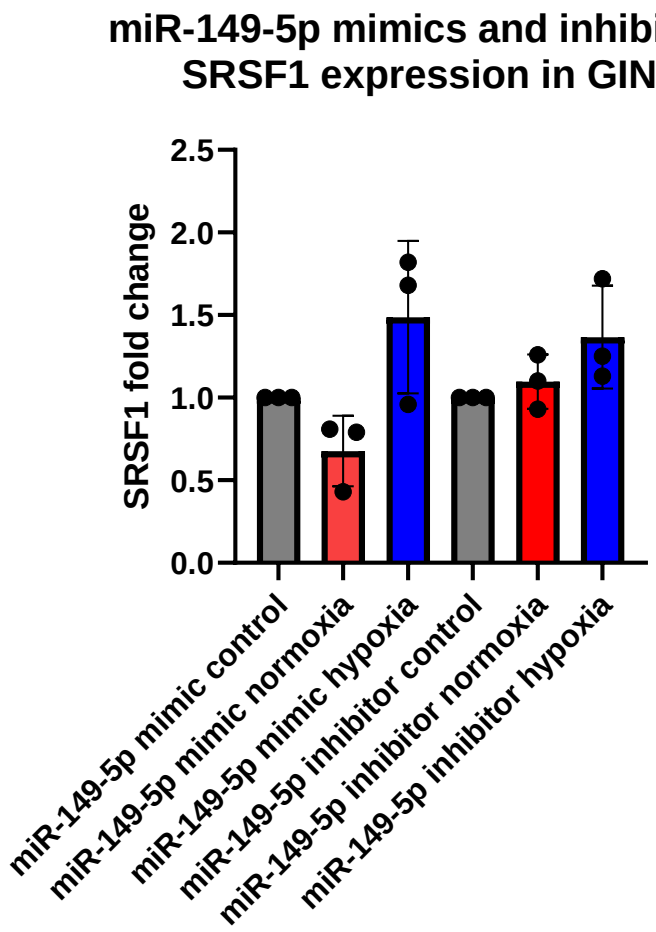

Figure 75. Effects of miR-149-5p mimics and inhibitors on SRSF1 expression in normoxic and hypoxic conditions in GIN31 cells.

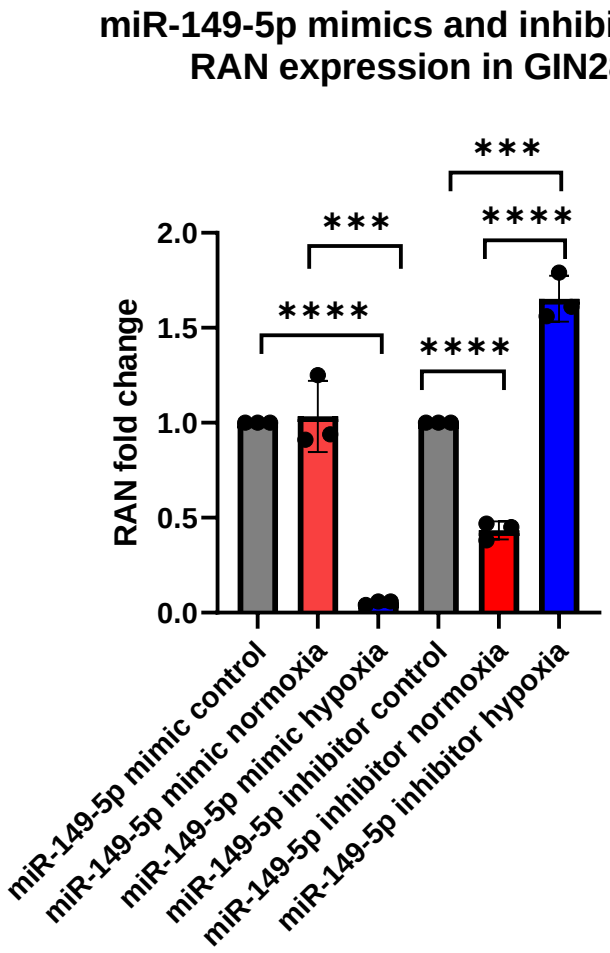

Figure 76. Effects of miR-149-5p mimics and inhibitors on RAN expression in normoxic and hypoxic conditions in GIN28 cells.

RAN, the second significant target of miR-149-5p, is a GTP-binding nuclear protein and is involved in nuclear transport in interphase and mitosis. In GIN28, no expression change in RAN is observed with miR-149-5p mimic and a significant decrease with the inhibitor in normoxia, however, in hypoxia, the mimic significantly depletes RAN expression and the inhibitor significantly increases RAN expression (figure 76). Also, in GIN31, RAN expression does not vary much across the mimics/inhibitors and hypoxia status as seen in figure 77.

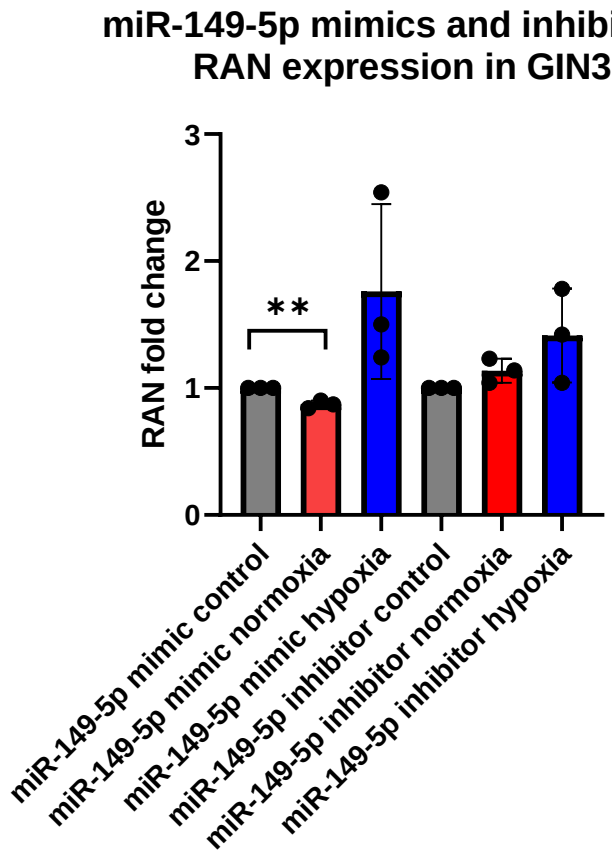

Figure 77. Effects of miR-149-5p mimics and inhibitors on RAN expression in normoxic and hypoxic conditions in GIN31 cells.

The third gene that was investigated as a target of miR-149-5p is HNRNPU which is a heterogeneous nuclear ribonucleoprotein U and is associated with pre-mRNA in the nucleus. In GIN28, HRNRPU expression is significantly lower than the control with the transfected miR-149-5p mimic in hypoxia but not significantly changed in normoxia (figure 78). The miR-149-5p inhibitor significantly increases HRNRPU expression in normoxia compared to hypoxia. In GIN31, there are no significant changes in HRNRPU expression in hypoxia with the mimic or inhibitor compared to the control (figure 79). The presence of miR-149-5p mimics and inhibitors in normoxia have significantly increased HRNRPU expression.

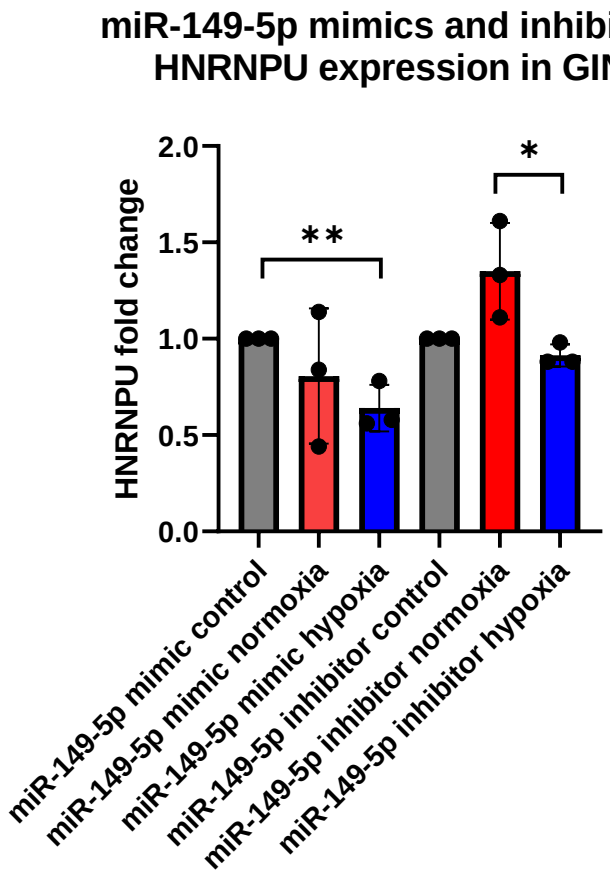

Figure 78. Effects of miR-149-5p mimics and inhibitors on HNRNPU expression in normoxic and hypoxic conditions in GIN28 cells.

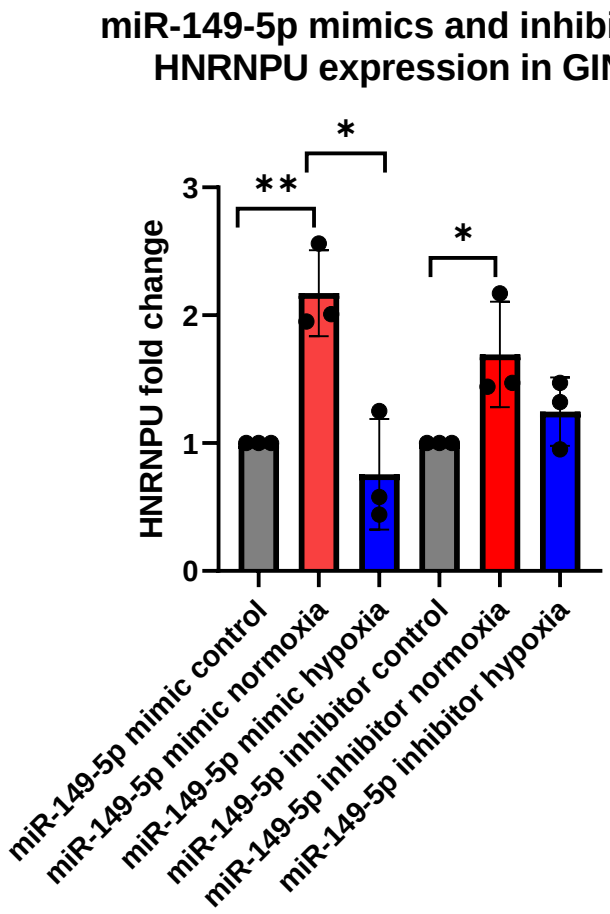

Figure 79. Effects of miR-149-5p mimics and inhibitors on HNRNPU expression in normoxic and hypoxic conditions in GIN31 cells.

In hypoxia miR-149-5p is acting as expected but to the extreme with all target genes as the mimics are decreasing the expression of target genes and the inhibitors are increasing target gene expression. However, this is not the case in normoxia indicating that this individual miRNA may be induced by hypoxia. This is further suggested as hypoxia is a pathway that is enriched with miR-149-5p targets.

5.5.1.1 Assessing effect of miR-149-5p expression on non-target genes

ACAA1 is acetyl-CoA acyltransferase 1 and is involved in the beta oxidation system of peroxisomes and is a gene target of miR-92a-3p. To assess if there is an indirect effect from miR-149-5p, the effect of miR-149-5p in hypoxia and normoxia was also analysed on miR-92a-3p gene targets. ACCA1 in GIN28 showed an increase in the gene with the mimic, figure 80, which is the inverse of what would be expected if the gene was a target. The differences seen may be solely the effect of hypoxia, however a larger increase was seen with the mimic than the inhibitor. In GIN31 no significant changes were seen in ACAA1 with mimics, figure 81, but a large significant increase was seen with the miR-149-5p inhibitor in normoxia but not in hypoxia.

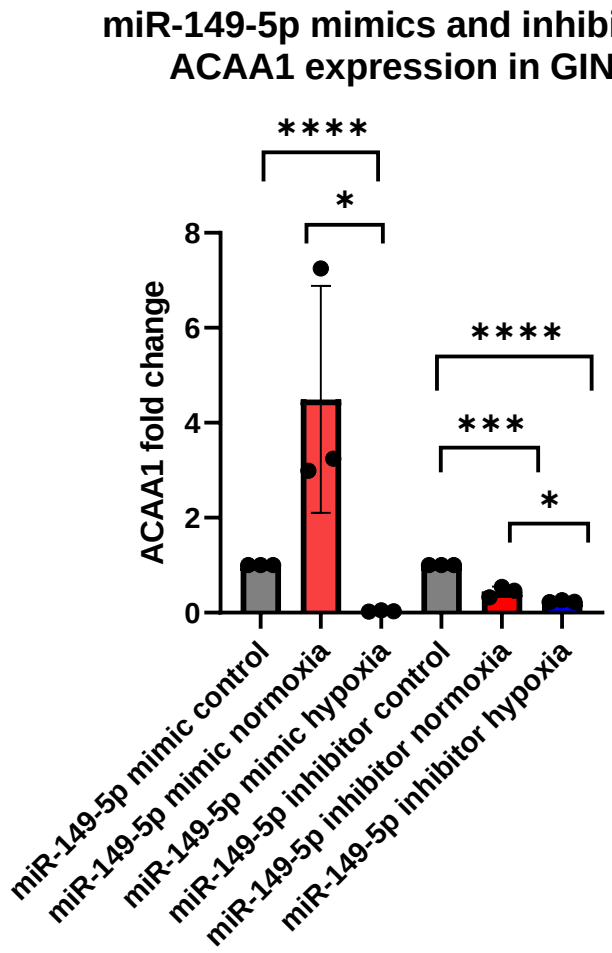

Figure 80. Effects of miR-149-5p mimics and inhibitors on ACAA1 expression in normoxic and hypoxic conditions in GIN28 cells.

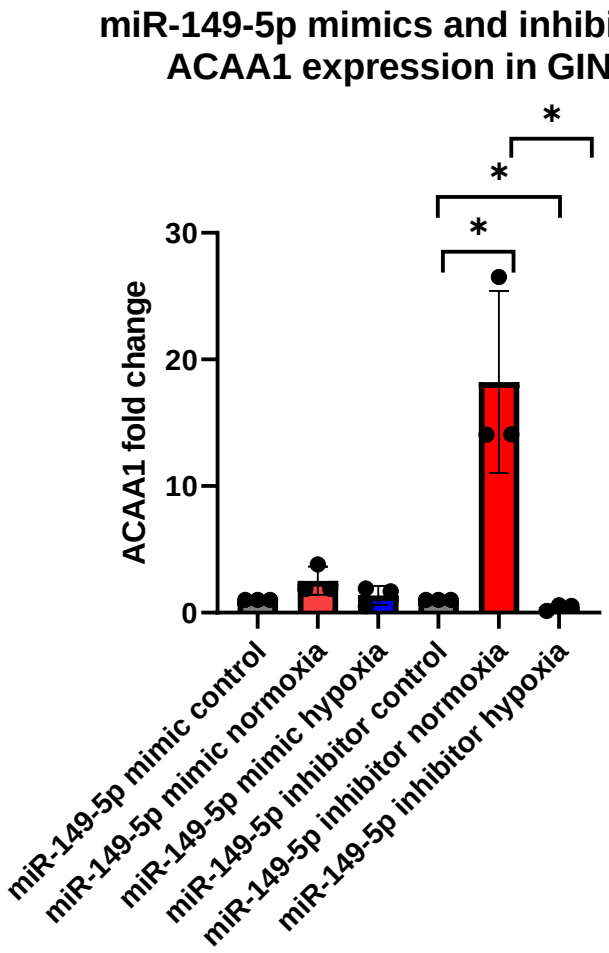

Figure 81. Effects of miR-149-5p mimics and inhibitors on ACAA1 expression in normoxic and hypoxic conditions in GIN31 cells.

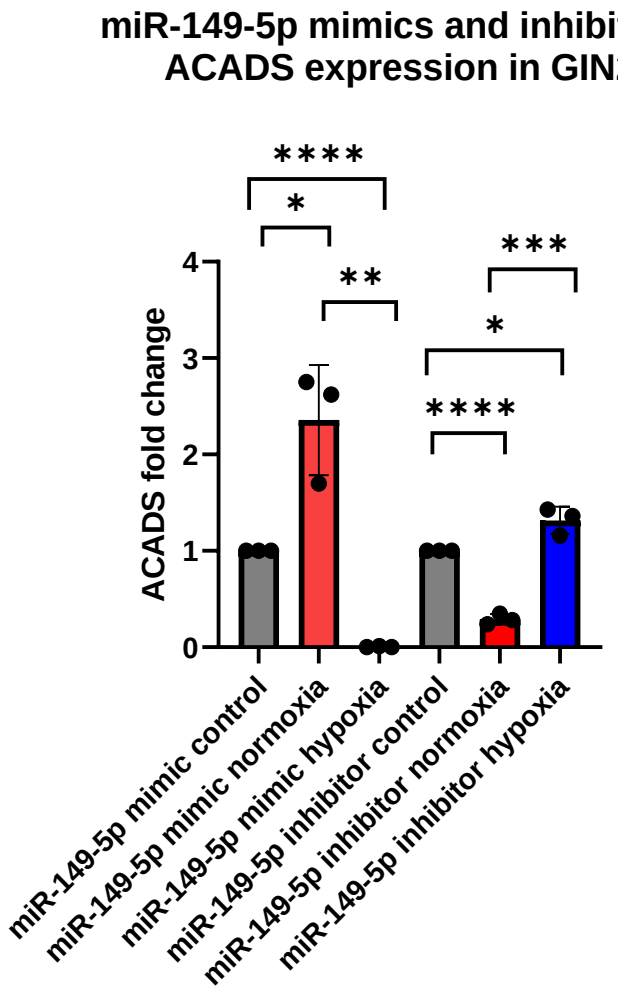

Figure 82. Effects of miR-149-5p mimics and inhibitors on ACADS expression in normoxic and hypoxic conditions in GIN28 cells.

The ACADS gene codes for Acyl-CoA dehydrogenase, C-2 to C-3 short chain catalyses the initial step of mitochondrial fatty acid beta-oxidation pathway and it is also associated with short-chain acyl-coenzyme A dehydrogenase deficiency. In GIN28, figure 82, the expression levels of ACADS so an effect from the mimic and inhibitor in hypoxic conditions but an inverse effect in normoxia. In GIN31, no significant changes are seen using the miR-149-5p mimic, but the inhibitor in normoxic conditions increased ACADS expression significantly (figure 83).

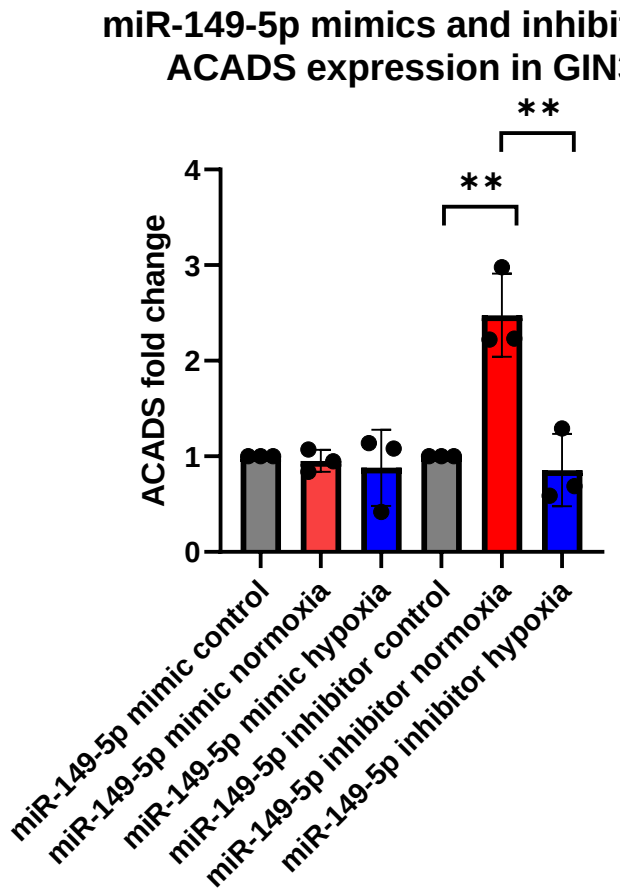

Figure 83. Effects of miR-149-5p mimics and inhibitors on ACADS expression in normoxic and hypoxic conditions in GIN31 cells.

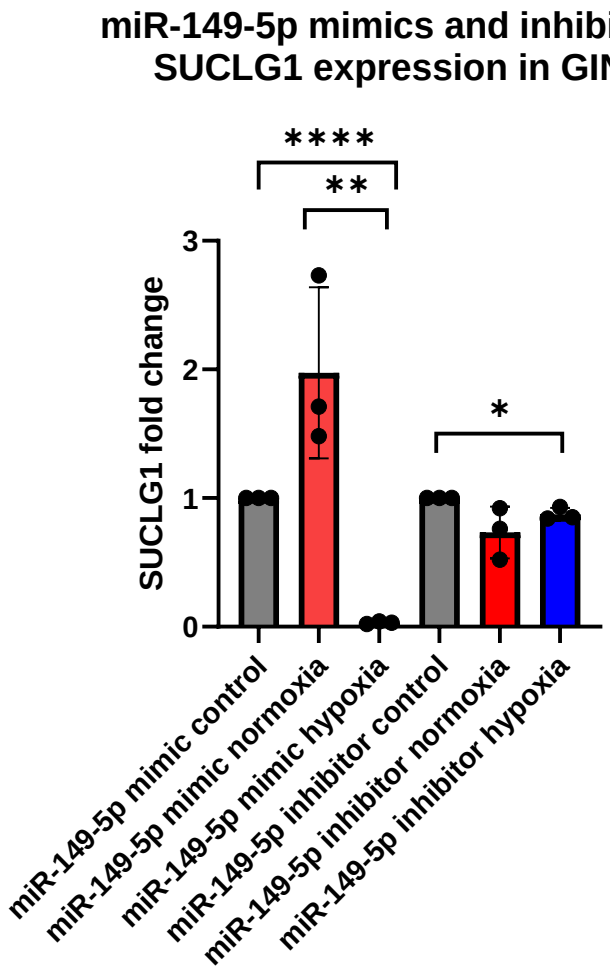

Figure 84. Effects of miR-149-5p mimics and inhibitors on SUCLG1 expression in normoxic and hypoxic conditions in GIN28 cells.

Succinyl-CoA ligase (GDP-forming) subunit alpha mitochondrial is an enzyme coded by SUCLG1, that can be phosphorylated or dephosphorylated and catalyses succinyl CoA and ADP/GDP to succinate and ATP/GTP. SUCLG1 expression in GIN28, figure 84, is very similar to the expression of ACADS in GIN28. SUCLG1 is significantly decreased in hypoxia with the mimic and increased in normoxia with the mimic. There is little change with the miR-149-5p inhibitor, with no

significant difference between control and normoxia, and a small significant decrease in hypoxia of SUCLG1 expression.

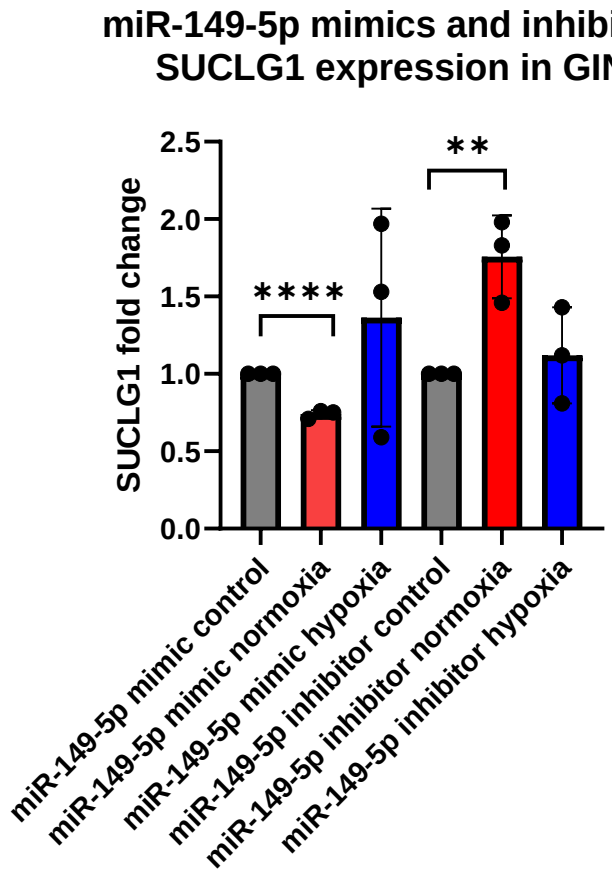

Figure 85. Effects of miR-149-5p mimics and inhibitors on SUCLG1 expression in normoxic and hypoxic conditions in GIN31 cells.

In GIN31, SUCLG1 expression is significantly decreased in normoxia with the miR-149-5p mimic and significantly increased with the miR-149-5p inhibitor (figure 85). These findings show that SUCLG1 is reacting to miR-149-5p as if it was a target in normoxia. However, in hypoxia, there is no significant change in SUCLG1 expression with either the miR-149-5p mimic or inhibitor.

5.5.2 qPCR of associated genes and miR-92a-3p expression

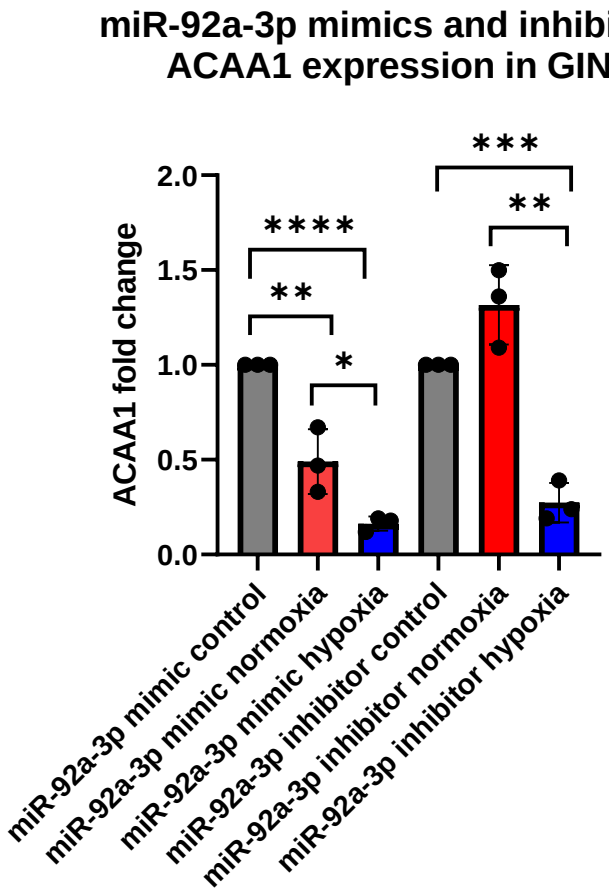

Figure 86. Effects of miR-92a-3p mimics and inhibitors on ACAA1 expression in normoxic and hypoxic conditions in GIN28 cells.

ACAA1 is a predicted gene target of miR-92-3p. The effect of miR-92a-3p mimic and inhibitor in normoxia has the desired effect as significantly decreasing and increasing ACAA1 expression respectively in GIN28, figure 86. However, the expression of ACAA1 is significantly decreased in hypoxia with both the miR-92a-3p mimic and inhibitor. Other hypoxic-related factors may have an indirect effect on ACAA1 expression rather than the result of miR-92a-3p.

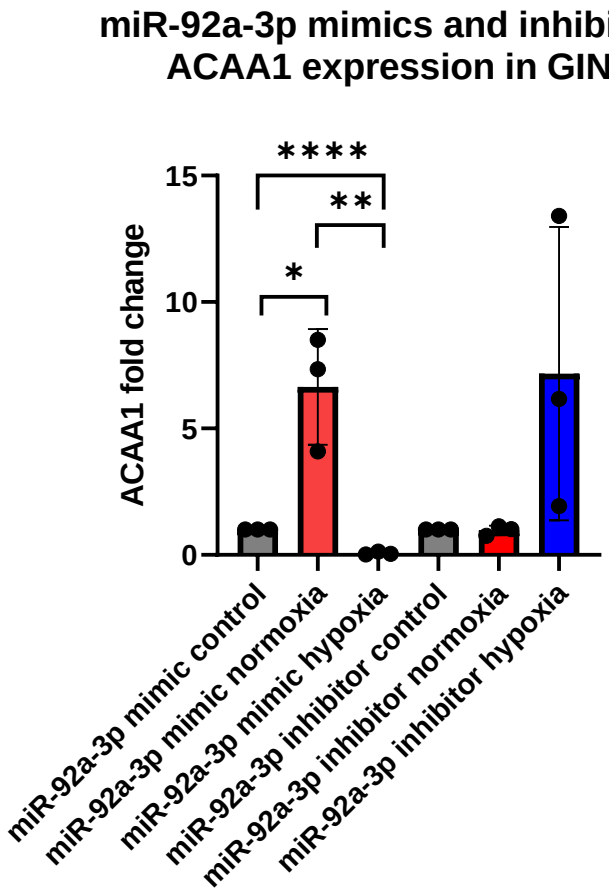

Figure 87. Effects of miR-92a-3p mimics and inhibitors on ACAA1 expression in normoxic and hypoxic conditions in GIN31 cells.

In GIN31, figure 87, the miR-92a-3p inhibitor has no significant effect in normoxia or hypoxia on ACAA1 expression. The miR-92a-3p mimic, has significantly decreased ACAA1 expression in hypoxia but increased ACAA1 expression in normoxia in GIN31.

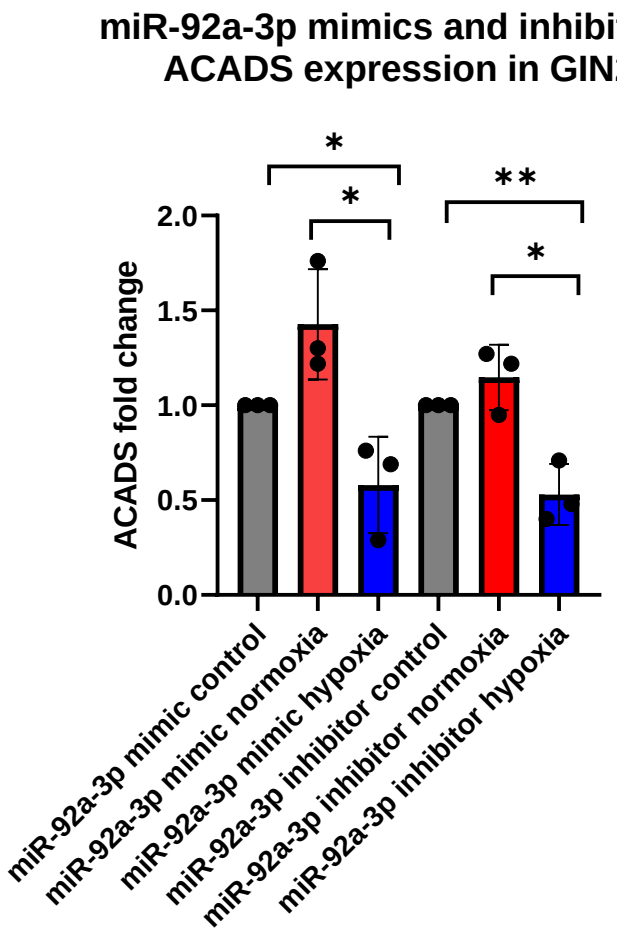

Figure 88. Effects of miR-92a-3p mimics and inhibitors on ACADS expression in normoxic and hypoxic conditions in GIN28 cells.

ACADS is a predicted target of miR-92a-3p. In GIN28, figure 88, ACADS expression is increased in normoxia and decreased in hypoxia regardless of miR-92a-3p mimics or inhibitors.

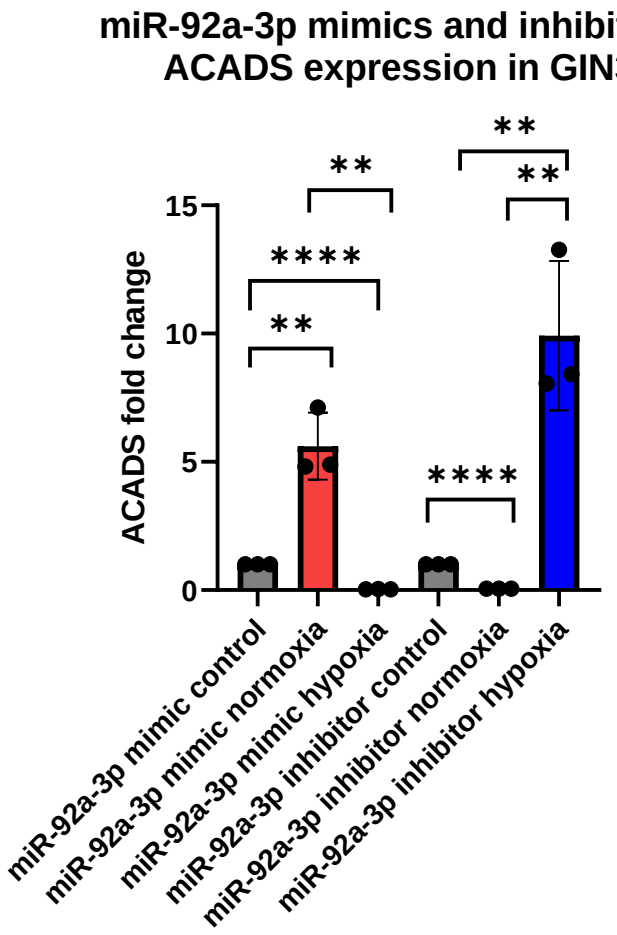

Figure 89. Effects of miR-92a-3p mimics and inhibitors on ACADS expression in normoxic and hypoxic conditions in GIN31 cells.

In GIN31, figure 89, the miR-92a-3p mimic significantly increases ACADS expression in normoxia, and significantly decreases ACADS expression in hypoxia. The inhibitor of miR-92a-3p significantly decreases ACADS expression in normoxia and significantly increases ACADS expression in hypoxia in GIN31.

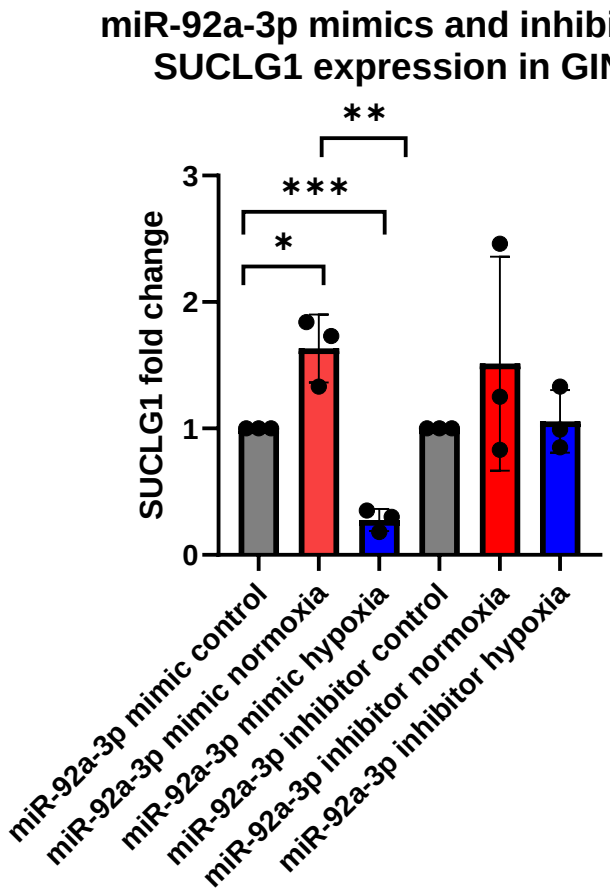

Figure 90. Effects of miR-92a-3p mimics and inhibitors on SUCLG1 expression in normoxic and hypoxic conditions in GIN28 cells.

SUCLG1 is a predicted target of miR-92a-3p. The miR-92a-3p mimic has the desired effect on SUCLG1 expression in hypoxia in GIN28, figure 90, by significantly decreasing its expression. SUCLG1 expression is significantly increased in normoxia with the miR-92a-3p mimic. There are no significant changes in SUCLG1 expression with miR-92a-3p inhibitor in either normoxic or hypoxic conditions.

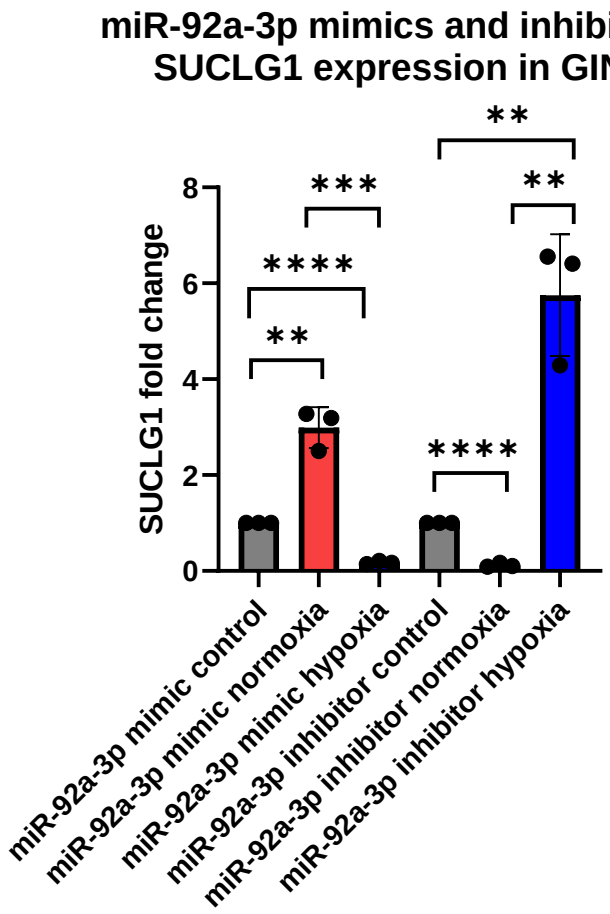

Figure 91. Effects of miR-92a-3p mimics and inhibitors on SUCLG1 expression in normoxic and hypoxic conditions in GIN31 cells.

In GIN31, figure 91, SUCLG1 expression is significantly affected by miR-92a-3p mimic and inhibitor in hypoxia with SUCLG1 expression significantly decreasing and increasing, respectively. However, the inverse was seen in normoxia with the miR-92a-3p mimic signicantly increasing SUCLG1 expression and miR-92a-3p inhibitor significantly decreasing SUCLG1 expression in GIN31.

5.5.2.1 Assessing effect of miR-92a-3p expression on non-target genes

SRSF1 is not a predicted target of miR-92a-3p but may be indirectly affected by miR-92a-3p expression. Figure 92 shows the effect of miR-92a-3p mimics and inhibitors in normoxia and hypoxia on SRSF1 expression in GIN28. SRSF1 expression is affected by miR-92a-3p mimic and inhibitor in hypoxia by significantly reducing and increasing SRSF1 expression respectively. SRSF1 expression is increased in normoxia significantly with both the miR-92a-3p mimic and inhibitor.

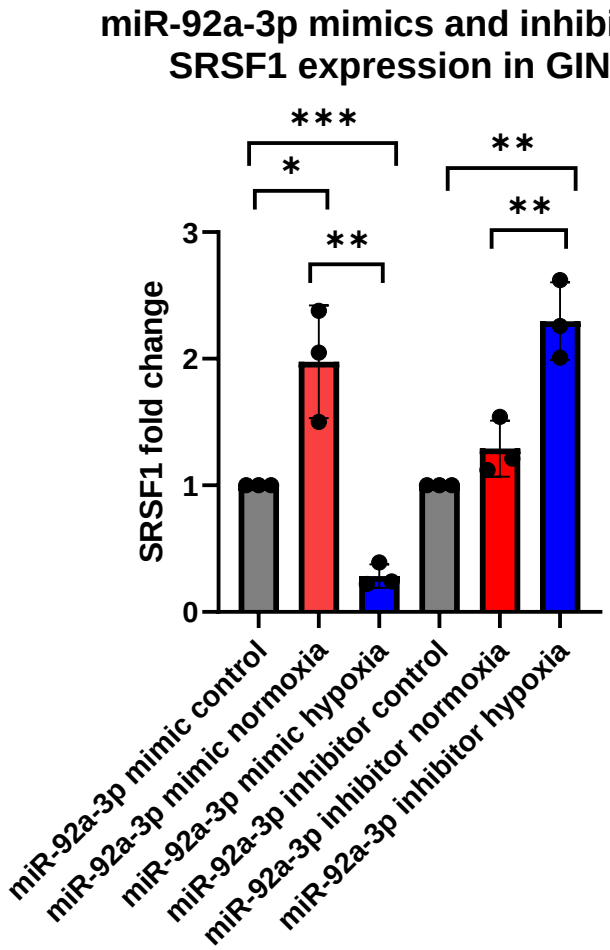

Figure 92. Effects of miR-92a-3p mimics and inhibitors on SRSF1 expression in normoxic and hypoxic conditions in GIN28 cells.

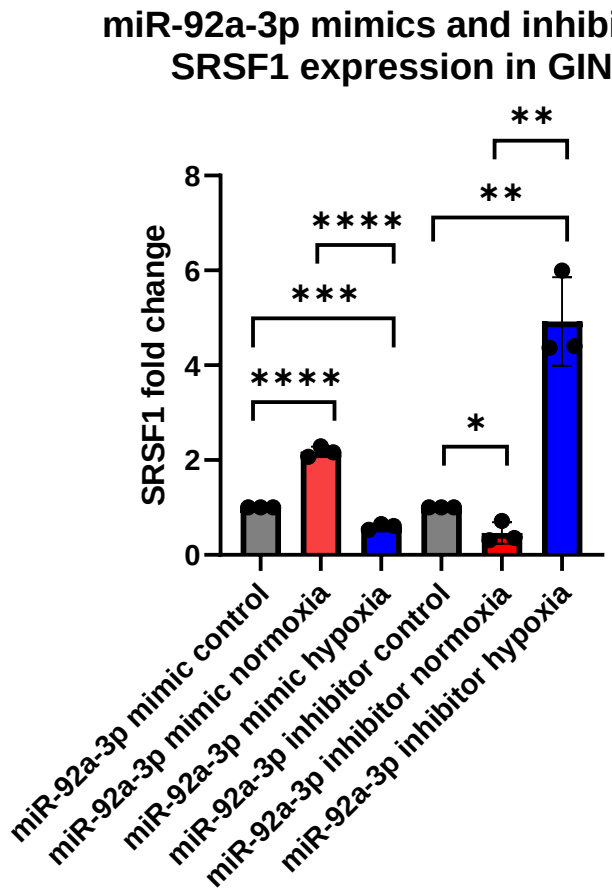

Figure 93. Effects of miR-92a-3p mimics and inhibitors on SRSF1 expression in normoxic and hypoxic conditions in GIN31 cells.

In GIN31, figure 93, SRSF1 expression is significantly increased in normoxia with miR-92a-3p mimic, and significantly decreased in hypoxia. The inverse is seen with the miR-92a-3p inhibitor with SRSF1 expression significantly decreased in normoxia and significantly increased in hypoxia.

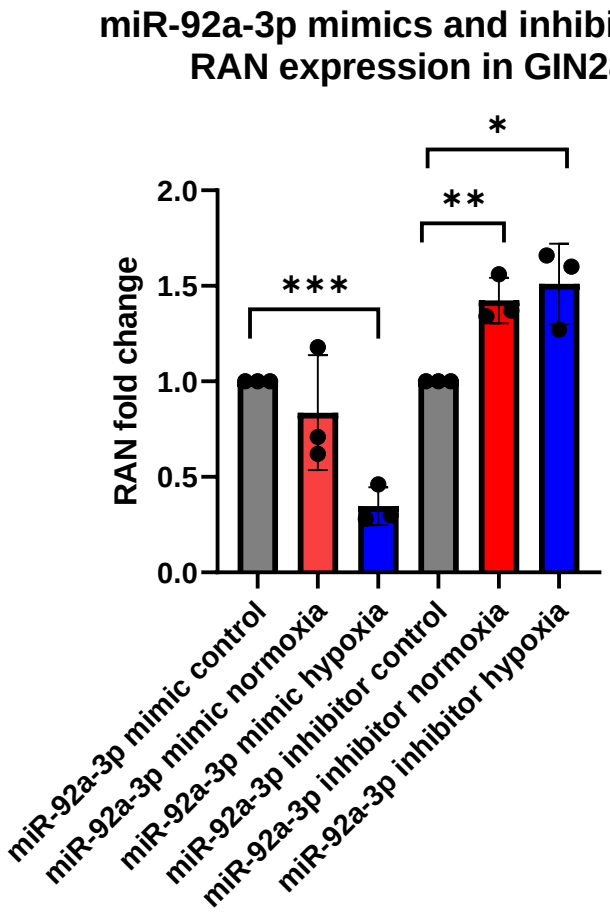

Figure 94. Effects of miR-92a-3p mimics and inhibitors on RAN expression in normoxic and hypoxic conditions in GIN28 cells.

RAN is also not a predicted target of miR-92a-3p, but qPCR is used to determine if it is indirectly affected by a change in miR-92a-3p expression. The miR-92a-3p mimic has no significant effect on RAN expression in normoxia on GIN28 cells, figure 94, but is significantly decreased with miR-92a-3p mimic in hypoxia. However, with the miR-92a-3p inhibitor, RAN expression increases significantly in both hypoxia and normoxia compared to the control. The hypoxic conditions with the miR-92a-3p mimic and inhibitor have the desired and expected effect on RAN expression in GIN28 if RAN was a direct target of miR-92a-3p.

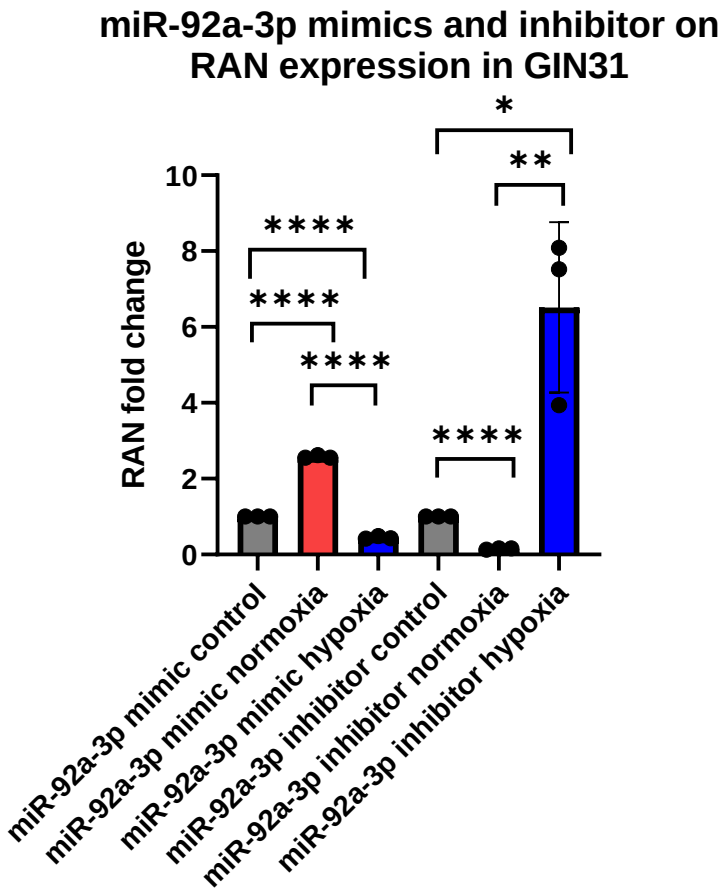

Figure 95. Effects of miR-92a-3p mimics and inhibitors on RAN expression in normoxic and hypoxic conditions in GIN31 cells.

In GIN31, RAN expression is significantly increased in normoxia with miR-92a-3p and decreased in hypoxia seen in figure 95. RAN expression is significantly decreased in normoxia and significantly increased with miR-92a-3p inhibitor. The hypoxic conditions with the miR-92a-3p mimic and inhibitor have the desired and expected effect on RAN expression in GIN31, if RAN was a direct target of miR-92a-3p.

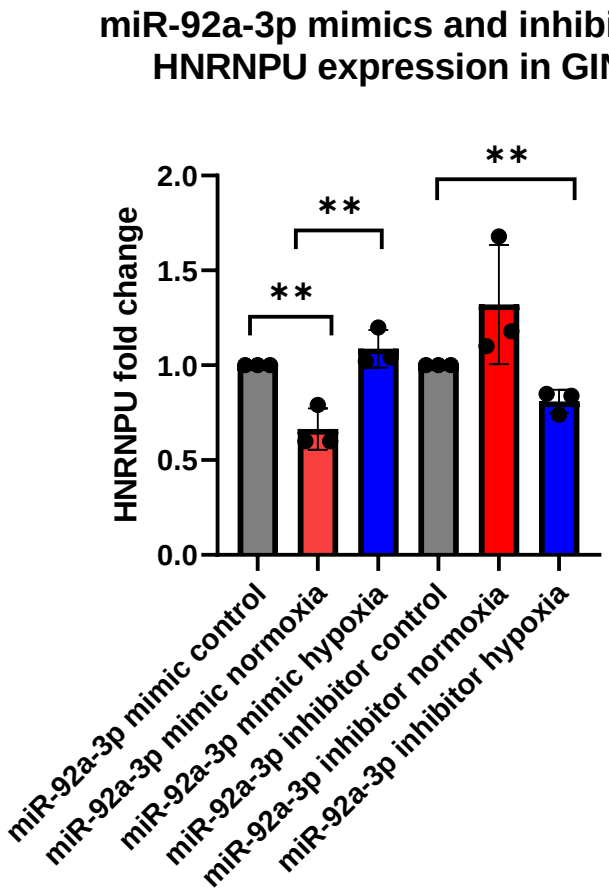

Figure 96. Effects of miR-92a-3p mimics and inhibitors on HRNRPU expression in normoxic and hypoxic conditions in GIN28 cells.

HNRNPU is a predicted target of miR-92a-3p but was not significant in the enrichment analysis. However, HNRNPU is significantly downregulated in normoxia with miR-92a-3p mimic in GIN28 cells seen in figure 96 and significantly increased in hypoxia. With the miR-92a-3p inhibitor, there was no significant increase in normoxia but a significant decrease in hypoxia.

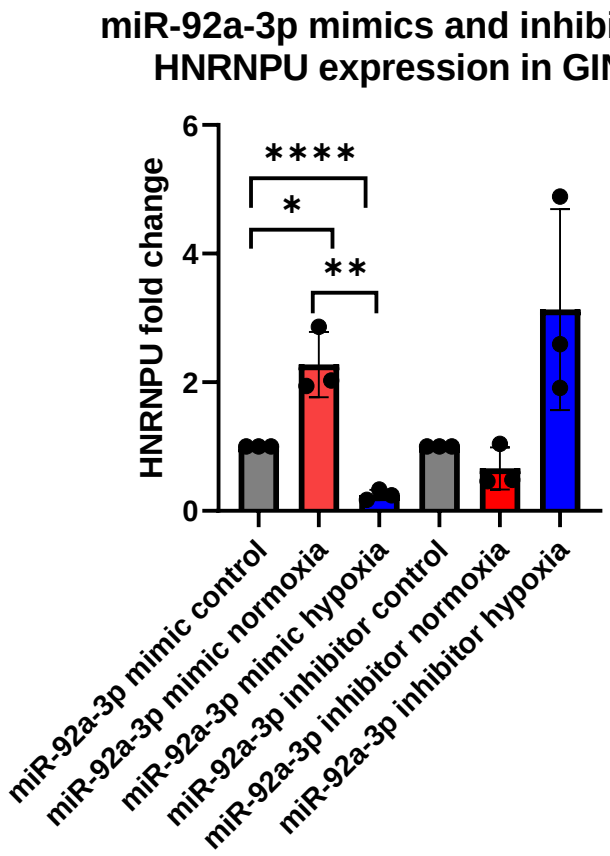

Figure 97. Effects of miR-92a-3p mimics and inhibitors on HRNRPU expression in normoxic and hypoxic conditions in GIN31 cells.

In GIN31, HNRNPU expression is significantly increased in normoxia with the miR-92a-3p mimic, and significantly decreased in hypoxia seen in figure 97. With the miR-92a-3p inhibitor, HNRNPU expression is not significantly changed in normoxia or hypoxia, however in hypoxia the HNRNPU expression is increased.

5.5.3 qPCR of core vs rim of target genes

To assess the expression of the target genes in glioblastoma tissues, qPCR was conducted to analyse the expression of the target genes within the core and rim regions of GBM patient samples.

Figure 98 shows a significantly lower expression of SRSF1 in the core within one patient which correlates with the significant higher expression of miR-149-5p in the core compared to the rim in patient 3. However, though patient 29 has higher miR-149-5p expression in the core, there is no significant difference in SRSF1 level between the core and the rim. Similarly, no significant difference of SRSf1 between tumour regions is seen in patient 58.

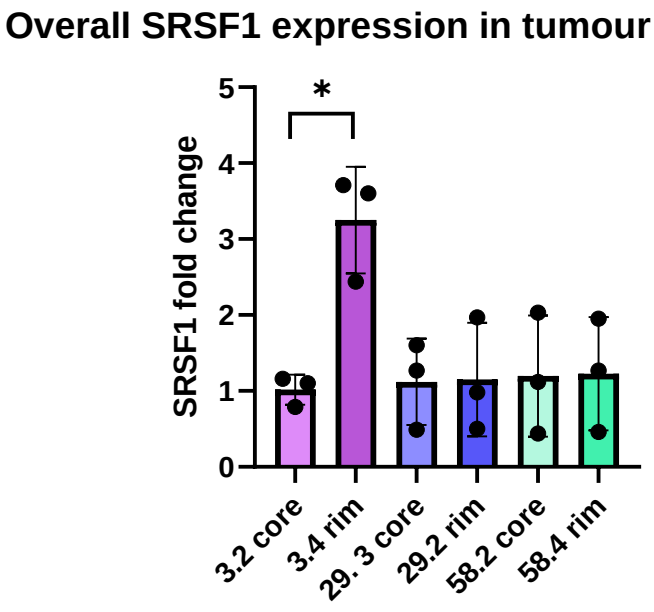

Figure 98. Graph showing SRSF1 expression in the core and rim of three glioblastoma patients

Patient tumour RAN expression, in figure 99, is significantly decreased in the core region of patient 29 compared to the rim region. Similar to SRSF1, this result negatively correlates with increased miR-149-5p expression within the core of patient 29 compared to the rim. Patient 29

and 58 do not have any significant changes in RAN expression between the core and rim regions of GBM tumour samples.

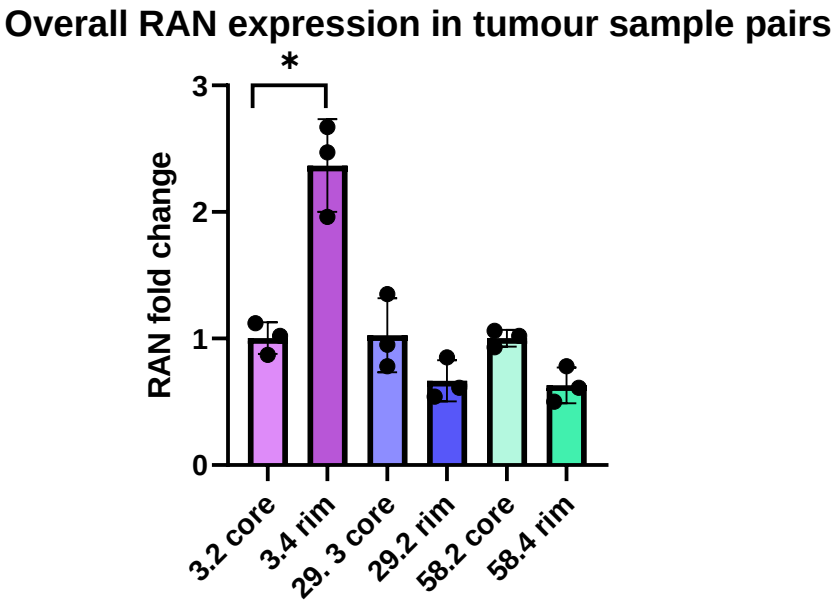

Figure 99. Graph showing RAN expression in the core and rim of three glioblastoma patients

HRNRPU has a small significant increase of expression within the core of the tumour in patient 3 compared with the rim. There are no significant differences of expression of HRNRPU between the core and rim in patients 29 and 58, as seen in figure 100.

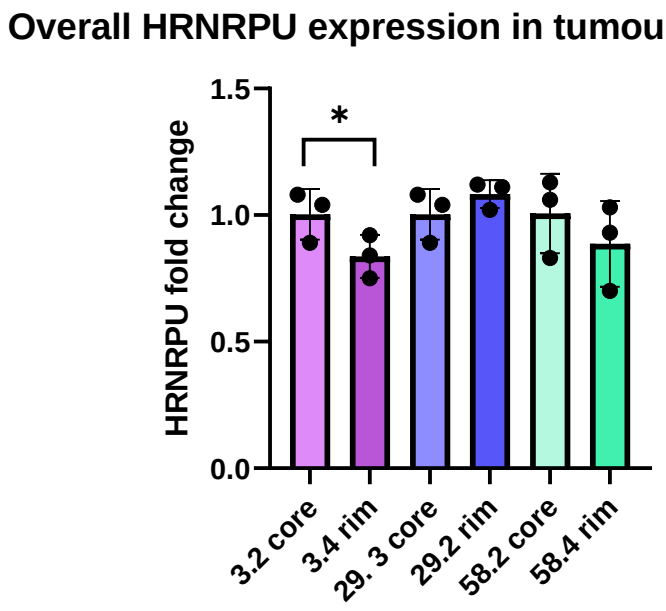

Figure 100. Graph showing HNRNPU expression in the core and rim of three glioblastoma patients.

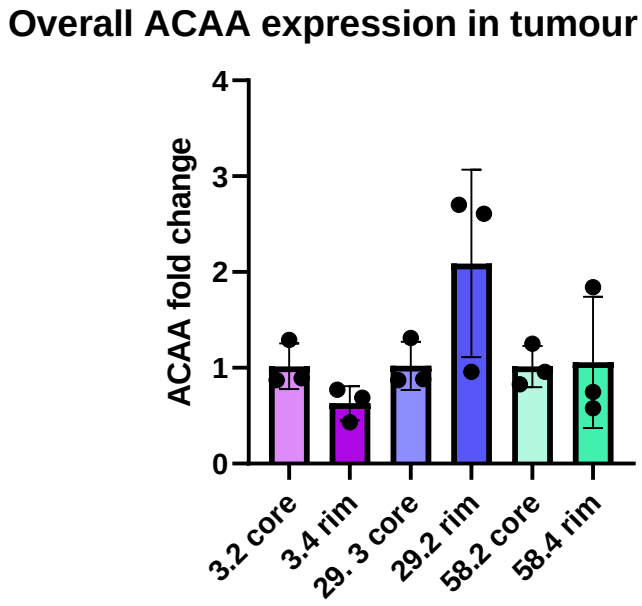

Figure 101. Graph showing ACAA1 expression in the core and rim of three glioblastoma patients.

No significant difference of expression was seen between tumour regions for miR-92a-3p target, ACAA as seen in figure 101.

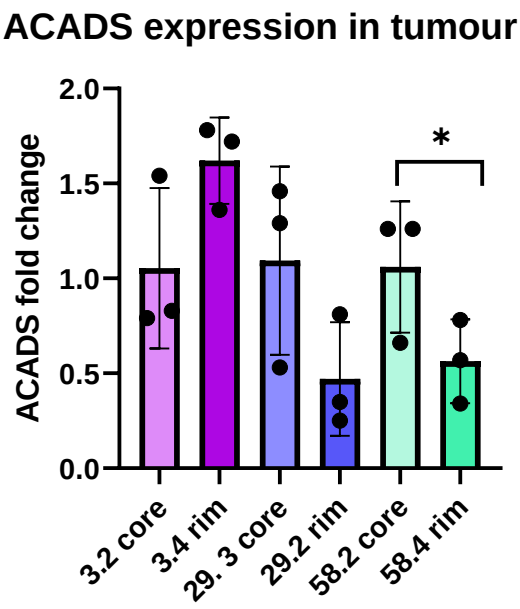

Figure 102. Graph showing ACADS expression in the core and rim of three glioblastoma patients

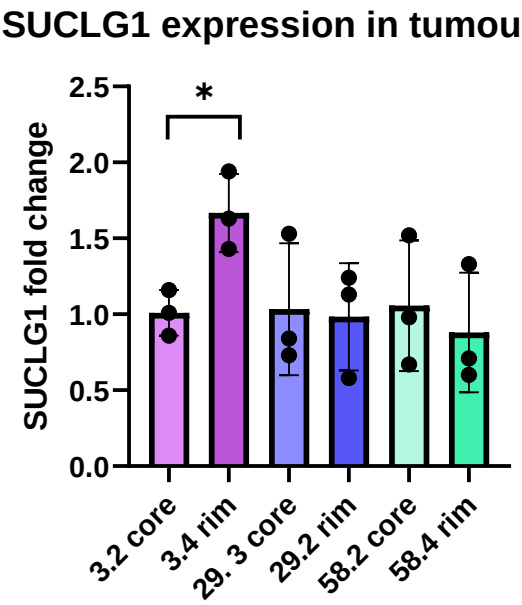

Figure 103. Graph showing SUCLG1 expression in the core and rim of three glioblastoma patients

In figure 102, ACADs expression varied widely with no significant changes seen between the core and rim of tumour samples in patients 3

and 29. However, in patient 58 ACADs expression was significantly increased in the core compared to the rim.

SUCLG1 expression was significantly decreased in the core of patient 3 compared to the rim, figure 103, which negatively correlates to the increase of miR-92a-3p expression in the core of this patient. No significant differences are seen in patient 29 and 58 in SUCLG1 expression between the core and rim regions.

5.5.4 Immunofluorescence of RAN

Immunofluorescence (IF) was used to visualise and determine the effect of hypoxia on RAN protein expression. In figure 104, RAN expression is determined in GIN28 cells, with a reduction of RAN protein seen under hypoxic influence which correlates with the qPCR data of RAN being under-expressed in hypoxia potentially due to increased miR-149-5p expression.

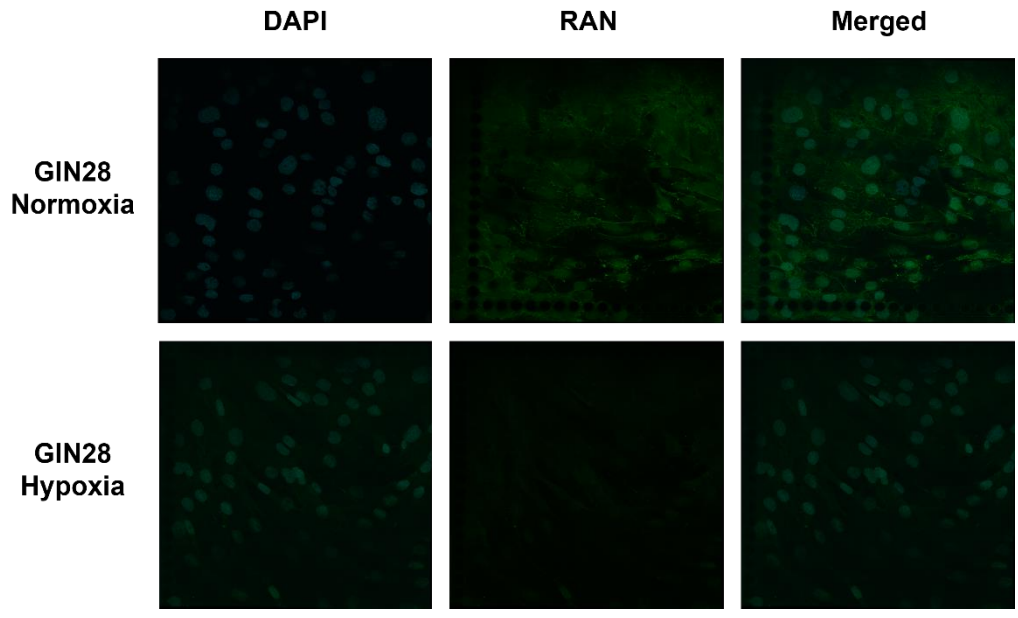

Figure 104. Immunofluorescence of RAN in GIN28 cells.

Figure 105 shows RAN staining using IF in GIN31 cells, with the opposite effect seen in GIN28. RAN expression is heavily increased with hypoxic exposure in GIN31 cells. RAN expression is also increased in GIN 8, figure 106, but to a much lesser level than seen in GIN31.

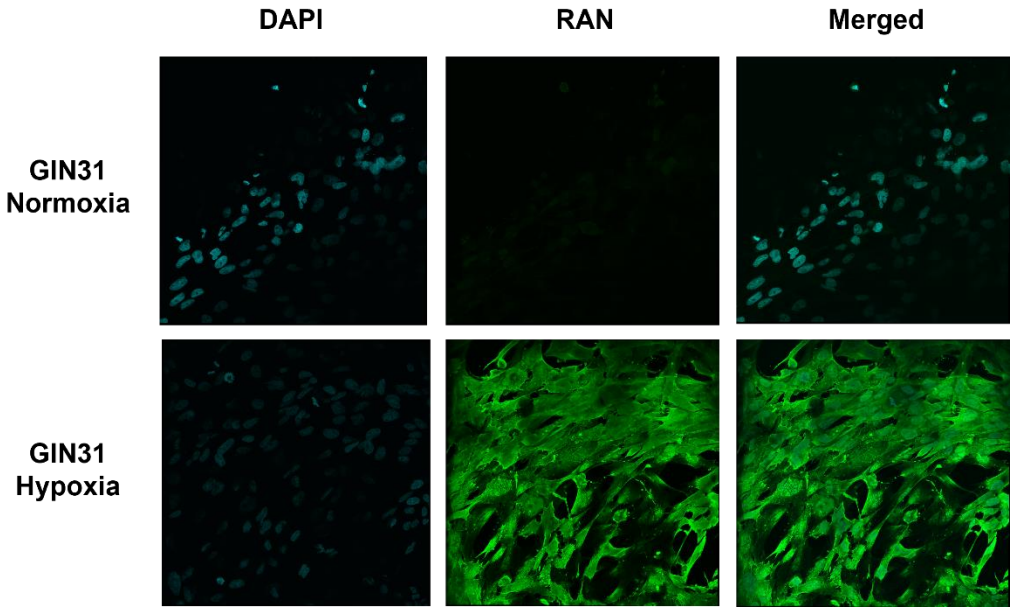

Figure 105. Immunofluorescence of RAN in GIN31 cells.

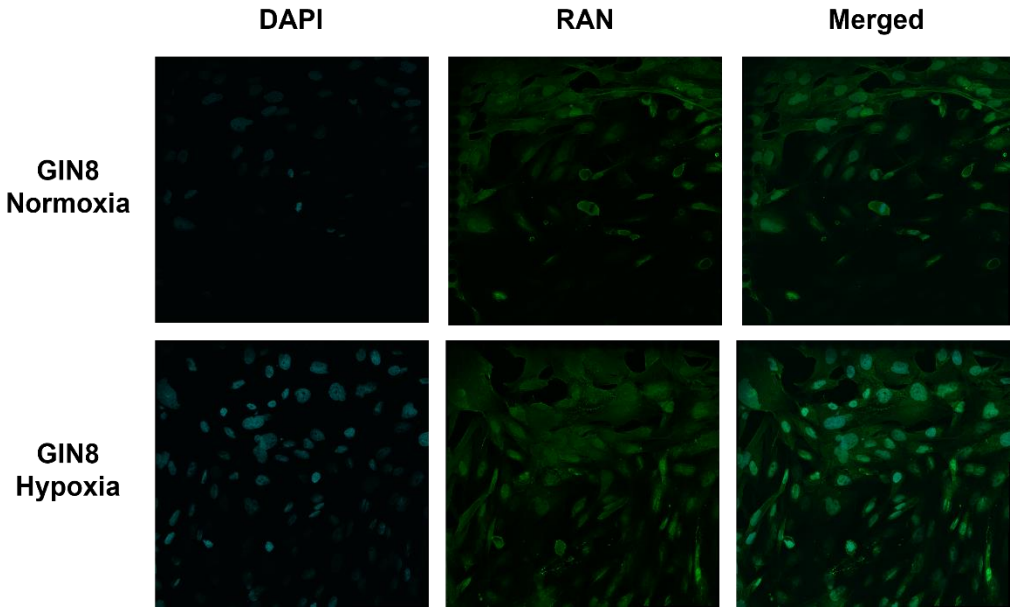

Figure 106. Immunofluorescence of RAN in GIN8 cells.

5.5.5 Immunohistochemical staining of RAN

To confirm the expression levels of RAN protein seen in the cell lines, IHC was used to assess the levels within tumour samples. RAN expression was not significantly changed between the different regions, however the RAN expression was slightly lower in the core than other regions as seen in figure 107.

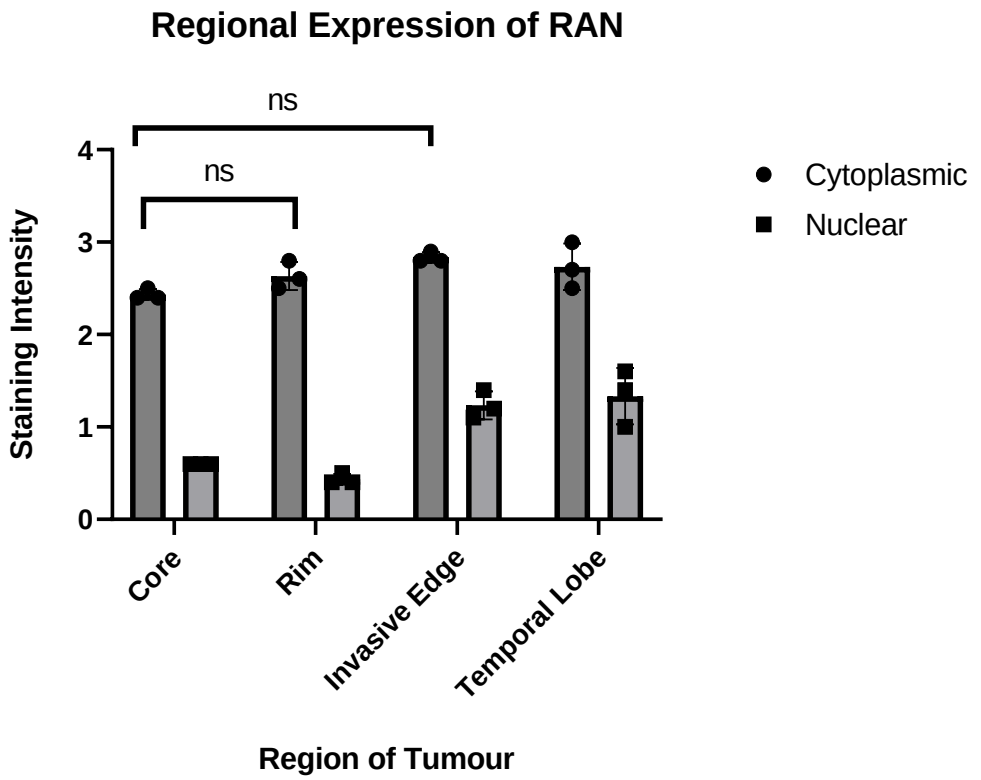

Figure 107. Immunohistochemical RAN expression in different GBM regions using patient tissues.

Figure 108 shows RAN staining within the temporal lobe and GBM core. Both regions have relatively strong staining of RAN expression, though less nuclear staining is seen within the GBM core compared to the temporal lobe.

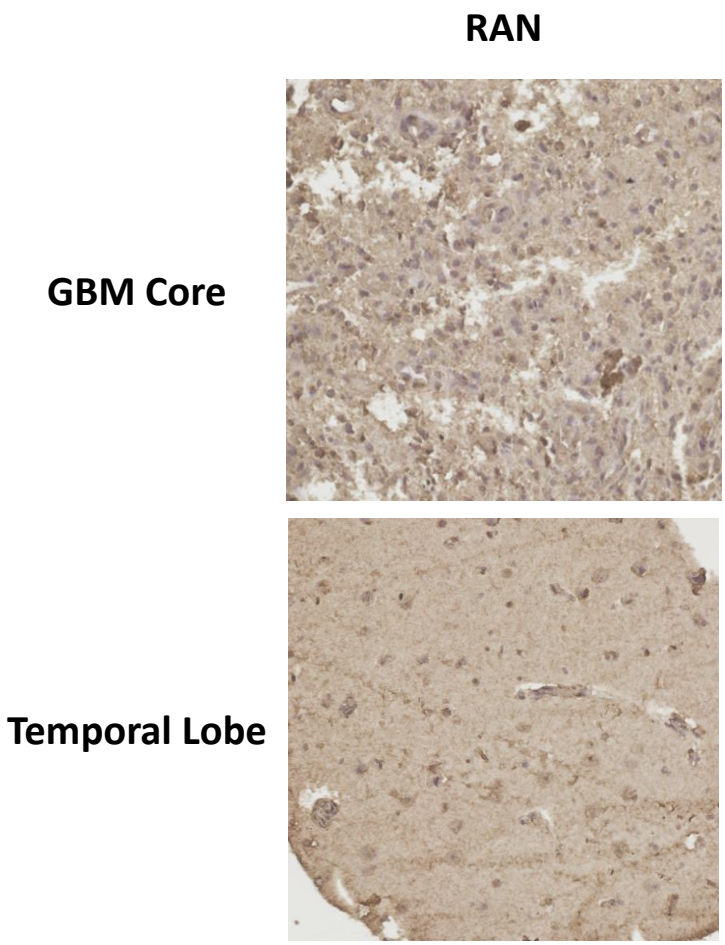

Figure 108. IHC staining of RAN in GBM core and temporal lobe.

RAN expression was assessed in each individual patient of the TMAs with substantially more RAN observed in the cytoplasm compared to the amount of nuclear staining in every patient which is seen in figures 109 and 110.

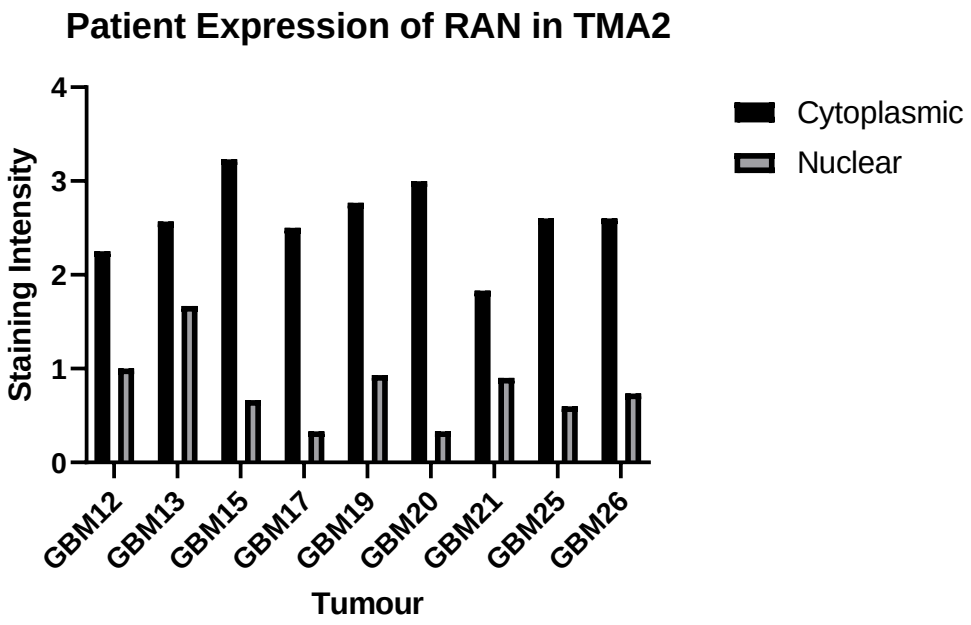

Figure 109. RAN staining in tumour samples in TMA2.

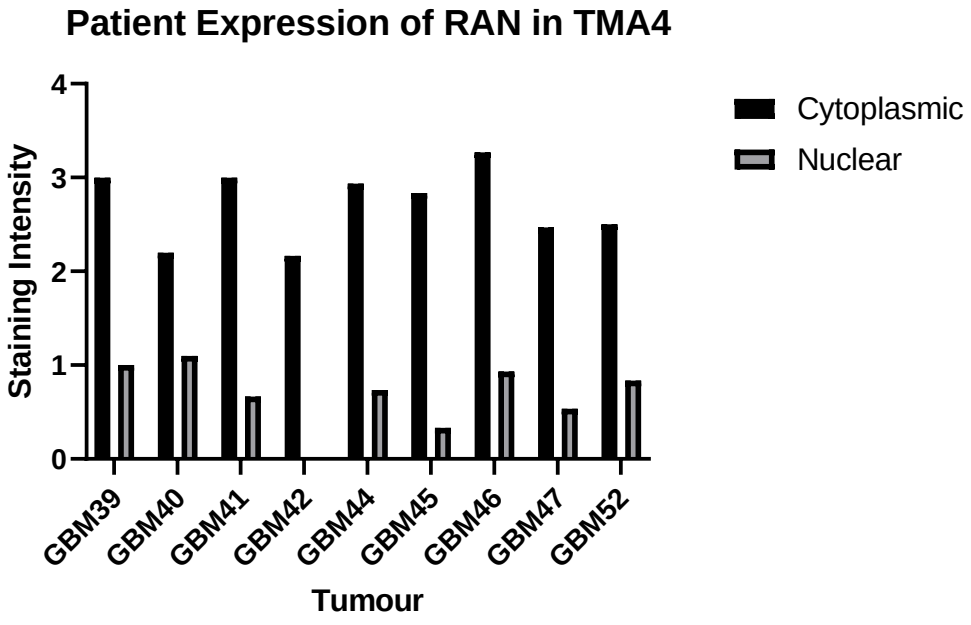

Figure 110. RAN staining in tumour samples in TMA4.

Figure 111. RAN staining intensity correlation with age of GBM patients.

A scatter graph was plotted to assess if a correlation between age and intensity of RAN expression. In figure 111 there is no correlation observed between age of GBM patients and amount of RAN expression. Assessing the distribution of high and low expression (low = 1, 2 stain score, high = 3, 4 stain score) of RAN within GBM patients, most patients, 17 out of 18, have high RAN expression as seen in figure 112. To determine if gender is a factor for high RAN expression, the amount of female and male patients for high RAN expression was assessed with 8 female and 9 male patients, as seen in figure 113, indicating that gender is not a factor to predict high RAN expression.

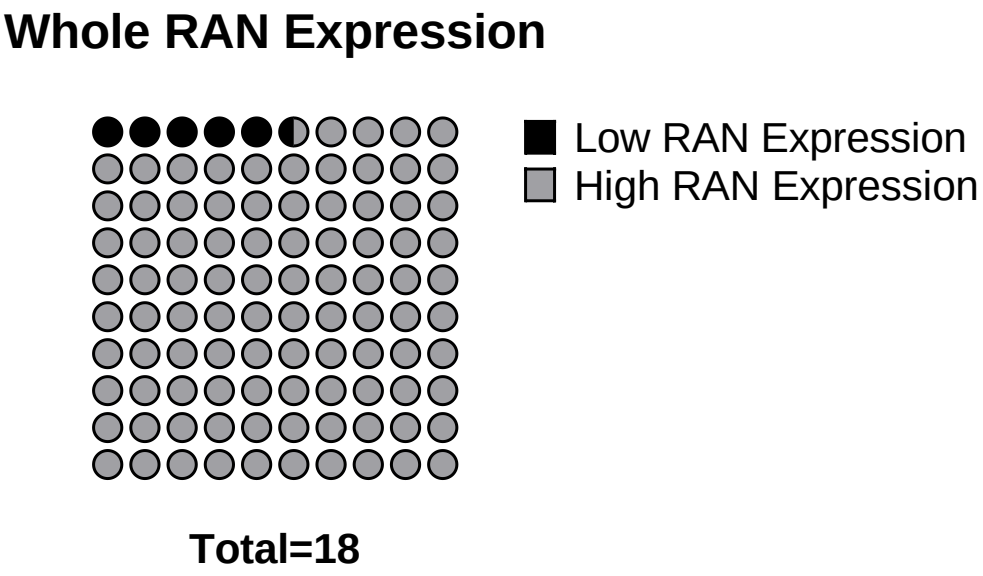

Figure 112 Schematic of low and high RAN expression amongst GBM patients.

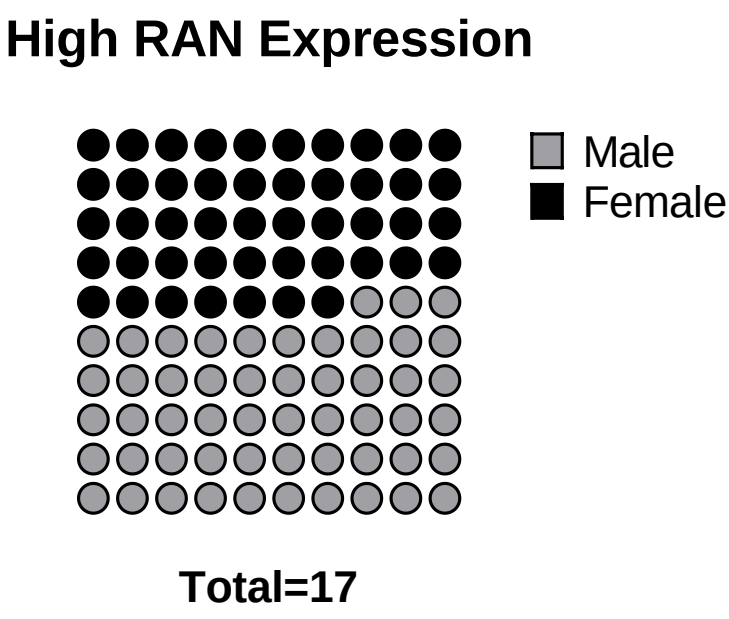

Figure 113. Schematic of female and male prevalence within high RAN expression amongst GBM patients.

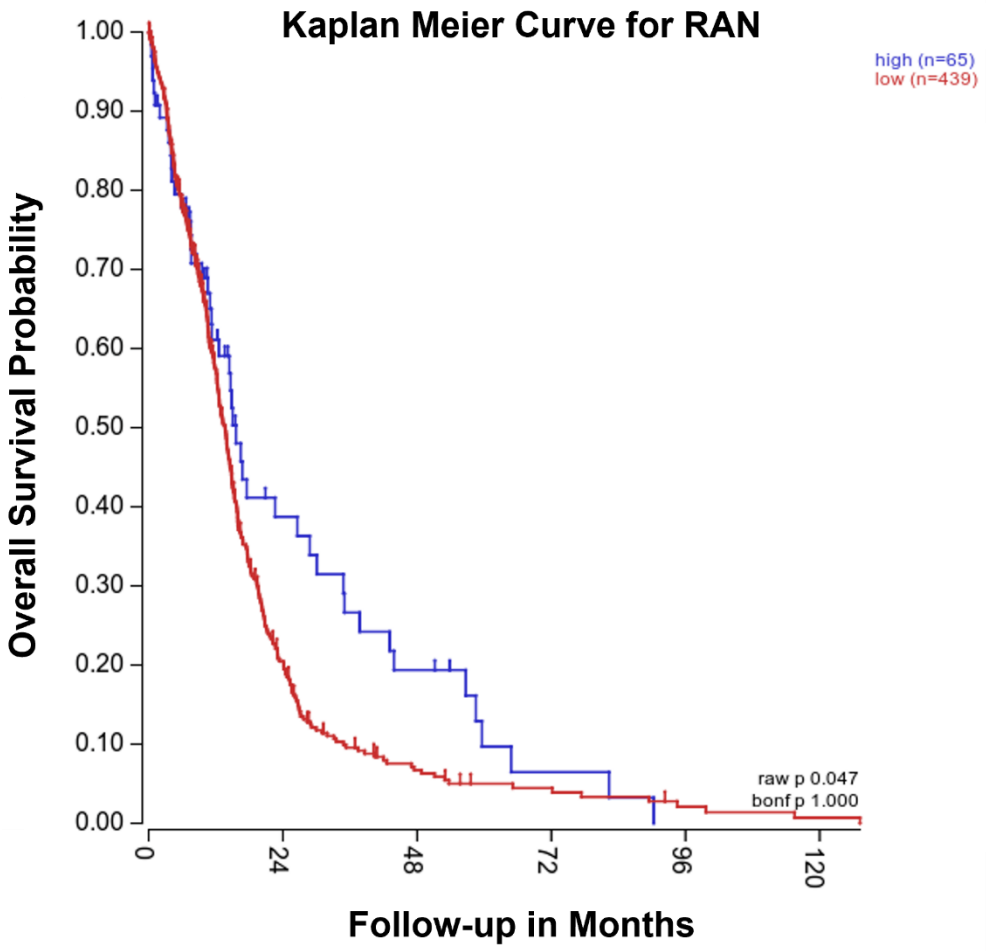

Figure 114. RAN survival curve in GBM patients using TCGA dataset of 540 patients

A Kaplan-Meier curve was produced using a TCGA dataset of glioblastomas with 540 patients as seen in figure 114 to determine the effect of RAN expression of survival. The graph assesses high RAN expression (n=65) and low RAN expression (n=439). Patients with low RAN expression have a lower overall survival probability within the first 60 months of follow-up compared with higher RAN expression. Low RAN expression and high CA9 hypoxic marker both have lower overall survival probability which potentiates their negative correlation.

5.6 Summary

5.6.1 Hypoxia in tumours samples

To confirm the presence of hypoxia in the tumour samples, CA9 was used as a hypoxic marker. The expression of CA9, determined by qPCR, was significantly increased in the core regions compared to the rim regions of the tumour samples, which confirms the assumption of hypoxia being more concentrated in the centre of the tumour. IHC staining of CA9 was also used to validate the level of CA9 which further confirmed the increase of hypoxia in the core region compared with the rim and invasive edge. The majority of tumour samples of the TMAs had low overall CA9 expression. The Kaplan-Meier curve indicated that the higher CA9 expression is significantly associated with lower overall survival, which correlates with a higher expression of hypoxia. However, the sample number in the Kaplan-Meier curve had a much higher sample number in the low CA9 expression in comparison to high CA9 expression. The miRNA qPCR data on tumour tissue samples does not consider overall CA9 expression but distinguishes CA9 expression in the core and rim regions. Though a large proportion of patients seem to have low CA9 expression, as it is an indirect marker, false negatives need to be considered and hypoxia is likely to be more present than the results seen based solely on CA9 expression. To validate the hypoxic findings and to ensure the cell lines exposed to hypoxia resulting in having a hypoxic effect, HIF-1 protein was identified using western blot and showed an increase in HIF-1 protein expression in the hypoxia-exposed cultures. GIN28 did show some HIF-1 expression in normoxic conditions but this

potentially may be due to slight over-confluency of the cells in the flask which can induce hypoxic conditions due to the increased density of cells. However, the hypoxic cultures of GIN28 had a much higher expression of HIF-1 in the western blot showing the hypoxic exposure causes the molecular changes within in the cells and increases HIF-1 expression.

Further experiments could be conducted to confirm the direct effect of hypoxia by staining for HIF-1 using IHC or performing qPCR to determine HIF-1 expression level, instead of using an indirect hypoxic marker such as CA9. To also look into the degree of hypoxia whether the effects are a result of acute or chronic hypoxia, HIF-2 associated with chronic hypoxia, could be investigated in a similar way. This may be interesting to see whether hypoxia-induced transcription is determined by HIF-1 or HIF-2 and the differences that consequently arise.

The cells used in culture are derived from the invasive margin. This is because the cells from these regions are more readily used and available in culture in the CBTRC. GCEs, cells derived in-house from the core region of GBM tumours, though initially may provide a better model for assessing hypoxia effects in GBM. GIN cell lines equally are representative of GBM tumours and will share a common origin with core cells and therefore may carry hypoxia-selected changes. It is also widely accepted and understood that GBMs harbour a high degree of heterogeneity within GBM tumours and between GBM patients, which contributes to the difference of hypoxia-responses between patient cell

lines and intra-tumour regions. Although, it is not known to the degree of how hardwired hypoxia-selected changes are and if these are long-standing changes differ between regions. Equally, it is important to evaluate the hypoxic pressure of cells in the invasive margin, as after surgical resection these are the cells that may remain and develop into further tumours which may become the core of recurrent GBMs and harbour hypoxic regions. Sequencing these cell lines from different regions in the future may give a better understanding of the changes that occur and differ in core cells to invasive cells and which cell lines may be a more appropriate model when investigating hypoxia. To also validate the changes in hypoxia and to further assess the differences, in the future the same experiments can be repeated in paired GCE lines, if possible, to determine if there is any significant difference between core and invasive cell lines.

A limitation of this experiment is the use of atmospheric oxygen, ~20%, as a normoxic value. In the brain, physiologically the normal oxygen levels vary between 2-9% oxygen (332), using a range of physiological values as normoxic oxygen could be more representative of the changes that occur in the brain tumours compared to surrounding normal brain cells. As tumours in the brain have been shown to have oxygen levels as low as 0.5% (332). However, experimentally this is challenging as physiological normoxic levels and hypoxic levels would not be able to be cultured at the same time, due to one hypoxic chamber, which could give rise to further variables between the conditions. To combat this, 3D

tumour models with an established hypoxic gradient (333) could be used to confirm the differences between hypoxic areas and the normoxic edge.

5.6.2 miR-92a-3p expression differences between cells and tissues

miR-92a-3p expression in tumour tissue samples in response to hypoxia is opposite as to what was seen in cell lines, upregulated, and downregulated respectively by qPCR. This may be because the tissues have other microenvironmental situations that can influence expression such as acidosis. To confirm if the expression of miR-92-3p is influenced by acidosis, which is known to reverse the effects of hypoxia and dominate, a future experiment would be to culture the cell lines in acidic and neutral media and then to PCR the miR-92a-3p levels to determine the effect overall. Other microenvironmental factors such as the immune system and extracellular matrix is likely to impact the expression of the miRNA and these components are not present in 2D culture which was used in this study. To further confirm if this impacts the expression of miRNA, 3D models could be used to assess the difference, which may provide more clinically relevant data though may be more difficult to assess the hypoxia gradient in a 3D model. However, 3D tumours models with a hypoxic gradient have been established (333). As previously discussed, GBM heterogeneity is exceptionally important and could also potentially contribute to be difference in miR-92a-3p expression in patient derived cell lines and patient tumour tissue samples.

5.6.3 miR-149-5p expression validated in tumour samples

miR-149-5p expression is upregulated in most tumour tissue samples in response to hypoxia which validates the results seen in GBM cell lines. In the literature miR-149-5p can be up or downregulated in glioblastomas and consequently effects different target genes such as caspase-2 or AKT1 respectively (199). miR-149-5p response to hypoxia in glioblastoma has not yet been reported, however the findings of increased miR-149-5p by qPCR links with the enrichment analysis of being involved with hypoxic pathway. This project has explored the effect of miR-149-5p expression in response to hypoxia on 3 target genes and the potential indirect effect on 3 other genes, emphasising that hypoxia effects miRNA and its targets. However, the mechanism by which miR-149-5p responds to hypoxia is yet to be elucidated and could be the focus of future work.

5.6.4 Apoptotic and senescence assays

Apoptotic and senescence assays were conducted to determine the effect on these biological processes depending on hypoxic status and miRNA expression. These two pathways were chosen to investigate as they were highlighted as important pathways during miRNA selection as both miR-92a-3p and miR-149-5p were predicted to be involved in them. Senescence and apoptosis are important mechanisms within cancer and can be both pro and anti-cancer. Both processes initiate cell death, in a pro-tumour situation, cells can enter apoptosis or senescence in order to allow for more proliferation though in this instance the rate of apoptosis

or senescence never exceeds the rate of proliferation. For these pathways to have an anti-cancer effect their rate must exceed the rate of proliferation.

The caspase-glo assay was conducted on 2 cell lines, GIN28 and GIN31 using miR-149-5p and miR-92a-3p mimics and inhibitors in both normoxic and hypoxic conditions. miRNA mimics had no effect on either cell line between hypoxic or normoxic conditions. miR-92a-3p inhibitors, lowering miR-92a-3p expression, increased the amount of apoptosis in both cell lines in hypoxia over normoxia. miR-92a-3p is widely involved in apoptosis and targets multiple pro-apoptotic genes. The added effect of hypoxia may contribute to the increase in apoptosis the miR-92a-3p inhibitor as well as influencing the expression of pro-apoptotic gene targets in attempt to balance out the hypoxic effect.

In GIN28, apoptosis is significantly increased in normoxia compared to hypoxia with miR-149-5p inhibitor transfected cells. In hypoxia miR-149-5p is upregulated, its inhibition in hypoxia from the transfected miR-149-5p inhibitor, results in lower levels of miR-149-5p. A pro-apoptotic gene, bcl-2, is a predicted target of miR-149-5p. Inhibition of miR-149-5p increases the amount of apoptosis by potentially causing an increase in bcl-2 expression, alongside the hypoxic environment which can enhance the rate of apoptosis. This suggests that lowering miR-149-5p expression, the opposite that is seen in hypoxia, can promote apoptosis in hypoxic conditions. This mechanism requires further investigation to

determine whether inducing apoptosis by increasing miR-149-5p expression has a significant anti-cancer effect and whether it is possible to exploit this pathway for treatment. To further validate the effect of miR-149-5p inhibitor in hypoxia on GIN28 cells, other apoptotic detection experiments can be conducted such as identifying annexin V in flow cytometry.

5.6.5 miR-92a-3p gene target expression

After analysing the effects of hypoxia on miR-92a-3p expression in apoptosis and senescence, further investigation of target genes was conducted using qPCR. The three top predicted target genes for miR-92a-3p are ACAA1, ACADS and SUCLG1.

ACAA1 codes for acetyl-CoA acyltransferase 1. It is a predicted gene target of miR-92-3p. The effect of miR-92a-3p mimic and inhibitor in normoxia is as expected which significantly decreases and increases ACAA1 expression respectively in GIN28. However, the expression of ACAA1 is significantly decreased in hypoxia with both the miR-92a-3p mimic and inhibitor. These results suggest that in normoxia, miR-92a-3p binds to ACAA1 as a target gene and in hypoxia, other pathways or influences may have caused the downregulation of ACAA1 in GIN28. In cell line GIN31, the miR-92a-3p inhibitor has no significant effect in normoxia or hypoxia on ACAA1 expression. The miR-92a-3p mimic, has significantly decreased ACAA1 expression in hypoxia which is an expected response but increased ACAA1 expression in normoxia in

GIN31. These results are not conclusive as to whether ACAA1 is targeted by miR-92a-3p. In colorectal cancer, upregulation of miR-92a-3p and downregulation of ACAA1 is associated with increased tumour progression (334). Similarly, non-small cell lung cancer (NSCLC) correlates downregulation of ACAA1 with poor prognosis and decreased immune infiltration of CD4+ T cells (335). Further experiments such as a luciferase assay as required to confirm that ACAA1 is a target of miR-92a-3p in GBM cells and to further validate its expression in GBM. No study reports on the effect of hypoxia on ACAA1 and in the tissue samples no significant difference of expression was seen between patient regions. This indicates that ACAA1 expression may not be influenced by hypoxia in GBM.

The second predicted gene target of miR-92a-3p that was analysed using qPCR using miRNA mimics and inhibitors in hypoxia and normoxia was ACADS. ACADS is a gene which codes for short-chain acyl-coenzymeA dehydrogenase (SCAD), an enzyme of the acyl-CoA family which initialises the first step of the mitochondrial fatty acid beta-oxidation. SCAD is most active in vitro with hexanoyl- and butyryl-CoA as substrates, but its physiologic role is specific to butyryl-CoA. Mutations within ACADS can cause ACADS deficiency. In the absence of SCAD, the by-products of butyryl-CoA accumulate including butyrylcarnitine, butyrylglycine, ethylmalonic acid (EMA), and methylsuccinic acid, in the blood, urine, and cells (336). EMA, the hallmark of ACADS deficiency, is likely formed by the carboxylation of excess butyryl-CoA by propionylCoA

carboxylase (336). Phenotypical features of ACADS deficiency are failure to thrive, metabolic acidosis, ketotic hypoglycemia, developmental delay, seizures, and neuromuscular symptoms such as myopathy and hypotonia (336). This disorder has been reported in infants, children, and adults.

In GIN28, ACADS expression is increased in normoxia and decreased in hypoxia regardless of miR-92a-3p mimics or inhibitors. This suggests that hypoxia, via a different mechanism, causes the downregulation of ACADS. It has not been reported that hypoxia induces ACADS deficiency, however these findings suggest that this is a possibility and further investigation of this is required. In GIN31, the miR-92a-3p mimic significantly increases ACADS expression in normoxia, and significantly decreases ACADS expression in hypoxia. The inhibitor of miR-92a-3p significantly decreases ACADS expression in normoxia and significantly increases ACADS expression in hypoxia in GIN31. This suggests that ACADS is targeted by miR-92a-3p in hypoxia in GIN31 but not in normoxia. In the tumour tissues, ACADS expression varied in one pair ACADS was increased in the core and the other two pairs it was increased in the rim, with one expression difference being significant. As the expression of ACADS varies, further experiments including repeating qPCR and IHC or western blots are required to confirm the expression of ACADS in hypoxia in glioblastomas.

Succinyl-CoA ligase (GDP-forming) subunit alpha mitochondrial is an enzyme coded by SUCLG1, which can be phosphorylated or dephosphorylated and catalyses succinyl CoA and ADP/GDP to succinate and ATP/GTP. SUCLG1 is another predicted target of miR-92a-3p. Elevated HIF-1α levels are correlated with elevated succinate levels (337). Though increased succinate levels are not solely dependent on SUCLG1 expression, increased SUCLG1 produces increased succinate. This suggests that within hypoxia, SUCLG1 expression potentially should be increased in hypoxia.

In the investigation of SUCLG1 expression by qPCR, the miR-92a-3p mimic has the expected effect on SUCLG1 expression in hypoxia in GIN28, by significantly decreasing its expression. Conversely, SUCLG1 expression is significantly increased in normoxia with the miR-92a-3p mimic. There are no significant changes in SUCLG1 expression with miR-92a-3p inhibitor in either normoxic or hypoxic conditions. In the second cell line, GIN31, SUCLG1 expression is significantly affected by miR-92a-3p mimic and inhibitor transfections in hypoxia resulting in SUCLG1 expression significantly decreasing and increasing, respectively. However, the opposite was seen with increased SUCLG1 in normoxia with the miR-92a-3p mimic and significantly decreased SUCLG1 expression in normoxia with the miR-92a-3p inhibitor in GIN31. Interestingly GIN31 in this case shows the expected results with miR-92a-3p targeting SUCLG1 in hypoxia but not in normoxia, potentially suggesting a hypoxia-induced effect. In GIN28 this effect was only

replicated with the miR-92a-3p mimic and not with the inhibitor in hypoxia. In the tumour tissues there are no significant differences between the core and rim in paired samples except for one patient in which SUCLG1 expression was significantly lower in the core than in the rim. This particular finding adds to the increase of miR-92a-3p in hypoxia, the core region, which causes lower SUCLG1 expression. Further validation techniques are required to confirm the SUCLG1 expression in relation to miR-92a-3p in hypoxia compared to normoxia in GBM cell lines and samples. As our expression levels of miR-92a-3p in hypoxia vary in cell lines and tissues, the literature suggests that SUCLG1 should be increased in hypoxia. If SUCLG1 was proven to be a target of miR-92a-3p, which can be confirmed using a luciferase assay, it would be suggested that low levels of miR-92a-3p in hypoxia correlate to increased SUCLG1 levels in hypoxia. SUCLG1 expression is reported to be affected by hypoxia, however further experiments are required to determine if its expression is regulated by miR-92a-3p in hypoxia.

5.6.6 miR-149-5p gene target expression

Similar to miR-92a-3p, after analysing the effects of hypoxia on miR-149-5p expression in apoptosis and senescence, further investigation of target genes was conducted using qPCR. The three top predicted target genes for miR-149-5p are SRSF1, RAN and HRNRPU.

The first predicted gene target of miR-149-5p is serine/arginine-rich splicing factor 1 (SRSF1). SRSF1 is involved in affecting pre-miRNA but

also mRNA decay and export, translation, miRNA processing and protein stimulation (338). It can autonomously work as a splicing factor but requires interaction with other splicing factors to activate silencing functions. SRSF1 is initially phosphorylated by serine residue protein-specific kinase 1 (SRPK1) and a second phosphorylation by CDC-like kinase 1 (CLK) occurs when SRSF1 is recruited to transcription sites for splicing regulation (338). SRSF1 is highlighted as oncogenic and overexpressed in many cancers and has been shown to be driven by hyperactivation of transcription factor MYC (339), which was identified in the miR-149-5p enrichment analysis pathways. SRSF1 has also been studied in GBM and is noted to be overexpressed compared to controls (340). Wu *et al* investigated SRSF1 and SRPK1 levels and found that SRSF1 mRNA levels are inhibited in hypoxia in GBM (341). The mechanism by which this occurs or further effects of SRSF1 depletion in hypoxia was not identified in this study as SRPK1 was the main focus. However, these studies validate our findings of SRSF1 mRNA levels downregulated in hypoxia, which now may possibly be the result of miR-149-5p elevation in GBM.

Analysing the expression of SRSF1 in GIN28, the miR-149-5p mimics and inhibitors show the opposite effect in normoxia compared to hypoxia. The mimic reduced the amount of SRSF1 expression significantly and the inhibitor significantly increased SRSF1 expression in hypoxia. These trends are expected to be observed by a target gene in response miRNA expression changes, potentially suggest that SRSF1-miR-149-5p binding

is induced in hypoxia. In GIN31, there are no significant changes to SRSF1 expression in response to the mimics and inhibitors in normoxia and hypoxia. This emphasises the differences and heterogeneity of glioblastoma tumours. This is also reflected in SRSF1 expression in tumour tissue samples with two tissue pairs showing no significant difference in SRSF1 expression between the core and the rim, but one patient with significantly lower SRSF1 expression in the core compared to the rim. This patient has higher expression levels of miR-149-5p in the hypoxic core which could contribute to the lower SRSF1 levels also observed in the core of the GBM tumour.

RAN (RAS-related nuclear protein) GTP-binding protein is a member of the RAS family and is often shared between the nucleus and cytoplasm. It has a central G domain for GTP binding and a unique acidic C-terminus tail which remains unstructured in an inactive state and changes conformation following activation to allow for interaction with other proteins (342). RAN has two main functions; during interphase, RAN regulates nucleo-cytoplasmic transport of molecules through the nuclear pore complex and in mitosis, RAN controls cell cycle progression through the regulation of the mitotic spindle and nuclear envelope formation (342). Small molecules diffuse through the nuclear envelope via nuclear pore complexes, however active transportation is required for proteins that are bigger than 5nm in diameter which involves nuclear transport receptors and RAN-GTP which feeds the metabolic energy for the process (342). This includes mediating the translocation of proteins and

receptors including androgen receptor (343). Deregulation of RAN has been reported in various types of cancers and is often increased, which is the same for glioblastoma (344). Though RAN is reported broadly in cancers, defined mechanisms of its tumorigenic role in GBM has not been elucidated, including its response to hypoxia.

In GIN28, no expression change in RAN is seen with miR-149-5p mimic and a significant decrease with the inhibitor in normoxia, but in hypoxia, the mimic significantly depletes RAN expression and the inhibitor significantly increases RAN expression. These findings suggest that miR-149-5p may be induced in hypoxia, as it effects RAN expression as predicted only in hypoxic conditions. This effect is the same seen with miR-1489-5p and SRSF1 in hypoxia. In tumour tissues RAN expression is significantly depleted in the core compared to the rim in one patient, which mirrors the effect seen using qPCR and miR-149-5p mimic in hypoxia in GIN28. However, the other two tumour tissue pairs have no significant change of RAN expression. In GIN31, RAN expression does not vary much across the mimics/inhibitors and hypoxia status.

Heterogeneous nuclear riblonucleoprotein U (HNRNRPU) is the third gene that was investigated as a target of miR-149-5p. HNRNPU binds to DNA and RNA protein that is involved in a vast range of biological processes including telomere-length regulation, mitotic cell progression and mRNA alternative splicing (345). HNRNPU is also a major factor in maintaining 3D chromatin architecture and regulates the formation of

chromatin loops, whose integrity depletes with reduced HNRNPU expression (345). HNRNPU has also been associated with promoting breast cancer cell proliferation, migration and invasion (346). Little has been studied about HNRNPU is glioblastoma, however, Pavlyukov *et al* identified HNRNPU as a spliceosomal protein which is exported from apoptotic GBM cells in a caspase-dependent manner (347). HNRNPU was only exported in a cleaved formation which removes the N-terminal DNA-binding domain which is required for chromatin formation and nuclear localisation (347). However, the role of HNRNPU in GBM is unknown as is its response to hypoxia.

From the qPCR analysis, in GIN28, HRNRPU expression is significantly lower than the control with the transfected miR-149-5p mimic in hypoxia but not significantly changed in normoxia. The miR-149-5p inhibitor significantly increases HNRNPU expression in normoxia compared to hypoxia. In GIN31, there are no significant changes in HRNRPU expression in hypoxia with the mimic or inhibitor compared to the control. The presence of miR-149-5p mimics and inhibitors in normoxia have significantly increased HNRNPU expression. None of these results indicate that miR-149-5p is binding to HNRNPU in these cell lines.

5.6.7 miRNAs indirectly affecting non-target gene expression

Though miRNAs affect the expression of their direct gene targets, it is not unlikely that miRNAs can indirectly affect the expression of genes that are not complimentary targets. This can occur as a result of altering the

expression target genes, which in turn dysregulates a biological or signalling pathway they are involved in, and then consequently affects the expression of other (downstream) genes without directly targeting them. As miR-92a-3p and miR-149-5p expression are both altered in response to hypoxia, it was investigated to determine if these miRNAs indirectly affect the target genes of the other miRNA. In the qPCR screening analysis to determine target miRNA, the dot plots showing the involvement of both miRNAs in differing diseases and biological pathways highlighted that both miR-149-5p and miR-92a-3p are involved in similar processes. Therefore, it was hypothesised that miR-92a-3p could potentially indirectly affect the expression of miR-149-5p targets and alter their expression in hypoxia and vice versa.

5.6.7.1 miR-92a-3p affecting miR-149-5p targets

The first miR-149-5p target gene analysed to determine if a change in expression is seen with miR-92a-5p is SRSF1. In normoxia, an increase in SRSF1 is seen with both the mimic and inhibitor of miR-92a-3p in GIN28. In normoxic cultures of GIN31, the mimic causes a significant increase in SRSF1 expression, and the inhibitor causes a significant decrease in SRSF1 expression. However, in both GIN28 and GIN31 the miR-92a-3p mimic cause a significant depletion of SRSF1 and the miR-92a-3p inhibitor causes a significant increase in SRSF1 in hypoxia. This indicates that miR-92a-3p may be interacting with SRSF1 in hypoxic conditions. Using miRNA prediction tools, SRSF3 and SRSF5 are predicted gene targets of miR-92a-3p and may also bind to the SRSF1

primers. However, these results need to be validated by conducting a luciferase assay in hypoxic and normoxic conditions to confirm or reject the possibility of SRSF1 being a miR-92a-3p target. If SRSF1 is confirmed to not be a target of miR-92a-3p, it is possible that it is indirectly affected, and that particular mechanism will require further elucidation.

The second miR-149-5p target is RAN. In normoxia in GIN28, the miR-92a-3p mimic results in not significant decrease of RAN, and the inhibitor shows a significant increase in RAN expression. In hypoxia in GIN28 the same results were seen, both at a significant level for mimic and inhibitors, suggesting that RAN is a target for miR-92a-3p. In GIN31 in normoxia the mimic causes a significant increase in RAN expression and the inhibitor causes a significant decrease in RAN expression. In hypoxia in GIN31, the same results were seen as in GIN28 in hypoxia conditions. Though RAN is a not a predicted target of miR-92a-3p, RAN-binding protein 9 (RANBP9) is a target of miR-92a-3p. The similarities of their sequences of RAN and RANBP9 is unknown. If the sequences are similar, it is likely that the RAN primers may not be specific to RAN, and also bind to RANBP9. To validate these results, a luciferase assay to determine if RAN is a miR-92a-3p target is required. However, RAN may be indirectly affected by miR-92a-3p expression by further downstream targets.

HRNRPU is a predicted target of miR-92a-3p but was not identified as significant in the enrichment analyses. In normoxia in GIN28, the mimics

and inhibitors of miR-92a-3p react as if miR-92a-3p targets HNRNPU and causes significant reduction and non-significant upregulation of HNRNPU respectively. In hypoxia, the mimic has no significant effect, and the inhibitor causes a small but significant decrease in HNRNPU expression. In GIN31, in normoxia the opposite to what is expected is observed however in hypoxia, HNRNPU expression is decreased significantly with the miR-92a-3p mimic and significantly increased with the miR-92a-3p inhibitor. These results indicate that miR-92a-3p does bind to HNRNPU, in normoxia for GIN28 and hypoxia for GIN31. To further validate that miR-92a-3p is a gene target in GBM, a luciferase assay is required. However with the enrichment analyses, HNRNPU does not yet indicate to be associated with hypoxia in glioblastomas.

5.6.7.2 miR-149-5p affecting miR-92a-3p targets

Similar to the section before, miR-92a-3p gene target expression was analysed to determine if miR-149-5p also interacts with these genes.

Firstly, ACAA1 is analysed with qPCR using miR-149-5p mimics and inhibitors. In GIN28, the miR-149-5p mimic causes an increase in ACAA1 expression in normoxia and a significant decrease in ACAA1 with the miR-149-5p inhibitor. In hypoxia, both the mimic and inhibitor cause a decrease in ACAA1 expression in GIN28 cells. In GIN31, the miR-149-5p mimic causes no significant change in ACAA1 expression in either normoxic or hypoxic conditions. The miR-149-5p inhibitor causes a significant increase in ACAA1 expression in normoxia and a significant

decrease in ACAA1 expression in hypoxia. The absence of a trend of ACAA1 expression with the mimics and inhibitors in either normoxic or hypoxic conditions, adds to the evidence that ACAA1 is not a target of miR-149-5p, which can further be validated with a luciferase assay.

The second target of miR-92a-3p that is examined using miR-149-5p mimics and inhibitors is ACADS. In GIN28, miR-149-5p mimic causes a significant increase of ACADS in normoxia and significant decrease of ACADS in hypoxia. The miR-149-5p inhibitor significantly decreases ACADS in normoixa and significantly increases ACADS expression in hypoxia. These results show that ACADS could potentially be a target for miR-149-5p in hypoxia or be indirectly affect by miR-149-5p expression in hypoxia in GIN28. In GIN31, there is no significant changes to ACADS expression in normoxia or hypoxia with miR-149-5p mimic and with miR-149-5p inhibitor, ACADS expression is significantly increased in normoxia and unchanged in hypoxia.

The third target gene of miR-92a-3p is SUCLG1. In GIN28, miR-149-5p mimics shows a significant increase in SUCLG1 expression in normoxia and a significant decrease in SUCLG1 expression in hypoxia. The miR-149-5p inhibitor has no significant effect in normoxia but causes a small but significant decrease in SUCLG1 in hypoxia in GIN28. In GIN31, miR-149-5p mimic shows a significant decrease in SUCLG1 in normoxia and no significant change in SUCLG1 expression in hypoxia. The miR-149-5p inhibitor shows a significant increase in SUCLG1 expression in

normoxia and no significant change in hypoxia in GIN31. Similar to ACAA1, with no trends seen in hypoxia or normoxia with mimics or inhibitors, it is likely that SUCLG1 is not a predicted gene target of miR-149-5p. To validate this experimentally, a luciferase assay should be conducted.

5.6.8 RAN expression in glioblastoma tumour tissue samples

RAN was selected as a gene target of miR-149-5p to explore and investigate further. RAN was chosen due to its hypoxia-response effect with miR-149-5p and as a potential novel hypoxia target due to limited literature reports. Firstly, the expression of RAN was validated in tumour tissue samples at the protein level using IHC and further in the cell lines using IF. Increased miR-149-5p due to hypoxic exposure would predict a decrease in RAN expression in hypoxia as RAN is a predicted target of miR-149-5p. The decrease of RAN protein expression is seen in the cell line GIN28 using immunofluorescence, the same cell line which saw a decrease of RAN gene expression in hypoxia with miR-149-5p mimic using qPCR. This emphasises the association between miR-149-5p and RAN expression in GIN28 cell line. However, using IF to identify RAN expression was also conducted on GIN31 and GIN8 cell lines. In GIN31 using IF RAN expression was increased in hypoxia which correlates with the qPCR analysis where RAN was increased in hypoxia with a miR-149-5p mimic. GIN8 also showed an increased expression of RAN with hypoxic exposure.

IHC was used to assess the protein expression of RAN in the tumour tissues to validate the changes seen the cell lines. The expression of RAN is marginally less in the core than the rim and invasive edge but not significantly different. The RAN protein expression is localised in the cytoplasm and most of the tissue sample patients have high RAN expression. The Kaplan-Meier curve shows that lower expression of RAN is associated with a poorer overall survival but is not statistically significant. A much smaller portion of the dataset exhibited low expression of RAN (12%) and only 5% of the tissue samples showed a low protein expression of RAN. However, a low protein expression of RAN, with a poor overall survival also correlates with high expression of miR-149-5p and hypoxic conditions.

RAN is a small GTPase protein that provides energy for nucleocytoplasmic transport and mitotic spindle assembly by hydrolysing guanosine triphosphate (GTP) into guanosine diphosphate (GDP) (348). RAN regulates the activities of the importin protein complexes that mediate nuclear import and export via the released energy (348). It is often deregulated in cancers including glioblastomas. It is associated with promoting proliferative signalling and shows that RAN activation is sufficient to initiate tumour progression and the stimulation of cell growth creates a positive feedback loop inducing RAN activity to promote the translocation of transcription factors such as NFKB and β-catenin to the nucleus (342). RAN may regulate the PI3K and MAPK pathways in two ways: upstream by stabilising Met-receptor and recruiting SoS protein

through RanBP9 and downstream by ensuring the traffic of transcription factors controlled by these pathways (342). RAN is also associated with resisting cell death by interacting with the protein survivin. The role of survivin in cell proliferation is associated with its ability to support mitosis in highly proliferating cancer cells, however, during interphase, survivin is absent in normal cells, but in cancer cells, it is stabilized and translocated to the cytoplasm and mitochondria where it exerts its antiapoptotic effect (349). During mitosis, survivin was shown to regulate microtubule dynamics, which is mediated by RAN and TPX2, and the loss of RAN results in mitotic defects similar to that of survivin inhibition (350). RAN is a key player for the cytoplasmic localisation of survivin and therefore participates in the acquisition of the antiapoptotic property of cancer cells (342). Another cancer hallmark RAN is associated with is invasion and metastasis and is associated with the oncogene MYC (342) which corresponds to the enrichment analysis as RAN was identified as a MYC target. MYC overexpression correlates with the expression of RAN and directly interacts with the RAN promoter to induce RAN expression (351). RAN mediates signalling of other oncogenes which are important in metastasis including LIN28B and glycophosphoprotein oestopontin (OPN) (342). These examples show the versatility and breadth of processes RAN is involved in to initiate and promote cancer progression. Further studies are required to characterise the involvement of RAN in glioblastoma. As hypoxia is an important microenvironmental condition in glioblastomas and often attributes to tumour progression, identifying the role RAN plays and by which mechanisms in glioblastoma,

is vital for glioblastoma research and to identify ways to exploit RAN as a novel target to combat glioblastoma.

As this chapter covers a large number of experimental findings the main overall conclusions can be summarised as follows:

- Hypoxia is significantly present in the core of tumour tissue samples as well as in the hypoxia-exposed cell lines in comparison to rim/invasive edge tissue and normoxia-exposed cells respectively.
- miR-149-5p is significantly upregulated in hypoxia in both cell lines and tumour tissue samples.
- miR-92a-5p expression is downregulated in hypoxia in the cell lines but upregulated in tumour tissue samples.
- Apoptosis is increased when using miRNA inhibitors in hypoxia-exposed cell lines.
- miR-149-5p targets RAN and SRSF1 are affected by miR-149-5p expression changes mainly in hypoxia. As miR-149-5p is increased in hypoxia, this is likely to lead to RAN and SRSF1 reduction in hypoxic conditions.
- Immunofluorescence and IHC have shown a reduction in RAN expression in hypoxic conditions compared to normoxic conditions.

6 Chapter 6: Discussion, conclusions, and future work

6.1 Overview and conclusions

This thesis addresses the importance of hypoxia within glioblastomas and endeavours to increase the knowledge of how this microenvironmental pressure influences the expression of miRNA and consequentially downstream targets. Glioblastomas are aggressive primary brain tumours with a median survival of 14 months with maximal treatment. Understanding more biological processes of GBMs may be able to inform future developments to target this cancer more effectively. Hypoxia is an important environmental condition which is associated with many hallmarks of cancer, enhancing pathways such as cell signalling, angiogenesis, cancer cell proliferation and metastasis. miRNAs are vital in regulating gene expression in many biological processes and their expression can be altered in response to many conditions, such as hypoxia, which consequently affects the expression of gene targets. There are many known oncogenic and tumour suppressive miRNAs that have important roles in tumorigenesis. The main aim of this thesis is to identify hypoxia-influenced miRNAs and to examine the expression of downstream targets in response to hypoxia and differing miRNA expression levels.

In chapter 3, a microarray was used to screen for differentially expressed miRNAs in response to hypoxia in a wide range of glioma cell lines. The

first hypothesis was that individual miRNAs are differentially expressed in hypoxic and normoxic conditions within gliomas. This hypothesis can be partially accepted as miRNAs were showed to differ between hypoxia and normoxia within the gliomas categories, however these results used unadjusted p-values of <0.01 as false discovery rate corrections rendered all the miRNAs insignificant. The microarray screened 800 individual miRNAs, however due to the loss of over half of the miRNAs due to background, it is possible that important and differentially expressed miRNAs were lost from this. The second hypothesis was that differentially expressed miRNAs in hypoxia compared to normoxia differs in high-grade gliomas compared to low-grade gliomas. Similar to the first hypothesis, this can be partially accepted (due to the statistical analysis) and different individual miRNA were identified to be expressed in hypoxia compared to normoxia in GBM and low-grade gliomas. As miR-138-5p, miR-576-3p, miR-128-1-5p, miR218-5p, miR-320a-5p, miR-608, miR-609, miR-301b-3p and miR-490-5p are differentially expressed in GBM in hypoxia and miR-2053, hsa-miR-217, hsa-miR-3615, hsa-miR-494-5p, hsa-miR-506-6p, hsa-miR-606 are differentially expressed in low-grade gliomas in hypoxia. This initial experiment provided a good basis to know that miRNAs can be differentially expressed in hypoxia but further experiments need to confirm and statistically validate the hypotheses generated in this chapter.

In chapter 4, a second screening method using custom qPCR plates were used to screen a hand-selected group of miRNAs. The same hypotheses

generated in the previous chapter were still used, as the hypotheses could not be fully accepted using the NanoString nCounter microarray. The first hypothesis is that individual miRNA levels are differentially expressed in hypoxic gliomas compared to normoxic glioma is accepted in this chapter. For each subgroup of gliomas, differentially expressed miRNAs were identified with a corrected p-value of <0.05. Similarly, the second hypothesis which was that differentially expressed miRNAs in hypoxia compared to normoxia differs in high-grade gliomas compared to low-grade gliomas is also accepted. Different miRNAs were differentially expressed in hypoxia in the different glioma subgroups, GBM, LGG and overall. After identifying the differentially expressed miRNAs, two were required to be selected for further investigation of their response to hypoxia. The GBM category was chosen, due to the readily availability and optimised culture of the cell lines, compared to the long growth time of the low-grade gliomas and the large amount of varying cell lines required for the overall category. The pathway analysis conducted on the GBM differentially expressed miRNAs highlighted the links to glioblastomas and hypoxia. The highest and lowest fold changed miRNAs were selected from GBM category and which are miR-149-5p and miR-92a-3p.

The fifth chapter 5 thesis focuses on validating the presence of hypoxia in cell lines and tumour tissues and focusing on the selected miRNAs from the previous chapter. It was important to validate that the hypoxic response was seen at the molecular level in the cell lines, confirmed by

the western blot, and in the tissue samples confirmed by CA9 PCR and IHC. The first hypothesis generated in this chapter is that the same changed expression of miR-149-5p and miR-92a-3p in hypoxia in GBM cell lines is also seen in GBM tumour tissue samples. This hypothesis can be accepted for miR-149-5p, as both cell lines and tissues saw an upregulation of miR-149-5p in hypoxia. The hypothesis is rejected for miR-92a-3p as the opposite was observed in the cell lines compared to the tissues. This need to be repeated to be validated, but as mentioned in chapter 5, there are many reasons way it may vary between cell lines and tissues. The second hypothesis is that altered expression in hypoxia (up or down-regulated) of miRNAs (miR-149-5p and miR-92a-3p) consequently results in differentially expressed gene targets in hypoxia compared to normoxia in GBM cells. This hypothesis was assessed using PCR and using miRNA mimics and inhibitors to change the miRNA expression and determine the effect of gene targets in hypoxia compared to normoxia. The six genes that were analysed, most showed differential expression between the mimics and inhibitors and within the hypoxic conditions, which confirms this hypothesis. This experiment highlights the possibility of miR-149-5p being a hypoxia-inducible miRNA. This is suggested as most of its targets bind as expected in hypoxic conditions and not in normoxia. This experiment is important as it insinuates the downstream effect the hypoxic change has on miRNAs. The hypoxia effect does not stop at miRNAs but continues cascading down into gene targets and consequently indirect targets. Following on from that discovery, the third hypothesis presents the presumption of miRNAs

effecting biological processes. Both apoptosis and senescence were investigated, as they were identified numerous times in the pathway analysis in chapter 4. Lastly, to confirm the changes seen in the gene targets were not limited to cell lines, one gene target, RAN, was also assessed in tumour tissue samples. This hypothesis was accepted as both IF and IHC confirmed the reduction of RAN in hypoxia in cell lines and tissues.

Overall, this work focusses on the screening miRNAs in hypoxia in glioblastoma to determine miRNAs of importance. The identification of miR-149-5p as a potential hypoxia-inducible miRNA which only binds in hypoxic conditions is vital for glioblastoma research. This knowledge and research could be used to produce targeted therapy to reduce the effect of hypoxic-induced pathways. As this research is only the first preliminary and initial process of identifying hypoxic-specific miRNAs in glioblastomas further work and research is required in order for the knowledge to develop to be able to exploit hypoxia within glioblastomas, as a possible therapy.

6.2 Future work

6.2.1 Luciferase assay

To further validate the work in this thesis, a luciferase assay to confirm the binding of miR-149-5p to RAN in hypoxic and normoxic conditions is required. This experiment will confirm the assumptions of miR-149-5p being a hypoxic-specific miRNA and having increased binding to its

targets in hypoxic conditions compared to normoxic conditions. The luciferase assay will robustly confirm the assumptions and findings made in this thesis of miR-149-5p. This experiment was planned to be completed during this thesis, however, QC issues and shipment delays rendered this impossible in the timeframe. The LightSwitch luciferase reporter assay system (cat no. 32031) was ordered. The GoClone vectors contain the 3′ UTR target of a miRNA, which is cloned downstream of the Renilla luciferase gene (RenSP) under the control of a constitutive promoter. The expression of luciferase will be reduced upon the binding of a miRNA mimic to the 3'UTR of its target. Go Clone vectors containing the 3' UTR sequences of RAN, β-actin, a random genomic fragment was purchased from Active Motif and the sequences are shown in table 26. An empty vector, the parental luciferase construct, contains no 3`UTR sequence would be used to assess any background noise signal. Secondly, a reporter vector that contains a random genomic fragment and a reporter vector that contains the 3'UTR of a housekeeping gene (β-Actin) would also be included for the purposes of normalisation against non-specific binding.

Table 26. Sequences of 3'UTRs cloned into the LightSwitch 3'UTR vector.

3' UTR type	Product Code (Active Motif)	Insert Length	3' UTR sequence
RAN	S806940	984	TTCCATCTCTTCGTCTAGGTTG CTCAGACAACTGCTCTCCCGGA TGAGGATGATGACCTG TGAGAATGAAGCTGGAGCCCA GCGTCAGAAGTCTAGTTTTATA GGCAGCTGTCCTGTGAT GTCAGCGGTGCAGCGTGTGTG CCACCTCATTATTATCTAGCTAA GCGGAACATGTGCTTC ATCTGTGGGATGCTGAAGGAGA TGAGTGGGCTTCGGAGTGAATG TGGCAGTTTAAAAAAT AACTTCATTGTTTGGACCTGCAT ATTTAGCTGTTTTGGAACGCAG TTGATTCCTTGAGTT TCATATATAAGACTGCTGCAGT CACATCACAATATTCAGTGGTG AAATCTTGTTTGTTAC TGTCATTCCCATTCCTTTTCGTT

			TAGAATCAGAATAAAGTTGTATT TCAAATATCTAAGC AAGTGAACTCATCCCTTGTTTAT AAATAGCATTTGGAAACCACTA AAGTAGGGAAGTTTT ATGCCATGTTAATATTTGAATTG CCTTGCTTTTATCACTTAATTTG AAATCTATTGGGTT AATTTCTCCCTATGTTTATTTTT GTACATTTGAGCCATGTCACAC AAACTGATGATGACA GGTCAGCAGTATTCTATTTGGT TAGAAGGGTTACATGGTGTAAA TATTAGTGCAGTTAAG CTAAAGCAGTGTTTGCTCCACC TTCATATTGGCTAGGTAGGGTC ACCTAGGGAAGCACTT GCTCAAAATCTGTGACCTGTCA GAATAAAAATGTGGTTTGTACAT ATCAAATAGATATTT TAAGGGTAATATTTTCTTTTATG GCAAAAGTAATCATGTTTTAATG TAGAACCTCAAACA GGATGGAACATCAGTGGATGG CAGGAGGTTGGGAATTCTTGCT

			GTTAAAAATAATTACAA ATTTTGCACTTTTTTGTTTGAAT GTTAGATGCTTAGTGTGAAGTT GATACGCAAGGAAAA TGGTCCATGTTTACCCACAGTT TT
ACTB	S804753	680	GGATCAGCAAGCAGGAGTATGA CGAGTCCGGCCCCTCCATCGT CCACCGCAAATGCTTCT AGGCGGACTATGACTTAGTTGC GTTACACCCTTTCTTGACAAAAC CTAACTTGCGCAGAA AACAAGATGAGATTGGCATGGC TTTATTTGTTTTTTTTGTTTTGTT TTGGTTTTTTTTTT TTTTTTGGCTTGACTCAGGATTT AAAAACTGGAACGGTGAAGGTG ACAGCAGTCGGTTGG AGCGAGCATCCCCCAAAGTTCA CAATGTGGCCGAGGACTTTGAT TGCACATTGTTGTTTT TTTAATAGTCATTCCAAATATGA GATGCGTTGTTACAGGAAGTCC CTTGCCATCCTAAAA GCCACCCCACTTCTCTCTAAGG

			AGAATGGCCCAGTCCTCTCCCA AGTCCACACAGGGGAG GTGATAGCATTGCTTTCGTGTA AATTATGTAATGCAAAATTTTTT TAATCTTCGCCTTAA TACTTTTTTATTTTGTTTTATTTT GAATGATGAGCCTTCGTGCCCC CCCTTCCCCCTTTT TTGTCCCCCAACTTGAGATGTA TGAAGGCTTTTGGTCTCCCTGG GAGTGGGTGGAGGCAG CCAGGGCTTACCTGTACACTGA CTTGAGACCAGTTGAATAAAAG TGCACACCTTAAAAAT GAGGCCAAGTGTGACTTTGT
Random genomic fragment	S890003	781	GTTTTCCTGTTTCCAGCACTTCA TGTGCCATGAGACTTTCCTTCT ATCTTGAAATGAAAC CAGGGAAGCCCACTCAGCACTT TCACAGCTTTGAAATATATGCCA GAATTATTCTTCTGA CAACCCCCATTACCTAAAACCA AGGCATTCAAACAAATGTGACA TAAATGCAGTTACACT TCTCACTACCACCATCCGCCAT

			ACTCACAAATATAAATGTTATCT GGAATATTAGCATCC TAAAGGAGGCAGTGTTTTACAT GATATTTTCAGGACTTCGCCAT CTGGGTCAACAGTATA CTTTCTAAAGAATTTTTAAGATG ACATCATAAAGAACTGATATAAT TGAACTTTTATATT AAAACTTCAATACTGACATGAAA TCACTATTTGGATATATATTTAA GCCAAGAAAATGCC TCATGTAGTTATGCTGTAACATT GTATAAAAGAAGACTTTAAAACA TGAATTTTACTGCA AAATGTCATGTTCACTCTGCAG GCATCTTGCTAAGATGATCAAC TGAATTCAAGGGATGT CTCTAGGATATCTTCAGATAGA AACCATTTACCACATTTGAGTTC TTGGTGAAAATTCAG AGACATAACACAATATTTATCAA AAATACTATTGGTAGAGATCAT GCCATAAAAATTTGC TAAAATTAAACAGACTAATTACC TTGGTAATTAACATCAATAGACA

			TGAGGCCATCTAGA TTATTCATAATAAAGTGAATACT GAAATTGTACACCACTCAGATT GATAAGGAAAACTGAT

6.2.1.1 Luciferase assay protocol

This luciferase protocol has been optimised by Huda Alfardus (43) and would be used, however further optimisation may be required. A 3'UTR bearing reporter vector at a 100ng final concentration will be mixed with the miR-149-5p mimic or non-targeting control (50nM final concentration) in serum-free media in tube 1. Empty vectors will be used as negative controls. The transfection reagent will be prepared in a separate tube for the required number of transfections. In tube 2, the DharmaFECT DUO Transfection Regent (Horizon Discovery) will be mixed in serum-free media. After 5-minute incubation at room temperature, 10µl from Tube 2 will be added to each prepared Tube 1 of vector plus miR-149-5p mimic or non-targeting control for a total volume of 20µl per transfection. The co-transfection solutions are found in table 27.

Table 27. Co-transfection solutions per replicate.

	Component	**Volume (µl)**
Tube 1	GoClone reporter vector (30ng stock)	3.33
	miRNA mimic or non-targeting mimic control (2µM stock)	5
	Serum-free media	1.67
Tube 2	DharmaFECT DUO transfection reagent	0.15
	Serum-free media	9.85

Each mixture will be incubated for 20 minutes at room temperature. After 20 minutes, 80µl of pre-warmed (37˚C), serum cell culture media will be added to each tube for a total of 100µl per transfection. The transfection media will be added on top of confluent GIN28 cells seeded into a 96-well solid bottom white cell culture plates (Avantor) 24h before transfection. Each well was seeded with 100µl of 3.125 x 104 cells/ml of GIN28 cells. The seeded plate will be removed from the incubator, and the media aspirated off from each well. Subsequently, 100µl of the transfection mixture will be added to each well, and the plate will incubate for 24hrs and a following further 24 hours in the allocated condition, normoxia or hypoxia. The plate will be removed from the incubator and covered with Foil Plate Sealing Tape (E&K Scientific) to protect from light

and placed in the -80˚C freezer. The plate is frozen for at least 6 hours in order to increase cell lysis and subsequently luciferase signal.

LightSwitch Luciferase Assay Kit (Active Motif) would be used to assess miRNA binding to its putative 3'UTR. The frozen plates will thaw at room temperature 30 minutes before applying the luciferase solution. To each well, 100µl of the LightSwitch assay solution was directly added, without aspirating the media, as shown in table 28.

Table 28. LightSwitch luciferase assay solution mixture.

Reagent	**Volume per well (µl)**
100x substrate	1
Assay buffer	99

Luminescence will be read with an emission filter gain of 3600 and a measurement interval time of 2 sec in the FLUOstar Omega microplate luminometer. The knockdown of luciferase expression can be calculated as the ratio of the signal of miR-149-5p mimic over the non-targeting control. This ratio can be calculated as (luminescence form a 3'UTR vector= miR-149-5p mimic/non-targeting control). The data can be normalised to the housekeeping, random, and empty constructs to control for non-3'UTR specific effects.

6.2.1.2 Luciferase assay outcome predictions

As the luciferase assay has not yet been performed, the results can only be assumed based off previous experimental results. The assumption is that the luciferase expression will decrease further using the RAN 3'UTR cloned vector and miR-149-5p mimic in hypoxic conditions compared to normoxic conditions. This is because in qPCR results, RAN expression was decreased significantly in hypoxia with the miR-149-5p mimic compared to normoxia, suggesting that miR-149-5p is further induced in hypoxic conditions. The decreased protein expression of RAN detected by IF and IHC in hypoxia increases the probability of hypoxia being the cause for its reduction. These results together suggest that in the luciferase assay, increased binding of RAN 3'UTR and miR-149-5p occurs in hypoxic conditions. If this experiment produces this predicted result, this robustly confirms the hypothesis that miR-149-5p is a hypoxia-inducible miRNA. Also, the empty vector, random genomic fragment and β-actin should have the same luciferase expression and remain unchanged in hypoxic and normoxic conditions.

To add onto the luciferase assay, analysing the binding between miR-149-5p and SRSF1 in hypoxia and normoxia will also be valuable as it exhibited a similar pattern to RAN in hypoxia. This method can be used on multiple miR-149-5p targets to fully understand the extent and identify which target genes are targeted in hypoxic conditions. This can be extended into analysing the hypoxia-targeted genes by miR-149-5p and completing bioinformatic analyses to determine if there are particular

mechanisms, processes or signalling pathways that are influenced by miR-149-5p changed expression in hypoxia in glioblastomas. This investigation could identify what role miR-149-5p plays in glioblastoma tumorigenesis by allowing the tumour to tolerate hypoxic conditions.

6.2.2 Other avenues of research

This project can easily diverge into many branches and further research avenues. Following on from luciferase assays, after confirming the binding in hypoxia, RAN and other miR-149-5p targets can be assessed at both a functional and mechanistical level in hypoxia to detect other pathways that miR-149-5p effects and how hypoxic exposure alters this. This can include using knockdown of target genes, by methods such as siRNA or CRISPR editing, causing decreased gene expression, which is similar to the effect caused by increased miR-149-5p. This can be used in functional assays such as cell proliferation, cell viability, invasion, apoptosis, senescence to confirm which pathways miR-149-5p/RAN other targets effect in hypoxia in glioblastomas. These experimental investigations will be able to confirm or reject the findings shown during bioinformatic analyses. Further research can include focusing on miR-149-5p gene targets such as SRSF1 and RAN and whether knock-ins compared to knockouts of these genes cause a significant anti-tumour effect. Currently here are no direct RAN-targeting drugs as GTPases have been labelled as ‘undruggable’ because of their exceptionally complex regulatory mechanisms and lack of deep pockets for ligand binding (352). However, Yin *et al* are using nuclear magnetic resonance

(NMR) spectroscopy techniques to develop early-stage drug discovery to target GTPases including RAN (352). If and when these potential drugs come to fruition, testing their effect on RAN in hypoxic and normoxic conditions within glioblastomas may produce a greater understanding of how to use these targets to aid the treatment of glioblastomas.

The qPCR screening identified multiple differentially expressed miRNAs in gliomas. Different miRNAs in glioblastomas can be examined further, similar to the research in this thesis to assess their response in hypoxia and the effect of their target genes. Also, further investigation can be initiated to identify the effect of hypoxia on miRNAs in low-grade gliomas. Very few studies have assessed the impact of hypoxia on low-grade gliomas, particularly the effect on miRNAs. This work would be very interesting to compare against the effect of hypoxia in glioblastomas, to determine if there are similarities or differences in the hypoxic response depending on the grade of tumour.

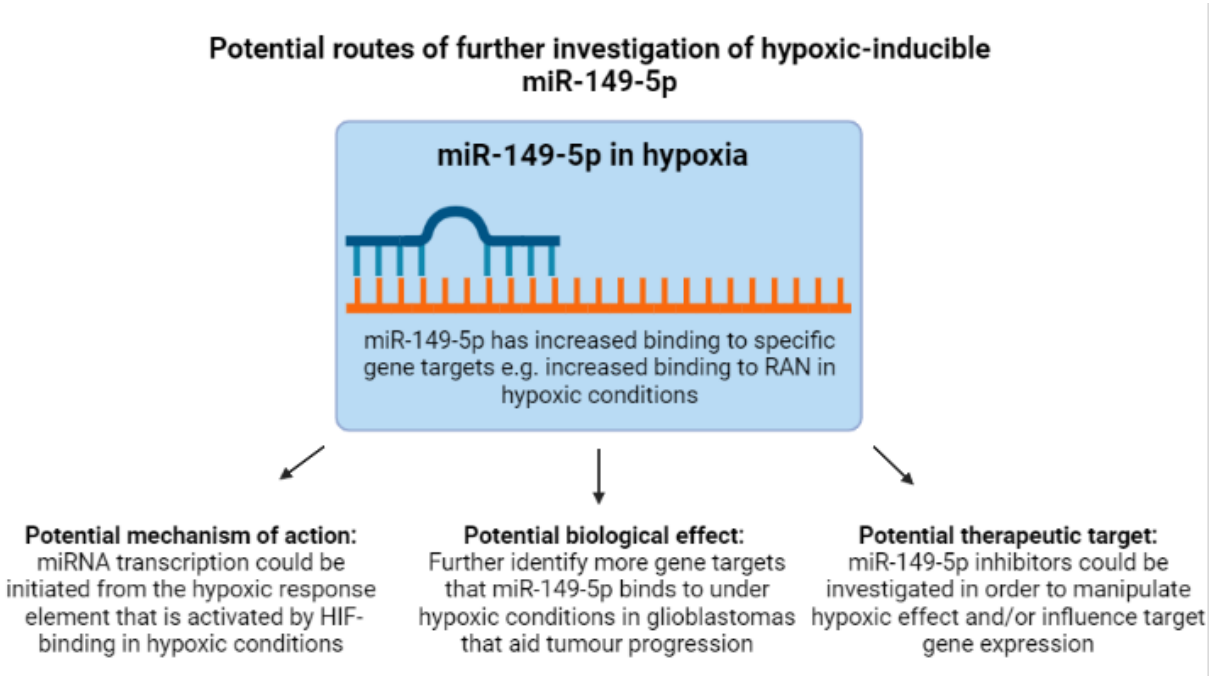

Figure 115. A schematic highlighting the possible avenues of future research to further investigate the hypoxic-inducible miR-149-5p in glioblastomas.

Figure 115 highlights the future avenues to explore of the newly discovered hypoxic-inducible miR-149-5p. Investigating the mechanism of action of how hypoxia influences the expression of miR-149-5p could provide vital information in understanding how hypoxia effects glioblastomas. A falsifiable emerging hypothesis to further study mechanism of action could be that 'miR-149-5p expression is induced by the hypoxic response element initiated by HIF in hypoxic conditions in glioblastomas. Other falsifiable hypotheses that should be studied to further the knowledge of the novel hypoxic-inducible miR-149-5p are:

- miR-149-5p levels can be manipulated in hypoxic conditions to reduce pro-tumorigenic pathways.
- miR-149-5p is significantly induced in hypoxia when compared to physiological levels of oxygen as a normoxic state.

- miR-149-5p significantly suppresses the expression of other target genes that lead to glioblastoma tumour progression in hypoxia compared to normoxia.

These hypotheses have the potential to increase the understanding of the relationship between hypoxia, miRNA and cancer as well as providing more in-depth and niche information about the newly discovered hypoxia-inducible miR-149-5p. Furthermore, for any of these future investigations to lead to possible therapeutics, other areas of research will need to be conducted. One namely includes looking into the stability of miRNAs and how to conquer this when assessing miRNAs as therapeutics. If this research is propelled closer to the clinic, miRNA stability within hypoxic and normoxic conditions needs to evaluated. This is because currently miRNAs are very unstable components and this has prevented their use in the clinic. These examples are just a fraction of the avenues that can be explored in this field to fully expand the knowledge of glioblastomas and how hypoxia and miRNAs fit into their landscape, and how they can potentially be exploited as therapeutic targets.

As shown in chapter 5, miR-92a-3p expression has varied in hypoxia in cell lines and tissues. Further validation of miR-92a-3p in hypoxia should include repeating the qPCR in different primary cell lines and tissues from different patients, to increase the sample number. Next generation sequencing can also be used to identify expression profiles of miRNAs, on normoxic and hypoxic-exposed samples (353). Further confirming the response of miR-92a-3p in hypoxia will be able to determine if there is a

consistent significant result and consequently investigating its potential influence and impact of target genes can begin.

The main scope of this thesis and consequent research is to increase the breadth of knowledge and research of the response of miRNAs in hypoxia in glioblastomas and gliomas. Enhancing, confirming and validating any hypotheses in this field emphasises the importance of miRNAs and hypoxia. Further in-depth work may highlight important pathways or molecular targets that can be exploited to potentially develop novel therapeutics, such as miRNA inhibitors, to help combat glioblastoma.

7 References

1. Mukherjee S. The Emperor of All Maladies: A Biography of Cancer. New York, Scribner; 2010.
2. Capasso LL. Antiquity of cancer. Int J Cancer. 2005;113(1):2–13.
3. Cancer Research UK. Cancer Research UK Statistics [Internet]. 2022 [cited 2022 Oct 3]. Available from: https://www.cancerresearchuk.org/health-professional/cancer-statistics-for-the-uk#heading-Four
4. De Kouchkovsky I, Abdul-Hay M. Acute myeloid leukemia: A comprehensive review and 2016 update. Blood Cancer J. 2016;6(7).
5. Hanahan D, Weinberg RA. Hallmarks of cancer: The next generation. Cell [Internet]. 2011;144(5):646–74. Available from: http://dx.doi.org/10.1016/j.cell.2011.02.013
6. Hanahan D, Weinberg RA. The Hallmarks of Cancer. Cell. 2000;100(1):57–70.
7. Duesberg P, Li R. Multistep carcinogenesis: a chain reaction of aneuploidizations. Cell cycle. 2003;2(3):201–9.
8. Pon JR, Marra MA. Driver and passenger mutations in cancer. Annu Rev Pathol Mech Dis. 2015;10:25–50.
9. Stratton MR, Campbell PJ, Futreal PA. The cancer genome. Nature [Internet]. 2009;458(7239):719–24. Available from: http://www.pubmedcentral.nih.gov/articlerender.fcgi?artid=2821689&tool=pmcentrez&rendertype=abstract
10. Abhinand CS, Raju R, Soumya SJ, Arya PS, Sudhakaran PR.

VEGF-A/VEGFR2 signaling network in endothelial cells relevant to angiogenesis. J Cell Commun Signal [Internet]. 2016;10(4):347–54. Available from: http://dx.doi.org/10.1007/s12079-016-0352-8

11. Claesson-Welsh L, Welsh M. VEGFA and tumour angiogenesis. J Intern Med. 2013;273(2):114–27.
12. Chan XY, Singh A, Osman N, Piva TJ. Role Played by Signalling Pathways in Overcoming BRAF Inhibitor Resistance in Melanoma. 2017;1–13.
13. Ksionda O, Mues M, Wandler AM, Donker L, Tenhagen M, Jun J, et al. Comprehensive analysis of T cell leukemia signals reveals heterogeneity in the PI3 kinase-Akt pathway and limitations of PI3 kinase inhibitors as monotherapy. 2018;
14. Wesseling P, Capper D. WHO 2016 Classification of gliomas. Neuropathol Appl Neurobiol. 2018;44(2):139–50.
15. Louis DN, Perry A, Wesseling P, Brat DJ, Cree IA, Figarella-Branger D, et al. The 2021 WHO classification of tumors of the central nervous system: A summary. Neuro Oncol. 2021;23(8):1231–51.
16. Cohen AL, Holmen SL, Colman H. IDH1 and IDH2 Mutations in Gliomas. Curr Neurol Neurosci Rep. 2013;13(5):345.
17. Fack F, Tardito S, Hochart G, Oudin A, Zheng L, Fritah S, et al. Altered metabolic landscape in IDH -mutant gliomas affects phospholipid, energy, and oxidative stress pathways . EMBO Mol Med. 2017;9(12):1681–95.

18. Han S, Liu Y, Cai SJ, Qian M, Ding J, Larion M, et al. IDH mutation in glioma: molecular mechanisms and potential therapeutic targets. Br J Cancer [Internet]. 2020;122(11):1580–9. Available from: http://dx.doi.org/10.1038/s41416-020-0814-x
19. Shi J, Sun B, Shi W, Zuo H. Decreasing GSH and increasing ROS in chemosensitivity gliomas with IDH1 mutation. 2015;655–62.
20. Kickingereder P, Sahm F, Radbruch A, Wick W, Heiland S, Deimling A Von, et al. IDH mutation status is associated with a distinct hypoxia / angiogenesis transcriptome signature which is non-invasively predictable with rCBV imaging in human glioma. Nat Publ Gr. 2015;(July):1–9.
21. Demidenko ZN, Blagosklonny M V. The purpose of the HIF-1 / PHD feedback loop. Cell cycle. 2011;10(10):1557–62.
22. Pugh CW, Ratcliffe PJ. Regulation of angiogenesis by hypoxia: role of the HIF system. Nat Med. 2003;9(6):677–84.
23. Xu W, Yang H, Liu Y, Yang Y, Wang P, Kim SH, et al. Oncometabolite 2-hydroxyglutarate is a competitive inhibitor of α-ketoglutarate-dependent dioxygenases. Cancer Cell [Internet]. 2011;19(1):17–30. Available from: http://dx.doi.org/10.1016/j.ccr.2010.12.014
24. The Cancer Genome Atlas Research Network. Comprehensive, Integrative Genomic Analysis of Diffuse Lower-Grade Gliomas. N Engl J Med. 2015;372(26):2481–98.
25. Wiestler B, Capper D, Holland-Letz T, Korshunov A, Von

Deimling A, Pfister SM, et al. ATRX loss refines the classification of anaplastic gliomas and identifies a subgroup of IDH mutant astrocytic tumors with better prognosis. Acta Neuropathol. 2013;126(3):443–51.

26. Paugh BS, Qu C, Jones C, Liu Z, Adamowicz-Brice M, Zhang J, et al. Integrated molecular genetic profiling of pediatric high-grade gliomas reveals key differences with the adult disease. J Clin Oncol. 2010;28(18):3061–8.

27. Phillips HS, Kharbanda S, Chen R, Forrest WF, Soriano RH, Wu TD, et al. Molecular subclasses of high-grade glioma predict prognosis, delineate a pattern of disease progression, and resemble stages in neurogenesis. Cancer Cell. 2006;9(3):157–73.

28. Verhaak RGW, Hoadley KA, Purdom E, Wang V, Qi Y, Wilkerson MD, et al. Integrated Genomic Analysis Identifies Clinically Relevant Subtypes of Glioblastoma Characterized by Abnormalities in PDGFRA, IDH1, EGFR, and NF1. Cancer Cell [Internet]. 2010;17(1):98–110. Available from: http://dx.doi.org/10.1016/j.ccr.2009.12.020

29. Colman H, Zhang L, Sulman EP, McDonald JM, Shooshtari NL, Rivera A, et al. A multigene predictor of outcome in glioblastoma. Neuro Oncol. 2010;12(1):49–57.

30. Zhang P, Xia Q, Liu L, Li S, Dong L. Current Opinion on Molecular Characterization for GBM Classification in Guiding Clinical Diagnosis, Prognosis, and Therapy. Front Mol Biosci. 2020;7(September):1–13.

31. Sharma A, Bendre A, Mondal A, Muzumdar D, Goel N, Shiras A. Angiogenic gene signature derived from subtype specific cell models segregate proneural and mesenchymal glioblastoma. Front Oncol. 2017;7(JUL).
32. Park AK, Kim P, Ballester LY, Esquenazi Y, Zhao Z. Subtype-specific signaling pathways and genomic aberrations associated with prognosis of glioblastoma. Neuro Oncol. 2019;21(1):59–70.
33. Teo WY, Sekar K, Seshachalam P, Shen J, Chow WY, Lau CC, et al. Relevance of a TCGA-derived Glioblastoma Subtype Gene-Classifier among Patient Populations. Sci Rep. 2019;9(1):1–10.
34. Park J, Shim JK, Yoon SJ, Kim SH, Chang JH, Kang SG. Transcriptome profiling-based identification of prognostic subtypes and multi-omics signatures of glioblastoma. Sci Rep [Internet]. 2019;9(1):1–11. Available from: http://dx.doi.org/10.1038/s41598-019-47066-y
35. Brito MB, Goulielmaki E, Papakonstanti EA. Focus on PTEN regulation. Front Oncol. 2015;5(July):1–15.
36. Delgado-Martín B, Medina MÁ. Advances in the Knowledge of the Molecular Biology of Glioblastoma and Its Impact in Patient Diagnosis, Stratification, and Treatment. Adv Sci. 2020;7(9).
37. Louis DN, Perry A, Reifenberger G, von Deimling A, Figarella-Branger D, Cavenee WK, et al. The 2016 World Health Organization Classification of Tumors of the Central Nervous System: a summary. Acta Neuropathol. 2016;131(6):803–20.
38. Oh JE, Ohta T, Nonoguchi N, Satomi K, Capper D, Pierscianek D,

et al. Genetic Alterations in Gliosarcoma and Giant Cell Glioblastoma. Brain Pathol. 2016;26(4):517–22.

39. Lowder L, Hauenstein J, Woods A, Chen HR, Rupji M, Kowalski J, et al. Gliosarcoma: distinct molecular pathways and genomic alterations identified by DNA copy number/SNP microarray analysis. J Neurooncol [Internet]. 2019;143(3):381–92. Available from: https://doi.org/10.1007/s11060-019-03184-1

40. Broniscer A, Tatevossian RG, Sabin ND, Klimo J, Dalton J, Lee R, et al. Clinical, radiological, histological and molecular characteristics of paediatric epithelioid glioblastoma. Neuropathol Appl Neurobiol. 2014;40(3):327–36.

41. Alexandrescu S, Korshunov A, Lai SH, Dabiri S, Patil S, Li R, et al. Epithelioid glioblastomas and anaplastic epithelioid pleomorphic xanthoastrocytomas - Same entity or first cousins? Brain Pathol. 2016;26(2):215–23.

42. Verbeek B, Southgate TD, Gilham DE, Margison GP. O6-Methylguanine-DNA methyltransferase inactivation and chemotherapy. Br Med Bull. 2008;85(1):17–33.

43. Alfardus H, de los Angeles Estevez Cebrero M, Rowlinson J, Lourdusamy A, Grundy R, Mcintyre A, et al. Microrna Analysis of the Invasive Margin of Glioblastoma Reveals Druggable Therapeutic Targets in Lipid Metabolism Pathways. Neuro Oncol. 2018;20(suppl_5):v348–v348.

44. Thakkar JP, Dolecek TA, Horbinski C, Ostrom QT, Lightner DD, Barnholtz-Sloan JS, et al. Epidemiologic and molecular

prognostic review of glioblastoma. Cancer Epidemiol Biomarkers Prev. 2014;23(10):1985–96.

45. Ohgaki H. Epidemiology of Brain Tumours. In: Cancer Epidemiology. Humana Press; 2009. p. 323–43.

46. Tamimi AF, Juweid M. Epidemiology and Outcome of Glioblastoma. In: Glioblastoma. Codon Publications; 2017. p. 143–53.

47. Ohgaki H, Kleihues P. Population-based studies on incidence, survival rates, and genetic alterations in astrocytic and oligodendroglial gliomas. J Neuropathol Exp Neurol. 2005;64(6):479–89.

48. Bastiancich C, Danhier P, Préat V, Danhier F. Anticancer drug-loaded hydrogels as drug delivery systems for the local treatment of glioblastoma. J Control Release [Internet]. 2016;243:29–42. Available from: http://dx.doi.org/10.1016/j.jconrel.2016.09.034

49. Delgado-López PD, Corrales-García EM. Survival in glioblastoma: a review on the impact of treatment modalities. Clin Transl Oncol. 2016;18(11):1062–71.

50. Delgado-López PD, Corrales-García EM, Martino J, Lastra-Aras E, Dueñas-Polo MT. Diffuse low-grade glioma: a review on the new molecular classification, natural history and current management strategies. Clin Transl Oncol. 2017;19(8):931–44.

51. Ricard D, Idbaih A, Ducray F, Lahutte M, Hoang-Xuan K, Delattre JY. Primary brain tumours in adults. Lancet [Internet]. 2012;379(9830):1984–96. Available from:

http://dx.doi.org/10.1016/S0140-6736(11)61346-9

52. Arita H, Matsushita Y, Machida R, Yamasaki K, Hata N, Ohno M, et al. TERT promoter mutation confers favorable prognosis regardless of 1p/19q status in adult diffuse gliomas with IDH1/2 mutations. Acta Neuropathol Commun [Internet]. 2020;8(1):1–11. Available from: https://doi.org/10.1186/s40478-020-01078-2

53. Jooma R, Waqas M, Khan I. Diffuse low-grade glioma – Changing concepts in diagnosis and management: A review. Asian J Neurosurg. 2019;14(2):356.

54. Duffau H, Taillandier L. New concepts in the management of diffuse low-grade glioma: Proposal of a multistage and individualized therapeutic approach. Neuro Oncol. 2015;17(3):332–42.

55. Bush NAO, Chang S. Treatment strategies for low-grade glioma in adults. J Oncol Pract. 2016;12(12):1235–41.

56. Nikitović M, Stanić D, Pekmezović T, Gazibara MS, Bokun J, Paripović L, et al. Pediatric glioblastoma: a single institution experience. Child's Nerv Syst. 2016;32(1):97–103.

57. Das KK, Mehrotra A, Nair AP, Kumar S, Srivastav AK, Sahu RN, et al. Pediatric glioblastoma: Clinico-radiological profile and factors affecting the outcome. Child's Nerv Syst. 2012;28(12):2055–62.

58. Suri V, Das P, Jain A, Sharma MC, Borkar SA, Suri A, et al. Pediatric glioblastomas: A histopathological and molecular genetic study. Neuro Oncol. 2009;11(3):274–80.

59. MacDonald T., Aguilera D, Kramm CM. Treatment of high-grade glioma in children and Adolescents. Neuro Oncol. 2011;13(10):1049–58.

60. Bar EE. Glioblastoma, cancer stem cells and hypoxia. Brain Pathol. 2011;21(2):119–29.

61. Evans SM, Judy KD, Dunphy I, Timothy Jenkins W, Hwang WT, Nelson PT, et al. Hypoxia is important in the biology and aggression of human glial brain tumors. Clin Cancer Res. 2004;10(24):8177–84.

62. Geoerger B, Hahn SM, Jenkins K, Stevens CW, Collins R, Koch CJ, et al. Comparative Measurements of Hypoxia in Human Brain Tumors Using Needle Electrodes and EF5 Binding. Cancer Res [Internet]. 2005;64(5):1886–92. Available from: http://www.ncbi.nlm.nih.gov/pubmed/14996753%0Ahttp://cancerres.aacrjournals.org/lookup/doi/10.1158/0008-5472.CAN-03-2424

63. Brahimi-Horn MC, Chiche J, Pouysségur J. Hypoxia and cancer. J Mol Med. 2007;85(12):1301–7.

64. Nyga A, Cheema U, Loizidou M. 3D tumour models : novel in vitro approaches to cancer studies. J Cell Commun Signal. 2011;5(3):239–48.

65. Merighi S, Benini A, Mirandola P, Gessi S, Varani K, Leung E, et al. Hypoxia Inhibits Paclitaxel-Induced Apoptosis through Adenosine-Mediated Phosphorylation of Bad in Glioblastoma Cells. Mol Pharmacol. 2007;72(1):162–72.

66. Padhani AR, Krohn KA, Lewis JS, Alber M. Imaging oxygenation

of human tumours. Eur Radiol. 2007;17(4):861–72.

67. Denko NC. Hypoxia, HIF1 and glucose metabolism in the solid tumour. Nat Commun. 2008;8(9):705–13.

68. Zagzag D, Lukyanov Y, Lan L, Ali MA, Esencay M, Mendez O, et al. Hypoxia-inducible factor 1 and VEGF upregulate CXCR4 in glioblastoma : implications for angiogenesis and glioma cell invasion. Nature. 2006;86(12):1221–32.

69. Yang L, Lin C, Wang L, Guo H, Wang X. Hypoxia and hypoxia-inducible factors in glioblastoma multiforme progression and therapeutic implications. Exp Cell Res [Internet]. 2012;318(19):2417–26. Available from: http://dx.doi.org/10.1016/j.yexcr.2012.07.017

70. Brown JM. Exploiting the hypoxic cancer cell : mechanisms and therapeutic strategies. Mol Med Today. 2000;6(4):157–62.

71. Semenza GL. Regulation of physiological responses to continuous and intermittent hypoxia by hypoxia-inducible factor 1. Exp Physiol. 2006;91(5):803–6.

72. Seagroves T, Johnson RS. Two HIFs may be better than one. Vol. 1, Cancer Cell. 2002. p. 211–3.

73. McLendon RE, Rich JN. Glioblastoma stem cells: A neuropathologist’s view. J Oncol. 2011;2011.

74. Zhao J, Du F, Luo Y, Shen G, Zheng F, Xu B. The emerging role of hypoxia-inducible factor-2 involved in chemo/radioresistance in solid tumors. Cancer Treat Rev [Internet]. 2015;41(7):623–33. Available from: http://dx.doi.org/10.1016/j.ctrv.2015.05.004

75. Keunen O, Johansson M, Oudin A, Sanzey M, Abdul SA, Fack F. Anti-VEGF treatment reduces blood supply and increases tumor cell invasion in glioblastoma. Proc Natl Acad Sci. 2011;108(9):3749–54.

76. Pore N, Gupta AK, Cerniglia GJ, Maity A. HIV Protease Inhibitors Decrease VEGF/HIF-1α Expression and Angiogenesis in Glioblastoma Cells. Neoplasia [Internet]. 2006;8(11):889–95. Available from: http://dx.doi.org/10.1593/neo.06535

77. Jensen RL, Ragel BT, Whang K, Gillespie D. Inhibition of hypoxia inducible factor-1α (HIF-1α) decreases vascular endothelial growth factor (VEGF) secretion and tumor growth in malignant gliomas. J Neurooncol. 2006;78(3):233–47.

78. Rumsey WL, Vanderkooi JM, Wilson DF. Imaging of phosphorescence: A novel method for measuring oxygen distribution in perfused tissue. Science (80-). 1988;241(4873):1649–51.

79. Clark LC, Wolf R, Granger D, Taylor Z. Contimozls Recording of Blood Oxygen Tensions by Pohzroognz~hyl. 1953;18:20. Available from: www.physiology.org/journal/jappl

80. Keeley TP, Mann GE. Defining Physiological Normoxia for Improved Translation of Cell Physiology to Animal Models and Humans. Physiol Rev. 2018;99(1):161–234.

81. Corroyer-Dulmont A, Chakhoyan A, Collet S, Durand L, MacKenzie ET, Petit E, et al. Imaging Modalities to Assess Oxygen Status in Glioblastoma. Front Med. 2015;2(August).

82. Bruehlmeier M, Roelcke U, Schubiger P a, Ametamey SM. Assessment of Hypoxia and Perfusion in Human Brain Tumors Using PET with 18F-Fluoromisonidazole and 15O-H2O. J Nucl Med. 2004;45:1851–9.

83. Mendichovszky I, Jackson A. Imaging hypoxia in gliomas. Br J Radiol. 2011;84(SPEC. ISSUE 2):145–58.

84. Lewis JS, McCarthy DW, McCarthy TJ, Fujibayashi Y, Welch MJ. Evaluation of 64Cu-ATSM in vitro and in vivo in a hypoxic tumor model. J Nucl Med [Internet]. 1999;40(1):177–83. Available from: http://www.ncbi.nlm.nih.gov/pubmed/9935074

85. Shibahara I, Kumabe T, Kanamori M, Saito R, Sonoda Y, Watanabe M, et al. Imaging of hypoxic lesions in patients with gliomas by using positron emission tomography with 1-(2-[18F] fluoro-1-[hydroxymethyl]ethoxy)methyl-2-nitroimidazole, a new 18F-labeled 2-nitroimidazole analog. J Neurosurg. 2009;113(2):358–68.

86. Linnik I V., Scott MLJ, Holliday KF, Woodhouse N, Waterton JC, O'Connor JPB, et al. Noninvasive tumor hypoxia measurement using magnetic resonance imaging in murine U87 glioma xenografts and in patients with glioblastoma. Magn Reson Med. 2014;71(5):1854–62.

87. Jensen RL, Mumert ML, Gillespie DL, Kinney AY, Schabel MC, Salzman KL. Preoperative dynamic contrast-enhanced MRI correlates with molecular markers of hypoxia and vascularity in specific areas of intratumoral microenvironment and is predictive

of patient outcome. Neuro Oncol. 2014;16(2):280–91.

88. Dunn JF, O'Hara JA, Zaim-Wadghiri Y, Lei H, Meyerand ME, Grinberg OY, et al. Changes in oxygenation of intracranial tumors with carbogen: A BOLD MRI and EPR oximetry study. J Magn Reson Imaging. 2002;16(5):511–21.

89. Evans SM, Jenkins KW, Chen HI, Jenkins WT, Judy KD, Hwang W-T, et al. The Relationship among Hypoxia, Proliferation, and Outcome in Patients with De Novo Glioblastoma: A Pilot Study. Transl Oncol. 2010;3(3):160–9.

90. Wijffels KIEM, Kaanders JHAM, Rijken PFJW, Bussink J, van den Hoogen FJA, Marres HAM, et al. Vascular architecture and hypoxic profiles in human head and neck squamous cell carcinomas. Br J Cancer. 2002;83(5):674–83.

91. Arteel GE, Thurman RG, Raleigh JA. Reductive metabolism of the hypoxia marker pimonidazole is regulated by oxygen tension independent of the pyridine nucleotide redox state. Eur J Biochem. 1998;253(3):743–50.

92. Raleigh JA, Chou SC, Calkins-Adams DP, Ballenger CA, Novotny DB, Varia MA. A clinical study of hypoxia and metallothionein protein expression in squamous cell carcinomas. Clin Cancer Res. 2000;6(3):855–62.

93. Kolenda J, Jensen SS, Aaberg-Jessen C, Christensen K, Andersen C, Brünner N, et al. Effects of hypoxia on expression of a panel of stem cell and chemoresistance markers in glioblastoma-derived spheroids. J Neurooncol. 2011;103(1):43–

58.

94. Vordermark D, Brown JM. Endogenous Markers of Tumor Hypoxia: Predictors of Clinical Radiation Resistance? Strahlentherapie und Onkol. 2003;179(12):801–11.

95. Supuran CT. Carbonuc anhydrases: catalytic and inhibition mechanisms, distribution and physiological roles. Carbon Anhydrase. 2004;13–36.

96. Potter C, Harris AL. Hypoxia inducible carbonic anhydrase IX, marker of tumour hypoxia, survival pathway and therapy target. Cell Cycle. 2004;3(2):164–7.

97. Thiry A, Dogné JM, Masereel B, Supuran CT. Targeting tumor-associated carbonic anhydrase IX in cancer therapy. Trends Pharmacol Sci. 2006;27(11):566–73.

98. Lal A, Peters H, St B, Haroon ZA, Mark W, Strausberg RL, et al. Transcriptional Response to Hypoxia in Human Tumors Background : The presence of hypoxic regions within solid tumors is associ- AND Serial Analysis of Gene Expression. J Natl Cancer Inst. 2001;93(17):1337–43.

99. Beasley NJP, Wykoff CC, Watson PH, Leek R, Turley H, Gatter K, et al. Carbonic Anhydrase IX, an Endogenous Hypoxia Marker, Expression in Head and Neck Squamous Cell Carcinoma and its Relationship to Hypoxia, Necrosis, and Microvessel Density. Cancer Res [Internet]. 2001;61(13):5262–7. Available from: http://cancerres.aacrjournals.org/content/61/13/5262.abstract

100. Wykoff CC, Beasley NJP, Watson PH, Turner KJ, Pastorek J,

Sibtain A, et al. Hypoxia-inducible expression of tumor-associated carbonic anhydrases. Cancer Res. 2000;60(24):7075–83.

101. Olive PL, Aquino-Parsons C, MacPhail SH, Liao SY, Stanbridge EJ, Raleigh JA, et al. Carbonic anhydrase 9 as an endogenous marker for hypoxic cells in cervical cancer. Cancer Res. 2001;61(24):8924–9.
102. Vaupel P, Mayer A. Hypoxia in cancer: Significance and impact on clinical outcome. Cancer Metastasis Rev. 2007;26(2):225–39.
103. Visone R, Croce CM. MiRNAs and cancer. Am J Pathol [Internet]. 2009;174(4):1131–8. Available from: http://dx.doi.org/10.2353/ajpath.2009.080794
104. Zhang L, Huang J, Yang N, Greshock J, Megraw MS, Giannakakis A, et al. MicroRNAs exhibit high frequency genomic alterations in human cancer. Proc Natl Acad Sci. 2006;103(24).
105. Lujambio A, Calin GA, Villanueva A, Ropero S, Blanco D, Montuenga LM, et al. A microRNA DNA methylation signature for human cancer metastasis. Proc Natl Acad Sci [Internet]. 2008;105(36):6. Available from: papers2://publication/uuid/11CFE67C-A5E9-4961-BE59-8A8DC7C5B622
106. O'Brien J, Hayder H, Zayed Y, Peng C. Overview of microRNA biogenesis, mechanisms of actions, and circulation. Front Endocrinol (Lausanne). 2018;9(AUG):1–12.
107. Ghildiyal M, Zamore PD. Small silencing RNAs: An expanding universe. Nat Rev Genet. 2009;10(2):94–108.

108. Yang JS, Lai EC. Alternative miRNA Biogenesis Pathways and the Interpretation of Core miRNA Pathway Mutants. Mol Cell [Internet]. 2011;43(6):892–903. Available from: http://dx.doi.org/10.1016/j.molcel.2011.07.024

109. Lee Y, Kim M, Han J, Yeom KH, Lee S, Baek SH, et al. MicroRNA genes are transcribed by RNA polymerase II. EMBO J. 2004;23(20):4051–60.

110. Ha M, Kim VN. Regulation of microRNA biogenesis. Nat Rev Mol Cell Biol [Internet]. 2014;15(8):509–24. Available from: http://www.ncbi.nlm.nih.gov/pubmed/25027649

111. Shenoy A, Blelloch R. Genomic Analysis Suggests that mRNA Destabilization by the Microprocessor Is Specialized for the Auto-Regulation of Dgcr8. PLoS One. 2009;4(9).

112. Lee Y, Ahn C, Han J, Choi H, Kim J, Yim J, et al. The nuclear RNase III Drosha initiates microRNA processing. 2003;425(September):1–5.

113. Lee Y, Jeon K, Lee J, Kim S, Kim VN. MicroRNA maturation: stepwise processing and subcellular localisation. EMBO J. 2002;21(17):4663–70.

114. Bohnsack MT, Czaplinski K, Go D. Exportin 5 is a RanGTP-dependent dsRNA-binding protein that mediates nuclear export of pre-miRNAs. 2004;185–91.

115. Park J, Heo I, Tian Y, Simanshu DK, Chang H, Jee D, et al. Dicer recognizes the 5 9 end of RNA for efficient and accurate processing. Nature [Internet]. 2011;475(7355):201–5. Available

from: http://dx.doi.org/10.1038/nature10198

116. Zhang H, Kolb FA, Jaskiewicz L, Westhof E, Filipowicz W. Single processing center models for human Dicer and bacterial RNase III. Cell. 2004;118(1):57–68.

117. Watson J, Khaled AR, Wyllie AH, Zha J, Vanderheiden MG, Liu A, et al. A Cellular Function for the RNA-Interference Enzyme Dicer in the Maturation of the let-7 Small Temporal RNA. Science (80-). 2001;293(August):834–9.

118. Hammond SM, Boettcher S, Caudy AA, Kobayashi R, Hannon GJ. Argonaute2 , a Link Between Genetic and Biochemical Analyses of RNAi. Science (80-). 2001;293(August):1146–51.

119. Gregory RI, Chendrimada TP, Cooch N, Shiekhattar R. Human RISC Couples MicroRNA Biogenesis and Posttranscriptional Gene Silencing. Cell. 2005;123:631–40.

120. Khvorova A, Reynolds A, Jayasena SD. Functional siRNAs and miRNAs Exhibit Strand Bias. Cell. 2003;115:209–16.

121. Martinez J, Patkaniowska A, Urlaub H, Lu R, Tuschl T. Single-Stranded Antisense siRNAs Guide Target RNA Cleavage in RNAi. Cell. 2002;110:563–74.

122. Jo MH, Shin S, Jung SR, Kim E, Song JJ, Hohng S. Human Argonaute 2 Has Diverse Reaction Pathways on Target RNAs. Mol Cell [Internet]. 2015;59(1):117–24. Available from: http://dx.doi.org/10.1016/j.molcel.2015.04.027

123. Krützfeldt J, Rajewsky N, Braich R, Rajeev KG, Tuschl T, Manoharan M, et al. Silencing of microRNAs in vivo with

"antagomirs." Nature. 2005;438(7068):685–9.

124. Jungers CF, Djuranovic S. Modulation of miRISC-Mediated Gene Silencing in Eukaryotes. Front Mol Biosci. 2022;9(February):1–14.
125. Nishihara T, Zekri L, Braun JE, Izaurralde E. MiRISC recruits decapping factors to miRNA targets to enhance their degradation. Nucleic Acids Res. 2013;41(18):8692–705.
126. Vasudevan S, Steitz JA. AU-Rich-Element-Mediated Upregulation of Translation by FXR1 and Argonaute 2. Cell. 2007;128(6):1105–18.
127. Ørom UA, Nielsen FC, Lund AH. MicroRNA-10a Binds the 5′UTR of Ribosomal Protein mRNAs and Enhances Their Translation. Mol Cell. 2008;30(4):460–71.
128. Shea A, Harish V, Afzal Z, Chijioke J, Kedir H, Dusmatova S, et al. MicroRNAs in glioblastoma multiforme pathogenesis and therapeutics. Cancer Med. 2016;5(8):1917–46.
129. Cosset E, Petty T, Dutoit V, Tirefort D, Otten-Hernandez P, Farinelli L, et al. Human tissue engineering allows the identification of active miRNA regulators of glioblastoma aggressiveness. Biomaterials [Internet]. 2016;107:74–87. Available from: http://dx.doi.org/10.1016/j.biomaterials.2016.08.009
130. Hwang HW, Mendell JT. MicroRNAs in cell proliferation, cell death, and tumorigenesis. Br J Cancer. 2006;94(6):776–80.
131. He L, Thomson JM, Hemann MT, Hernando-Monge E, Mu D, Goodson S, et al. A microRNA polycistron as a potential human

oncogene. Nature. 2005;435(7043):828–33.

132. Takamizawa J, Nagino, MasatoKonishi H, Endoh H, Osada H, Harano T, Tomida S, et al. Reduced Expression of the let-7 MicroRNAs in Human Lung Cancers in Association with Shortened Postoperative Survival. Cancer Res [Internet]. 2005;64(11):3753–6. Available from: http://www.ncbi.nlm.nih.gov/pubmed/15172979%0Ahttp://cancerres.aacrjournals.org/lookup/doi/10.1158/0008-5472.CAN-04-0637

133. Chan JA, Krichevsky AM, Kosik KS. MicroRNA-21 is an antiapoptotic factor in human glioblastoma cells. Cancer Res [Internet]. 2005;65(14):6029–33. Available from: http://www.ncbi.nlm.nih.gov/pubmed/16024602

134. Masoudi MS, Mehrabian E, Mirzaei H. MiR-21: A key player in glioblastoma pathogenesis. J Cell Biochem. 2018;119(2):1285–90.

135. Rezaei O, Honarmand K, Nateghinia S, Taheri M, Ghafouri-Fard S. miRNA signature in glioblastoma: Potential biomarkers and therapeutic targets. Exp Mol Pathol [Internet]. 2020;117(September):104550. Available from: https://doi.org/10.1016/j.yexmp.2020.104550

136. Gabriely G, Yi M, Narayan RS, Niers JM, Wurdinger T, Imitola J, et al. Human glioma growth is controlled by microRNA-10b. Cancer Res. 2011;71(10):3563–72.

137. Chen Y, Li R, Pan M, Shi Z, Yan W, Liu N, et al. MiR-181b modulates chemosensitivity of glioblastoma multiforme cells to

temozolomide by targeting the epidermal growth factor receptor. J Neurooncol. 2017;133(3):477–85.

138. Zhang X, Yu J, Zhao C, Ren H, Yuan Z, Zhang B, et al. MiR-181b-5p modulates chemosensitivity of glioma cells to temozolomide by targeting Bcl-2. Biomed Pharmacother [Internet]. 2019;109(August 2018):2192–202. Available from: https://doi.org/10.1016/j.biopha.2018.11.074
139. Guessous F, Zhang Y, Kofman A, Catania A, Li Y, Schiff D, et al. microRNA-34a is tumor suppressive in brain tumors and glioma stem cells. Cell Cycle. 2010;9(6):1031–6.
140. Wang Y, Wang L. miR-34a attenuates glioma cells progression and chemoresistance via targeting PD-L1. Biotechnol Lett. 2017;39(10):1485–92.
141. Huang X, Ding L, Bennewith KL, Tong RT, Welford SM, Ang KK, et al. Hypoxia-Inducible mir-210 Regulates Normoxic Gene Expression Involved in Tumor Initiation. Mol Cell [Internet]. 2009;35(6):856–67. Available from: http://dx.doi.org/10.1016/j.molcel.2009.09.006
142. Huang X, Le QT, Giaccia AJ. MiR-210 - micromanager of the hypoxia pathway. Trends Mol Med [Internet]. 2010;16(5):230–7. Available from: http://dx.doi.org/10.1016/j.molmed.2010.03.004
143. Chang W, Lee CY, Park JH, Park MS, Maeng LS, Yoon CS, et al. Survival of hypoxic human mesenchymal stem cells is enhanced by a positive feedback loop involving mir-210 and hypoxia-inducible factor 1. J Vet Sci. 2013;14(1):69–76.

144. Dang K, Myers KA. The role of hypoxia-induced miR-210 in cancer progression. Int J Mol Sci. 2015;16(3):6353–72.
145. Crosby ME, Kulshreshtha R, Ivan M, Glazer PM. MicroRNA regulation of DNA repair gene expression in hypoxic stress. Cancer Res. 2009;69(3):1221–9.
146. Feng Z, Scott SP, Bussen W, Sharma GG, Guo G, Pandita TK, et al. Rad52 inactivation is synthetically lethal with BRCA2 deficiency. Proc Natl Acad Sci U S A. 2011;108(2):686–91.
147. Devlin C, Greco S, Martelli F, Ivan M. MiR-210: More than a silent player in hypoxia. IUBMB Life. 2011;63(2):94–100.
148. Yang W, Sun T, Cao J, Liu F, Tian Y, Zhu W. Downregulation of miR-210 expression inhibits proliferation, induces apoptosis and enhances radiosensitivity in hypoxic human hepatoma cells in vitro. Exp Cell Res [Internet]. 2012;318(8):944–54. Available from: http://dx.doi.org/10.1016/j.yexcr.2012.02.010
149. Cui H, Grosso S, Schelter F, Mari B, Krüger A. On the pro-metastatic stress response to cancer therapies: Evidence for a positive co-operation between TIMP-1, HIF-1α, and miR-210. Front Pharmacol. 2012;3 JUL(July):1–6.
150. Huang S wei, Ali N da, Zhong L, Shi J. MicroRNAs as biomarkers for human glioblastoma: progress and potential. Acta Pharmacol Sin. 2018;39(9):1405–13.
151. Ahir BK, Ozer H, Engelhard HH, Lakka SS. MicroRNAs in glioblastoma pathogenesis and therapy: A comprehensive review. Crit Rev Oncol Hematol [Internet]. 2017;120(October):22–33.

Available from: https://doi.org/10.1016/j.critrevonc.2017.10.003

152. Gao YT, Chen XB, Liu HL. Up-regulation of miR-370-3p restores glioblastoma multiforme sensitivity to temozolomide by influencing MGMT expression. Sci Rep. 2016;6(August):1–9.

153. Guo X, Luo Z, Xia T, Wu L, Shi Y, Li Y. Identification of miRNA signature associated with BMP2 and chemosensitivity of TMZ in glioblastoma stem-like cells. Genes Dis [Internet]. 2020;7(3):424–39. Available from: https://doi.org/10.1016/j.gendis.2019.09.002

154. Zhao C, Guo R, Guan F, Ma S, Li M, Wu J, et al. MicroRNA-128-3p Enhances the Chemosensitivity of Temozolomide in Glioblastoma by Targeting c-Met and EMT. Sci Rep. 2020;10(1):1–12.

155. Shatsberg Z, Zhang X, Ofek P, Malhotra S, Krivitsky A, Scomparin A, et al. Functionalized nanogels carrying an anticancer microRNA for glioblastoma therapy. J Control Release [Internet]. 2016;239:159–68. Available from: http://dx.doi.org/10.1016/j.jconrel.2016.08.029

156. Jiang G, Chen H, Huang J, Song Q, Chen Y, Gu X, et al. Tailored Lipoprotein-Like miRNA Delivery Nanostructure Suppresses Glioma Stemness and Drug Resistance through Receptor-Stimulated Macropinocytosis. Adv Sci. 2020;7(5).

157. Ofek P, Calderón M, Mehrabadi FS, Krivitsky A, Ferber S, Tiram G, et al. Restoring the oncosuppressor activity of microRNA-34a in glioblastoma using a polyglycerol-based polyplex. Nanomedicine Nanotechnology, Biol Med [Internet].

2016;12(7):2201–14. Available from: http://dx.doi.org/10.1016/j.nano.2016.05.016

158. Czauderna F, Fechtner M, Dames S, Aygün H, Klippel A, Pronk GJ, et al. Structural variations and stabilising modifications of synthetic siRNAs in mammalian cells. Nucleic Acids Res. 2003;31(11):2705–16.

159. Pottoo FH, Javed MN, Rahman JU, Abu-Izneid T, Khan FA. Targeted delivery of miRNA based therapeuticals in the clinical management of Glioblastoma Multiforme. Semin Cancer Biol [Internet]. 2021;69(April 2020):391–8. Available from: https://doi.org/10.1016/j.semcancer.2020.04.001

160. Fu Q, Zhao Y, Yang Z, Yue Q, Xiao W, Chen Y, et al. Liposomes actively recognizing the glucose transporter GLUT1 and integrin αvβ3 for dual-targeting of glioma. Arch Pharm Weinheim. 2019;352(2).

161. Jacobs VL, Valdes PA, Hickey WF, de Leo JA. Current review of in vivo GBM rodent models: Emphasis on the CNS-1 tumour model. ASN Neuro. 2011;3(3):171–81.

162. Waggott D, Chu K, Yin S, Wouters BG, Liu FF, Boutros PC. NanoStringNorm: An extensible R package for the pre-processing of nanostring mRNA and miRNA data. Bioinformatics. 2012;28(11):1546–8.

163. Wang H, Wang C. The NanoStringDiff package. 2019;17.

164. Li X, Liu Y, Granberg KJ, Wang Q, Moore LM, Ji P, et al. Two mature products of MIR-491 coordinate to suppress key cancer

hallmarks in glioblastoma. Oncogene. 2015;34(13):1619–28.

165. Hoa NN, Shimizu T, Zhou ZW, Wang ZQ, Deshpande RA, Paull TT, et al. Mre11 Is Essential for the Removal of Lethal Topoisomerase 2 Covalent Cleavage Complexes. Mol Cell [Internet]. 2016;64(3):580–92. Available from: http://dx.doi.org/10.1016/j.molcel.2016.10.011

166. Otero-Albiol D, Carnero A. Cellular senescence or stemness: hypoxia flips the coin. J Exp Clin Cancer Res. 2021;40(1):1–20.

167. Welford SM, Giaccia AJ. Hypoxia and senescence: The impact of oxygenation on tumor suppression. Mol Cancer Res. 2011;9(5):538–44.

168. van Wijnen AJ, Bagheri L, Badreldin AA, Larson AN, Dudakovic A, Thaler R, et al. Biological functions of chromobox (CBX) proteins in stem cell self-renewal, lineage-commitment, cancer and development. Bone [Internet]. 2021;143(September 2020):115659. Available from: https://doi.org/10.1016/j.bone.2020.115659

169. Chen Y, Xu S, Liu X, Jiang X, Jiang J. CircSEC24A upregulates TGFBR2 expression to accelerate pancreatic cancer proliferation and migration via sponging to miR-606. Cancer Cell Int [Internet]. 2021;21(1):1–16. Available from: https://doi.org/10.1186/s12935-021-02392-y

170. Lunn M-L, Mouritzen P, Faber K, Jacobsen N. MicroRNA quantitation from a single cell by PCR using SYBR® Green detection and LNA-based primers. Nat Methods. 2008;5(2):iii–iv.

171. Mo B, Wu X, Wang X, Xie J, Ye Z, Li L. miR-30e-5p Mitigates Hypoxia-Induced Apoptosis in Human Stem Cell-Derived Cardiomyocytes by Suppressing Bim. Int J Biol Sci. 2019;15(5):1042–51.
172. Hua X, Chu H, Wang C, Shi X, Wang A, Zhang Z. Targeting USP22 with miR-30-5p to inhibit the hypoxia-induced expression of PD-L1 in lung adenocarcinoma cells. Oncolgy Reports. 2021;46(4).
173. Zhang K, Fu G, Pan G, Li C, Shen L, Hu R, et al. Demethylzeylasteral inhibits glioma growth by regulating the miR-30e-5p/MYBL2 axis. Cell Death Dis. 2018;9(10).
174. Vaitkiene P, Pranckeviciene A, Stakaitis R, Steponaitis G, Tamasauskas A, Bunevicius A. Association of miR-34a expression with quality of life of glioblastoma patients: A prospective study. Cancers (Basel). 2019;11(3):1–11.
175. Wang N, Feng Y, Xu J, Zou J, Chen M, He Y, et al. miR-362-3p regulates cell proliferation, migration and invasion of trophoblastic cells under hypoxia through targeting Pax3. Biomed Pharmacother [Internet]. 2018;99(January):462–8. Available from: https://doi.org/10.1016/j.biopha.2018.01.089
176. Yin CY, Kong WEI, Jiang J, Xu HAO, Zhao WEI. miR-7-5p inhibits cell migration and invasion in glioblastoma through targeting SATB1. Oncol Lett. 2019;17(2):1819–25.
177. Song H, Zhang Y, Liu N, Zhao S, Kong Y, Yuan L. MiR-92a-3p exerts various effects in glioma and glioma stem-like cells

specifically targeting CDH1/β-catenin and notch-1/Akt signaling pathways. Int J Mol Sci. 2016;17(11).

178. Rafat M, Moraghebi M, Afsa M, Malekzadeh K. The outstanding role of miR-132-3p in carcinogenesis of solid tumors. Hum Cell [Internet]. 2021;34(4):1051–65. Available from: https://doi.org/10.1007/s13577-021-00544-w

179. Burek M, König A, Lang M, Fiedler J, Oerter S, Roewer N, et al. Hypoxia-Induced MicroRNA-212/132 Alter Blood-Brain Barrier Integrity Through Inhibition of Tight Junction-Associated Proteins in Human and Mouse Brain Microvascular Endothelial Cells. Transl Stroke Res. 2019;10(6):672–83.

180. Epis MR, Giles KM, Candy PA, Webster RJ, Leedman PJ. MiR-331-3p regulates expression of neuropilin-2 in glioblastoma. J Neurooncol. 2014;116(1):67–75.

181. Chen HH, Zong J, Wang SJ. LncRNA GAPLINC promotes the growth and metastasis of glioblastoma by sponging miR-331-3p. Eur Rev Med Pharmacol Sci. 2019;23(1):262–70.

182. Wang M, Wu Q, Fang M, Huang W, Zhu H. miR-152-3p sensitizes glioblastoma cells towards cisplatin via regulation of SOS1. Onco Targets Ther. 2019;12:9513–25.

183. Tamanini A, Fabbri E, Jakova T, Gasparello J, Manicardi A, Corradini R, et al. A peptide-nucleic acid targeting miR-335-5p enhances expression of cystic fibrosis transmembrane conductance regulator (CFTR) gene with the possible involvement of the CFTR scaffolding protein NHERF1.

Biomedicines. 2021;9(2):1–21.

184. Liu F, Gong J, Huang W, Wang Z, Wang M, Yang J, et al. MicroRNA-106b-5p boosts glioma tumorigensis by targeting multiple tumor suppressor genes. Oncogene. 2014;33(40):4813–22.

185. Shi Y, Zhang B, Zhu J, Huang W, Han B, Wang Q, et al. miR-106b-5p inhibits IRF1/IFN-β signaling to promote M2 macrophage polarization of glioblastoma. Onco Targets Ther. 2020;13:7479–92.

186. Huang W, Shi Y, Han B, Wang Q, Zhang B, Qi C, et al. LncRNA GAS5-AS1 inhibits glioma proliferation, migration, and invasion via miR-106b-5p/TUSC2 axis. Hum Cell [Internet]. 2020;33(2):416–26. Available from: https://doi.org/10.1007/s13577-020-00331-z

187. Chen YY, Ho HL, Lin SC, Ho TDH, Hsu CY. Upregulation of miR-125b, miR-181d, and miR-221 Predicts Poor Prognosis in MGMT Promoter-Unmethylated Glioblastoma Patients. Am J Clin Pathol. 2018;149(5):412–7.

188. Yuan M, Da Silva ACAL, Arnold A, Okeke L, Ames H, Correa-Cerro LS, et al. MicroRNA (miR) 125b regulates cell growth and invasion in pediatric low grade glioma. Sci Rep. 2018;8(1):1–14.

189. Macharia LW, Muriithi W, Heming CP, Nyaga DK, Aran V, Mureithi MW, et al. The genotypic and phenotypic impact of hypoxia microenvironment on glioblastoma cell lines. BMC Cancer. 2021;21(1):1–20.

190. Mutalifu N, Du P, Zhang J, Akbar H, Yan B, Alimu S, et al. Circ_0000215 Increases the Expression of CXCR2 and Promoted the Progression of Glioma Cells by Sponging miR-495-3p. Technol Cancer Res Treat. 2020;19(1984):1–11.
191. Liao K, Qian Z, Zhang S, Chen B, Li Z, Huang R, et al. The LGMN pseudogene promotes tumor progression by acting as a miR-495-3p sponge in glioblastoma. Cancer Lett [Internet]. 2020;490(May):111–23. Available from: https://doi.org/10.1016/j.canlet.2020.07.012
192. Wang P, Yan Q, Liao B, Zhao L, Xiong S, Wang J, et al. The HIF1α/HIF2α-miR210-3p network regulates glioblastoma cell proliferation, dedifferentiation and chemoresistance through EGF under hypoxic conditions. Cell Death Dis [Internet]. 2020;11(11). Available from: http://dx.doi.org/10.1038/s41419-020-03150-0
193. Wang ZQ, Zhang MY, Deng ML, Weng NQ, Wang HY, Wu SX. Low serum level of miR-485-3p predicts poor survival in patients with glioblastoma. PLoS One. 2017;12(9):1–11.
194. Zhao H, Shen J, Hodges TR, Song R, Fuller GN, Heimberger AB. Serum microRNA profiling in patients with glioblastoma: A survival analysis. Mol Cancer. 2017;16(1):1–7.
195. Acanda de la Rocha AM, Gonzalez-Huarriz M, Guruceaga E, Mihelson N, Tejada-Solis S, Diez-Valle R, et al. miR-425-5p, a SOX2 target, regulates the expression of FOXJ3 and RAB31 and promotes the survival of GSCs. Arch Clin Biomed Res. 2020;4(3):221.

196. Saravanan PB, Vasu S, Yoshimatsu G, Darden CM, Wang X, Gu J, et al. Differential expression and release of exosomal miRNAs by human islets under inflammatory and hypoxic stress. Diabetologia. 2019;62(10):1901–14.
197. Shin J, Shim HG, Hwang T, Kim H, Kang SH, Dho YS, et al. Restoration of miR-29b exerts anti-cancer effects on glioblastoma. Cancer Cell Int. 2017;17(1):1–9.
198. Iacona JR, Lutz CS. miR-146a-5p: Expression, regulation, and functions in cancer. Wiley Interdiscip Rev RNA. 2019;10(4):1–22.
199. He Y, Yu D, Zhu L, Zhong S, Zhao J, Tang J. miR-149 in human cancer: A systemic review. J Cancer. 2018;9(2):375–88.
200. Shen L, Sun C, Li Y, Li X, Sun T, Liu C, et al. MicroRNA-199a-3p suppresses glioma cell proliferation by regulating the AKT/mTOR signaling pathway. Tumor Biol. 2015;36(9):6929–38.
201. Zhao JL, Tan B, Chen G, Che XM, Du ZY, Yuan Q, et al. Hypoxia-induced glioma-derived exosomal mirna-199a-3p promotes ischemic injury of peritumoral neurons by inhibiting the mtor pathway. Oxid Med Cell Longev. 2020;2020.
202. Zhang B Le, Dong FL, Guo TW, Gu XH, Huang LY, Gao DS. MiRNAs Mediate GDNF-Induced Proliferation and Migration of Glioma Cells. Cell Physiol Biochem. 2018;44(5):1923–38.
203. Wang Z, Li Z, Fu Y, Han L, Tian Y. MiRNA-130a-3p inhibits cell proliferation, migration, and TMZ resistance in glioblastoma by targeting Sp1. Am J Transl Res. 2019;11(12):7272–85.
204. Xu L, Wu Q, Yan H, Shu C, Fan W, Tong X, et al. Long

noncoding RNA KB-1460A1.5 inhibits glioma tumorigenesis via miR-130a-3p/TSC1/mTOR/YY1 feedback loop. Cancer Lett [Internet]. 2022;525(October 2021):33–45. Available from: https://doi.org/10.1016/j.canlet.2021.10.033

205. Hu M, Fu Q, Jing C, Zhang X, Qin T, Pan Y. LncRNA HOTAIR knockdown inhibits glycolysis by regulating miR-130a-3p/HIF1A in hepatocellular carcinoma under hypoxia. Biomed Pharmacother [Internet]. 2020;125(September 2019):109703. Available from: https://doi.org/10.1016/j.biopha.2019.109703

206. Milani R, Brognara E, Fabbri E, Manicardi A, Corradini R, Finotti A, et al. Targeting miR-155-5p and miR-221-3p by peptide nucleic acids induces caspase-3 activation and apoptosis in temozolomide-resistant T98G glioma cells. Int J Oncol. 2019;55(1):59–68.

207. Litak J, Bogucki J, Petniak A, Kocki J, Rahnama-hezavah M, Roszkowski M, et al. PD-L1/miR-155 Interplay in Pediatric High-Grade Glioma. Brain Sci. 2022;1–9.

208. Robertson ED, Wasylyk C, Ye T, Jung AC, Wasylyk B. The oncogenic microRNA hsa-miR-155-5p targets the transcription factor ELK3 and links it to the hypoxia response. PLoS One. 2014;9(11).

209. Ni W, Xia Y, Bi Y, Wen F, Hu D, Luo L. FoxD2-AS1 promotes glioma progression by regulating miR-185- 5P/HMGA2 axis and PI3K/AKT signaling pathway. Aging (Albany NY). 2019;11(5):1427–39.

210. Gu J, Shi JZ, Wang YX, Liu L, Wang SB, Sun JT, et al. LncRNA FAF attenuates hypoxia/ischaemia-induced pyroptosis via the miR-185-5p/PAK2 axis in cardiomyocytes. J Cell Mol Med. 2022;26(10):2895–907.
211. Lee H, Shin CH, Kim HR, Choi KH, Kim HH. MicroRNA-296-5p promotes invasiveness through downregulation of nerve growth factor receptor and caspase-8. Mol Cells. 2017;40(4):254–61.
212. Alrfaei BM, Clark P, Vemuganti R, Kuo JS. MicroRNA miR-100 Decreases Glioblastoma Growth by Targeting SMARCA5 and ErbB3 in Tumor-Initiating Cells. Technol Cancer Res Treat. 2020;19:1–13.
213. Zheng H, Sun Y, Shu X, Gao Q, Chen X. Overexpression of microRNA-100-5p attenuates the endothelial cell dysfunction by targeting HIPK2 under hypoxia and reoxygenation treatment. J Mol Histol [Internet]. 2021;52(5):1115–25. Available from: https://doi.org/10.1007/s10735-021-10002-4
214. Krell A, Wolter M, Stojcheva N, Hertler C, Liesenberg F, Zapatka M, et al. MiR-16-5p is frequently down-regulated in astrocytic gliomas and modulates glioma cell proliferation, apoptosis and response to cytotoxic therapy. Neuropathol Appl Neurobiol. 2019;45(5):441–58.
215. Kurogi R, Nakamizo A, Suzuki SO, Mizoguchi M, Yoshimoto K, Amano T, et al. Inhibition of glioblastoma cell invasion by hsa-miR-145-5p and hsa-miR-31-5p co-overexpression in human mesenchymal stem cells. J Neurosurg. 2019;130(1):44–55.

216. Wu D, Chen T, Zhao X, Huang D, Huang J, Huang Y, et al. HIF1α-SP1 interaction disrupts the circ-0001875/miR-31-5p/SP1 regulatory loop under a hypoxic microenvironment and promotes non-small cell lung cancer progression. J Exp Clin Cancer Res [Internet]. 2022;41(1):1–22. Available from: https://doi.org/10.1186/s13046-022-02336-y

217. Wang J, Quan Y, Lv J, Gong S, Dong D. BRD4 promotes glioma cell stemness via enhancing miR-142-5p-mediated activation of Wnt/β-catenin signaling. Environ Toxicol. 2020;35(3):368–76.

218. Zhan L, Lei S, Li W, Zhang Y, Wang H, Shi Y, et al. Suppression of microRNA-142-5p attenuates hypoxia-induced apoptosis through targeting SIRT7. Biomed Pharmacother [Internet]. 2017;94:394–401. Available from: http://dx.doi.org/10.1016/j.biopha.2017.07.083

219. Salmani T, Ghaderian SMH, Hajiesmaeili M, Rezaeimirghaed O, Hoseini MS, Rakhshan A, et al. Hsa-miR-27a-3p and epidermal growth factor receptor expression analysis in glioblastoma FFPE samples. Asia Pac J Clin Oncol. 2021;17(5):e185–90.

220. Xu H, Shen J, Xie L. Effect of miR-148b-3p on invasion and migration of glioma cells by regulating Wnt signaling pathway. Chinese J Oncol. 2020;42(7):565–9.

221. Chen L, Chen XR, Chen FF, Liu Y, Li P, Zhang R, et al. MicroRNA-107 inhibits U87 glioma stem cells growth and invasion. Cell Mol Neurobiol. 2013;33(5):651–7.

222. Yamakuchi M, Lotterman CD, Bao C, Hruban RH, Karim B,

Mendell JT, et al. P53-induced microRNA-107 inhibits HIF-1 and tumor angiogenesis. Proc Natl Acad Sci U S A. 2010;107(14):6334–9.

223. Wang G, Li Y, Li J, Zhang D, Luo C, Zhang B, et al. microRNA-199a-5p suppresses glioma progression by inhibiting MAGT1. J Cell Biochem. 2019;120(9):15248–54.
224. Raimondi L, Amodio N, di Martino MT, Altomare E, Leotta M, Caracciolo D, et al. Targeting of multiple myeloma-related angiogenesis by miR-199a-5p mimics: In vitro and in vivo anti-tumor activity. Oncotarget. 2014;5(10):3039–54.
225. Wang Z, Wang X, Cheng F, Wen X, Feng S, Yu F, et al. Rapamycin inhibits glioma cells growth and promotes autophagy by miR-26a-5p/DAPK1 axis. Cancer Manag Res. 2021;13:2691–700.
226. Yan G, Wang J, Fang Z, Yan S, Zhang Y. MiR-26a-5p targets WNT5A to protect cardiomyocytes from injury due to hypoxia/reoxygenation through the wnt/β-catenin signaling pathway. Int Heart J. 2021;62(5):1145–52.
227. Wang J, Chen C, Yan X, Wang P. The role of miR-382-5p in glioma cell proliferation, migration and invasion. Onco Targets Ther. 2019;12:4993–5002.
228. Seok JK, Lee SH, Kim MJ, Lee YM. MicroRNA-382 induced by HIF-1α is an angiogenic miR targeting the tumor suppressor phosphatase and tensin homolog. Nucleic Acids Res. 2014;42(12):8062–72.

229. Wen X, Li S, Guo M, Liao H, Chen Y, Kuang X, et al. miR-181a-5p inhibits the proliferation and invasion of drug-resistant glioblastoma cells by targeting F-box protein 11 expression. Oncol Lett. 2020;20(5):1–9.
230. Marisetty A, Wei J, Kong LY, Ott M, Fang D, Sabbagh A, et al. Mir-181 family modulates osteopontin in glioblastoma multiforme. Cancers (Basel). 2020;12(12):1–16.
231. Meng X, Deng Y, Lv Z, Liu C, Guo Z, Li Y, et al. LncRNA SNHG5 promotes proliferation of glioma by regulating mir-205-5p/ZEB2 axis. Onco Targets Ther. 2019;12:11487–96.
232. Wang X, Yu M, Zhao K, He M, Ge W, Sun Y, et al. Upregulation of miR-205 under hypoxia promotes epithelial–mesenchymal transition by targeting ASPP2. Cell Death Dis. 2016;7(12).
233. Chen XR, Zhang YG, Wang Q. miR-9-5p Mediates ABCC1 to Elevate the Sensitivity of Glioma Cells to Temozolomide. Front Oncol. 2021;11(August):1–7.
234. Cai X, Li B, Wang Y, Zhu H, Zhang P, Jiang P, et al. CircJARID2 Regulates Hypoxia-Induced Injury in H9c2 Cells by Affecting miR-9-5p-Mediated BNIP3. J Cardiovasc Pharmacol. 2021;78(1):E77–85.
235. Yi B, Li H, Cai H, Lou X, Yu M, Li Z. LOXL1-AS1 communicating with TIAR modulates vasculogenic mimicry in glioma via regulation of the miR-374b-5p/MMP14 axis. J Cell Mol Med. 2022;26(2):475–90.
236. Toda H, Seki N, Kurozumi S, Shinden Y, Yamada Y, Nohata N, et

al. RNA-sequence-based microRNA expression signature in breast cancer: tumor-suppressive miR-101-5p regulates molecular pathogenesis. Mol Oncol. 2020;14(2):426–46.

237. Qin N, Tong GF, Sun LW, Xu XL. Long noncoding RNA MEG3 suppresses glioma cell proliferation, migration, and invasion by acting as a competing endogenous RNA of miR-19a. Oncol Res. 2017;25(9):1471–8.

238. Fu Q, Mo TR, Hu XY, Fu Y, Li J. miR-19a mitigates hypoxia/reoxygenation-induced injury by depressing CCL20 and inactivating MAPK pathway in human embryonic cardiomyocytes. Biotechnol Lett. 2021;43(2):393–405.

239. Wong HKA, Fatimy R El, Onodera C, Wei Z, Yi M, Mohan A, et al. The cancer genome atlas analysis predicts MicroRNA for targeting cancer growth and vascularization in glioblastoma. Mol Ther [Internet]. 2015;23(7):1234–47. Available from: http://dx.doi.org/10.1038/mt.2015.72

240. Wu H, Liu L, Zhu JM. MIR-93-5p inhibited proliferation and metastasis of glioma cells by targeting MMP2. Eur Rev Med Pharmacol Sci. 2019;23(21):9517–24.

241. Wu Y, Wu M, Yang J, Li Y, Peng W, Wu M, et al. Silencing CircHIPK3 Sponges miR-93-5p to Inhibit the Activation of Rac1/PI3K/AKT Pathway and Improves Myocardial Infarction-Induced Cardiac Dysfunction. Front Cardiovasc Med. 2021;8(April):1–12.

242. Xue J, Yang M, Hua LH, Wang ZP. MiRNA-191 functions as an

oncogene in primary glioblastoma by directly targeting NDST1. Eur Rev Med Pharmacol Sci. 2019;23(14):6242–9.

243. Sharma S, Nagpal N, Ghosh PC, Kulshreshtha R. P53-miR-191-SOX4 regulatory loop affects apoptosis in breast cancer. Rna. 2017;23(8):1237–46.

244. Guo S, Zhang J, Zhao YY, Zhou LY, Xie Y, Wu XY, et al. The expressions of miR-151a-5p and miR-23b in lung cancer tissues and their effects on the biological functions of lung cancer A549 cells. Eur Rev Med Pharmacol Sci. 2020;24(12):6779–85.

245. De Santi C, Melaiu O, Bonotti A, Cascione L, Di Leva G, Foddis R, et al. Deregulation of miRNAs in malignant pleural mesothelioma is associated with prognosis and suggests an alteration of cell metabolism. Sci Rep. 2017;7(1):1–11.

246. Du P, Luo K, Li G, Zhu J, Xiao Q, Li Y, et al. Long non-coding RNA VCAN-AS1 promotes the malignant behaviors of breast cancer by regulating the miR-106a-5p-mediated STAT3/HIF-1α pathway. Bioengineered [Internet]. 2021;12(1):5028–44. Available from: https://doi.org/10.1080/21655979.2021.1960774

247. Xu W, Liu M, Peng X, Zhou P, Zhou J, Xu K, et al. MiR-24-3p and miR-27a-3p promote cell proliferation in glioma cells via cooperative regulation of MXI1. Int J Oncol. 2013;42(2):757–66.

248. Roscigno G, Puoti I, Giordano I, Donnarumma E, Russo V, Affinito A, et al. MiR-24 induces chemotherapy resistance and hypoxic advantage in breast cancer. Oncotarget [Internet]. 2017;8(12):19507–21. Available from:

www.impactjournals.com/oncotarget/

249. Miao W, Li N, Gu B, Yi G, Su Z, Cheng H. Mir-27b-3p suppresses glioma development via targeting yap1. Biochem Cell Biol. 2020;98(4):466–73.

250. Moriondo G, Scioscia G, Soccio P, Tondo P, De Pace CC, Sabato R, et al. Effect of Hypoxia-Induced Micro-RNAs Expression on Oncogenesis. Int J Mol Sci. 2022;23(11):6294.

251. Hao SC, Ma H, Niu ZF, Sun SY, Zou YR, Xia HC. HUC-MSCs secreted exosomes inhibit the glioma cell progression through PTENP1/MIR-10a-5p/PTEN pathway. Eur Rev Med Pharmacol Sci. 2019;23(22):10013–23.

252. Wang F, Jiang H, Wang S, Chen B. Dual Functional MicroRNA-186-5p Targets both FGF2 and RelA to Suppress Tumorigenesis of Glioblastoma Multiforme. Cell Mol Neurobiol. 2017;37(8):1433–42.

253. Du F, Guo T, Cao C. Silencing of Long Noncoding RNA SNHG6 Inhibits Esophageal Squamous Cell Carcinoma Progression via miR-186-5p/HIF1α Axis. Dig Dis Sci [Internet]. 2020;65(10):2844–52. Available from: https://doi.org/10.1007/s10620-019-06012-8

254. Qin Y, Zheng Y, Huang C, Li Y, Gu M, Wu Q. Downregulation of miR-181b-5p Inhibits the Viability, Migration, and Glycolysis of Gallbladder Cancer by Upregulating PDHX Under Hypoxia. Front Oncol. 2021;11(August):1–11.

255. Gao K, Wang T, Qiao Y, Cui B. MiR-23b-5p promotes the chemosensitivity of temozolomide via negatively regulating TLR4

in glioma. Acta Biochim Biophys Sin (Shanghai). 2021;53(8):979–87.

256. Shao NY, Wang DX, Wang Y, Li Y, Zhang ZQ, Jiang Q, et al. MicroRNA-29a-3p Downregulation Causes Gab1 Upregulation to Promote Glioma Cell Proliferation. Cell Physiol Biochem. 2018;48(2):450–60.

257. Catanzaro G, Sabato C, Russo M, Rosa A, Abballe L, Besharat ZM, et al. Loss of miR-107, miR-181c and miR-29a-3p promote activation of Notch2 signaling in pediatric high-grade gliomas (pHGGs). Int J Mol Sci. 2017;18(12).

258. Xie P, Wang Y, Liao Y, Han Q, Qiu Z, Chen Y, et al. MicroRNA-628-5p inhibits cell proliferation in glioma by targeting DDX59. J Cell Biochem. 2019;120(10):17293–302.

259. Wang N, Tan HY, Feng YG, Zhang C, Chen F, Feng Y. microRNA-23a in human cancer: Its roles, mechanisms and therapeutic relevance. Cancers (Basel). 2019;11(1):1–22.

260. Agrawal R, Pandey P, Jha P, Dwivedi V, Sarkar C, Kulshreshtha R. Hypoxic signature of microRNAs in glioblastoma: Insights from small RNA deep sequencing. BMC Genomics. 2014;15(1):1–16.

261. Xue W, Chen J, Liu X, Gong W, Zheng J, Guo X, et al. PVT1 regulates the malignant behaviors of human glioma cells by targeting miR-190a-5p and miR-488-3p. Biochim Biophys Acta - Mol Basis Dis [Internet]. 2018;1864(5):1783–94. Available from: https://doi.org/10.1016/j.bbadis.2018.02.022

262. Zhang MY, Guo Y, Wu J, Chen FH, Dai ZJ, Fan SS, et al. Roles

of microRNA-99 family in human glioma. Onco Targets Ther. 2016;9:3603–12.

263. Wang Y, Chen R, Zhou X, Guo R, Yin J, Li Y, et al. miR-137: A Novel Therapeutic Target for Human Glioma. Mol Ther - Nucleic Acids [Internet]. 2020;21(September):614–22. Available from: https://doi.org/10.1016/j.omtn.2020.06.028

264. Li DM, Chen QD, Wei GN, Wei J, Yin JX, He JH, et al. Hypoxia-Induced miR-137 Inhibition Increased Glioblastoma Multiforme Growth and Chemoresistance Through LRP6. Front Oncol. 2021;10(February):1–12.

265. Simionescu N, Nemecz M, Petrovici A, Nechifor IS, Buga R, Dabija MG, et al. Microvesicles and Microvesicle-Associated microRNAs Reflect Glioblastoma Regression : Microvesicle-Associated miR-625-5p Has Biomarker Potential. 2022;

266. Wang M, Hu M, Li Z, Qian D, Wang B, Liu DX. miR-141-3p functions as a tumor suppressor modulating activating transcription factor 5 in glioma. Biochem Biophys Res Commun [Internet]. 2017;490(4):1260–7. Available from: http://dx.doi.org/10.1016/j.bbrc.2017.05.179

267. Sun S, Ma J, Xie P, Wu Z, Tian X. Hypoxia-responsive miR-141–3p is involved in the progression of breast cancer via mediating the HMGB1/HIF-1α signaling pathway. J Gene Med. 2020;22(10):1–11.

268. Li D, Li L, Chen X, Yang W, Cao Y. Circular RNA SERPINE2 promotes development of glioblastoma by regulating the miR-

361-3p/miR-324-5p/BCL2 signaling pathway. Mol Ther - Oncolytics [Internet]. 2021;22(270):483–94. Available from: https://doi.org/10.1016/j.omto.2021.07.010

269. Kit OI, Pushkin AA, Alliluyev IA, Timoshkina NN, Gvaldin DY, Rostorguev EE, et al. Differential expression of microRNAs targeting genes associated with the development of high-grade gliomas. Egypt J Med Hum Genet [Internet]. 2022;23(1). Available from: https://doi.org/10.1186/s43042-022-00245-5

270. Kannathasan T, Kuo WW, Chen MC, Viswanadha VP, Shen CY, Tu CC, et al. Chemoresistance-associated silencing of mir-4454 promotes colorectal cancer aggression through the gnl3l and nf-κb pathway. Cancers (Basel). 2020;12(5).

271. Wozniak M, Peczek L, Czernek L, Düchler M. Analysis of the miRNA profiles of melanoma exosomes derived under normoxic and hypoxic culture conditions. Anticancer Res. 2017;37(12):6779–89.

272. Yang R, Liu G, Han L, Qiu Y, Wang L, Wang M. MiR-365a-3p-Mediated Regulation of HELLS/GLUT1 Axis Suppresses Aerobic Glycolysis and Gastric Cancer Growth. Front Oncol. 2021;11(March):1–11.

273. Liu YZ, Sun Y. High expression of GAS5 promotes neuronal death after cerebral infarction by regulating miR-365a-3p. Eur Rev Med Pharmacol Sci. 2018;22(16):5270–7.

274. Yang B, Xia S, Ye X, Jing W, Wu B. MiR-379–5p targets microsomal glutathione transferase 1 (MGST1) to regulate human

glioma in cell proliferation, migration and invasion and epithelial-mesenchymal transition (EMT). Biochem Biophys Res Commun [Internet]. 2021;568:8–14. Available from: https://doi.org/10.1016/j.bbrc.2021.05.099

275. Khalil S, Fabbri E, Santangelo A, Bezzerri V, Cantù C, Di Gennaro G, et al. miRNA array screening reveals cooperative MGMT-regulation between miR-181d-5p and miR-409-3p in glioblastoma. Oncotarget. 2016;7(19):28195–206.
276. Wang X, Xiao H, Wu D, Zhang D, Zhang Z. MiR-335-5p regulates cell cycle and metastasis in lung adenocarcinoma by targeting CCNB2. Onco Targets Ther. 2020;13:6255–63.
277. Garrido-cano I, Const V, Adam-artigues A, Lameirinhas A, Sim S, Ortega B, et al. Circulating miR-99a-5p Expression in Plasma : A Potential Biomarker for Early Diagnosis of Breast Cancer. 2020;
278. Xia J, Jiang N, Li Y, Wei Y, Zhang X. The long noncoding RNA THRIL knockdown protects hypoxia-induced injuries of H9C2 cells through regulating miR-99a. 2019;26(5):564–74.
279. Lee CC, Ho KH, Huang TW, Shih CM, Hsu SY, Liu AJ, et al. A regulatory loop among CD276, miR-29c-3p, and Myc exists in cancer cells against natural killer cell cytotoxicity. Life Sci [Internet]. 2021;277(January):119438. Available from: https://doi.org/10.1016/j.lfs.2021.119438
280. Sun XH, Fan WJ, An ZJ, Sun Y. Inhibition of long noncoding RNA CRNDE increases chemosensitivity of medulloblastoma cells by targeting miR-29c-3p. Oncol Res. 2020;28(1):95–102.

281. Gu W, Wang L, Deng G, Gu X, Tang Z, Li S, et al. Knockdown of long noncoding RNA MIAT attenuates cigarette smoke-induced airway remodeling by downregulating miR-29c-3p–HIF3A axis. Toxicol Lett [Internet]. 2022;357:11–9. Available from: https://doi.org/10.1016/j.toxlet.2021.12.014
282. Hu Y, Li Y, Wu C, Zhou L, Han X, Wang Q, et al. MicroRNA-140-5p inhibits cell proliferation and invasion by regulating VEGFA/MMP2 signaling in glioma. Tumor Biol. 2017;39(4).
283. Wang D-W, Lou X-Q, Liu Z-L, Zhang N, Pang L. LncRNA SNHG1 protects SH-Sy5Y cells from hypoxic injury through miR-140-5p/Bcl-XL axis. Int J Neurosci. 2021;131(4):336–45.
284. Feng L, Ma J, Ji H, Liu Y, Hu W. MiR-184 Retarded the Proliferation, Invasiveness and Migration of Glioblastoma Cells by Repressing Stanniocalcin-2. Pathol Oncol Res. 2018;24(4):853–60.
285. Yuan Q, Gao W, Liu B, Ye W. Upregulation of miR-184 enhances the malignant biological behavior of human glioma cell line A172 by targeting FIH-1. Cell Physiol Biochem. 2014;34(4):1125–36.
286. Zhang Y, Ta W-W, Sun P-F, Meng Y-F, Zhao C-Z. Diagnostic and prognostic significance of serum miR-145-5p expression in glioblastoma. Int J Clin Exp Pathol [Internet]. 2019;12(7):2536–43. Available from: http://www.ncbi.nlm.nih.gov/pubmed/31934080%0Ahttp://www.pubmedcentral.nih.gov/articlerender.fcgi?artid=PMC6949540
287. Chen LP, Zhang NN, Ren XQ, He J, Li Y. miR-103/miR-195/miR-

15b regulate SALL4 and inhibit proliferation and migration in glioma. Molecules. 2018;23(11).

288. Balzeau J, Menezes MR, Cao S, Hagan JP. The LIN28/let-7 pathway in cancer. Front Genet. 2017;8(MAR):1–16.

289. Weng M, Feng Y, He Y, Yang W, Li J, Zhu Y, et al. Hypoxia-Induced LIN28A mRNA Promotes the Metastasis of Colon Cancer in a Protein-Coding-Independent Manner. Front Cell Dev Biol. 2021;9(February):1–15.

290. Li Z, Qian R, Zhang J, Shi X. MiR-218-5p targets LHFPL3 to regulate proliferation, migration, and epithelial–mesenchymal transitions of human glioma cells. Biosci Rep. 2019;39(3):1–14.

291. Li Y, Wang X, Zhao Z, Shang J, Li G, Zhang R. LncRNA NEAT1 promotes glioma cancer progression via regulation of miR-98-5p/BZW1. Biosci Rep. 2021;41(7):1–15.

292. Dong L, Cao X, Luo Y, Zhang G, Zhang D. A Positive Feedback Loop of lncRNA DSCR8/miR-98-5p/STAT3/HIF-1α Plays a Role in the Progression of Ovarian Cancer. Front Oncol. 2020;10(September):1–12.

293. Meng Q, Li S, Liu Y, Zhang S, Jin J, Zhang Y, et al. Circular RNA circSCAF11 Accelerates the Glioma Tumorigenesis through the miR-421/SP1/VEGFA Axis. Mol Ther - Nucleic Acids [Internet]. 2019;17(September):669–77. Available from: https://doi.org/10.1016/j.omtn.2019.06.022

294. Ge X, Liu X, Lin F, Li P, Liu K, Geng R, et al. MicroRNA-421 regulated by HIF-1α promotes metastasis, inhibits apoptosis, and

induces cisplatin resistance by targeting E-cadherin and caspase-3 in gastric cancer. Oncotarget. 2016;7(17):24466–82.

295. Wang X, Sun S, Tong X, Ma Q, Di H, Fu T, et al. MiRNA-154-5p inhibits cell proliferation and metastasis by targeting PIWIL1 in glioblastoma. Brain Res [Internet]. 2017;1676:69–76. Available from: https://doi.org/10.1016/j.brainres.2017.08.014

296. Wang L, Sun L, Liu R, Mo H, Niu Y, Chen T, et al. Long non-coding RNA MAPKAPK5-AS1/PLAGL2/HIF-1α signaling loop promotes hepatocellular carcinoma progression. J Exp Clin Cancer Res. 2021;40(1):1–18.

297. Sárközy M, Kahán Z, Csont T. A myriad of roles of miR-25 in health and disease. Oncotarget. 2018;9(30):21580–612.

298. Vandesompele J, De Preter K, Pattyn F, Poppe B, Van Roy N, De Paepe A, et al. Accurate normalization of real-time quantitative RT-PCR data by geometric averaging of multiple internal control genes. Genome Biol. 2002;3(7):reserach0034.1-0034.11.

299. Zhao H, Xing F, Yuan J, Li Z, Zhang W. Sevoflurane inhibits migration and invasion of glioma cells via regulating miR-34a-5p / MMP-2 axis. Life Sci [Internet]. 2020;256(1):117897. Available from: https://doi.org/10.1016/j.lfs.2020.117897

300. Chen L, Li Z yang, Xu S yi, Zhang X jun, Zhang Y, Luo K, et al. Upregulation of miR-107 Inhibits Glioma Angiogenesis and VEGF Expression. Cell Mol Neurobiol. 2016;36(1):113–20.

301. Zhou W, Yu X, Sun S, Zhang X, Yang W, Zhang J, et al. Increased expression of MMP-2 and MMP-9 indicates poor

prognosis in glioma recurrence. Biomed Pharmacother [Internet]. 2019;118(August):109369. Available from: https://doi.org/10.1016/j.biopha.2019.109369

302. Fujiwara S, Nakagawa K, Harada H, Nagato S, Furukawa K, Teraoka M, et al. Silencing hypoxia-inducible factor-1α inhibits cell migration and invasion under hypoxic environment in malignant gliomas. Int J Oncol. 2007;30(4):793–802.
303. Huang M, Gong X. Let-7c inhibits the proliferation, invasion, and migration of glioma cells via targeting E2F5. Oncol Res. 2018;26(7):1103–11.
304. Lee SY, Yang J, Park JH, Shin HK, Kim WJ, Kim SY, et al. The MicroRNA-92a/Sp1/MyoD Axis Regulates Hypoxic Stimulation of Myogenic Lineage Differentiation in Mouse Embryonic Stem Cells. Mol Ther [Internet]. 2020;28(1):142–56. Available from: https://doi.org/10.1016/j.ymthe.2019.08.014
305. Huang H-T, Liu Z-C, Wu K-Q, Gu S-R, Lu T-C, Zhong C-J, et al. MiR-92a regulates endothelial progenitor cells (EPCs) by targeting GDF11 via activate SMAD2/3/FAK/Akt/eNOS pathway. Ann Transl Med. 2019;7(20):563–563.
306. Camps C, Saini HK, Mole DR, Choudhry H, Reczko M, Guerra-Assunção JA, et al. Integrated analysis of microRNA and mRNA expression and association with HIF binding reveals the complexity of microRNA expression regulation under hypoxia. Mol Cancer. 2014;13(1):1–21.
307. Casanova-Salas I, Rubio-Briones J, Fernández-Serra A, López-

Guerrero JA. MiRNAs as biomarkers in prostate cancer. Clin Transl Oncol. 2012;14(11):803–11.

308. Grobbelaar C, Ford AM. The Role of MicroRNA in Paediatric Acute Lymphoblastic Leukaemia: Challenges for Diagnosis and Therapy. J Oncol. 2019;2019.

309. De Robertis M, Poeta ML, Signori E, Fazio VM. Current understanding and clinical utility of miRNAs regulation of colon cancer stem cells. Semin Cancer Biol [Internet]. 2018;53(August):232–47. Available from: https://doi.org/10.1016/j.semcancer.2018.08.008

310. Varrone F, Caputo E. The miRNAs role in melanoma and in its resistance to therapy. Int J Mol Sci. 2020;21(3).

311. Enokida H, Yoshino H, Matsushita R, Nakagawa M. The role of microRNAs in bladder cancer. Investig Clin Urol. 2016;57:S60–76.

312. Shi K, Sun H, Zhang H, Xie D, Yu B. MiR-34a-5p aggravates hypoxia-induced apoptosis by targeting ZEB1 in cardiomyocytes. Biol Chem. 2019;400(2):227–36.

313. Kong S, Fang Y, Wang B, Cao Y, He R, Zhao Z. miR-152-5p suppresses glioma progression and tumorigenesis and potentiates temozolomide sensitivity by targeting FBXL7. J Cell Mol Med. 2020;24(8):4569–79.

314. Regazzo G, Terrenato I, Spagnuolo M, Carosi M, Cognetti G, Cicchillitti L, et al. A restricted signature of serum miRNAs distinguishes glioblastoma from lower grade gliomas. J Exp Clin

Cancer Res [Internet]. 2016;35(1):1–11. Available from: http://dx.doi.org/10.1186/s13046-016-0393-0

315. Gong Q, Xie J, Li Y, Liu Y, Su G. Enhanced ROBO4 is mediated by up-regulation of HIF-1α/SP1 or reduction in miR-125b-5p/miR-146a-5p in diabetic retinopathy. J Cell Mol Med. 2019;23(7):4723–37.
316. Jeremias I, David A, Aditya PA, Rizky N. MiRNA-regulated HspB8 as potent biomarkers in low-grade gliomas. Res J Biotechnol. 2021;16(1):17–25.
317. Zhu L, Deng H, Hu J, Huang S, Xiong J, Deng J. The promising role of miR-296 in human cancer. Pathol Res Pract [Internet]. 2018;214(12):1915–22. Available from: https://doi.org/10.1016/j.prp.2018.09.026
318. Monteiro A, Hill R, Pilkington G, Madureira P. The Role of Hypoxia in Glioblastoma Invasion. Cells. 2017;6(4):45.
319. Zhang H, Liang F, Yue J, Liu P, Wang J, Wang Z, et al. MicroRNA-137 regulates hypoxia-mediated migration and epithelial-mesenchymal transition in prostate cancer by targeting LGR4 via the EGFR/ERK signaling pathway. Int J Oncol. 2020;57(2):540–9.
320. Sawai S, Wong P-F, Ramasamy TS. Hypoxia-regulated microRNAs: the molecular drivers of tumour progression. Crit Rev Biochem Mol Biol. 2022;
321. Zhou Y, Huang Y, Hu K, Zhang Z, Yang J, Wang Z. HIF1A activates the transcription of lncRNA RAET1K to modulate

hypoxia-induced glycolysis in hepatocellular carcinoma cells via miR-100-5p. Cell Death Dis [Internet]. 2020;11(3). Available from: http://dx.doi.org/10.1038/s41419-020-2366-7

322. Li Y, Kuscu C, Banach A, Zhang Q, Pulkoski-Gross A, Kim D, et al. miR-181a-5p inhibits cancer cell migration and angiogenesis via downregulation of matrix metalloproteinase-14. Cancer Res. 2015;75(13):2674–85.

323. Wang L, Ma J, Wang X, Peng F, Chen X, Zheng B, et al. Kaiso (ZBTB33) Downregulation by Mirna-181a Inhibits Cell Proliferation, Invasion, and the Epithelial-Mesenchymal Transition in Glioma Cells. Cell Physiol Biochem. 2018;48(3):947–58.

324. Shen X, Li J, Liao W, Wang J, Chen H, Yao Y, et al. MicroRNA-149 targets caspase-2 in glioma progression. Oncotarget. 2016;7(18):26388–99.

325. She X, Yu Z, Cui Y, Lei Q, Wang Z, Xu G, et al. MiR-128 and miR-149 enhance the chemosensitivity of temozolomide by Rap1B-mediated cytoskeletal remodeling in glioblastoma. Oncol Rep. 2014;32(3):957–64.

326. Wang Q, Teng Y, Wang R, Deng D, You Y, Peng Y, et al. The long non-coding RNA SNHG14 inhibits cell proliferation and invasion and promotes apoptosis by sponging miR-92a-3p in glioma. Oncotarget. 2018;9(15):12112–24.

327. Liu PJ, Ye YX, Wang YX, Du JX, Pan YH, Fang XB. MiRNA-92a promotes cell proliferation and invasion through binding to KLF4 in Glioma. Eur Rev Med Pharmacol Sci. 2019;12(15):6612–20.

328. Niu H, Wang K, Zhang A, Yang S, Song Z, Wang W, et al. miR-92a is a critical regulator of the apoptosis pathway in glioblastoma with inverse expression of BCL2L11. Oncol Rep. 2012;28(5):1771–7.

329. Ghosh AK, Shanafelt TD, Cimmino A, Taccioli C, Volinia S, Liu CG, et al. Aberrant regulation of pVHL levels by microRNA promotes the HIF/VEGF axis in CLL B cells. Blood. 2009;113(22):5568–74.

330. Li M, Guan X, Sun Y, Mi J, Shu X, Liu F, et al. MiR-92a family and their target genes in tumorigenesis and metastasis. Exp Cell Res [Internet]. 2014;323(1):1–6. Available from: http://dx.doi.org/10.1016/j.yexcr.2013.12.025

331. Krock BL, Skuli N, Simon MC. Hypoxia-Induced Angiogenesis: Good and Evil. Genes and Cancer. 2011;2(12):1117–33.

332. Colwell N, Larion M, Giles AJ, Seldomridge AN, Sizdahkhani S, Gilbert MR, et al. Hypoxia in the glioblastoma microenvironment: Shaping the phenotype of cancer stem-like cells. Neuro Oncol. 2017;19(7):887–96.

333. Ando Y, Siegler EL, Ta HP, Cinay GE, Zhou H, Gorrell KA, et al. Evaluating CAR-T Cell Therapy in a Hypoxic 3D Tumor Model. Adv Healthc Mater. 2019;8(5).

334. Wang S, Lu J. 25-hydroxycholesterol Regulates Migration , Invasion and EMT of Colorectal Cancer through miR-92a- 3p / ACAA1 / NF- κ B Pathway - PREPRINT. Res Sq. 2021;

335. Feng H, Shen W. ACAA1 Is a Predictive Factor of Survival and Is

Correlated With T Cell Infiltration in Non-Small Cell Lung Cancer. Front Oncol. 2020;10(October).

336. Jethva R, Bennett MJ, Vockley J. Short-chain acyl-coenzyme A dehydrogenase deficiency. Mol Genet Metab [Internet]. 2008;95(4):195–200. Available from: http://dx.doi.org/10.1016/j.ymgme.2008.09.007

337. Tretter L, Patocs A, Chinopoulos C. Succinate, an intermediate in metabolism, signal transduction, ROS, hypoxia, and tumorigenesis. Biochim Biophys Acta - Bioenerg [Internet]. 2016;1857(8):1086–101. Available from: http://dx.doi.org/10.1016/j.bbabio.2016.03.012

338. Lo Giudice A, Asmundo MG, Broggi G, Cimino S, Morgia G, Di Trapani E, et al. The Clinical Role of SRSF1 Expression in Cancer: A Review of the Current Literature. Appl Sci. 2022;12(5).

339. Das S, Anczuków O, Akerman M, Krainer AR. Oncogenic Splicing Factor SRSF1 Is a Critical Transcriptional Target of MYC. Cell Rep. 2012;1(2):110–7.

340. Barbagallo D, Caponnetto A, Brex D, Mirabella F, Barbagallo C, Lauretta G, et al. CircSMARCA5 regulates VEGFA mRNA splicing and angiogenesis in glioblastoma multiforme through the binding of SRSF1. Cancers (Basel). 2019;11(2):1–12.

341. Wu Q, Chang Y, Zhang L, Zhang Y, Tian T, Feng G, et al. SRPK1 dissimilarly impacts on the growth, metastasis, chemosensitivity and angiogenesis of glioma in normoxic and hypoxic conditions. J Cancer. 2014;4(9):727–35.

342. Boudhraa Z, Carmona E, Provencher D, Mes-Masson AM. Ran GTPase: A Key Player in Tumor Progression and Metastasis. Front Cell Dev Biol. 2020;8(May).
343. Williamson M, De Winter P, Masters JR. Plexin-B1 signalling promotes androgen receptor translocation to the nucleus. Oncogene. 2016;35(8):1066–72.
344. Guvenc H, Pavlyukov MS, Joshi K, Kurt H, Banasavadi-Siddegowda YK, Mao P, et al. Impairment of glioma stem cell survival and growth by a novel inhibitor for survivin-ran protein complex. Clin Cancer Res. 2013;19(3):631–42.
345. Wavelet-vermuse C, Odnokoz O, Xue Y, Lu X, Cristofanilli M. CDC20-Mediated hnRNPU Ubiquitination Regulates Chromatin Condensation and Anti-Cancer Drug Response. Cancers (Basel). 2022;14(3723):1–21.
346. Zhou J, Guo Y, Huo Z, Xing Y, Fang J, Ma G, et al. Identification of therapeutic targets and prognostic biomarkers from the hnRNP family in invasive breast carcinoma. Aging (Albany NY). 2021;13(3):4503–21.
347. Pavlyukov MS, Yu H, Bastola S, Minata M, Shender VO, Lee Y, et al. Apoptotic Cell-Derived Extracellular Vesicles Promote Malignancy of Glioblastoma Via Intercellular Transfer of Splicing Factors. Cancer Cell [Internet]. 2018;34(1):119-135.e10. Available from: https://doi.org/10.1016/j.ccell.2018.05.012
348. Sheng KL, Pridham KJ, Sheng Z, Lamouille S, Varghese RT. Functional blockade of small GTPase RAN inhibits glioblastoma

cell viability. Front Oncol. 2019;9(JAN):1–12.

349. Wheatley SP, Altieri DC. Survivin at a glance. J Cell Sci. 2019;132(7).

350. Cheung CHA, Chen HH, Kuo CC, Chang CY, Coumar MS, Hsieh HP, et al. Survivin counteracts the therapeutic effect of microtubule de-stabilizers by stabilizing tubulin polymers. Mol Cancer. 2009;8:1–15.

351. Yuen HF, Gunasekharan VK, Chan KK, Zhang SD, Platt-Higgins A, Gately K, et al. RanGTPase: A candidate for myc-mediated cancer progression. J Natl Cancer Inst. 2013;105(7):475–88.

352. Yin G, Lv G, Zhang J, Jiang H, Lai T, Yang Y, et al. Early-stage structure-based drug discovery for small GTPases by NMR spectroscopy. Pharmacol Ther [Internet]. 2022;236:108110. Available from: https://doi.org/10.1016/j.pharmthera.2022.108110

353. Zhang N, Hu G, Myers TG, Williamson PR. Protocols for the analysis of microRNA expression, biogenesis and function in immune cells. Curr Protoc Immunol. 2019;126(1):e78.